



universität
wien

MASTERARBEIT / MASTER'S THESIS

Titel der Masterarbeit / Title of the Master's Thesis

“Detection, Quantification and Influence of Groundwater at Lake Steiβlingen based on the Measurement of Physical, Chemical and Isotopic Parameters”

verfasst von / submitted by

Anna Sophia Magdalena Mathis (BSc)

Angestrebter akademischer Grad / in partial fulfilment of the requirements for the degree of
Master of Science (MSc)

Wien, 2018

Studienkennzahl lt. Studienblatt /
degree programme code as it appears on
the student record sheet:

A 066 815

Studienrichtung lt. Studienblatt /
degree programme as it appears on
the student record sheet:

Masterstudium Erdwissenschaften UG2002

Betreut von / Supervisor:

Univ. – Prof. Dr. habil. Thilo Hofmann

Acknowledgments

First of all, I would like to express my gratitude to my supervisor Univ. – Prof. Dr. habil. Thilo Hofmann for making it possible to write this thesis extern at ISF Langenargen and moreover to experience the scientific exchange.

I would also like to thank Dr. Vera Winde who spent a lot of time discussing and explaining scientific questions with me. Moreover, she helped me not to lose the right track during the writing process.

Also, I owe a great debt of gratitude to Dr. Albrecht Leis and Till Harum for the scientific input concerning chemical and isotopically questions.

Last but not least, I would like to thank the institution for lake research (ISF) in Langenargen for employing me and involving me to the SeeZeichen project.

I am deeply grateful to my parents Uli and Hansjörg and my uncle Otto for supporting me mentally and financially during my studies. Without you and your love this could not have been possible.

Also, I would like to thank my friends for always making me laugh whenever I had a tough time.

Abstract

Groundwater can be a driving factor for the hydrochemistry, mixture dynamic and water budget of a lake system. This study is part of the SeeZeichen project for which various observation and measurement methods were applied concerning groundwater tracing and quantification, mainly at Lake Constance, but also at Lake Steißlingen and Ammersee Lake. Within this thesis, Lake Steißlingen is observed. Former surveys of Lake Steißlingen mainly regarded its historical climatic data and sediments. Thereby, it became clear that Lake Steißlingen gets fed mainly by groundwater, which leads to a more detailed observation for groundwater detection and quantification within this study.

In this study, measurements of physical, chemical and isotopic parameters, in combination with Phreeqc inverse modelling, are evaluated in its applicability and portability to Lake Steißlingen, which was currently verified as an appropriate method for the quantification and detection of groundwater at Lake Constance. Another aim of this master's thesis was to examine the aquifer layer where groundwater is originating from and to which extent it influences the lakes stratification through seasonal-mixing- and circulation-behavior.

To close research gaps concerning groundwater quantification and localization at Lake Steißlingen, physical, chemical and isotopic parameters were measured along depth profiles and close to the sediment through water sampling, CTD-measurement and analysis in the laboratory at regular intervals in 2016/2017. Additionally, a permanent measuring station was installed on-site between December 2016 and December 2017. For a more accurate evaluation of groundwater ratio and the ascertainment of the saturation index for calcite, Phreeqc modelling and inverse modelling was applied. All applied methods, e.g. measurements of $\text{NO}_3\text{-N}$ or $\delta^{18}\text{O}$, show that groundwater enters the lake through a quaternary, carbonatic high permeable aquifer lens, fed by local precipitation, at a depth of ~15m. This causes the formation of a distinct water layer above the hypolimnion between spring and fall months. The exchange processes between the hypolimnion and the groundwater layer cause a complete mixture and homogeneity of the hypolimnion during fall/winter. Influenced by warmer incoming groundwater to the lake in connection with the homogeneity of the hypolimnion Lake Steißlingen indicates a temporary inverse stratification in winter. Due to slight differences in water temperature and density between epi- and hypolimnion within this period of the year, a mixing event only gets approached by exchange processes. The occurrence of a mixing approach is proven by a chemical and isotopically homogeneity along the entire water column in spring.

An accumulation of groundwater in the hypolimnion was observed between spring and fall months up to 77.2% in September 2017, which supports the stabilization of the lakes stratification. The highest groundwater ratios calculated by Phreeqc are located in the middle and north-eastern side of the lake in September 2017.

Zusammenfassung

Grundwasser kann aufgrund vieler Faktoren einen erheblichen Einfluss auf Seesysteme nehmen, wie beispielsweise auf den Hydrochemismus, die Mischdynamik und den Wasserhaushalt. Diese Studie war Teil des SeeZeichen Projektes, welches sich mit der räumlichen Verteilung und der saisonalen Dynamik unterschiedlicher Eintragspfade in Seen, wie beispielsweise Grundwasser, befasste. Zur Identifikation von Grundwasserzutritten wurden im Projekt verschiedene physikalische, chemische und isotopische Methoden einzeln und in Kombination getestet. Hauptuntersuchungsgebiet war der Bodensee. Die entwickelten Methoden wurden auf Übertragbarkeit auf andere Seen, wie den Steißlinger See und den Ammersee, überprüft und verifiziert. In dieser Arbeit lag das Augenmerk auf den Untersuchungen des Steißlinger Sees. Bisherige Studien widmeten sich hauptsächlich der Klimahistorie und den Sedimentabfolgen des Steißlinger Sees, wobei unter anderem beobachtet wurde, dass der See vermutlich zu einem Großteil durch Grundwasser gespeist wird. Aufgrund der seit Jahren bestehenden Annahme, dass der Steißlinger See hauptsächlich durch Grundwasser gespeist und beeinflusst wird, lag der Fokus dieser Studie auf der Detektion und Quantifikation des Grundwassers.

Für die Datenerfassung wurden physikalische, chemische und isotopische Parameter gemessen und anschließend eine inverse Modellierung mit Phreeqc durchgeführt. Außerdem wurde die als für die Quantifizierung und Detektion von Grundwasser am Bodensee geeignete Methode auf dessen Anwendbarkeit und Übertragbarkeit auf den Steißlinger See eingesetzt. Ein weiteres Ziel dieser Studie war die Lokalisierung der Aquifer-Schicht des einströmenden Grundwassers und dem damit in Verbindung stehenden Einfluss auf die Seeschichtung sowie die Erfassung der saisonalen Durchmischung und Zirkulation des Steißlinger Sees.

Um die Herkunft und Quantität des einströmenden Grundwassers am Steißlinger See zu verifizieren, wurden im Jahr 2016 und 2017 in regelmäßigen Intervallen physikalische, chemische und isotopische Parameter entlang von Tiefenprofilen und in Sedimentnähe gemessen, Wasserproben genommen, CTD-Messungen durchgeführt und Analysen im Labor gemacht. Außerdem wurde für hochaufgelöste Messungen der zeitlichen Variabilität zwischen Dezember 2016 und Dezember 2017 eine Dauermessstation an der seetiefsten Stelle betrieben. Für eine präzise Ermittlung des Grundwasseranteils und der Bestimmung des Sättigungsindex von Kalzit, wurde zusätzlich zu den Messungen eine Modellierung sowie inverse Modellierung mittels Phreeqc durchgeführt. Alle angewendeten Methoden, wie zum Beispiel die Messung von $\text{NO}_3\text{-N}$ oder $\delta^{18}\text{O}$, zeigten, dass das Grundwasser durch eine quartäre, karbonatische und stark durchlässige Aquifer-Linse in einer Tiefe von ~15 m eintritt, welche durch lokalen Niederschlag gespeist wird. Durch das Eintreten des Grundwassers in dieser Tiefe bildet sich zwischen den Frühlings- und Herbstmonaten im See eine ausgeprägte Grundwasserschicht oberhalb des Hypolimnions. Die Austauschprozesse zwischen Hypolimnion und Grundwasserschicht führen dazu, dass sich während den Herbst- und

Wintermonate ein homogener Wasserkörper im Hypolimnion ausgebildet. Aufgrund des fortlaufend infiltrierenden Grundwassers in den See und der Homogenität des Hypolimnions, weist der Steißlinger See in den Wintermonaten eine temporäre inverse Stratifizierung auf. Durch einen leichten Unterschied der Wassertemperatur und der Wasserdichte zwischen Epi- und Hypolimnion im Winter, bleibt ein vollständiger Mischungsprozess aus und wird nur annähernd erreicht, was auch an der isotopischen und chemischen Homogenität entlang der Wassersäule im Frühling erkennbar ist.

Eine Akkumulation des Grundwassers wurde zwischen Frühling- und Herbstmonaten bis hin zu 77,2 % im September 2017 im Hypolimnion beobachtet, was unter anderem zu einer Stabilisierung der Seeschichtung führt. Die Berechnungen des Grundwasseranteils mittels Phreeqc zeigen die höchsten Werte im September 2017 im Nord-Osten und in der Mitte des Sees.

TABLE OF CONTENTS

ACKNOWLEDGEMENT	I
ABSTRACT	II
ZUSAMMENFASSUNG	III
TABLE OF CONTENTS	V
1 Introduction	1
2 Material and Methods	6
2.1 Area of Research	6
2.1.1 Geographical Location	6
2.1.2 Geology	7
2.1.2.1 Regional Geology	7
2.1.2.2 Description Geological Section	12
2.1.2.3 Limnological Setting	13
2.2 Groundwater Detection of Lake Steißlingen	19
2.2.1 Measurement of in-situ physical-chemical parameters (CTD)	20
2.2.2 Depth specific Sampling within Lake Steißlingen	22
2.2.3 Determination of physical-chemical Parameters through Titration	23
2.2.4 Determination of Anions and Cations with Ion Chromatography Measurement (IC)	24
2.2.5 Determination of $\delta^{18}\text{O}$ and $\delta^2\text{H}$ Isotopes with a Laser Spectrometer	25
2.2.6 Calculation of Inorganic Carbonic Species with CO_2sys	26
2.3 Seasonal Quantification and Water Chemistry through Groundwater Influence (Phreeqc)	27
2.4 Stratification and Mixtures within Lake Steißlingen: Permanent measuring station	29
3 Results	30
3.1 Detection of Groundwater Inlets within Lake Steißlingen	31

3.1.1 Physical Parameters (T, EC, dissolved oxygen, oxygen saturation, turbidity, pH, Chlorophyll A)	31
3.1.2 Chemical Parameters (TA, Water Hardness, Anions, Cations)	40
3.1.3 Isotopic Parameters ($\delta^{2}\text{H}$, $\delta^{18}\text{O}$)	54
3.2 Quantification of groundwater inlets of Lake Steißlingen	58
3.3 Stratification and mixing dynamics within Lake Steißlingen (EnviWatch)	61
4 Discussion	63
4.1 Error Discussion	63
4.2 Hydrochemistry and Stratification of Lake Steißlingen	65
4.3 Groundwater Inflow to Lake Steißlingen	75
4.4 Impacts on Lake Steißlingen through Groundwater Inflow	86
5 Conclusion	91
6 References	93
Appendix:	
A) Table of Figures	
B) List of Tables	
C) Physical, Chemical and Isotopic Parameters	
D) Results of Phreeqc $\text{SI}_{\text{Calcite}}$ and Inverse Modeling	

1 Introduction

The last decades showed humanity that anthropogenic activities and global warming do have a tremendous impact on the hydrological system of the earth (Boehrer et al., 2008). Therefore, it is crucial that mankind antagonize further impact and thus ensure a sustainable and worth living future for example by gaining a better understanding for environmental processes (Boehrer et al., 2008).

In the world of science, surface water and groundwater were seen as two separate entities until the middle of the last century. Nowadays these expressions get summarized as limnology, which is explained by the importance of the interaction between ground- and surface water (Fleckenstein et al., 2010). The earth's groundwater reservoir was estimated to be approximately 21.9 million km³ by Gleeson et al. (2015), which corresponds to about 30.8% of the planets fresh water. Despite the fact that continental surface waters, as for example lakes, make up a small part with 0.3% of the earths freshwater reservoir, it is an essential component of the environment regarded by a hydrogeological and ecological point of view (BMU, 2008). The relevance within the research area of limnology (The science of fresh water ecosystems) and hydrogeology (The science of water in the earth's crust) increases constantly. This can be explained on the one hand by a growing nutrient input in surface and ground waters through anthropogenic activities (Rosenberry et al., 2015) which can influence the eutrophication and water quality of a lake (Hofmann et al., 2011). On the other hand, Krause et al. (2010) emphasizes the importance of an innovative and sustainable future for water – and land-management of water systems.

Even though several measurement methods were developed for examinations in the field of ground- and surface-water-interactions in the last 20 years, the state of research is still insufficient due to Fleckenstein et al. (2010). Groundwater was often ignored in history because it was not considered that the amount of in – and outflowing water is small, but the interstitial surface of the two water bodies is large, that it is often not visible and that its quantification method is not applicable to every lake system (Rosenberry et al., 2015).

The study of Hofmann et al. (2011) reveals how groundwater can change lake systems according to several factors, such as its hydrochemistry, its seasonal groundwater inlet and its isotopic composition. Moreover, groundwater inflow can change the circulation of lakes and thus its stratification, which can influence the alteration of water densities (Boehrer et al., 2008).

A considerable step in the research development of ex- and infiltrating of groundwater in surface waters is the implementation of multidisciplinary research in the fields of hydrology, biogeochemistry and ecology (Krause et al., 2010). Hereby, it is remarkable that the interdisciplinary research is crucial for a better understanding because most processes, which can be observed in the interstitial interface between surface water and groundwater, can be

explained chemically, physical and/or biologically. The processes, which can be found in the water body of the lake and the locations where groundwater ex-and infiltrates, are controlled by following parameters and processes: mixture of groundwater and surface water, transport and spatial-temporal distribution of oxygen, nutrient input, physical-chemical parameters (e.g. water temperature, electrical conductivity, pH, water hardness, anion, cation), redox conditions, meteorology (e.g. wind, rain), redox reactions and chemical gradients. The above-mentioned processes and parameters can change water quality and can influence internal lake circulation, lake eutrophication grade and the saturation index of minerals (Hofmann et al., 2011; Kalbus et al., 2006; Rosenberry et al., 2015; Spirkaneder, 2016). Furthermore, the geological and geometrical setting of the surrounding area of a lake effects the locations of groundwater in- and outflows and its flow path. This gets also influenced by lake depth, permeability and slope of the lake ground (Genereux et al., 2001).

For the examination of groundwater in- and exfiltration mostly indirect measurement methods are applied to determine different parameters (Rosenberry et al., 2015). A short overview of methods and its measured parameters will be given as follows, and for this thesis relevant ones will be explained in more detail.

The determination of physical-chemical parameters (Water temperature (T), dissolved oxygen, electrical conductivity (EC), pH..) is crucial within the research field of groundwater-surface water-interactions, which can be explained by its influence on water quality, the distribution of dissolved oxygen, lake water circulations and general seasonal fluctuations of involved factors. Therefore, seasonal in-situ measurements along depth profiles within lakes are applied, for example with a multi parameter probe (Hofmann et al., 2011). To localize groundwater inlets, results of temperature (Anibas et al., 2009) and EC measurements are used (Vogt et al., 2010). Hereby, the observations focus of the alteration of EC (Vogt et al., 2009) or temperature (Sebok et al., 2013) lies along the sediment surface and possible groundwater entrances. The survey of Hofmann et al. (2011) indicates that incoming groundwater to a lake can change its nutrient budget through biogenic fluctuations of pH, among other things.

The parameter of alkalinity can be determined with the Gran plot method in the field and is defined as the quantitative ability of an aqueous solution to neutralize an acid (Apello et al., 2005). According to lakes, alkalinity mainly gets controlled by the concentration of dissolved hydrogen carbonates due to its natural pH range and can therefore be influenced by the precipitation of carbonates in a lake (Hofmann et al., 2011).

For the observation of lakes, the hardness of water plays an important role because it can give information about the concentration of Ca^{2+} and Mg^{2+} and thus the type of aquifer that the groundwater is originating from, among other things (Langguth et al., 2004; Tepe et al., 2005). Whereas water hardness is dependent on the type of minerals found in the surroundings that the water passed through (Tepe et al., 2005).

The analysis of anions and cations can be for example done by ion chromatography, which represents the nutrient budget and water constitution of the lake (Hofmann et al., 2011).

For the detection of groundwater in lakes isotopic ratios between ^{16}O and ^{18}O as well as ^1H and ^2H are utilized as a natural tracer because they are already available as H_2O in the environment (LaBaugh et al., 1997). Due to minimal mass differences between the isotopes of oxygen and hydrogen, respectively, the lighter or heavier isotope gets enriched or depleted in the water body, which is dependent on the process (evaporation, condensation). The isotopic signatures of inflowing groundwater to the lakes are applied to determine origin and/or seasonal fluctuations (Hofmann et al., 2011). Furthermore, Radon-222 can be used as a groundwater tracer due to its radioactive decay in rocks (Arnoux et al., 2017) and the resulting accumulation in groundwater (Dimova et al., 2013).

To get a better understanding of groundwater- and surface-water-interactions it is common that various methods are applied in combination (Rosenberry et al., 2015).

The investigated ecosystem of this thesis is Lake Steißlingen, of which several studies, e.g. the analysis of pollen and sediment, were already conducted (Eusterhues 2000; Lechterbeck, 2000; Peschtrich, 2005). Eusterhues (2000) showed that the sediments at the bottom of Lake Steißlingen are mainly seasonally laminated and indicate ages back to the late- and postglacial periods, whereat, high concentrations of autochthonous calcite, organic matter and sulfate were found. Therefore, previous studies (Eusterhues 2000; Lechterbeck, 2000; Peschtrich, 2005) show that the research area of Lake Steißlingen is still in fledgling stages according to the knowledge of its hydrogeology and limnology.

In this thesis the focus lies within observations of groundwater output in Lake Steißlingen and the resulting interaction between groundwater and lake because there is still a little understanding for its processes and dynamics (Fleckenstein et al., 2010).

This master's thesis is part of the joint research project "SeeZeichen" (funding measures ReWaM (BMBF)), conducted by Institute of Lake Research, Federal State Institute for the Environment Baden-Württemberg, that dealt with the spatial distribution and seasonal dynamics of different pathways in lakes, for example of groundwater. For the identification of groundwater inlets, various physical, isotopic and chemical methods were applied and tested separately and in combination at Lake Constance. Hereby, the developed methods were also applied and verified at other lakes, such as Lake Steißlingen.

Lake Steißlingen is located north-westerly of Lake Constance and lies within the administrative district of Constance (Baden-Württemberg) with an area of 11.2 ha. Due to minimal inflow of surface water, but present recurring biological productivity in the epilimnion, it is believed that the nutrients enter Lake Steißlingen mainly through groundwater inflow (Eusterhues, 2000). Eusterhues (2000) assumes that in this connection the stratification and mixture pattern of the

lake water determines the distribution of the nutrient matter and hence the eutrophication, which is defined as “mesotroph”(LUBW, 2014). As a result of calculations, it is known that Lake Steißlingen has a considerable groundwater ratio of 70 % of its total input, which was observed in spring and summer months by Gilfedder et al. (2018). It gets presumed that the groundwater originates from geological layers in the subsurface and indicates a recharge rate of 11 l/s (Gilfedder et al., 2018). The quantity of incoming groundwater can influence water balance (Hofmann et al., 2011), hydrochemistry (Boehrer et al., 2008; Hofmann et al., 2011), isotopic composition (Hofmann et al., 2011) and the circulations in the water body (Boehrer et al., 2008; Hofmann et al., 2011), among other things. According to Lake Steißlingen it gets supposed that the groundwater carrying geological layers could be on the western shoreline outcropping as “Obere Meeresmolasse” and/or on the eastern side and the centre of the lake outcropping as quaternary layer. The two potential aquifers show different isotopic and chemical contents and can therefore be distinguished. From a hydrochemical point of view it is mentionable that the inflowing groundwater is anoxic and contains significant values of methane, nitrite and partly iron (Spirkaneder, 2016).

Due to insufficient knowledge of groundwater – surface water interactions at Lake Steißlingen and based on previous studies, following hypothesis and research questions for this thesis were proposed:

- Can the methods for groundwater detection that were developed for Lake Constance also be applied at Lake Steißlingen?
- Where are the locations of groundwater inlets and from which geological layer is it originating from?
- How much groundwater ratio can be quantified in Lake Steißlingen?
- To which extent does groundwater mix and distribute within Lake Steißlingen and how does this influence its stratification, mixing and circulation?
- Are there seasonal fluctuations according to groundwater recharge?

The hot spots of groundwater inlets of Lake Steißlingen will get identified and seasonally and spatially quantified, for which defined depth profiles within a measuring grid were recorded in regular intervals (June 2016, November 2016, March 2017, July 2017, September 2017). For the in-situ measurements a multi parameter probe was applied (Water temperature, electrical conductivity, dissolved oxygen, turbidity, chlorophyll A). Additionally, various chemical tracers (Anions, cations, stable isotopes) were measured in the laboratory for selected depths within the measuring grid. Moreover, a permanent measuring station was installed at the lakes deepest zone between December 2016 and December 2017 to gain a more accurate data set for the water parameters of temperature, electrical conductivity, pH and oxygen as well as

meteorological data. Depending on the month, some physical-chemical parameters (Temperature, electrical conductivity, pH, TA, water hardness) were measured in the vicinity of the lake including relevant groundwater springs and its in- and outlets. Furthermore, the biogeochemical modelling program Phreeqc (Tool: Inverse Modelling) was applied for calculating saturation indices and the mixing ratios of the water samples with different end members (inlet water, groundwater, lake water).

2 Material and Methods

2.1 Area of Research

2.1.1 Geographical Location

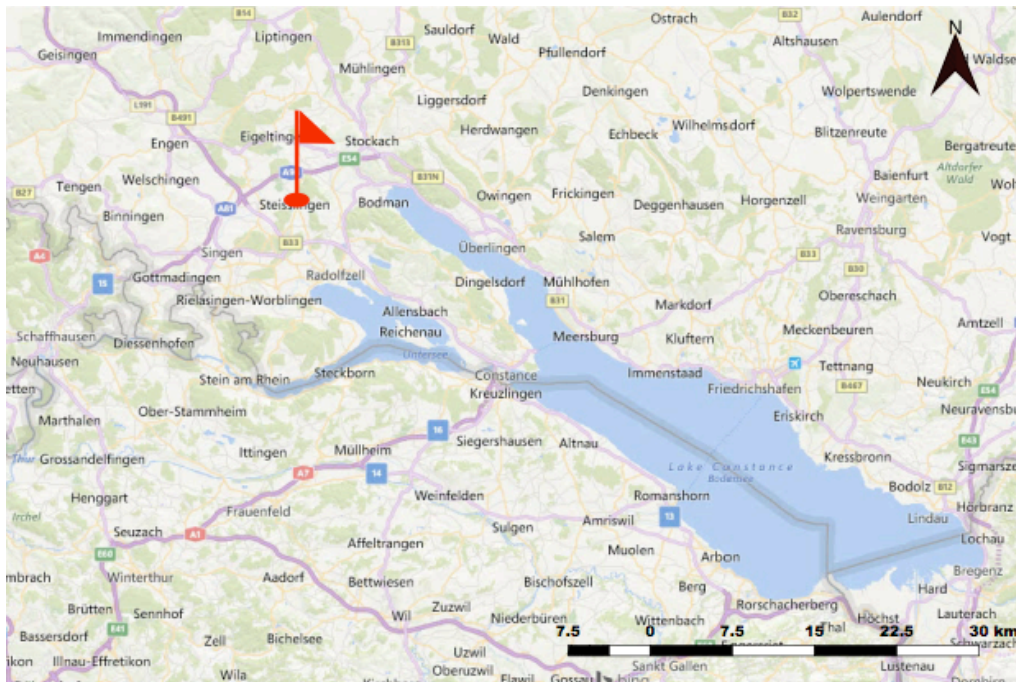


Figure 1 Geographical location of the research area (constructed with QGIS OpenLayers plugin, print composer)

The object that is observed within this master's thesis is Lake Steißlingen that lies on a sea level of 445.56NN and has an area of 11.2 ha (Eusterhues, 2000; LUBW, 2014). Regarding it at a large scale the small hard water lake is in the very southwestern part of Germany, near Lake Constance, southerly of the Swabian Alb, and south-easterly of the Black Forest, where river Danube originates (Eusterhues, 2002). Focusing on its small scale Lake Steißlingen is situated in the western part of Steißlingen and gets circumvented in the west by Hill Fronholz that is located in the centre of the rural district of Constance (Peschtrich, 2005). Steißlingen lays 7 km north westerly of the city of Radolfzell, about 6 km north-easterly of Singen and northerly of "Untersee" which is part of Lake Constance (Kürfgen, 1999). Due to its geographical location and an average precipitation rate of 820 mm/y between 1981 and 2010 (Deutscher Wetterdienst,

2017), Lake Steißlingen belongs to the temperate central European climate zone, which is defined as the changeover between the temperate oceanic climate and the temperate continental climate. Investigations of LUBW (Landesanstalt für Umwelt Baden-Württemberg) exhibit that climate change can also be seen regionally within the province of Baden-Württemberg, which moreover might change climatic conditions minimally (LUBW, 2013).

2.1.2 Geology

2.1.2.1 Regional Geology

The region of the research area is part of the Molasse Basin, which is known as the foreland basin along the northern margin of the Alps. The part of the Molasse Basin, which can be found in the area of Steißlingen, is surrounded by the Alps in the south-east, the Black Forest in the north-west, Swabian Alb and Jura in the north and the west (Hötzl, 1996; Figure 1). The formation of the Molasse Basin was caused by the converging of the European and Adriatic plate, which started about 35 Ma ago, in the late Eocene, Tertiary. This tectonic process induced the downward movement of the Molasse Zone (Schlunegger et al., 2015; Garfunkel et al., 2010).

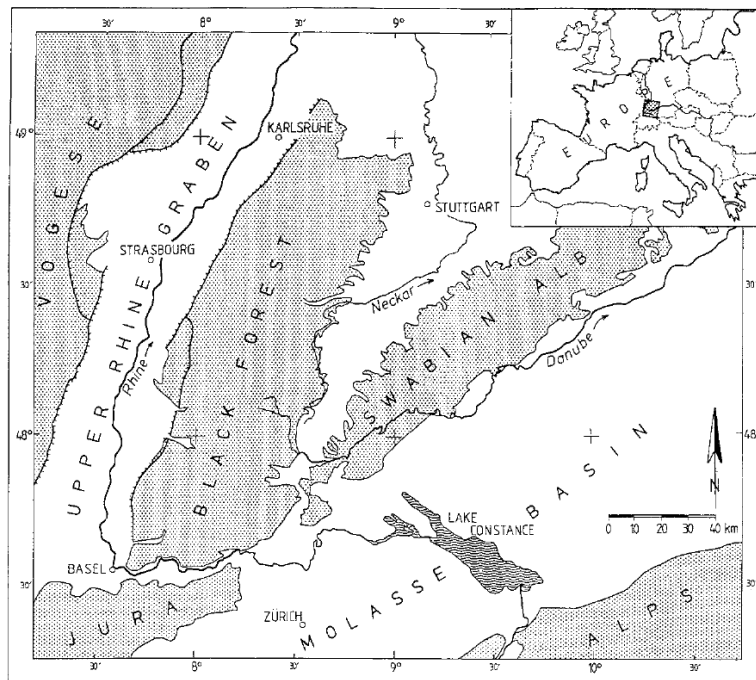


Figure 2 Geology of Southwestern-Germany, France and Switzerland (Hötzl, 1996)

During the orogenic processes of the Alps, huge amounts of tertiary sediment loads were deposited alternately, depending on the existence or absence of the Tethys, under shallow marine and fluvial lacustrine conditions through erosion within the Molasse Basin (Schlunegger et al., 2015; Eusterhues, 2000). The subdivision of the Molasse Basin from bottom to top gets

defined as follows: The Lower Marine Molasse (tUM, early Oligocene), Lower Freshwater Molasse (tUS, late Oligocene to early Miocene), Upper Marine Molasse (tOM, early Miocene) and Upper Freshwater Molasse (tOS, middle to late Miocene) (Garfunkel et al., 2010). The molasse basin gets overlain by Pleistocene layers which were formed during the glacial periods of Mindel, Riß and Würm (BGR, 2007). The tUS consists of marl and sandstone which possesses an alternating stratification, whereat the tOM mainly comprises sands and marls, mostly bearing glauconite as well as bivalves (Eusterhues, 2000). The tertiary layers of the tOS are deposited within the surrounding area of Steißlingen, yet do not occur in the zone of Lake Steißlingen according to LGRB (Landesamt für Geologie, Rohstoffe und Bergbau) (2017). The geological layer of tUM does not appear in the area of Steißlingen.

tUS cannot be found in the very circumference of Lake Steißlingen due to erosion processes. The overlain layers of the Molasse basin were formed by the ensuing quaternary period, more precisely within the Würm phase of the Rhine glacier. Characteristic settings of glacial activity such as ground – and terminal moraines with its related gravel terraces and dead ice holes appear in the landscape of Steißlingen (Peschtrich, 2005)

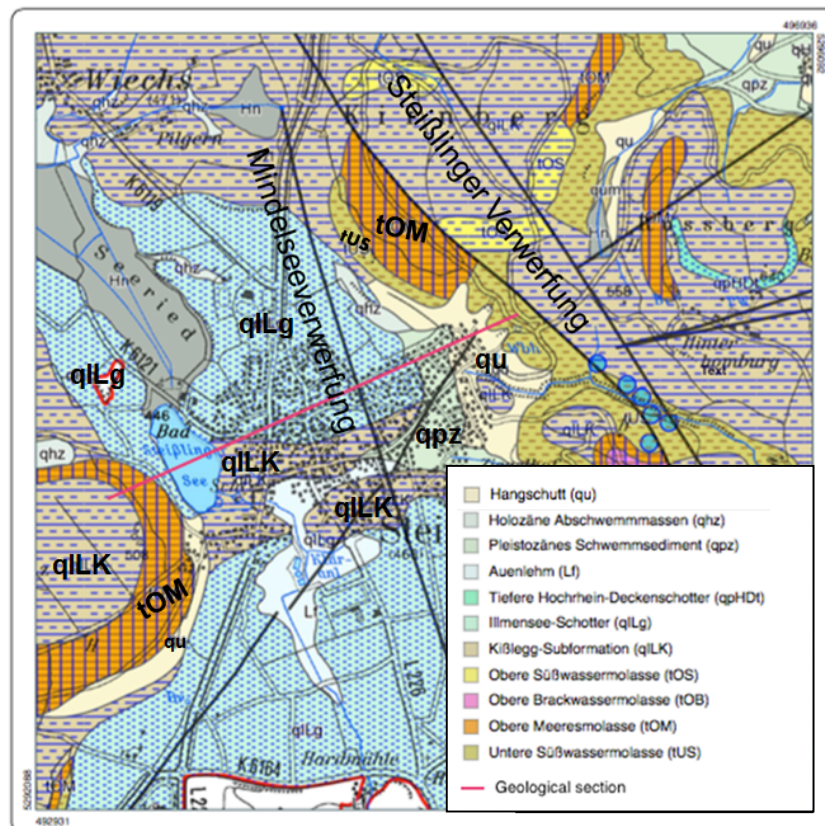


Figure 3 Geological map of the research area Steißlingen (LGRB, 2017). The denomination and interpretation of the faults is based on the study of Barnikol-Schlamm (1994).

The survey area indicates a geomorphological setting of a NW-SE running glacier tongue that was formed by the pre-existing Rhine glacier (Peschtrich, 2005).

Therefore, a prerequisite for the formation of Lake Steißlingen was the deposition of a block of dead ice, which can be clearly perceived through the lake's steep margins and its location dominated by the Rhine glacier during the Würm period (Eusterhues, 2002, 2000; Kürfgen, 1999). When regarding the structural geology, four different faults can be distinguished in the tectonical setting of Steißlingen (LGRB, 2017; Figure 3). Observations show that north-easterly of Steißlingen (Kirnberg) two faults with an offset of 50 m between tUM and tOM, denominated as "Mindelseeverwerfung", strike in NW-SE direction (Barnikol-Schlamm, 1994). Another fault gets assumed according to literature that is denominated as "Steißlinger Verwerfung" and gets supposed in the southeast of Steißlingen as a potential bench of the "Mindelseeverwerfung" (Barnikol-Schlamm, 1994).

According to preliminary, geological observations of and around Lake Steißlingen, which mainly comprises tOM, tUM and Würm layers, following lithologies get defined by LGRB (2017) (Figure 3) from bottom to top:

Pleistozänes Schwemmsediment (qpz):

- Sediments with various grain sizes and lithologies, which is dependent on the present and deposited substrates in its adjacencies
- Mostly stratified
- Extremely low permeability, due to "HK50-Vorschlag" in "Hydrogeologie-Einführung in die Allgemeine und Angewandte Hydrogeologie" (Hölting et al., 2013) the k_f -value is about $1 \cdot 10^{-10}$ m/s to 10^{-9} m/s
- No aquifer type defined
- Hydrogeochemical type or rock: calcareous/siliceous (LUBW, 2017)

Hangschutt (qu):

- Debris
- Mostly clayey
- Partly solifluction
- Alluvial gravel
- Landslides
- At hillside toe often interlocked with alluviums
- Low permeability, no aquifer type defined, due to "HK50-Vorschlag" in "Hydrogeologie-Einführung in die Allgemeine und Angewandte Hydrogeologie" (Hölting et al., 2013) k_f -value is about $1 \cdot 10^{-6}$ m/s to $1 \cdot 10^{-5}$ m/s
- Hydrogeochemical type of rock: calcareous/siliceous

Illmensee Schotter (qILg):

- Fluvial gravels and sands formed by a glacier advance
- Locally deposited diamicts, belonging to „Äußere Jungendmoräne“ and „Altmoränen-Innenwall“ (old drift moraine)
- High permeability, defined as porous aquifer type, due to “HK50-Vorschlag” in “Hydrogeologie-Einführung in die Allgemeine und Angewandte Hydrogeologie” (Hölting et al., 2013) kf- value is around $1.2 \cdot 10^{-5}$ m/s to $2.3 \cdot 10^{-3}$ m/s

Kißlegg Formation (qILK):

- Diamicts
- Gravel
- Sands and fine sediments originate from alpine and local areas during glacier advance of Rhine glacier and formation of the „Äußere Jungendmoräne“
- Moderate permeability, alternating sequences cause alternating aquifer type between aquitard and aquifer, due to “HK50-Vorschlag” in “Hydrogeologie-Einführung in die Allgemeine und Angewandte Hydrogeologie” (Hölting et al., 2013) kf- value for Kißlegg Formation is $8 \cdot 10^{-6}$ m/s
- Hydrogeochemical type of rock: calcareous/siliceous

Untere Süßwassermolasse (tUS):

- Marl stone
- Sandstone
- Partially mica and claystone
- Found in various stratifications, sometimes interlocked with layers of conglomerate, in lower section limnic limestone is deposited, often pisolitic, breccia like, presence of fossils (mainly gastropodes)
- Low permeability, defined as aquitard, due to “HK50-Vorschlag” in “Hydrogeologie-Einführung in die Allgemeine und Angewandte Hydrogeologie” (Hölting et al., 2013) kf- value is between $1 \cdot 10^{-6}$ m/s and $1 \cdot 10^{-5}$ m/s (Hölting et al., 2013).
- Hydrogeochemical type of rock: siliceous/calcareous

Obere Meeresmolasse (tOM):

- Sand
- Sandstone
- Silt
- Glauconitic
- Rich of mica
- Partly calcareous
- Sometimes obliquely bedded

- Marl stone
- „Schalentrümmerkalk“
- Coarse sand to fine gravel
- Alternating aquifer type between aquitard and aquifer, due to “HK50-Vorschlag” in “Hydrogeologie-Einführung in die Allgemeine und Angewandte Hydrogeologie” (Hölting et al., 2013) for the aquitard and aquifer are respectively $1 \cdot 10^{-10}$ m/s to $1 \cdot 10^{-5}$ m/s and $1 \cdot 10^{-5}$ m/s to $1 \cdot 10^{-2}$ m/s
- Hydrogeochemical type of rock: siliceous/calcareous

2.1.2.2 Description Geological Section

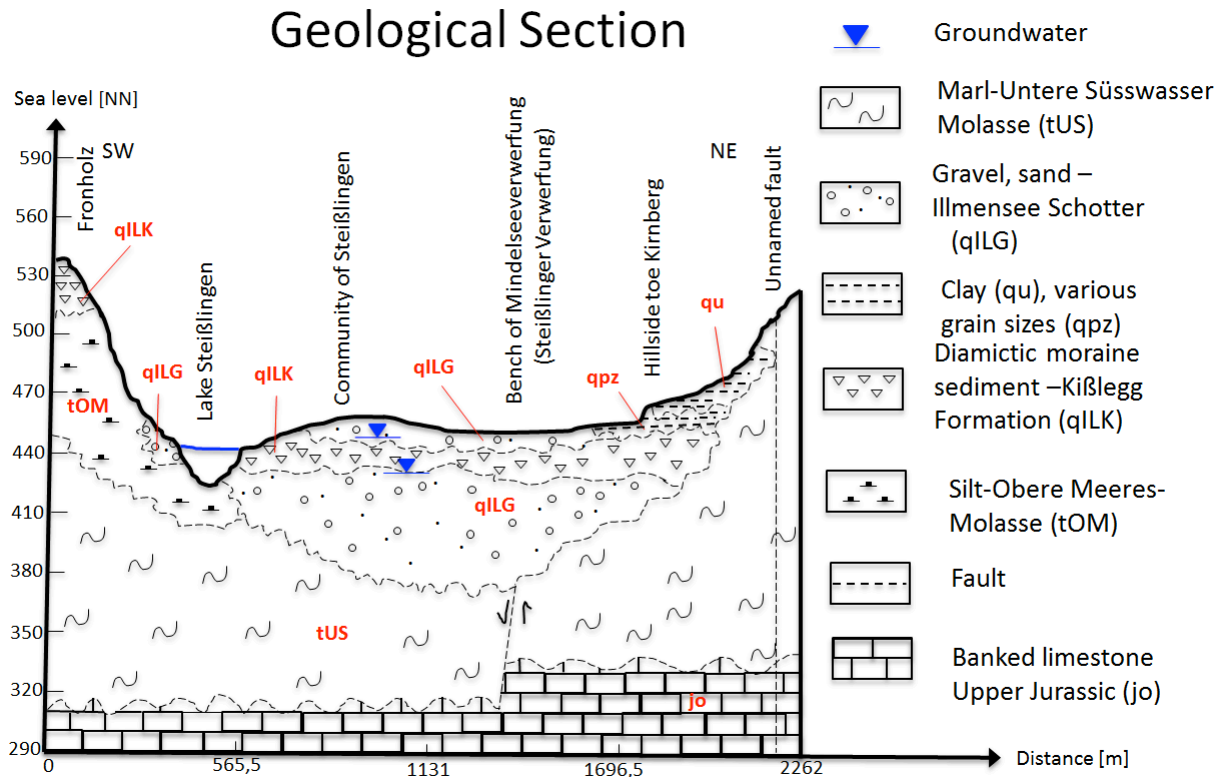


Figure 4 Geological section of the survey area Lake Steißlingen; drawn manually and digitalized by Microsoft PowerPoint integrating data of LRGB (2017), LUBW and GDI-BW (2017).

Data sets of LRGB, LUBW and GDI-BW (Landesamt für Geoinformation und Landentwicklung Baden-Württemberg) (2017) were used for the construction of a geological section that runs from Hill Fronholz in the southwest to an unnamed fault in the northeast within the area of Lake Steißlingen (See Figure 4).

The top of Hill Fronholz and the south-western side of Lake Steißlingen get characterized by its accumulation of diamictic moraine sediment Kißlegg Formation (qILK) which got formed by glacial movements (LRGB, 2017). The Illmensee Schotter (qILG) occurs in the subsurface at the north-eastern side of Lake Steißlingen and gets confined by a moderate permeable layer of diamictic moraine sediments (qILK) on top. Geological maps of LRGB (2017) exhibit a high permeability for qILG, thus it gets assumed as main aquifer layer that recharges the lake in 11.0 m-14.0 m depth (Gilfedder et al., 2018).

Farther north-east of the lake a lens of qILG crops out and runs through Steißlingen and ends shortly before the hillside toe of Kirnberg. A low permeable sequence of pleistocenic alluvial sediments (qpz) and clay (qu) crops out between Steißlinger Verwerfung and an unnamed fault.

Below the quaternary sections at the south-western side of Lake Steißlingen, a layer of tOM with an alternating stratification of aquiclude and aquifer and a thickness of 30 m to 60 m gets assumed (LUBW, 2017). Due to literature and core profiles of the surrounding area, it is known that tUM sediments are just below tOM whereat the upper end of tUM was interpreted to start at a height of about 460 NN and gets defined as aquiclude (Garfunkel et al., 2010; LUBW, 2017). The tUM is not present within this geological section due to assumption of erosion processes in the past. tUS occurs within the whole geological section between SW and NE, assumed to be at a sea level between 290 m to 440 m (LUBW, 2017). The geological observations in the area of Steißlingen indicate that the Late Jurassic formation builds up the fundament of the subsurface and gets supposed in around 300 m depth (Bertleff, 2005). An offset of 50 m, similar to the Mindelseeverwerfung, gets assumed for the fault between tUS and tOM.

2.1.2.3 Limnological Setting

According to measurements of LUBW (2014) Lake Steißlingen has a water volume of 1152286 m³ during average water level of 445.56 NN and a maximum depth of 21.4 m about 150 m northerly of the southern shore.

The adjacent land use and vegetation of Lake Steißlingen is defined as “Grünland”, “Streuobst”, “Laub- und Nadelholz”, “Ackerland” and “Siedlungsfläche” (Figure 5). Lake Steißlingen is a private property but gets used for human activities such as bathing on the north-east shore side and fishing farming (Fig. 5; Wolf, 1994).

In the circumference of the research area two drainage channels, that are responsible for the low hydrological surface input of the lake, are situated in the northern (Seeriedgraben) and the eastern (Drainagegraben) side (Figure 5).

Moreover, an artificial outflow at the south eastern side of the lake (Figure 5) was constructed during the last century that subsequently flows into Radolfzeller Aach around Singen and finally discharges into Lake Constance farther south (Wolf, 1994). Figure 5 shows the surface catchment area of Lake Steißlingen with 2 km² is small when comparing it to other lakes in this area such as Lake Constance and a surface catchment area of 11500 km².

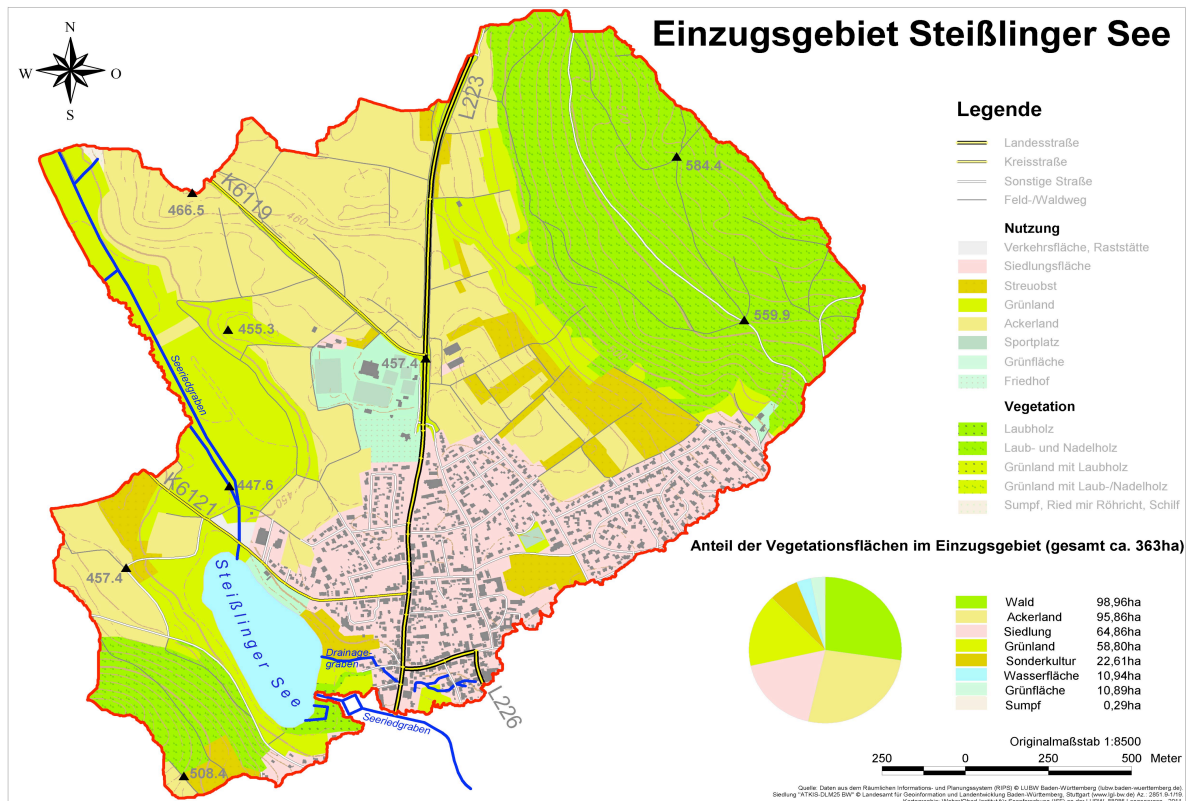


Figure 5 Surface catchment area of Lake Steißlingen (Compiled by LUBW (Obad) copyright by LUBW Baden-Württemberg based on "räumlichen Informations- und Planungssystem" (RIPS) and Siedlung „ATKIS-DLM25 BW“ copyright Landesamt für Geoinformation und Landentwicklung Baden-Württemberg, Stuttgart (www.lgl-bw.de) Az 2851 (2011))

Lake Steißlingen gets classified as mainly meromictic, and therefore presumes that its deepest layer never mixes with the layers above, which is due to a strong density difference between epilimnion and hypolimnion (Spirkaneder, 2016). According to Eusterhues (2000) the unchanging density stratification of the lake is caused by external factors such as ice layers, warm summers and non-turbulent weather conditions rather than biological productivity (Eusterhues, 2000). Through observations the stratification of Lake Steißlingen was subdivided as follows: Epilimnion until 4 m depth, thermocline, also metalimnion, in a depth between 6-8 m and the hypolimnion, which lies at a depth of 8 m to 21.4 m and was determined as a low oxygen containing layer (Spirkaneder, 2016).

Due to minimal inflow of surface water, but present recurring biological productivity in the epilimnion, it is believed that the main number of nutrients enter lake Steißlingen through groundwater inflow (Eusterhues, 2000). Therefore, Eusterhues (2000) assumes that the stratification and mixture pattern of the lake determines the distribution of nutrient matter and hence the eutrophication status, which is defined as “mesotroph” (LUBW, 2014). Spirkneder

(2016) used ^{222}Rn measurements for tracing and locating groundwater inflow to Lake Steißlingen and reveals that high ^{222}Rn activities prevail in the hypolimnion at the middle and north to north-eastern part of the lake at a depth of 11 to 14 meters. The accumulation of ^{222}Rn rather indicates groundwater inlet areas than punctual groundwater incomes which get caused by the combination of diffusion and the disability of ^{222}Rn to degas immediately due to an overlying denser thermocline (Spirkaneder, 2016). However, a large-area of groundwater income gets excluded, whereas a punctual groundwater inlet gets presumed due to unremarkable ^{222}Rn activities in the remaining part of the lake (Spirkaneder, 2016). Conforming to Gilfedder et al. (2018) Lake Steißlingen indicates a considerable groundwater ratio of 70 % and a recharge rate of 11 l/s in the months of April and June. This furthermore, can be crucial, among other things, in terms of water balance, hydrochemistry, isotopic composition and the circulations in the water body (Boehrer et al., 2008; Hofmann et al., 2011; Spirkaneder, 2016).

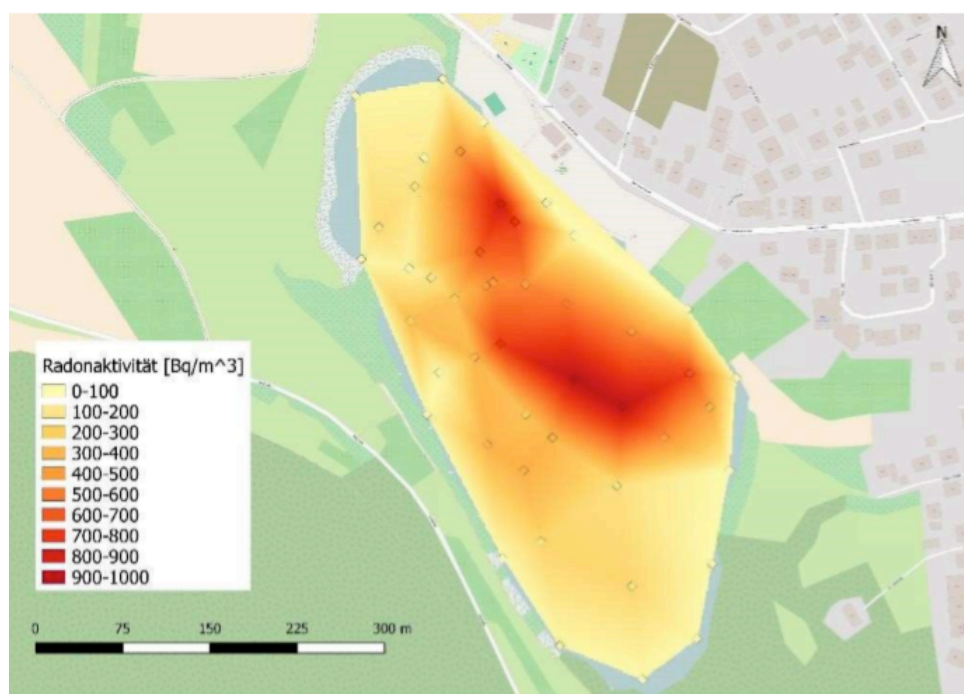


Figure 6 Interpolation of measured ^{222}Rn activities and assumed groundwater inlets (black mark) at the bottom of Lake Steißlingen (Spirkaneder, 2016)

Measuring campaigns concerning Lake Steißlingen were carried out in different intervals by LUBW (2014) during the years of 2014 (February - December) and 1987 (February, April – November) (See Figure 7). Hereby annual average values were calculated for several parameters during 1987 and 2014.

In 2014 the average water temperature of Lake Steißlingen is 11.5°C, the dissolved average oxygen content was recorded to be 6.8 mg/l, a mean water hardness value of 5.4 ½ mmol/l was measured and average concentrations of calcium and magnesium were 84 mg/l and 24 mg/l, respectively (See Figure 8). These results show slightly increased values when comparing them to 1987. Moreover, the concentrations of chloride and sulphate in 2014 indicate enhanced values compared to 1987 and other small lakes in Baden-Württemberg which is mainly due to salt spreading in winter (LUBW, 2014).

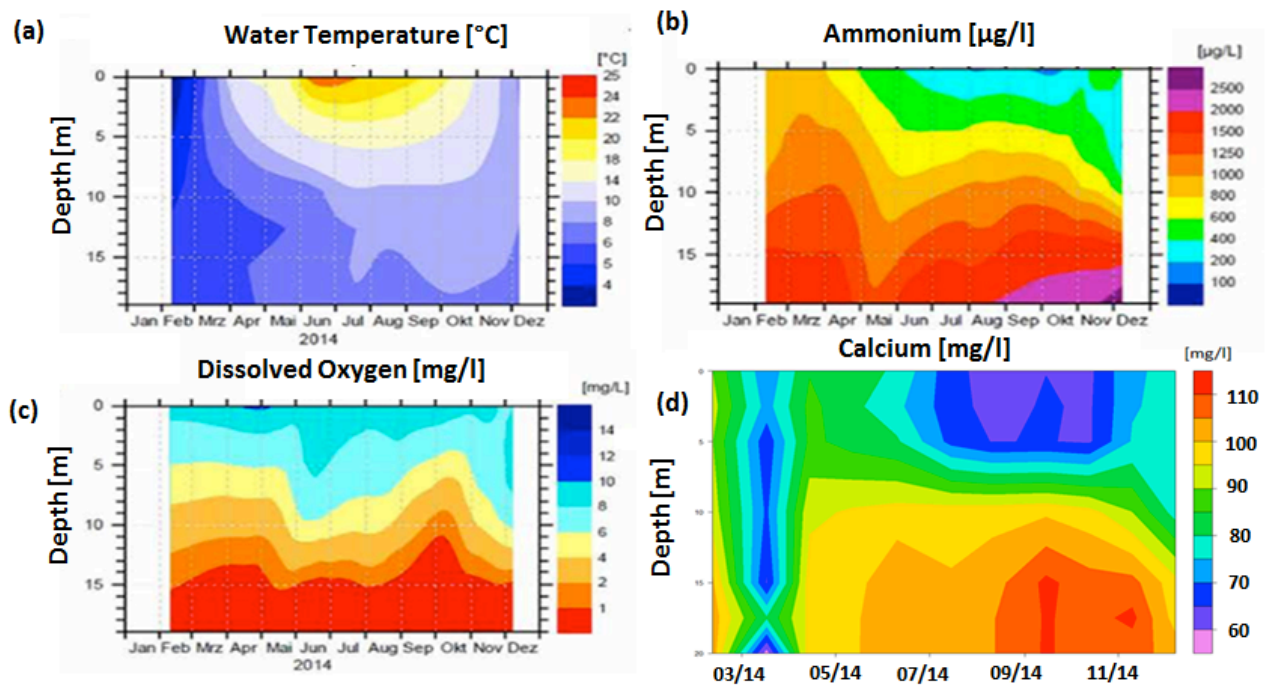


Figure 7 Isopleth map of (a) water temperature (b) ammonium (c) O₂ and (d) Ca²⁺ in 2014.

In 2014 a data evaluation according to seasonal fluctuations of physical-chemical parameters was carried out by LUBW (2014). Due to a high difference in water temperature with depth in summer, the stratification indicates a higher stability compared to winter (See Figure 7).

Steißlinger See Parameter	Einheit	1987 (Feb, Apr-Nov)*	2014 (Feb-Dez)* ¹
Vol.-gew. Jahresmittel			
Temp.	°C	9,7	11,5
Sichtt.	m	2,1	3,5
O ₂	mg/l	6,7	6,8
pH-Wert		7,8	7,9
Leitf.	µS/cm	563	590
SBV	mmol/l	4,8	5,3
Härte	1/2 mmol/l	6	6,4
PO ₄ -P	µg/l	0,8	1,8
gelöst P	µg/l	3,2	5,9
gesamt P	µg/l	29	19
NO ₃ -N	µg/l	561	745
NH ₄ -N	µg/l	875	776
an.-N	µg/l	1472	1642
SiO ₂ -Si	µg/l	2888	4450
Fe	µg/l	43	9,5
Mn	µg/l		11
Cl	mg/l	29	33
SO ₄	mg/l	40	43
Ca gel.	mg/l		84
Mg gel.	mg/l		24
Li gel.	µg/l		8,5
Ba gel.	µg/l		102
Sr gel.	µg/l		529
As gel.	µg/l		<0,5 (BG)
Al gel.	µg/l		3,8* ²
Zn gel.	µg/l		1,3* ²
Cu gel.	µg/l		0,8
U gel.	µg/l		17
Chl a (0–10 m)	µg/l	5,6	8,9

* Juli, November: zwei Messungen pro Monat vorhanden

*¹ Metalle: nur April, August

*² zur Berechnung des Mittelwerts wurde die halbe Bestimmungsgrenze verwendet, wenn einzelne Messwerte unter der Bestimmungsgrenze liegen.

Figure 8 Physical-chemical parameters of Lake Steißlingen in 2014 and 1987 (LUBW, 2014)

According to seasonal fluctuations of dissolved oxygen a significant descent from 10 mg/l down to 0-1 mg/l in the hypolimnion between 0 m and 15m-20 m was observed within Lake Steißlingen the entire year (See Figure 7; LUBW, 2014). In the months from April 2014 to September 2014 increased oxygen concentrations compared to the surface water were recorded at a depth of around 5m due to high photosynthetic activity (LUBW, 2014). According to Spirkaneder (2016) the locations of incoming groundwater in Lake Steißlingen anoxic conditions and significant values of methane, nitrite and iron were measured.

When regarding calcium content in March 2014 a homogeneous concentration of 65 mg/l to 80 mg/l was observed within the entire water column. Moreover, noticeable low calcium contents (60 mg/l-70 mg/l) were recorded in the upper 5m of Lake Steißlingen between July 2014 and November 2014 (LUBW, 2014) (See Figure 7).

Referring to N-NH_4^+ increased concentrations were recorded in the hypolimnion of the lake throughout the entire year (LUBW, 2014) (See Figure 7). The alkalinity value measured for Lake Steißlingen indicates a good buffer capacity with a stable pH of 8 (LUBW, 2014).

2.2 Groundwater Detection of Lake Steißlingen

This study comprised measurements and samplings in regular intervals within a defined measuring grid and along determined depth profiles in the period between June 2016 and September 2017 (June 2016, November 2016, March 2017, July 2017, September 2017) (Figure 9). In June 2016 additional physical- and chemical data was used, which was actually measured and evaluated for a study of Uni Bayreuth (sampling points SS2, SS4 and SS5).

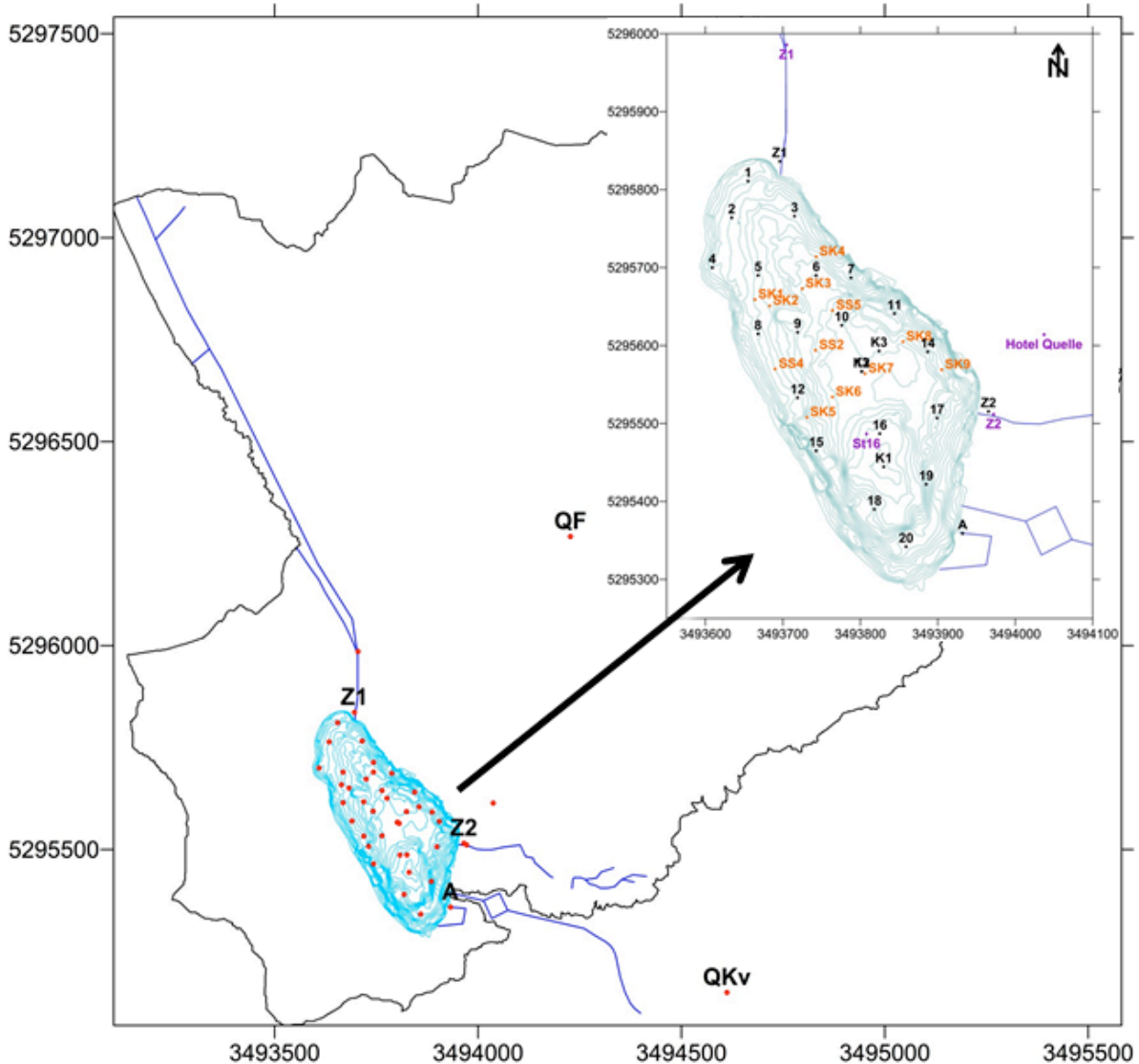


Figure 9 Defined measuring Grid in Gauß-Krüger coordinate system with black sampling points (data LUBW), orange sampling points (University of Bayreuth) and purple sampling points (data GFZ Potsdam that gets involved in chapter 4) (constructed with Surfer®)

The depth profiles were taken with a water sampler on a rubber boat at locations where groundwater inlets were assumed as well as at the shore zones of the lake (See Figure 9). Besides sampling the water of the lake, also its surface outlet A (Abfluss) was examined

The second end members used are the wells QF (Quelle Friedhof) and QKv (Quelle Kreisverkehr) that represent the presumed groundwater composition.

The third end members are the surface inlets Z1 (Zufluss 1) and Z2 (Zufluss 2), which get excluded for the calculation of groundwater ratio due to its minimal impact on Lake Steißlingen (LUBW, 2014). Simultaneously to regular sampling, a permanent measuring station was installed for depth profile measurements along K1, which also represents the deepest possible point within Lake Steißlingen.

Apart from a big data set, the survey also comprises some measurement lacks. In November 2016 QF could not be sampled due an inhibition of the well. The sampling of Z1 (Zufluss 1) and Z2 (Zufluss 2) (See Figure 9) was dependent on its availability of water and thus the seasonal desiccation of the channel. Therefore, no samples were taken at Z1 and Z2 in July 2017. No data is available for Z1, Z2 and A as well in June 2016, because it was not yet part of the measuring campaign. In the month of November 2016, the measurement of oxygen content was not possible due to a defect of the CTD, therefore it was calculated by known oxygen saturation.

For a better insight to the mixture path and behavior of Lake Steißlingen the determination of water quality, seasonal fluctuations, the distribution of dissolved oxygen and certain physical-chemical-isotopical parameters was carried out. Therefore, physical measurements were done in situ with a CTD and measuring probes, followed by a hydro chemical analysis in the laboratory at ISF Langenargen. A detailed description of the methodologies and techniques that were applied within this study will be handled in chapters 2.2 to 2.4. The results of all measurements get described in chapter 3 which were all rounded to a feasible decimal place.

2.2.1 Measurement of in-situ physical-chemical parameters (CTD)

A part of physical-chemical parameters was measured with a “Sea & Sun CTD 90 m Memory Probe”, where physical and optical sensors can be connected. The CTD equipment is quite sensitive and thus a sensor protection cage that surrounds the whole instrumentation was used. The ascertainment of water depth was calculated with the pressure values that were measured with the CTD and a conversion factor of 1.01955. The sensors and instruments were fixed either on the bottom of the memory probe and were applied in “offline mode” for the parameter measurements at Lake Steißlingen.

For the water temperature (T), which was measured in Celsius [°C] with the temperature sensor SST Pt100 by Sea & Sun GmbH, that is a resistor out of platinum situated in a ceramic carrier,

was applied. The measurement principle for temperature measuring instrument is based on the temperature dependent resistance of the platinum element. The sensors accuracy lies within $\pm 0.005^{\circ}\text{C}$ and its calibration is done automatically by the instrumentation.

In order to identify electrical conductivity (EC) in $[\mu\text{S}/\text{cm}]$ a “SST 7-pole” conductivity cell by Sea & Sun GmbH was utilized and basically measures the currency that flows through the water sample. The accuracy of the probe is $\pm 3 \mu\text{S}/\text{cm}$ and for its calibration potassium chloride with known conductivity was used.

For the determination of oxygen (O_2) measurements were done on the one hand in [%], which shows oxygen saturation, and on the other hand in $[\text{mg}/\text{l}]$ that indicates dissolved oxygen. In November 2016 the oxygen sensor of the CTD was not completely functioning, so oxygen saturation values were converted from [%] to oxygen content values in $[\text{mg}/\text{l}]$ with following equation (Baur, 1997):

$$\text{O}_2 [\text{mg}/\text{l}] = \text{O}_2 [\%] \cdot (0.0048 \cdot T^2 - 0.3609 \cdot T + 14.085) / 100$$

T=Temperature in situ: $\text{O}_2 [\%]$ =oxygen saturation; $\text{O}_2 [\text{mg}/\text{l}]$ =oxygen concentration

Oxygen saturation and thus dissolved oxygen is inversely proportional to temperature (Galler, 2017) and was verified with a fast-optical oxygen sensor by Sea & Sun GmbH. The measurement principle is based on a red-light excitation that shows luminescence within the NIR (near infrared), whereat oxygen molecules attach to some of the micro molecules within the probe and get subsequently excited by an orange light. Hereby micro molecules without an attached oxygen molecule respond with a dark red fluorescence light whereat the ones attached to an oxygen molecule attenuate the fluorescence light. Furthermore, the attenuated dark red fluorescence light gets detected and increases when oxygen increases. Due to installed software included at the logger an automatic calibration is given and the probe shows an accuracy of $\pm 2\%$.

To determine the turbidity, a “Seapoint Turbidity Meter” of Ocean Instruments Ltd. was applied, which basically measures the scattered light from suspended particles within a small volume in the liquid in Formazin Turbidity Units (FTU). Within the equipment light gets emitted in a circumference of 5 cm and subsequently gets scattered by suspending particles, which is proportional to the turbidity. The instrumentation gets calibrated internally by the manufacturers and its accuracy shows a deviation of $<2\%$ within 0-750 FTU.

A chlorophyll A sensor with “Chlorophyll in vivo Blue excitation (concentration of minimum detection limit: $0.03 \mu\text{g}/\text{l}$) and Red excitation (concentration of minimum detection limit: $0.3 \mu\text{g}/\text{l}$)” was utilized for the examination of the chlorophyll A content. The principle of the method is the phenomena of fluorescence whereat the photon of a certain wavelength gets adsorbed by a chlorophyll A pigment within the phytoplankton and subsequently emits fluorescent light with a lower energy state compared to the incoming light, which finally gets detected by the sensor that measures the intensity of fluorescence and thus chlorophyll A concentration, which shows a

direct proportionality. The sensor gets calibrated internally by the company and shows an accuracy of 2%.

For the determination of physical-chemical parameters at sampling points around Lake Steißlingen (QKv, QF, Z1 and Z2) on the one hand an YSI Professional Optical Dissolved Oxygen (Pro ODO) instrument was applied, which measures oxygen saturation, dissolved oxygen and temperature in [%], [mg/l] and [°C] with an accuracy of $\pm 2\% \pm 1\%$, $\pm 0.2^\circ\text{C}$, respectively. On the other hand, a WTW ProfiLine Conductivity Meter LF 197 electrical conductivity probe was used for the verification of electrical conductivity in [$\mu\text{S}/\text{cm}$] that was calibrated with a conductivity Mettler Toledo standard solution 1413 $\mu\text{S}/\text{cm}$ at a water temperature of 25°C and has an accuracy of $\pm 0.5\%$.

2.2.2 Depth specific Sampling within Lake Steißlingen

For the seasonal quantification and identification of groundwater inlets, a depth specific sampling in combination with a subsequent analysis in the laboratory was carried out in regular intervals between July 2016 and September 2017. Hereby for all sampling points bottom water samples were taken and for some selected points a complete depth profile with an interval of 5m was recorded. During the year of 2016 less samples were taken, compared to 2017 when the measuring campaign was expanded.

Firstly the preparation for the sampling, that includes washing and labeling the sampling bottles according to its observing parameters, was done. Afterwards the samples were taken in specific depths along the measuring grid with a rubber boat equipped with a Hydro-Bios PWS water sampler fixed on a winch. Shortly before sampling the bottles were rinsed out with sample two times to avoid contamination and thus falsifying the results. Then the water was filled up in prepared PE bottles, whereby a 250 ml bottle was used for the ensuing titration, 500 ml were sampled for the ion chromatograph analysis in the laboratory and a 100 ml PE bottle was filled up for the isotopic measurement. After this step it was necessary to cool the samples as soon as possible to avoid a warming up of the water, and thus changing living conditions for microbes, that could change the results.

The preparation for the ion chromatograph was done in the laboratory right after fieldwork at the end of the day. Therefore, the according water samples were filtered with a filter cartridge and Sartorius 11106--47N membrane filter ($0.45\ \mu\text{m}$) cellulose acetate and were finally filled up for cation and anion measurement in reaction tubes (Sarstedt or Corning®) with a volumetric capacity of 50 ml. Subsequently the tubes for the cation measurement were acidified with 2 mol/l HNO_3 (100 μl) to avoid decomposition of NH_4 . Finally, a part of the samples, which had been prepared for measurement, were stored at a temperature of 4°C .

2.2.3 Determination of physical-chemical Parameters through Titration

One part of the laboratory work was done with a Metrohm 905 Titrando, equipped with an 814 Sample Processor and three Metrohm 800 Dosinos, for the measurement of physical-chemical parameters. For the titration stored samples with a volume of 250 ml were used for the determination of electrical conductivity, pH, water hardness and alkalinity (TA), whereat temperature was only measured for referencing the results.

After the electrodes got equilibrated with deionized water for titration, a standard solution was measured, followed by a subsequent preparation through calibration.

The temperature was measured in [°C] by a Metrohm Pt1000 sensor that is included in the pH- and EC electrode and shows an accuracy of 0.1 °C.

In order to determine EC, a Metrohm 856 Conductivity Module in combination with a Metrohm 5-ring conductivity measuring cell [6.0915.100], equipped with a Metrohm Pt 1000 temperature sensor, was applied. The parameter gets measured in [$\mu\text{S}/\text{cm}$] with an accuracy of $\pm 1\%$, which was tested before with a 0.001 mol/l potassium chloride standard solution to relativize possible measuring errors. In principle the equipment measures the electric resistance of an applied electrical voltage between two platinum electrodes submerged in the liquid to be examined. The electrical conductivity depends on water temperature and is directly proportional to it. So, all measured values firstly get converted to a reference temperature of 20°C, followed by a conversion to a reference temperature of 25°C. Therefore, following equations were used for referencing and thus a uniform and comparable resulting data set:

$$\text{EC}(20) = \text{EC}_{\text{roh}} / (0.02 + 1 \cdot (T - 20))$$

$$\text{EC}(25) = \text{EC}_{\text{roh}} / (0.02 + 1 \cdot (T - 25))$$

The pH is measured with a Metrohm LL-Aquatrode plus electrode equipped with a Pt1000 sensor, which was firstly calibrated with a Metrohm buffer solution of pH 4 and pH 9. The equipment, that indicates an accuracy of 0.01, measures an electrical potential difference in [mV], whereat an electrical voltage is applied within the pH electrode, and gets then converted into pH unit.

The parameter of alkalinity gets defined as the quantitative ability of an aqueous solution to neutralize an acid (Appelo et al., 2005). It is therefore the concentration of species, which is removed from the system, before the pH changes in response to the acid gradually added during titration. The value of alkalinity increases with the buffer capacity of the solution.

A Metrohm 800 Dosino, Metrohm LL-Aquatrode plus and a Metrohm 802 stirrer was used for the ascertainment of alkalinity (acid capacity) TA in [mmol/l].

After the calibration of the pH electrode with a Metrohm buffer solution of pH 4 and pH 9, the water samples ($V=100$ ml) were stirred for simultaneous pH measurements followed by titration. For that a 0.1 M HCl was used until the pH end point of 4.3 was reached, whereat from this point on all HCO_3^- will be converted to H_2CO_3 , which causes an increase of H^+ linearly to volume of

acid/ H^+ added. For the determination of TA the volume of consumed acid was measured in [mmol/l] and the alkalinity was recorded in [mVal].

The water hardness was measured in [$\frac{1}{2}$ mmol/l]. To analyze the water hardness, the pH firstly gets increased with a $CuNH_4$ solution up to 10 in combination with a titration of an EDTA solution ($c(Na_2EDTA)=0.1$ mol/l). This enables the formation of complexes with metallic ions, such as Ca^{2+} and Mg^{2+} and leads to the determination of water hardness which gets calculated and converted by a software of the instrumentation.

2.2.4 Determination of Anions and Cations with Ion Chromatography Measurement (IC)

For the cation (Ca^{2+} , Mg^{2+} , Na^+ , K^+ , NH_4-N) - and anion (Cl^- , SO_4^{2-} , NO_3^- -N) -analysis of the water samples a Metrohm 850 Professional IC combined with a 858 Professional Sample Processor was applied and determined in [mg/l] and [μ g/l]. For the implementation the IC got calibrated with an appropriate standard solution of the ions to be examined, which is made up of mother liquids with known concentrations of cations and anions prepared with element standards of Bernd Kraft GmbH and VWR PROLAB. Subsequently the samples were filled up in 8 ml tubes and put into the auto sampler wherefrom water samples get injected. For the determination of the anions an eluent solution comprising 64.0 mmol/l Na_2CO_3 and 20 mmol/l $NaHCO_3$ is used. To measure cations, its sample firstly got acidified with HNO_3 ($c=1$ mol/l) and then a pyridine-2,6-dicarboxylic acid functioning as an eluent was applied. The analysis of anion and cation samples were done separately, wherefore each got mixed up with an eluent (anion eluent: solution out of 64 mmol/l Na_2CO_3 and 20 mmol/l $NaHCO_3$; cation eluent: HNO_3 1 mol/l). Together, the eluent blended with the sample, forms the mobile phase, which gets transported to the separation column that temporarily separates the solved ions based on different affinities between the resin on the column and the anions/cations to be analyzed. Subsequently the anions/cations dissolve again which is caused by the eluents chemical exchange property and depends on the ions retention time on the column. The method of IC measurement is based on relative affinities between anions/cations and the resin on the column, the retention time of different ions on the column and when the ions get eluted by the eluent ion. Subsequently, the detector measures the conductivity of the eluent that passed through, by presence of each separated species a conductivity change occurs and its concentration and retention time signals get recorded.

To ensure that measurement conditions stay constant, standards and blanks were measured simultaneously with the samples in regular intervals. The measurement of cations and anions (Na^+ , NH_4-N , K^+ , Ca^{2+} , Mg^{2+} , Cl^- , NO_3^- -N, SO_4^{2-}) show following accuracies, respectively: $\pm 1.1\%$, $\pm 13.0\%$, $\pm 3.4\%$, $\pm 1.7\%$, $\pm 0.8\%$, $\pm 0.8\%$, $\pm 15.3\%$, $\pm 0.5\%$, $\pm 2.1\%$.

2.2.5 Determination of $\delta^{18}\text{O}$ and $\delta^2\text{H}$ Isotopes with a Laser Spectrometer

Water consists of hydrogen and oxygen, whereat each element indicates three isotopic configurations (Kralik et al., 2015). Known oxygen isotopes are ^{16}O (most abundant one), ^{17}O and ^{18}O . The element hydrogen shows ^1H (most abundant one), ^2H (Deuterium) and ^3H (Tritium). The isotopic ratio of a water sample is dependent on its origin and passed physical processes, such as evaporation or precipitation in a lake (Hofmann et al., 2011; Kralik et al., 2015). For this study isotopic ratios (R_{Sample} referring to $^2\text{H}/^1\text{H}$ or $^{18}\text{O}/^{16}\text{O}$) got compared with an internationally determined standard Vienna standard of marine ocean water (R_{VSMOW}). The deviation between R_{Sample} and R_{VSMOW} in [‰] gets defined as δ and calculated as follows:

$$\delta[\text{‰}] = \left(\frac{R_{\text{Sample}}}{R_{\text{VSMOW}}} - 1 \right) * 10^3$$

Relevant isotopic parameters of this master's thesis are $\delta^{18}\text{O}$ and $\delta^2\text{H}$ which is used for localizing and tracing groundwater dynamics. The isotopic signature of $\delta^{18}\text{O}$ and $\delta^2\text{H}$ can be positive or negative for which following is applied:

$\delta < 0$ (enriched in light isotopes)

$\delta > 0$ (enriched in heavy isotopes)

Halder et al. (2013) emphasizes natural isotopic tracer methods compared to artificial tracers because of its simple, cheap and non-environmentally-disturbing application.

Therefore, $\delta^{18}\text{O}$ and $\delta^2\text{H}$ (δD) were used for a first approximation of the binare mixing of groundwater with lake water in the period of 2016/2017 and got calculated with following equation:

$$X_L = \left(\frac{\delta^{18}\text{O}_{\text{Lake sample}} - \delta^{18}\text{O}_{\text{Lake water}}}{\delta^{18}\text{O}_{\text{Groundwater}} - \delta^{18}\text{O}_{\text{Lake water}}} \right) * 100$$

$\delta^{18}\text{O}_{\text{Lake sample}}$ refers to every water sample taken, $\delta^{18}\text{O}_{\text{Lake water}}$ shows results of surface water samples or surface runoff and QF represents $\delta^{18}\text{O}_{\text{Groundwater}}$.

The measurement for the determination of the isotopic composition was carried out by JR-AquaConSol in Graz, whereat a L1102-i from PICARRO CRDS wavelength-scanned cavity ring-down spectroscopy system (WS-CRDS) was applied. For the isotopic analysis an automatic measurement interval of 9 min/sample in high precision laboratory mode was predefined. After measurement preparation the water samples were put into a PAL auto sampler from Leap Technologies, Carrboro, NC, USA, where about 1.8 μl of each sample got injected three times into the evaporator, which was heated up to 110°C before and where then H_2O (l) was converted into H_2O (g). Subsequently H_2O (g) got mixed up homogeneously with a N_2 processor gas which gets carried into the Cavity measuring cell, followed by a multiple measurement process. The

program then calculated the mean value for each sample measured. Simultaneously the equipment got flushed with N₂ as preparation for the next injection process.

One sampling sequence comprised the measurement of 54 samples and 10 standards. Afterwards the results got normalized to the international VSMOW scale that based on specific isotopic water standards „LIMS“(Labor Information Management System). The analytical precision for stable isotope measurements in water is ± 0.8 ‰ for δD and ± 0.08 ‰ for $\delta^{18}O$ for the high precision (standard) mode.

2.2.6 Calculation of Inorganic Carbonic Species with CO₂sys

To gain the parameters of dissolved CO₂ and CO₃²⁻ the CO₂ calculation system “CO₂sys.xls” by Lewis and Wallace (1998) was applied. CO₂sys.xls calculates two missing parameters of all parameters of the CO₂ system in water (TA; total inorganic carbon, pH and pCO₂), provided that two of these species are known.

To calculate the missing parameters in this study, the constants K1 and K2 by Millero et al. (2006) were used with given TA and pH. For the pH the NBS scale was chosen and the partial pressure of CO₂ pCO₂ was used. The input parameters for the calculation were TA, water temperature and pH, which were already measured. The salinity was assumed to be 0.2.

2.3 Seasonal Quantification and Water Chemistry through Groundwater Influence (Phreeqc)

For the determination of seasonal groundwater quantification Phreeqc Interactive 3.4.0-12927 (1999) was applied. It is a thermodynamic equilibrium model by Appelo and Parkhurst to calculate various geochemical parameters, constants and reactions in aqueous systems (Parkhurst et al., 1999). Part of the master's thesis was the calculation of the saturation index (SI) of calcite and the application of inverse modelling for the determination of groundwater ratio in a sample.

For the calculation of SI_{Calcite} the major parameters of each sample, measured during the five measuring campaigns, were used for the input file template of each solution in Phreeqc (pH, T [°C], alkalinity as HCO_3^- [mg/l], dissolved oxygen [mg/l], Ca^{2+} [mg/l], Mg^{2+} [mg/l], K^+ [mg/l], Na^+ [mg/l], N(5) as NH_4^+ [mg/l], Cl [mg/l], N(-3) as NO_3^- [mg/l], S(6) as SO_4^{2-} [mg/l], ^2H [‰], ^{18}O [‰]). For the precision of the calculation, the species of $\text{NH}_4\text{-N}$, $\text{NO}_3\text{-N}$, SO_4^{2-} and alkalinity were written as N(5) as NH_4^+ , N(-3) as NO_3^- , S(6) as SO_4^{2-} and alkalinity as HCO_3^- . Another reason why alkalinity was written as “alkalinity as HCO_3^- ” is because in natural waters at a pH between 7.3-8.3 alkalinity is approximately the HCO_3^- content. When TA is written as alkalinity only, Phreeqc uses $M=1/z \cdot M_{\text{CaCO}_3}$ for the calculation instead of $M=1/z \cdot M_{\text{HCO}_3^-}$, which would falsify the results. Saturation indices are calculated by dividing the ion activity product, of the species building a certain mineral, by the thermodynamic constant of this mineral.

For the inverse modelling possible end members of a given mixing solution have to be assumed. The endmembers of our model include the average lake composition, the groundwater (QF, QKv), assumed as the main water source of the lake, and surface inlets (Z1, Z2). The known mixing solution was assumed to be the lake bottom water of each sample included, where most of the groundwater gets presumed.

To start with, input files were constructed for each month and sample included and measured (June 2016, November 2016, March 2017, July 2017 and September 2017) á 5 solutions comprising the assumed end members (average lake water, Z1, Z2, QKv and QF) and its mixing solution (Bottom water sample in different depths and months). To get plausible results for the inverse modelling calculations, non-conservative parameters of the system (dissolved oxygen, NO_3^- , NH_4^+ , partly SO_4^{2-}) were omitted. This is because the species of dissolved oxygen, NO_3^- , SO_4^{2-} and NH_4^+ experience strong concentration changes due to adsorption processes and redox reactions, which could lead to non-plausible models found by Phreeqc. Additionally, the phase of calcite and CO_2 (g) was integrated and considered in the model which could either dissolve or precipitate, even though most lakes are calcite oversaturated. The dissolution and precipitation of calcite was integrated because calcite was already proven in the system, which

might dissolve at the bottom of the lake through bacterial respiration of organic material and its resulting formation of CO_2 . Also, the phenomenon of mixture corrosion can occur, which can happen when two slightly oversaturated solutions with different water temperatures and calcium concentrations (groundwater and lake water) mix. This mixing process can lead to an excess of CO_2 that results in calcite dissolution. Additionally, calcite can dissolve at the location of a groundwater inflow due to an increased dissolved CO_2 content originating from the aquifer. Moreover, Phreeqc depicts more plausible results, when including calcite dissolution. In June 2016 no temperature values were available for QKv and QF so they were assumed to be the same as in July 2017. Moreover, the end member of QF was not available in November 2016, so parameters were assumed to be the mean of all other months that were measured in 2016/2017. All chemical parameters were specified in mg/l thus TA^- , Ca^{2+} -, Mg^{2+} - values were converted from molar mass to mg/l.

To see if the templates of the input file are working within the applications of inverse modeling, first of all high uncertainties were assumed. The templates worked, so uncertainties were determined within a range between 0.01 and 0.8 depending on the season and the environmental conditions (not lower than the measuring accuracy). After the first try of modeling, including all end members, the solutions of surface inlets (Z1, Z2) were excluded because Phreeqc did not calculate feasible groundwater ratios. This can be explained by the fact that surface inlets indicate a relatively small catchment area and do not have a strong impact to the hydrochemistry of Lake Steißlingen due to a dry up in summer months and a low precipitation rate in winter months. For the depiction of groundwater ratio data one convenient model per sampling point was chosen as a representative because they only differ in some decimal places.

2.4 Stratification and Mixtures within Lake Steißlingen: Permanent measuring station

To quantify the stratification and mixture behavior of Lake Steißlingen, a permanent measuring station (“EnviWatch”) was developed and installed for a year at the deepest point around K1 (November 2016-December 2017). Therefore, physical-chemical parameters (temperature, EC, dissolved oxygen) were recorded every 20 minutes by EnviWatch-YSI-probes, a thermistor chain for a depth specified measurement was installed and a meteorological station (“Meteo”) was mounted on top. The “Meteo” is a multi-sensor permanent measuring station that recorded following meteorological parameters: wind velocity [km/h], air temperature [°C], air pressure [hPa], precipitation [mm] and incident solar radiation [W/m²]. The thermistor chain was equipped with 35 thermistors, including temperature sensors [°C], in intervals of 1 meter, running from the floating drum of the measuring station on top to the bottom of the lake. Moreover, the platform comprised EnviWatch-YSI-probes that measured temperature [°C], electrical conductivity [µS/cm] and dissolved oxygen [mg/l].

The automatically long-distance data transmission was realized via a programmed logger “enviLog Maxi” that transferred data through GPRS and internet to the computer.

3 Results

In this chapter, the delineation and description of physical, chemical and isotopic parameters. In June 2016 additional data was used, which is part of the SeeZeichen project and in cooperation with ISF. All measured data points that are plotted on the graphs, are marked in the sampling map (See Figure 10). For the sampling points of surface inlets (Z1, Z2), surface outlets (A) and potential groundwater samples (QKv, QF) a realistic estimated depth was assigned to simplify the comparison of the results. The decision if sampling points QKv, QF, Z1, Z2 and A get delineated on the graph, was dependent on whether they were occurring within or close to the value range of the lake samples.

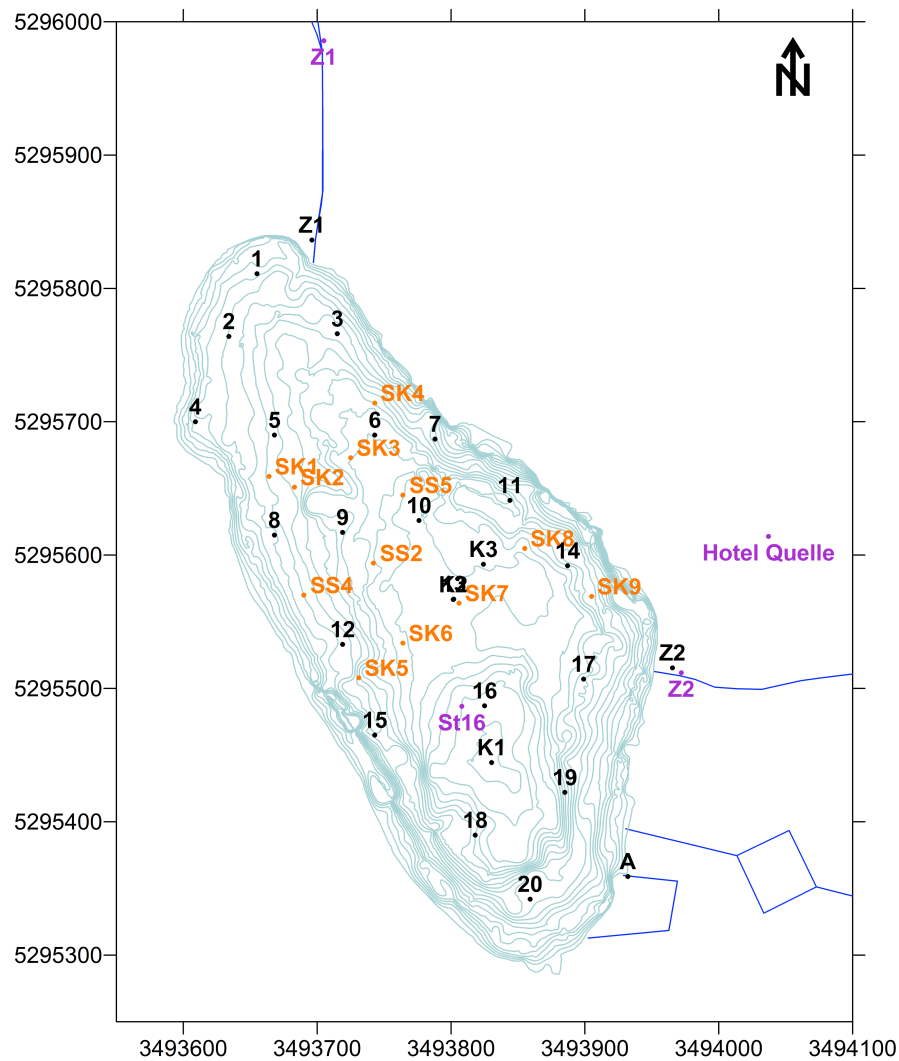


Figure 10 Measuring grid map of Lake Steißlingen in Gauß-Krüger coordinates.

3.1 Detection of Groundwater Inlets within Lake Steißlingen

3.1.1 Physical Parameters (T, EC, dissolved oxygen, oxygen saturation, turbidity, pH, Chlorophyll A)

Water Temperature

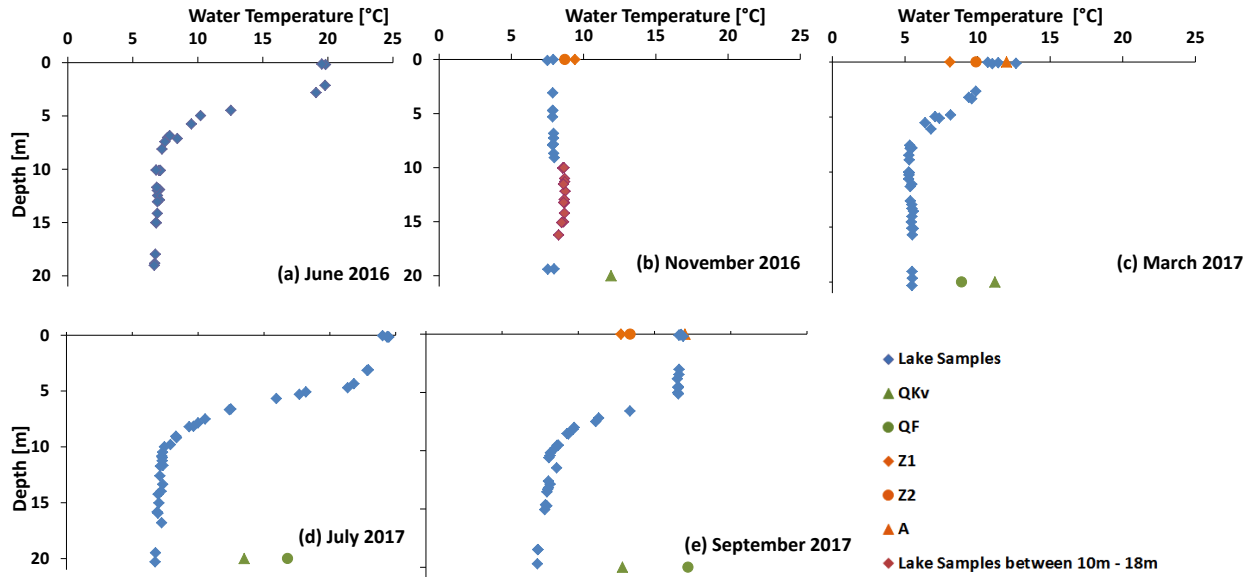


Figure 11 Data of water temperature measurements of Lake Steißlingen from different seasons with the references Z, Q and A against water depth. (a) June 2016, (b) November 2016, (c) March 2017, (d) July 2017 and (e) September 2017. The x-axis demonstrates water temperature in [°C] and the y-axis shows water depth in [m].

In June 2016 surface water temperatures of 19.5°C to 19.8°C prevail. Between 0.0 m and 10.0 m water temperature decreases wherefrom it stays almost constant with values between 6.7°C and 7.1°C from 10.0 m to 21.0 m.

It can be seen from the results of November 2016 that the water temperature of the lake lays within 7.5°C and 9.4°C and thus it is supposed to be almost constant within the entire water column. QKv, Z1 and Z2 have a water temperature of 11.9°C, 9.4°C and 8.7°C, respectively.

The results in March 2017 indicate that average surface water temperatures between 10.7°C and 12.6°C decrease until a depth of 7.8 m wherefrom values stay almost constant down to the lakes deepest part with 5.2°C to 5.6°C. Regarding the sampling points QF, QKv, A, Z1 and Z2 in the surrounding area of Lake Steißlingen, water temperatures of 8.9°C, 11.2°C, 12°C, 8.1°C, 9.9°C were measured, respectively.

According to July 2017 the water temperature data does not show any remarkable outliers. At the top of the water column water temperatures measured are between 24.0°C and 24.5° . Subsequently, water temperature decreases down to a depth of 7.5m wherefrom barely any fluctuations occur until 21.4 m with between 6.7°C and 10.5°C. The results of QF, A and QK do show following temperatures: 16.8°C, 26.3°C and 13.5°C.

In September 2017 almost constant water temperatures within 16.5°C and 16.9°C occur between 0.0 m and 4.6 m. Temperature values decrease until 9.7 m from where they show barely any fluctuations with values between 7.3°C and 8.6°C down to the deepest point of the lake. Regarding the sampling points QKV, QF, Z1, Z2 and A, in the surrounding area of Lake Steißlingen, it can be seen that they have temperature values of 12.9°C, 17.2°C, 12.8 °C, 13.4 °C and 17.0 °C, respectively.

Electrical Conductivity

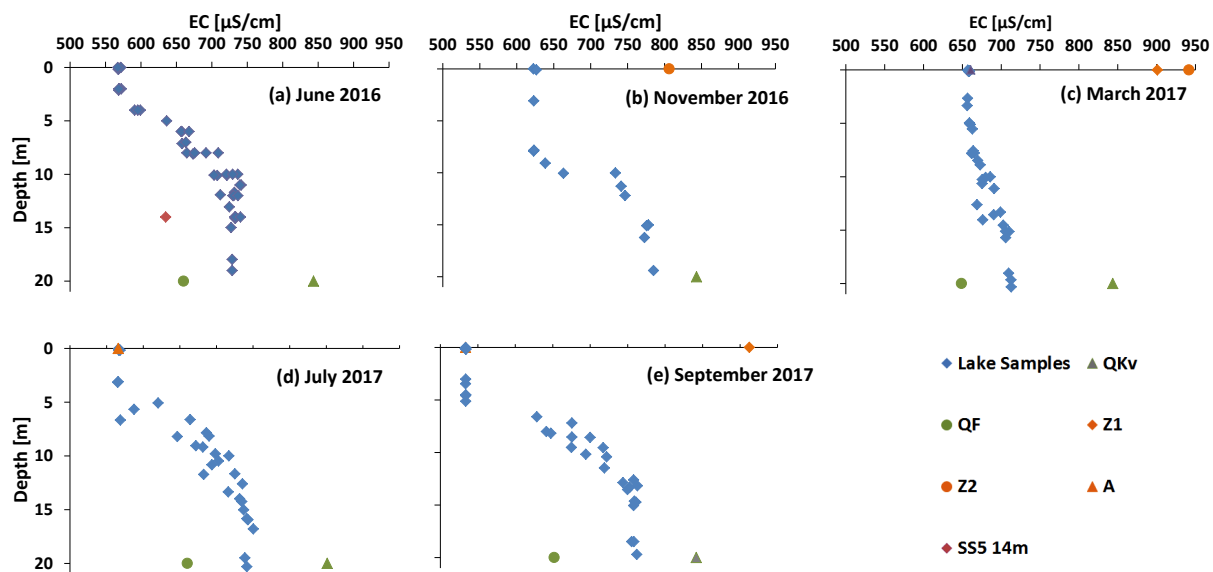


Figure 12 Depth profiles of EC measured by titration ($T=25^{\circ}\text{C}$) in $[\mu\text{S}/\text{cm}]$ (x-axis) vs. depth (y-axis) for the months of (a) June 2016, (b) November 2016, (c) March 2017, (d) June 2017 and (e) September 2017.

At the surface of the lake electrical conductivity values between 568 $\mu\text{S}/\text{cm}$ and 572 $\mu\text{S}/\text{cm}$ were measured in June 2016. From 0.0 m to 2.0 m EC stays constant with values measured between 567 $\mu\text{S}/\text{cm}$ and 572 $\mu\text{S}/\text{cm}$, wherefrom it increases down to a depth of 10.0 m with results between 703 $\mu\text{S}/\text{cm}$ and 737 $\mu\text{S}/\text{cm}$. From 10.0 m to the deepest point of the lake values do not show very strong fluctuations with conductivities between 712 $\mu\text{S}/\text{cm}$ and 741 $\mu\text{S}/\text{cm}$. An exception shows SS5 at 14.0 m and a comparatively low conductivity of 635 $\mu\text{S}/\text{cm}$. The EC of QF is 660 $\mu\text{S}/\text{cm}$ and QKv shows a deviating value of 844 $\mu\text{S}/\text{cm}$.

As it can be seen from the data of November 2016 EC values barely fluctuate between 622 $\mu\text{S/cm}$ and 639 $\mu\text{S/cm}$ from 0.0 m to 9.1 m. A sudden rise in conductivity was measured around 10.0 m wherefrom it stays constant again down to the deepest point of the lake with conductivities between 773 $\mu\text{S/cm}$ and 785 $\mu\text{S/cm}$. The EC of QKv, Z1 and Z2 indicates a value of 843 $\mu\text{S/cm}$, 901 $\mu\text{S/cm}$ and 806 $\mu\text{S/cm}$, respectively.

The data of March 2017 shows that little differences of EC were measured along the water column with values between 656 $\mu\text{S/cm}$ and 713 $\mu\text{S/cm}$, whereat the deeper layers of the lake show slightly higher conductivities. QF indicates a value of 649 $\mu\text{S/cm}$, A indicates 661 $\mu\text{S/cm}$. Z1, Z2 and QKv show conductivities of 901 $\mu\text{S/cm}$, 942 $\mu\text{S/cm}$ and 844 $\mu\text{S/cm}$, respectively.

In July 2017 the upper 3.2 m indicate a constant EC between 565 $\mu\text{S/cm}$ and 569 $\mu\text{S/cm}$. Subsequently, conductivity starts to increase down to a depth of 15.0 m wherefrom it stays almost constant to the deepest part of the lake with values from 737 $\mu\text{S/cm}$ to 750 $\mu\text{S/cm}$. When comparing it to the other results, a lowered conductivity of 569 $\mu\text{S/cm}$ was measured at a depth of 6.7 m at sampling point 10. Measured data indicates that QF, QKv and A show values of 653 $\mu\text{S/cm}$, 842 $\mu\text{S/cm}$ and 563 $\mu\text{S/cm}$, respectively.

In September 2017 the upper part of the lake, at a depth between 0.0 m and 5.0 m, shows similar data that ranges between 533 $\mu\text{S/cm}$ and 534 $\mu\text{S/cm}$. The results depict a continuous ascent of electrical conductivity between 5.0 m and 13.5m, wherefrom it stays almost constant down to the deepest point of the lake. The conductivities measured from 13.5m to 21.4 m lay within 758 $\mu\text{S/cm}$ and 762 $\mu\text{S/cm}$. The results of QKv, Z1, A, QF and Z2 are 842 $\mu\text{S/cm}$, 912 $\mu\text{S/cm}$, 534 $\mu\text{S/cm}$, 652 $\mu\text{S/cm}$ and 952 $\mu\text{S/cm}$, respectively.

Dissolved Oxygen

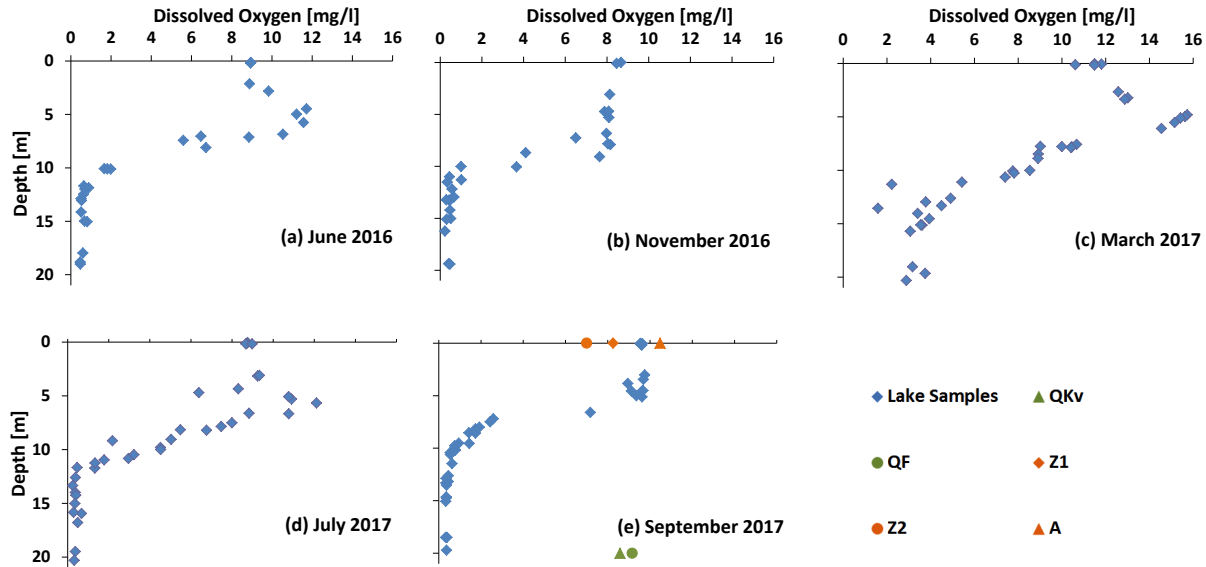


Figure 13 The plots of (a) June 2016, (b) November 2016, (c) March 2017, (d) July 2017 and (e) September 2017 show dissolved oxygen in [mg/l] plotted on the x-axis and depth in [m].

In June 2016 dissolved oxygen is 8.9 mg/l and 9.0 mg/l at the water surface. An increase of dissolved oxygen was recorded between 11.2 mg/l and 11.7 mg/l at a depth of 5.0 m. Between 5.0 m and 10.0 m a decrease of dissolved oxygen with depth is measured showing results from 1.7 mg/l to 2.0 mg/l. The lowermost part of the water column from 10.0 m to 21.4 m indicates a recurring slight descent of dissolved oxygen within 0.5 mg/l and 0.9 mg/l.

At the surface of the water column oxygen content of sampling point 10 and K1 in November 2016 lays at 10.1 mg/l and 11.0 mg/l. Between 3.0 m and 8.0 m data shows constant O_2 concentrations between 7.9 mg/l and 8.2 mg/l with an exception of sampling point 8 and an oxygen content of 6.5 mg/l. A sudden decrease of dissolved oxygen can be seen at around 8.0 m to 10.0 m wherefrom values stay almost constant down to the deepest point of the lake with O_2 concentrations between 0.2 mg/l and 1.0 mg/l.

Regarding data of dissolved oxygen in March 2017 values between 10.6 mg/l and 11.8 mg/l are measured at the surface. Increased O_2 contents from 15.2 mg/l to 15.7 mg/l were measured down to 5.0 m. Between 5.0 m and 14.0 m dissolved oxygen decreases strongly followed by constant concentrations between 2.9 mg/l and 3.9 mg/l.

According data of dissolved oxygen in July 2017, values between 8.7 mg/l and 9.0 mg/l were measured at the surface, followed by an increase down to 5m where O_2 contents from 10.8 mg/l to 12.1 mg/l were recorded. At a depth of 4.7 m a deviating value of 6.4 mg/l at sampling point 1 was measured. Oxygen concentrations decrease strongly between 5m and 11.5m from where they stay almost constant between 0.2 mg/l and 1.3 mg/l down to the bottom of the lake.

The graph of September 2017 shows that oxygen content stays almost constant in the upper 5.4 m of the water column, with values between 8.9 mg/l and 9.7 mg/l. This gets followed by a decrease down to 10 m wherefrom values stay constant until 21.4 m with concentrations measured from 0.3 mg/l to 0.6 mg/l. QKv, QF, Z1, Z2 and A indicate following results: 8.6 mg/l, 9.2 mg/l, 10.5 mg/l, 7.0 mg/l and 8.3 mg/l.

Oxygen Saturation

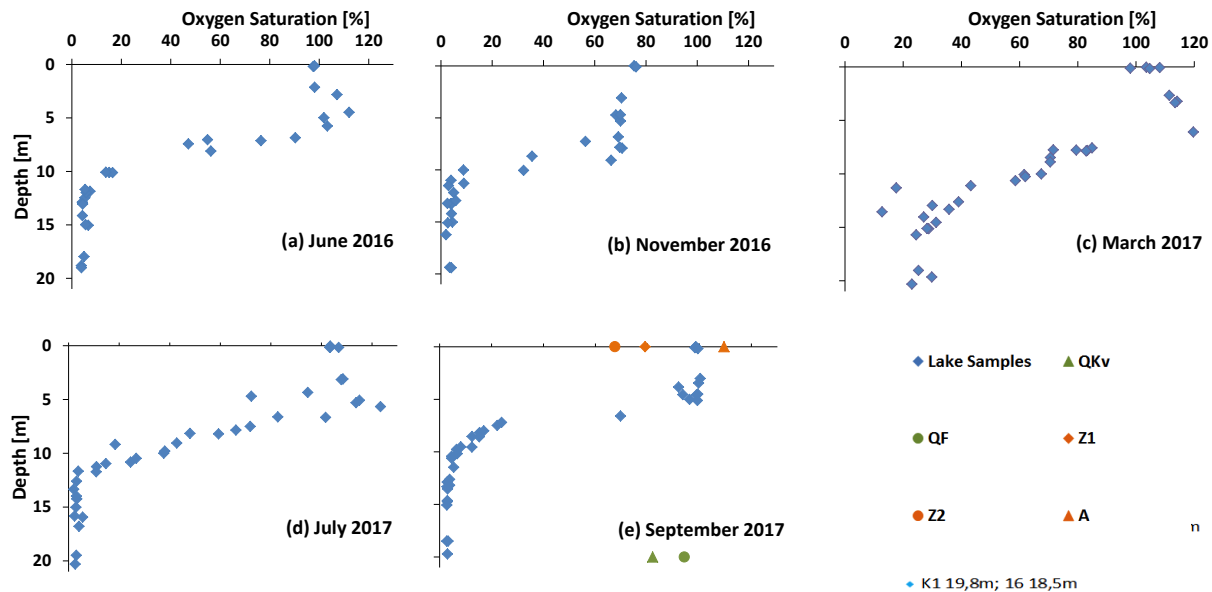


Figure 14 Oxygen saturation in [%] vs. depth in [m] in (a) June 2016 (b) November 2016 (c) March 2017 (d) July 2017 and (e) September 2017.

In June 2016 oxygen saturations of 97.6 % and 98.1 % were recorded at the water surface. The results indicate an increase of oxygen saturation at a depth of around 5.0 m, where values between 101.9% and 112.1 % were measured. Between 5.0 m and 10.0 m a decrease of dissolved oxygen with depth is measured from 13.8% to 16.5% at 10 m. The lowermost part of the water column from 10.0 m to 21.4 m indicates a recurring slight descent down to 3.8% and 7.4%.

On top of the water column an oxygen saturation of 88.0% and 98.5% was measured in November 2016. Between 3.0 m and 8.0 m data shows constant saturation values between 68.3% and 70.7%, with an exception of 56.4% at 7.3 m. A sudden decrease of O₂ saturation can be seen between 8 m and 10 m wherefrom values stay almost constant down to the deepest point of the lake between 2.0% and 9.0%.

According to oxygen saturation in March 2017 values from 98.0% to 108.2% were measured at the surface, followed by an increase around 5.0 m between 123.7% and 133.1%. Between 5.0 m and 14.0 m saturation of oxygen decreases strongly and subsequently stays almost constant down to the deepest point of the lake with values from 23.0 % to 31.3%.

Regarding O₂ saturation in July 2017 values between 103.3% and 106.8% were measured at the surface, followed by an increase to around 5.0 m with results from 113.8% to 123.3%. At a depth of 4.7 m a deviating value of 72.3% was measured. Oxygen saturations decrease strongly between 5m and 11.5m from where they stay almost constant down to 21.4 m with O₂ saturations between 2.1% and 11.0%.

The data of September 2017 shows that oxygen saturation, with values between 91.2% and 100.3%, stays almost constant from the surface until a depth of 5.4 m. This is followed by a decrease down to 10.0 m wherefrom values stay unchanged until 21.4 m with saturations measured from 2.7% to 5.4%. QKv, QF, Z1, Z2 and A indicate following results, respectively: 82.0%, 94.2%, 109.5%, 67.5% and 79.1%.

Turbidity

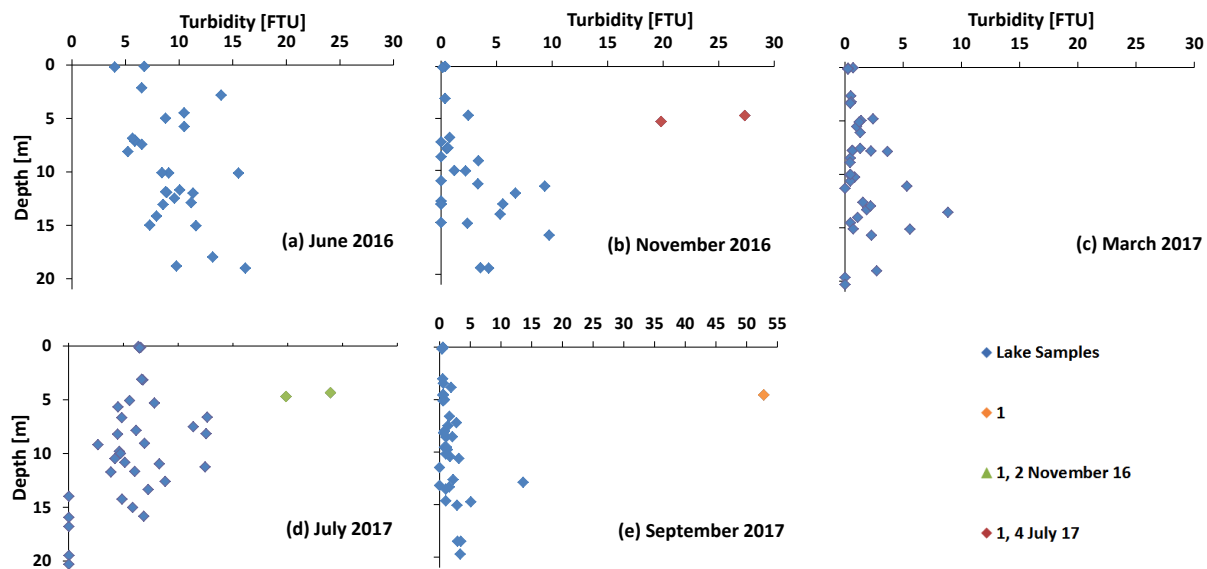


Figure 15 The delineation shows turbidity in FTU (x-axis) versus depth in [m] (y-axis) of the sampling campaigns in (a) June 2016, (b) November 2016, (c) March 2017, (d) July 2017 and (e) September 2017 of Lake Steißlingen. A different scale for the graph of September 2017 was chosen, because sampling point 1 is deviating strongly due to plant growth.

As seen from data in June 2016 turbidity fluctuates between 4.0 and 16.1 along the entire water column, whereat no specific trend can be distinguished.

From the surface to the bottom of the lake turbidity fluctuates slightly in November 2016 with values from 0.0 to 9.7. Exceptions show sampling points 1 and 2 with values of 27.3, and 19.8 at depths of 4.8 m and 5.3 m.

In March 2017 turbidity results between 0.0 and 2.7 were measured within the whole water column, whereat a slight increase up to 8.8 was recorded in 13.5m.

In July 2017 turbidity values fluctuate from 2.7 to 12.7 between 0.0 m to around 15.0 m. From around 15m down to the deepest point of the lake turbidity values are 0.0. Deviating values indicate sampling points 1 and 4 at around 5m with a turbidity of 19.8 and 23.9, respectively.

In September 2017 turbidity values do show slight fluctuations along the entire water column between 0.0 and 5.1. The result of sampling point 1 deviates strongly with 52.8 at a depth of 4.8 m.

pH-value

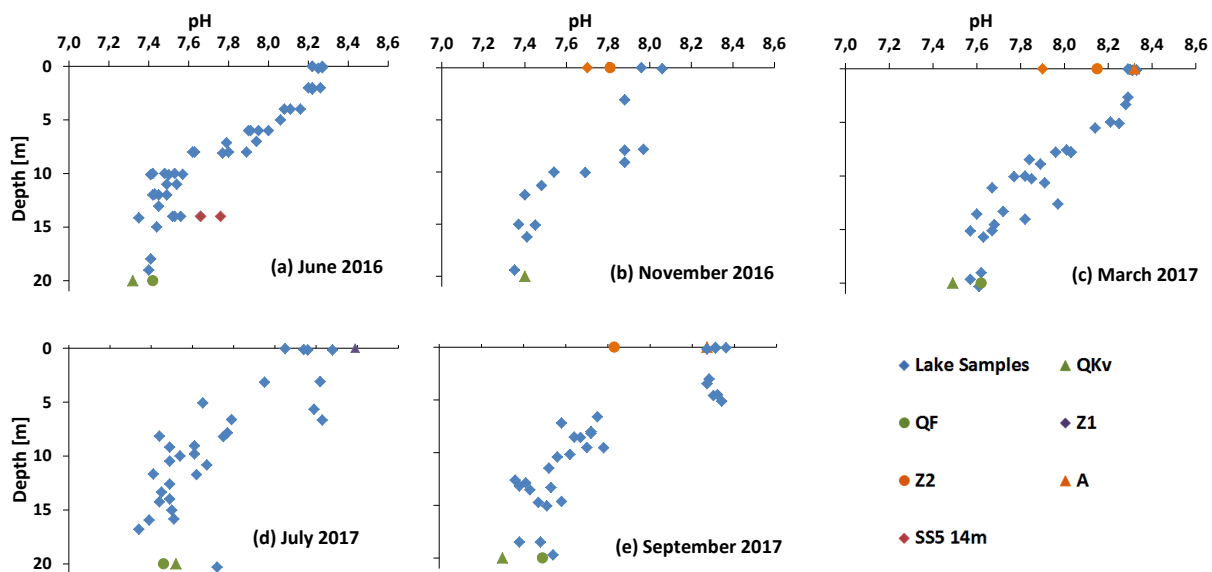


Figure 16 pH-value vs. water depth in [m] in (a) June 2016, (b) November 2016, (c) March 2017, (d) July 2017 and (e) September 2017.

In June 2016 pH decreases from values at the surface between 8.22 and 8.27 down to values from 7.41 to 7.57 at 10.0 m depth, wherefrom pH only shows slight fluctuations between 7.35 and 7.57 down to the deepest point of the lake at 21.4 m. At sampling point SS5 and SS2 at a

depth of 14.0 m pH increased values of 7.76 and 7.6 were measured. The pH of QF and QKv is 7.45 and 7.32, respectively.

The results of November 2016 indicate pH values of 7.96 and 8.06 at the surface of the water column. From 3.0 m to around 10.0 m an almost constant pH between 7.88 and 7.97 was measured. From around 10.0 m to the bottom of the lake pH does not fluctuate strongly with values from 7.35 to 7.69. QKv, Z1 and Z2 indicate a pH of 7.40, 7.70 and 7.81, respectively.

When regarding results of March 2017 in the upper 5m of Lake Steißlingen constant pH values between 8.14 and 8.33 were measured, followed by a continuous descent down to the deepest points of the lake, where values between 7.57 and 7.62 are recorded. For QKv, QF, Z1, Z2 and A following results are recorded respectively: 7.49, 7.62, 7.90, 8.15 and 8.32.

In the upper 6.7 m of the water column pH shows enhanced values between 7.95 and 8.34 in July 2017. From 6.7 m to around 15.0 m a descent in pH was recorded. In the lowermost water layer, pH stays almost constant with values between 7.34 and 7.54 down to deepest point of the lake. The pH values of QKv, QF, A are 7.52, 7.46 and 8.39, respectively.

A clear decrease of pH with depth can be distinguished in September 2017. All results show almost constant values between 8.27 and 8.36 in the uppermost layer from 0.0 m to around 5m of the water column, wherefrom pH decreases continuously down to around 10.0 m where results from 7.56 to 7.78 were recorded. Hereby sampling point 18 deviates strongly to a lower pH of 7.43 at a depth of 5.3 m. Between 10.0 m and 21.4 m values fluctuate slightly between 7.47 and 7.58. Hereby sampling points 17, 14, 6 and 18 between 10.6 m and 13.1 m show slightly lower pH values from 7.36 and 7.41 compared with data between 10.0 m and 21.0 m. As seen from the pH data of September 2017 QKv, QF, A, Z1 and Z2 show values of 7.3, 7.5, 8.3, 7.8 and 7.8, respectively.

Chlorophyll A

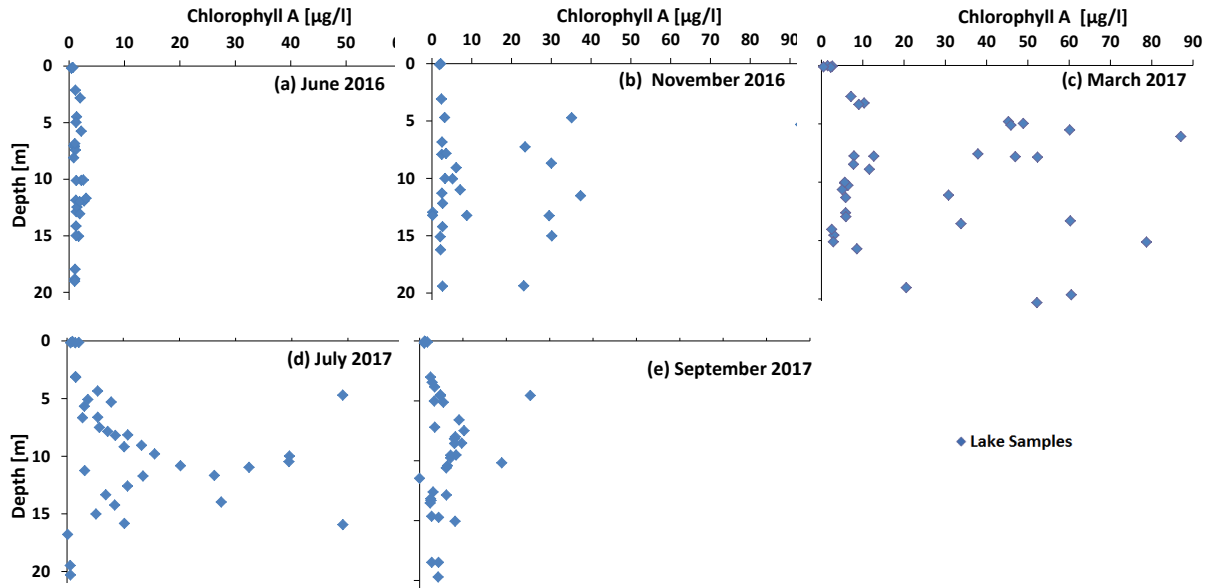


Figure 17 Chlorophyll A contents in $\mu\text{g/l}$ on the x-axis vs. depth in m on the y-axis in (a) June 2016, (b) November 2016, (c) March 2017, (d) July 2017 and (e) September 2017. Because of strong Chlorophyll A fluctuations between the seasons, different scales were chosen depending on the concentration range.

Basically, Chlorophyll A values are close to $0.0 \mu\text{g/l}$ at the surface of the lake throughout the whole year.

Recorded values in June 2016 show a consistency with depth of about $0.4 \mu\text{g/l}$ - $2.6 \mu\text{g/l}$.

In November 2017 measurements show that Chlorophyll A values fluctuate from $0.2 \mu\text{g/l}$ to $8.8 \mu\text{g/l}$ between 0.0 m and 15.0 m . Remarkable high Chlorophyll A concentrations with values between $18.1 \mu\text{g/l}$ and $37.4 \mu\text{g/l}$ appear between 4.7 m and 19.5 m . For sampling point 2 (5.3 m) strongly increased values of $92.7 \mu\text{g/l}$ were recorded.

In March 2017 concentration of Chlorophyll A lies within $0.5 \mu\text{g/l}$ and $2.6 \mu\text{g/l}$ at the water surface. Further down at around 5.0 m - 7.8 m results show increased values between $37.9 \mu\text{g/l}$ and $87.0 \mu\text{g/l}$. At a depth of 15.0 m there is a recurring increase with a Chlorophyll A concentration of $78.7 \mu\text{g/l}$. At a depth of around 21.4 m high concentrations of $52.2 \mu\text{g/l}$ and $60.5 \mu\text{g/l}$ were measured.

In July 2017 Chlorophyll A slightly fluctuates between 0.0 m and 7.5 m with values from $0.6 \mu\text{g/l}$ to $7.9 \mu\text{g/l}$. A noticeable deviating value of $49.1 \mu\text{g/l}$ is measured at sampling point 1 at around 5.0 m . Between 7.5 m and 10.0 m results indicate a concentration rise up to $39.6 \mu\text{g/l}$. From 10.0 m to 15 m concentrations of Chlorophyll A decrease again wherefrom they fluctuate slightly down to the bottom of the lake within a range between $0.1 \mu\text{g/l}$ and $10.2 \mu\text{g/l}$. Hereby, one value deviates with a concentration of $49.1 \mu\text{g/l}$ at 16.0 m .

In September 2017 Chlorophyll A concentrations at the water surface lay within 1.1 µg/l and 1.8 µg/l wherefrom they increase continuously to around 8.0 m where values from 8.0 µg/l to 10.2 µg/l were measured. From 12.5m to 21.4 m decreased concentrations between 2.6 µg/l and 4.4 µg/l can be distinguished. At a depth of 4.6 m and 10.2 m slightly increased values of 6.1 µg/l and 8.2 µg/l occur.

3.1.2 Chemical Parameters (TA, Water Hardness, Anions, Cations)

Alkalinity

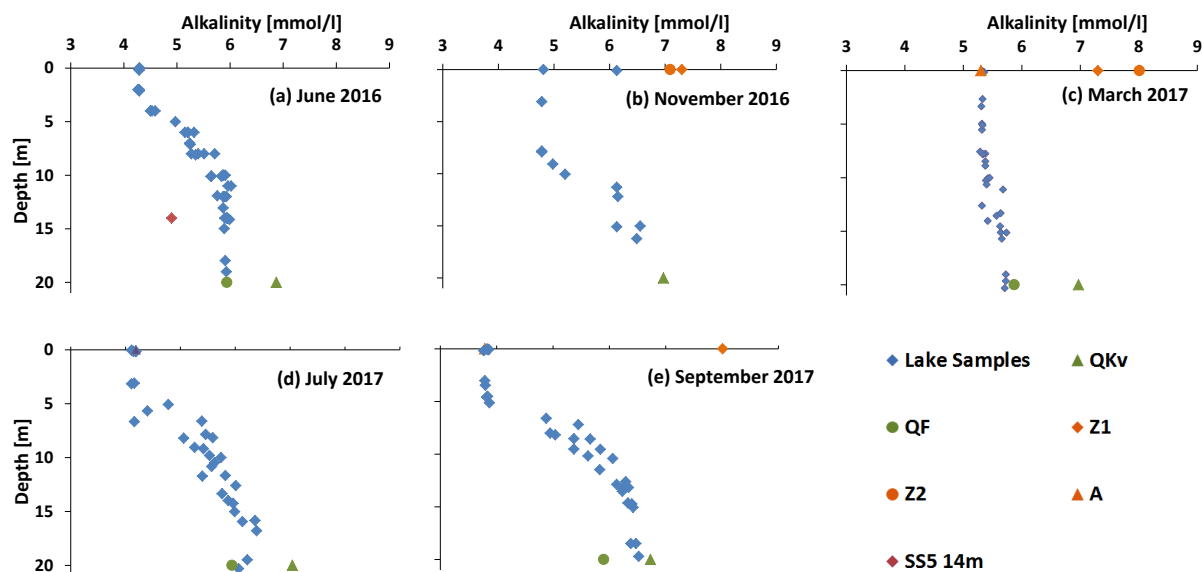


Figure 18 The results of TA in (a) June 2016, (b) November 2016, (c) March 2017, (d) July 2017 and (e) September 2017 plotted in [mmol/l] on the x-axis vs. depth in [m] on the y-axis.

According to June 2016 alkalinity stays constant in the upper layer of the water column between 0.0 m and 2.0 m with a value of 4.3 mmol/l. From 2.0 m down to 10.0 m an increase of alkalinity is recorded wherefrom values stay constant down to the bottom of the lake. In the range of 10.0 m to 21.4 m alkalinity values were measured between 5.6 mmol/l and 6.0 mmol/l. A lower alkalinity of 4.6 mmol/l is measured at sampling point SS5 (14.0 m). Sampling points QF and QKv have alkalinities of 5.9 mmol/l and 6.9 mmol/l.

When regarding the graph of November 2016 it can be perceived that alkalinity barely fluctuates from 0 m to around 11.0 m because data shows that values between 4.8 mmol/l and 5.2 mmol/l were measured. An exception indicates sampling point K1 (10.0 m) with an alkalinity of 6.0 mmol/l. From 11.0 m to 21.4 m only increased values between 6.1 mmol/l and 7.0 mmol/l were

recorded. The alkalinity of QKv, Z1 and Z2 shows following values: 7.0 mmol/l, 7.3 mmol/l and 7.0 mmol/l.

In the month of March 2017 there are slight fluctuations of alkalinity within the water column between 0.0 m-21.4 m, which shows a range of about 0.4 mmol/l between 5.3 mmol/l and 5.7 mmol/l. The values for QKv, QF, Z1, Z2 and A are 7.0 mmol/l, 5.9 mmol/l, 7.3 mmol/l, 8.0 mmol/l and 5.3 mmol/l, respectively.

The results of July 2017 show that alkalinity indicates consistency at the upper 4.1 m of the water column where values between 4.1 mmol/l and 4.2 mmol/l were measured. Data shows an increase of alkalinity to around 15m wherefrom it only shows slight alterations down to the deepest point of the lake with values between 6.0 mmol/l to 6.4 mmol/l. The alkalinity of QKv, QF and A is 7.0 mmol/l, 5.9 mmol/l and 4.2 mmol/l, respectively.

In September 2017 alkalinity is constant with values of 3.8 mmol/l to 3.9 mmol/l until 5.0 m, followed by a continuous increase to a maximum of 6.5 mmol/l down to a depth of 21.4 m. For QKv, QF, Z1, Z2 and A following concentrations were measured: 6.7 mmol/l, 5.9 mmol/l, 8.0 mmol/l, 9.4 mmol/l and 3.8 mmol/l, respectively.

Water Hardness

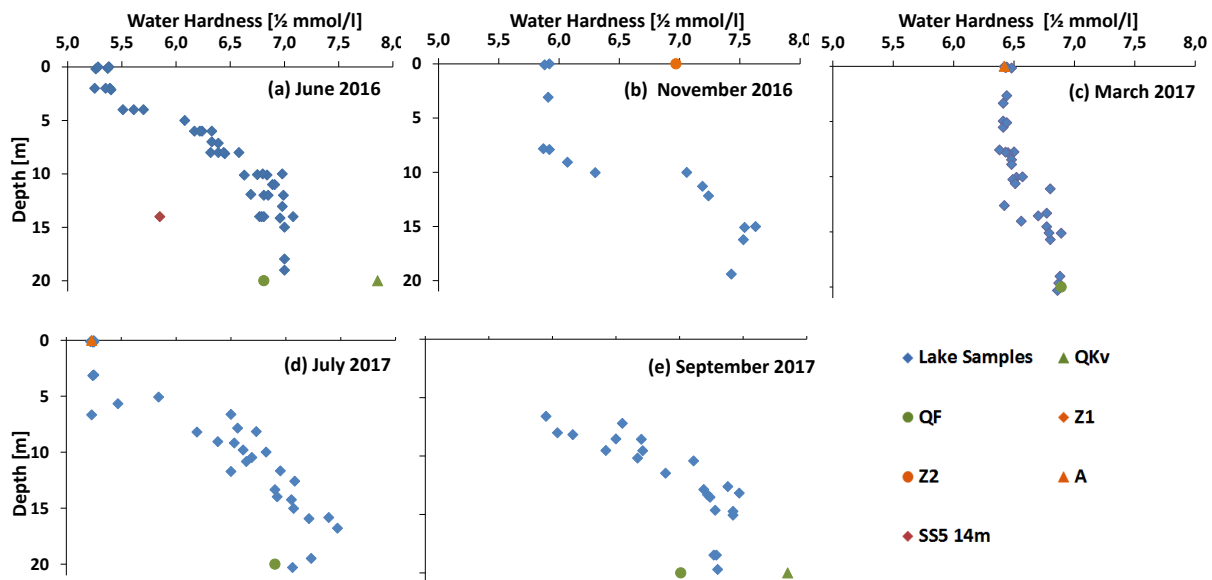


Figure 19 The results of Lake Steißlingen for water hardness were plotted on the x-axis in [$\frac{1}{2}$ mmol/l] with corresponding depths on the y-axis in [m] in (a) June 2016, (b) November 2016, (c) March 2017, (d) July 2017 and (e) September 2017.

The graph of June 2016 indicates that water hardness stays constant between 0.0 m and 2.0 m with values from 5.3 ½ mmol/l to 5.4 ½ mmol/l, followed by an increase until 10.0 m wherefrom water hardness does not indicate further change. From 10.0 m to the deepest point of the lake values between 5.9 ½ mmol/l and 7.1 ½ mmol/l were measured. QF and QKv indicate a water hardness of 6.8 ½ mmol/l and 7.9 ½ mmol/l.

In November 2016 the upper layer of the water column to around 10.0 m show constant values from 5.9 ½ mmol/l to 6.3 ½ mmol/l. A recurring increase of water hardness is recorded between 10.0 m and 15.0 m and then stays constant from a depth of 15.0 m to the deepest part of the lake with values of 7.4 ½ mmol/l to 7.6 ½ mmol/l. QKv, Z1 and Z2 indicate a water hardness of 8.1 ½ mmol/l 9.5 ½ mmol/l and 7.0 ½ mmol/l.

According to recorded data in March 2017, it can be seen that measured values between 6.4 ½ mmol/l and 6.9 ½ mmol/l show a consistency in water hardness within the entire column. The water hardness of QKv, QF, Z1, Z2 and A indicates a value 8.1 ½ mmol/l, 6.9 ½ mmol/l, 10.3 ½ mmol/l, 9.3 ½ mmol/l and 6.4 ½ mmol/l, respectively.

In July 2017 water hardness indicates unchanging values between 5.2 ½ mmol/l and 5.3 ½ mmol/l in the upper 3.1 m of the water column. Subsequently, water hardness increases continuously to around 15.0 m. From around 15.0 m to the bottom of the lake slightly changing values between 7.1 ½ mmol/l and 7.5 ½ mmol/l were measured. For sampling points QKv, QF and A following values were measured: 8.0 ½ mmol/l, 6.9 ½ mmol/l and 5.2 ½ mmol/l.

Regarding the month of September 2017, it can be seen that water hardness shows constant values of 4.9 ½ mmol/l from surface water to a depth of around 5.0 m. Subsequently water hardness increases continuously to 15.0 m followed by constant values between 7.3 ½ mmol/l and 7.4 ½ mmol/l down to 21.4 m. Raised water hardness values are shown by QKv, QF, Z1 and Z2 of 7.9 ½ mmol/l 7.0 ½ mmol/l 9.6 ½ mmol/l and 10.1 ½ mmol/l respectively.

Chloride

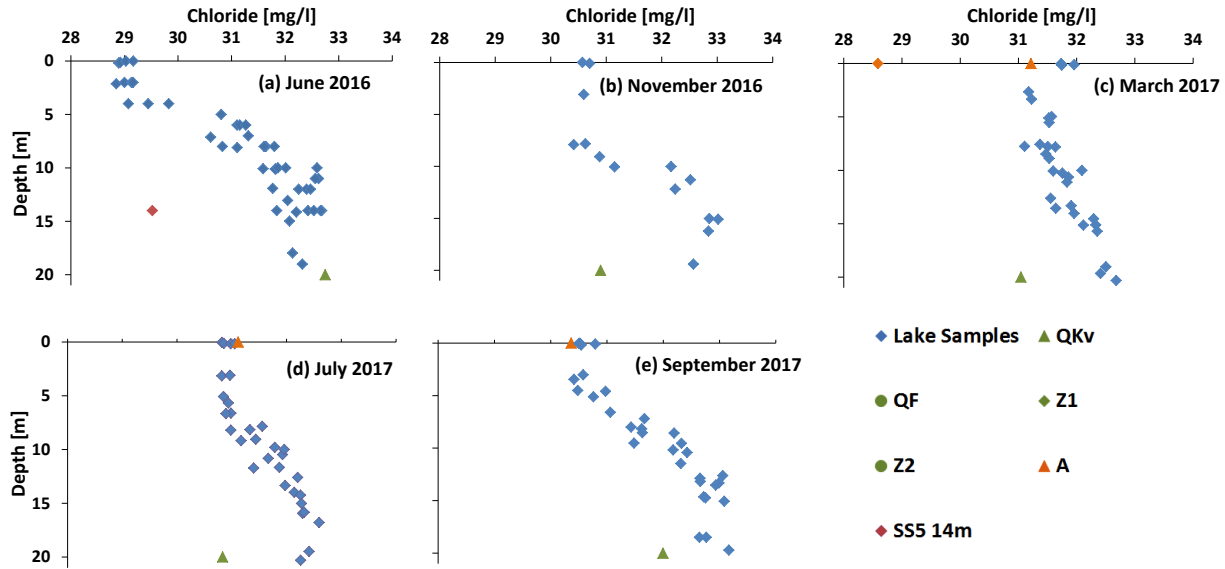


Figure 20 Chloride concentration in [mg/l] on the x-axis vs. depth in [m] in the months of (a) June 2016, (b) November 2016, (c) March 2017, (d) July 2017 and (e) September 2017.

The results of June 2016 show that chloride concentrations stay constant from 0.0 m to 4.0 m with values between 28.8 mg/l and 29.4 mg/l. An increase of Cl^- concentration is occurring between 4.0 m and 10.0 m followed by unchangeable concentrations from 10.0 m to 21.4 m with values from 31.8 mg/l to 32.7 mg/l. QF and QKv show a concentration of 8.9 mg/l and 32.7 mg/l, respectively.

The measurements of November 2016 show slight fluctuations along the entire water column between 30.4 mg/l and 33.0 mg/l. QKv, Z1 and Z2 do have chloride concentrations of 30.9 mg/l, 23.3 mg/l and 8.8 mg/l.

According to March 2017 concentrations of chloride change slightly within the whole lake profile with results from 31.1 mg/l and 32.7 mg/l, whereat slightly increased values were recorded close to the deepest part of the lake. The sampling points QKv, QF, Z1, Z2 and A show results of 31.0 mg/l, 8.5 mg/l, 28.6 mg/l, 11.3 mg/l and 31.2 mg/l, respectively.

In July 2017 the concentration of chloride stays almost constant between 0.0 m and 6.6 m with values from 30.8 mg/l to 31.1 mg/l. There is a concentration increase from 6.6 m to 15m followed by an unchanging concentration value between 32.3 mg/l and 32.6 mg/l down to 21.4 m. QKv, QF and A indicate following results: 30.8 mg/l, 8.9 mg/l and 31.1 mg/l.

When regarding chloride concentrations in September 2017, it can be seen that they stay almost unchanged with values that lay in a range between 30.4 mg/l and 31.0 mg/l from 0.0 m to 5.0 m.

Subsequently the concentrations of chloride increase continuously down to the deepest point of the lake where a value of 33.2 mg/l was measured. QKv, QF, Z1, Z2 and A show values of 32.0 mg/l, 8.5 mg/l, 22.7 mg/l, 8.6 mg/l and 30.4 mg/l.

Sulfate

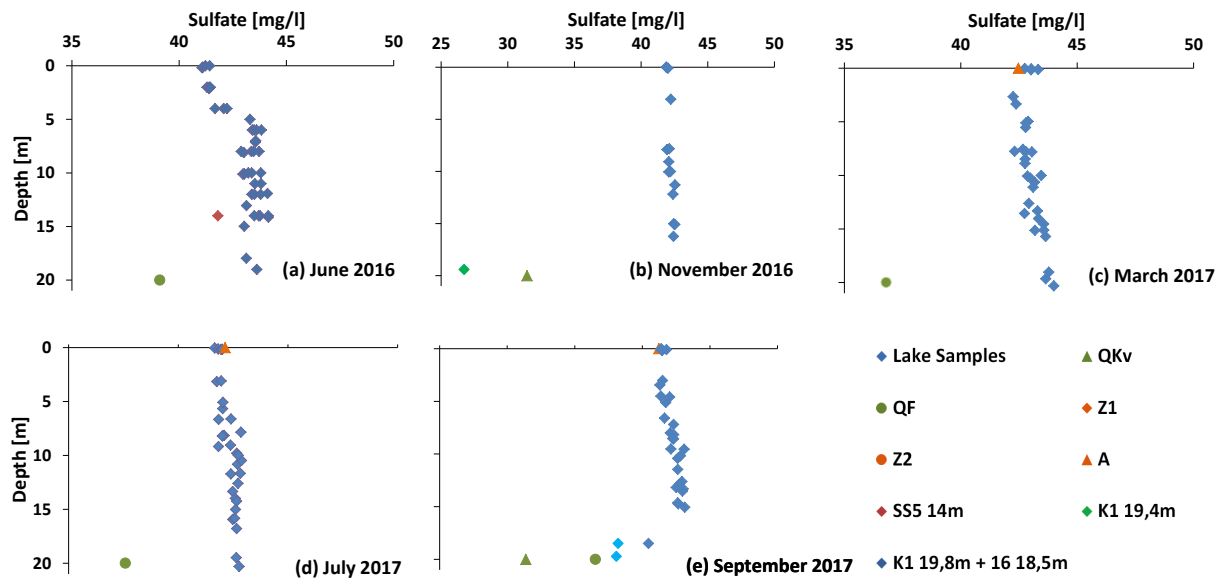


Figure 21 Sulfate concentration in [mg/l] on the x-axis vs. depth in [m] on the y-axis in (a) June 2016, (b) November 2016, (c) March 2017, (d) July 2017 and (e) September 2017.

The measuring campaign in June 2016 shows constant sulfate concentrations between 41.0 mg/l and 42.2 mg/l from 0.0 m to 4.0 m. A sudden change in sulfate content was measured around 5.0 m wherefrom values stay slightly increased down to the deepest point of the lake indicating concentrations from 42.9 mg/l and 44.2 mg/l. The sampling points of QF and QKv show concentrations of 39.1 mg/l and 31.8 mg/l.

Measurements of November 2016 show that sulfate concentrations stay almost constant within the entire water column with values between 41.0 mg/l and 42.5 mg/l. Hereby sampling point K1 deviates strongly at a depth of 19.5 m and a concentration of 26.7 mg/l. QKv, Z1 and Z2 indicate contents of 31.4 mg/l, 66.5 mg/l and 69.1 mg/l, respectively.

Measurements of March 2017 show that sulfate concentrations stay almost constant within the entire water column with values between 42.0 mg/l and 44.0 mg/l. For Z1, Z2, Hotel Quelle and A following values were recorded in February 2017: 75.5 mg/l, 84.4 mg/l, 28.1 mg/l and 42.3 mg/l. In March 2017 QKv, QF, Z1, Z2 and A show sulfate contents of 31.1 mg/l, 36.8 mg/l, 60.6 mg/l, 107.0 mg/l and 42.5 mg/l, respectively.

Regarding the results of July 2017 it can be distinguished that sulfate concentrations barely fluctuate along the depth profile with values from 41.7 mg/l and 42.9 mg/l. For sampling points QKv, QF and A following results were measured: 31.2 mg/l, 37.6 mg/l and 42.1 mg/l, respectively.

In September 2017 sulfate values show a consistency at a depth from 0.0 m to 15.0 m with results between 40.5 mg/l and 43.1 mg/l. Close to the deepest point the lake low results from 38.1 mg/l to 38.2 mg/l were measured. QKv, QF, Z1, Z2 and A indicate a sulfate concentration of 31.4 mg/l, 36.5 mg/l, 61.3 mg/l, 67.8 mg/l and 41.2 mg/l, respectively.

NO₃-N

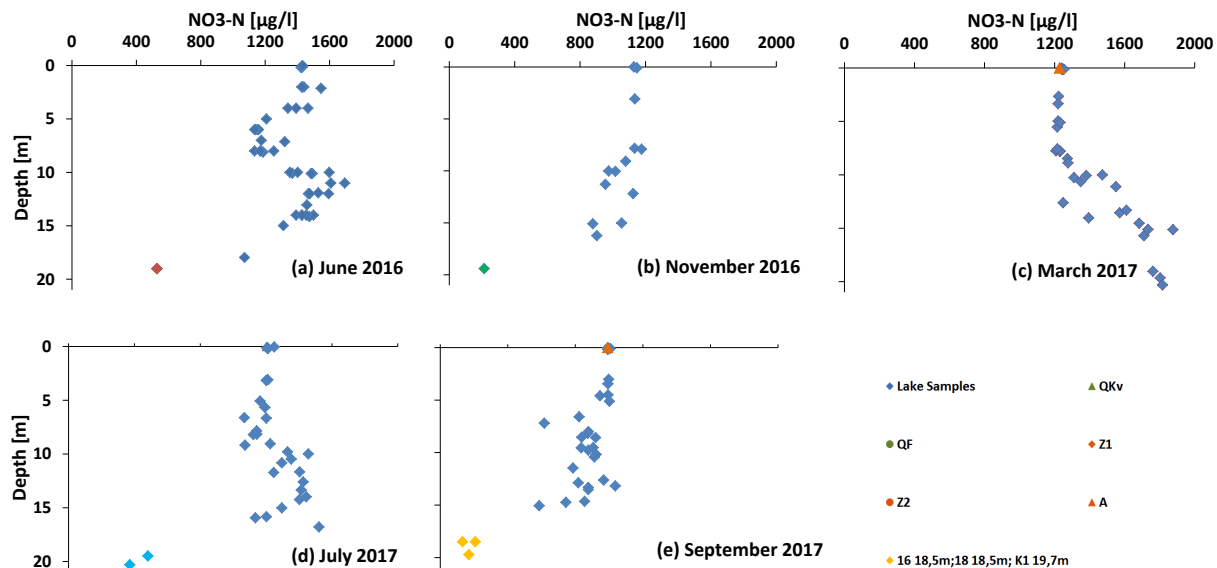


Figure 22 NO₃-N values on the x-axis in [µg/l] vs. depth in [m] on the y-axis in (a) June 2016, (b) November 2016, (c) March 2017, (d) July 2017 and (e) September 2017.

In June 2016 NO₃-N values fluctuate slightly between 1341 µg/l and 1547 µg/l at the surface layer of the lake from 0.0 m to 4.0 m. Decreased values within 1134 µg/l and 1321 µg/l were measured from 6 m to 8 m. At a depth of 10.0 m to 15m NO₃-N concentrations are increased again fluctuating between 1315 µg/l and 1694 µg/l. A concentration descent was measured between 15m and 21.4 m with measured values of 528 µg/l and 1072 µg/l. QF and QKv indicate nitrate concentrations of 3277 µg/l and 7731 µg/l, respectively.

Little fluctuations of NO₃-N concentrations are measured between 902 µg/l and 1176 µg/l from 0.0 m to 16 m within the depth profile of November 2016. In the lowest part of the water column

a decreased value of 213 µg/l was measured at sampling point K1. QKv, Z1 and Z2 show high NO₃-N concentrations of 7279 µg/l, 7877 µg/l and 3000 µg/l.

In March 2017 values between 1215 µg/l and 1253 µg/l show a consistency of NO₃-N concentration from 0.0 m to 7.6 m. Subsequently, NO₃ contents decrease continuously with depth down to 1816 µg/l measured at 21.4 m. In 15.0 m depth a slightly deviating value of 1876 µg/l was recorded. For QKv, QF, Z1, Z2 and A following concentrations were measured: 7285 µg/l, 2920 µg/l, 7335 µg/l, 3172 µg/l and 1228 µg/l, respectively.

According to July 2017 NO₃-N concentrations fluctuate hardly between 1068 µg/l and 1250 µg/l were measured until a depth of 9.2 m. Slightly higher values from 9.2 m to 15.0 m between 1247 µg/l and 1457 µg/l were recorded. Between 15.0 m and the deepest part of the lake concentrations decrease down to 373 µg/l. QKv, QF and A show concentrations of 7426 µg/l, 2970 µg/l and 1203 µg/l, respectively.

In September 2017 between 0.0 m and 10.0 m NO₃-N content barely changes with measured values between 823 µg/l and 1008 µg/l. At a depth of 7.2 m a deviating NO₃ concentration of 616 µg/l was measured. In a depth between 10.0 m and 15.0 m NO₃-N fluctuates and lays within 586 µg/l and 1037 µg/l. At the lower part of the water column close to the deepest point of the lake decreased values of 132 µg/l, 170 µg/l and 207 µg/l were recorded at sampling points 16, 18 and K1. For QKv, QF, Z1, Z2 and A NO₃-N concentrations are 7383 µg/l, 2913 µg/l, 5832 µg/l, 6996 µg/l and 992 µg/l, respectively.

NH₄-N

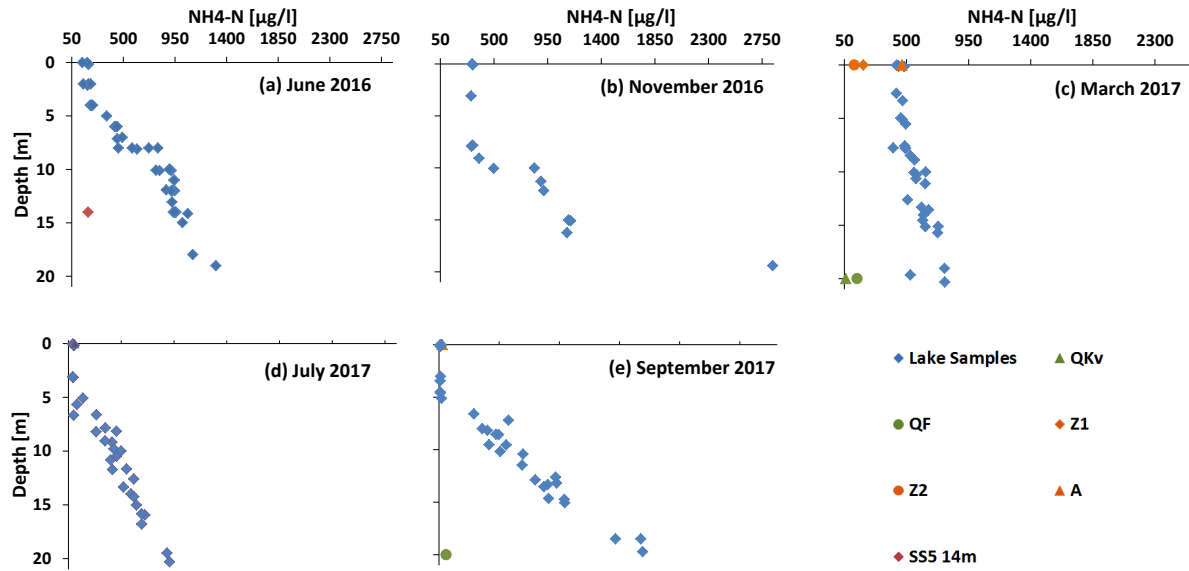


Figure 23 Ammonium concentration on the x-axis in [µg/l] vs. depth in [m] on the y-axis in (a) June 2016, (b) November 2016, (c) March 2017, (d) July 2017 and (e) September 2017.

The data of NH₄-N in June 2016 shows that constant concentrations between 142 µg/l and 233 µg/l are recorded from 0.0 m to 4.0 m. Between 4.0 m and 21.4 m values continuously increase up to 19 µg/l. An exception indicates sampling point SS5 with 193 µg/l at 14.0 m depth. QF and QKv show NH₄-N concentrations of 47 µg/l and 19 µg/l, respectively.

The results from 0.0 m to 7.9 m within the water column show unchanging NH₄-N concentrations between 308 µg/l and 322 µg/l in November 2016. From 7.9 m to 21.4 m NH₄-N increases continuously with depth up to 2838 µg/l. QKv, Z1 and Z2 indicate concentrations of 322 µg/l, 10 µg/l, 19 µg/l and 23 µg/l.

It can be seen from data of March 2017 that NH₄ concentration increases in almost regular intervals from top to the bottom of the water column with values from around 427 µg/l to 778 µg/l. Sampling point 3(7.8 m) and 17(12.6 m) do show different results compared to the rest of the values in the same depth of 404 µg/l and 509 µg/l, respectively. Following results were recorded for QKv, QF, Z1, Z2 and A, respectively: 61 µg/l, 143 µg/l, 188 µg/l, 122 µg/l, 468 µg/l.

Almost constant NH₄-N concentrations between 87 µg/l and 99 µg/l were measured within 0.0 m-3.1 m in July 2017, wherefrom values start to increase down to the deepest point of the lake where contents from 890 µg/l and 912 µg/l were recorded.

NH₄ concentrations indicate stable values from 58 µg/l to 70 µg/l between 0.0 m and 5.0 m. At around 5.0 m ammonium starts to increase continuously up to 1573 µg/l to the deepest

measured point within the lake at 21.4 m. The recorded values for QKv, QF, Z1, Z2 and A are as follows: 5 µg/l, 103 µg/l, 26 µg/l, 40 µg/l, 75 µg/l.

It can be seen that NH₄-N rises with depth between 0.0 m and 21.4 m during all seasons when regarding the graphs of June 2016, November 2016, March 2017, July 2017 and September 2017 which show following value ascents, respectively: from about 193 µg/l to 1307 µg/l, 322 µg/l to 2838 µg/l, 428 µg/l to 777 µg/l, 87 µg/l to 912 µg/l, 75 µg/l to 1559 µg/l.

Sodium

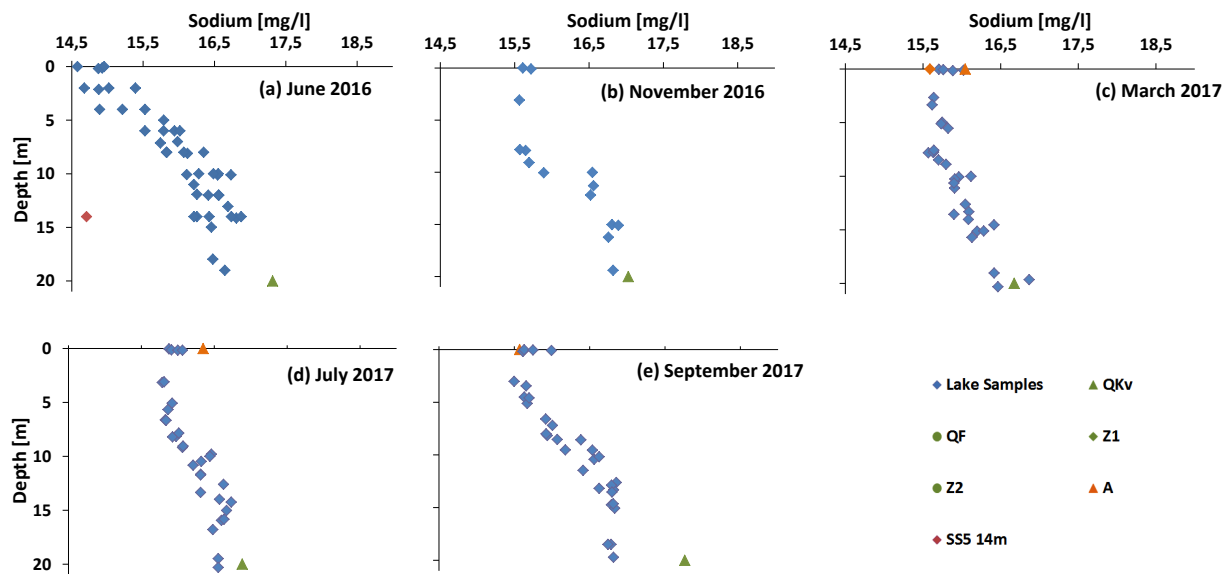


Figure 24 Sodium concentration in [mg/l] on the x-axis and depth in [m] on the y-axis in (a) June 2016, (b) November 2016, (c) March 2017, (d) July 2017 and (e) September 2017.

In June 2016 sodium concentrations increase with depth whereat at the surface values of 14.6 mg/l to 15.0 mg/l were measured and close to the bottom concentrations of 16.5 mg/l and 16.6 mg/l were recorded. Sampling point SS5 (14.0 m) with 14.7 mg/l shows deviating values. QKv and QF indicate concentrations of 17.3 mg/l and 4.6 mg/l.

The measurements of November 2016 show unchanging values between 15.6 mg/l and 15.7 mg/l from 0.0 m to 7.9 m, wherefrom concentrations increase up to 16.8 mg/l down to the deepest point of the lake. The sodium concentrations of QKv, Z1 and Z2 have values of 17.0 mg/l, 12.8 mg/l and 5.7 mg/l.

In March 2017 sodium concentrations slightly increase with depth within the whole water column, whereat surface values were measured between 15.7 mg/l and 16.0 mg/l and close to the bottom concentrations of 16.3 mg/l and 16.5 mg/l were recorded. Hereby at a depth of 16.4

m a lowered sodium concentration of 14.5 mg/l was measured. QKv, QF, Z1, Z2 and A show following values: 16.7 mg/l, 4.5 mg/l, 15.6 mg/l, 9.1 mg/l and 16.0 mg/l.

For the top of the water column from 0.0 m to 5.0 m almost constant values were measured between 15.8 mg/l and 16.1 mg/l in July 2017, which is followed by an increase up to 16.7 mg/l at around 15,0 m depth. Between 15.0 m and 21.4 m sodium concentration fluctuates slightly from 16.5 mg/l to 16.7 mg/l. The results for QKv, QF and A indicate concentrations of 16.9 mg/l, 4.5 mg/l and 16.3 mg/l, respectively.

According to September 2017 the top layer of the lake from 0.0 m to 5.0 m indicates little fluctuations in sodium with results between 15.5 mg/l and 16.0 mg/l followed by an increase until 15.0 m, wherefrom concentrations indicate a consistency of 16.8 mg/l down to the bottom of the lake. For the sampling points QKv, QF, Z1, Z2 and A following sodium concentrations were recorded: 17.8 mg/l, 4.4 mg/l, 12.5 mg/l, 7.1 mg/l and 15.6 mg/l.

Potassium

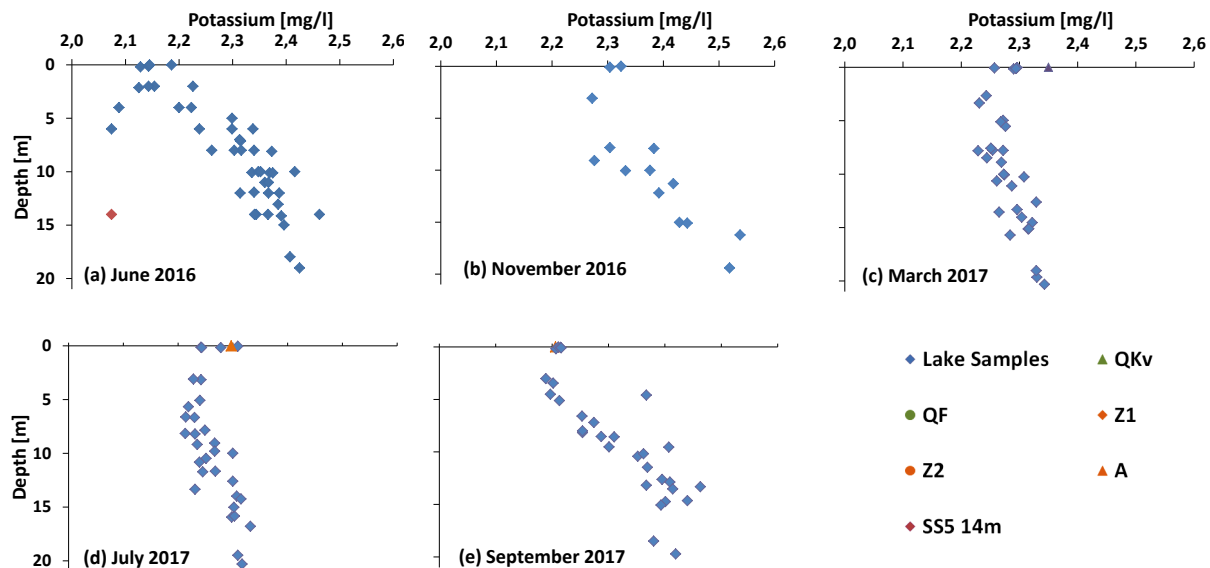


Figure 25 The illustration of potassium concentrations on the x-axis in [µg/l] with depth in [m] on the y-axis in (a) June 2016, (b) November 2016, (c) March 2017, (d) July 2017 and (e) September 2017.

In June 2016 potassium concentrations between 2.07 mg/l and 2.46 mg/l were measured and slightly increase with depth. With an exception of sampling point SS5 of 2.07 mg/l in 14.0 m. QF and QKv indicate values of 1.08 mg/l and 12.46 mg/l.

In November 2016 concentrations between 2.27 mg/l and 2.44 mg/l of potassium were measured in the upper 15m of the water column. From 15.0 m to 21.4 m slightly increased

potassium values of 2.52 mg/l and 2.53 mg/l were recorded. The values of QKv, Z1 and Z2 are as follows: 11.76 mg/l, 1.73 mg/l and 3.7 mg/l, respectively.

Potassium concentrations barely fluctuate between 2.21 mg/l and 2.34 mg/l within the whole water column in March 2017 and July 2017. For QKv, QF, Z1, Z2 and A concentrations of 11.43 mg/l, 1.11 mg/l, 1.79 mg/l, 11.77 mg/l and 2.35 mg/l were measured in March 2017. In July 2017 QKv, QF and A indicate concentrations of 11.36 mg/l, 1.07 mg/l and 2.30 mg/l.

In September 2017 in a depth between 0.0 m and 5.0 m measurements show a potassium concentration between 2.20 and 2.28 mg/l at the water surface. Between 5.0 m and 21.4 m the concentration of K^+ increases steadily to around 2.46 mg/l measured at the deepest point of the lake. For the sampling points QKv, QF, Z1, Z2 and A following sodium concentrations were recorded: 11.72 mg/l, 1.10 mg/l, 1.52 mg/l, 7.85 mg/l and 2.21 mg/l.

Calcium

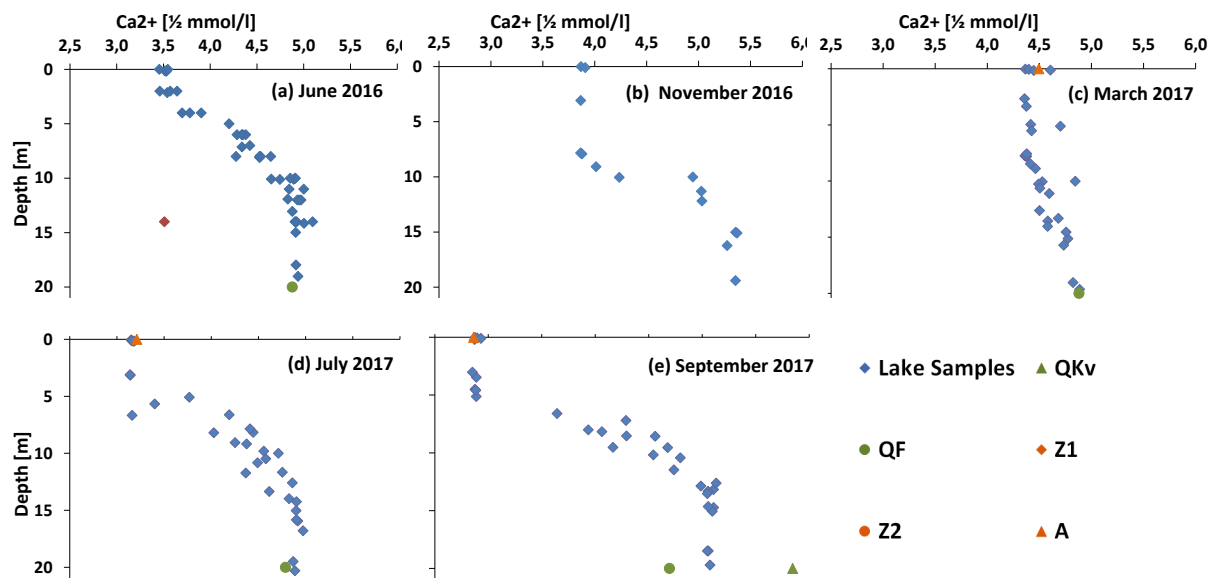


Figure 26 Calcium concentration at Lake Steißlingen in (a) June 2016, (b) November 2016, (c) March 2017, (d) July 2017 and (e) September 2017. The x-axis demonstrates calcium in [$\frac{1}{2}$ mmol/l] and the y-axis shows water depth in [m].

The results of June 2016 exhibit that calcium concentrations stay constant from 0.0 m to 3.5m with results between 3.46 and 3.64 mmol/l. Concentrations increase down to around 10.0 m where values from 4.65 mmol/l to 4.91 mmol/l were measured. At the lower layer of the water column from 10.0 m to 21.4 m concentrations only fluctuate slightly between 4.83 mmol/l and 5.09 mmol/l, whereat an exception indicates sampling point SS5 (14.0 m) with 3.51 mmol/l. QF and QKv are 4.88 mmol/l and 6.01 mmol/l.

According to November 2016 a constant calcium concentration of 3.86 mmol/l to 3.91 mmol/l was measured between 0.0 m to 7.8 m. Between 7.8 m and 15.0 m concentrations increase and subsequently stay constant within the water column from 15.0 m to 21.4 m with values from 5.27 mmol/l to 5.37 mmol/l. For QKv, Z1 and Z2 following concentrations were measured: 6.12 mmol/l, 7.84 mmol/l and 7.80 mmol/l.

In March 2017 calcium concentrations show a slight increase from values of 4.37 mmol/l to 4.48 mmol/l at the surface to 4.82 mmol/l to 4.89 mmol/l at the deepest point of the water column. Ca^{2+} concentration of QKv, QF, Z1, Z2 and A are: 6.15 mmol/l, 4.88 mmol/l, 7.73 mmol/l, 9.00 mmol/l and 4.50 mmol/l.

The measurements of July 2017 show that between 0.0 m and 3.0 m the concentrations of calcium indicate almost unchanging values of 3.14 mmol/l to 3.19 mmol/l. From 3.0 m to around 15.0 m an increase of calcium was measured wherefrom it stays constant down to the bottom of the lake with values measured between 4.87 mmol/l and 4.97 mmol/l. In July 2017 QKv, QF and A indicate a concentration of 6.06 mmol/l, 4.79 mmol/l and 3.21 mmol/l, respectively.

At a depth of 0.0 m to 5.0 m a calcium concentrations of 2.85 mmol/l to 2.93 mmol/l was measured in September 2017. Subsequently calcium content increases up to 5.13 mmol/l within the water column until a depth of 12.6 m wherefrom results do not indicate further changes down to the bottom of the lake with values between 4.98 mmol/l and 5.13 mmol/l. QKv, QF, Z1, Z2 and A show a calcium concentration of 5.85 mmol/l, 4.69 mmol/l, 7.84 mmol/l, 8.53 mmol/l and 2.86 mmol/l, respectively.

Magnesium

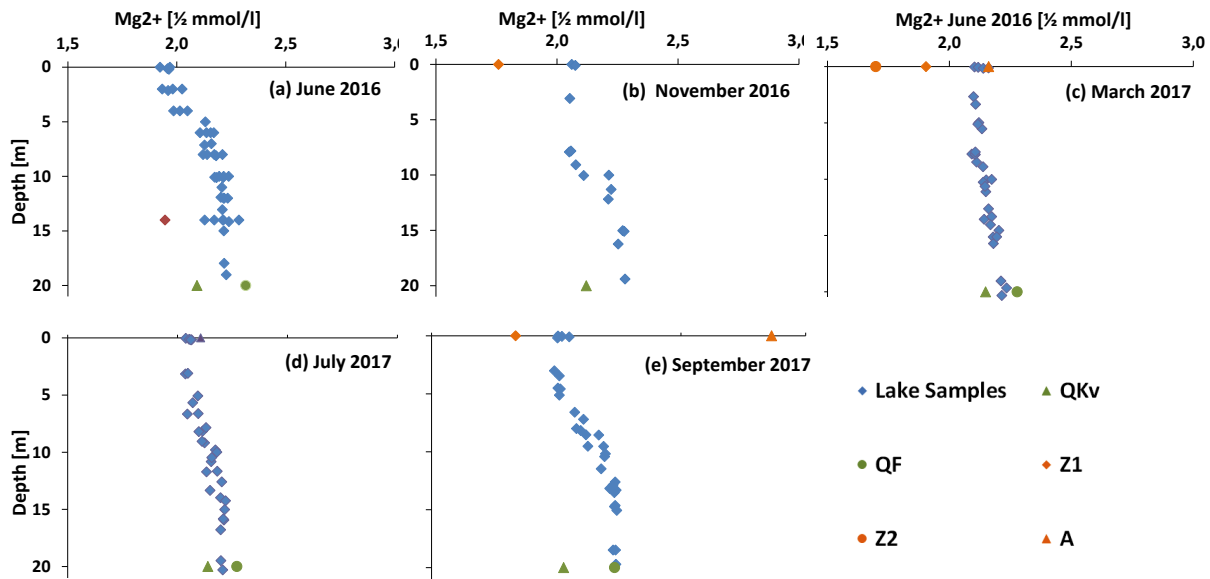


Figure 27 Magnesium concentration in and around Lake Steißlingen in (a) June 2016, (b) November 2016, (c) March 2017, (d) July 2017 and (e) September 2017. The x-axis demonstrates magnesium in [$\frac{1}{2}$ mmol/l] and the y-axis shows depth in [m].

A slight continuous increase of Mg concentration was measured in June 2016 within the entire water column, whereat values of surface water fluctuate between 1.92 mmol/l and 1.97 mmol/l and magnesium contents close to the lake ground lay at 2.23 mmol/l. Sampling point SS5 (14.0 m) indicates a low concentration of 1.95 mmol/l compared with other results within this depth. QF and QKv show values of 2.32 mmol/l and 2.09 mmol/l, respectively.

From 0.0 m to 7.8 m the lake shows a magnesium content between 2.05 mmol/l and 2.08 mmol/l in November 2016. Between 10.0 m and 15.0 m a slight increase of Mg concentration was measured up to 2.27 mmol/l which does not show strong alterations for the remaining part of the water column down to the deepest point of the lake. QKv, Z1 and Z2 have concentrations of 2.12 mmol/l, 1.76 mmol/l and 1.92 mmol/l, respectively.

In March 2017 consistent Mg concentrations from 2.09 mmol/l to 2.23 mmol/l were measured within the entire depth profile of the lake. For QKv, QF, Z1, Z2 and A values of 2.15 mmol/l, 2.28 mmol/l, 1.90 mmol/l, 1.70 mmol/l and 2.16 mmol/l were measured.

The entire water column indicates constant Mg concentrations in July 2017 that fluctuate slightly between 2.04 mmol/l and 2.22 mmol/l. The sampling points QKv, QF and A exhibit a concentration of 2.14 mmol/l, 2.27 mmol/l and 2.11 mmol/l.

The measurements of September 2017 indicate that Mg concentration stays unchanged between 0.0 m and 5.0 m with values of 1.99 mmol/l to 2.05 mmol/l. Down to 15.0 m a slight

increase of Mg concentration up to 2.24 mmol/l was measured, which subsequently stays unchanged down to the deepest measured part of the lake. The sampling points QKv, QF, Z1, Z2 and A show a concentration of 2.03 mmol/l, 2.23 mmol/l, 1.83 mmol/l, 1.35 mmol/l and 2.00 mmol/l, respectively.

3.1.3 Isotopic Parameters ($\delta^2\text{H}$, $\delta^{18}\text{O}$)

$\delta^{18}\text{O}$ Oxygen Isotopes

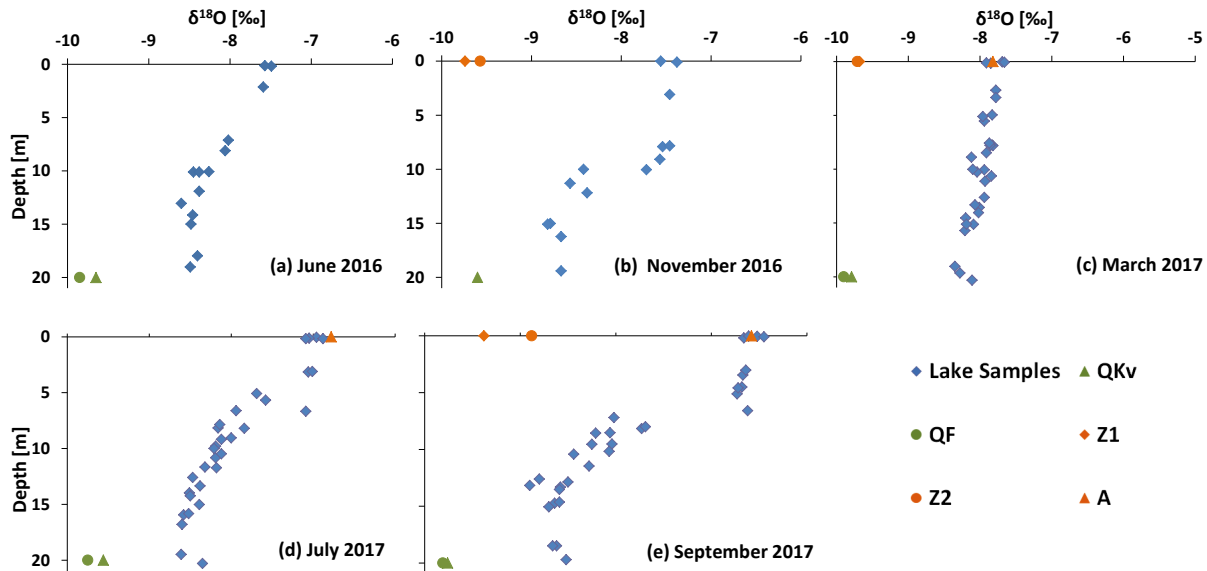


Figure 28 $\delta^{18}\text{O}$ values in [‰] on x-axis vs. depth in [m] on y-axis in (a) June 2016, (b) November 2016, (c) March 2017, (d) July 2017 and (e) September 2017.

In June 2016 $\delta^{18}\text{O}$ ratio decreases from values between -7.57‰ and -7.49‰ at the water surface to -8.45‰ to -8.26‰ measured at a depth of 10.0 m. From 10.0 m to 21.4 m isotopic signatures stay almost unchanged with values between -8.60‰ and -8.26‰ . QKv and QF indicate $\delta^{18}\text{O}$ ratios of -9.85‰ and -9.65‰ .

According to November 2016 in the upper 7.8 m $\delta^{18}\text{O}$ ratios stay almost constant with values from -7.56‰ to -7.38‰ . Between 7.8 m to 21.4 m isotopic signatures of $\delta^{18}\text{O}$ indicate a descent down to 15.0 m from where they stay almost constant with ratios between -8.82‰ and -8.67‰ . QKv, Z1 and Z2 show $\delta^{18}\text{O}$ signatures of -9.60‰ , -9.74‰ and -9.75‰ , respectively.

Due to data from March 2017 it can be distinguished that $\delta^{18}\text{O}$ values indicate slight fluctuations between -8.35‰ and -7.66‰ within the entire water column. QKv, QF, Z1, Z2 and A are -9.79‰ , -9.90‰ , -9.68‰ , -9.71‰ and -7.82‰ , respectively.

A constant $\delta^{18}\text{O}$ ratio between -7.01‰ and -6.88‰ was measured within the upper 3.1 m of the water column in July 2017. Subsequently a continuous descent down to -8.58‰ to -8.39‰ occurs at a depth of around 15.0 m. From 15.0 m to the deepest point of the lake $\delta^{18}\text{O}$ values do not show further changes. QKv, QF and A have isotopic ratios of -9.56‰ , -9.75‰ and -6.78‰ .

In the month of September 2017 $\delta^{18}\text{O}$ ratios slightly fluctuate between -6.73‰ and -6.45‰ within the upper 6.6 m of the water column. Between 6.6 m and 12.6 m the lake water gets continuously enriched in light ^{16}O isotopes with depth. From 12.6 m to the deepest point of the lake $\delta^{18}\text{O}$ values do only show slight alterations between -8.90‰ and -8.50‰ . QKv and QF show similar values of -9.76‰ and -9.81‰ . The $\delta^{18}\text{O}$ ratio for Z1, Z2 and A is -9.38‰ , -8.88‰ and -6.58‰ .

$\delta^2\text{H}$ Hydrogen Isotopes

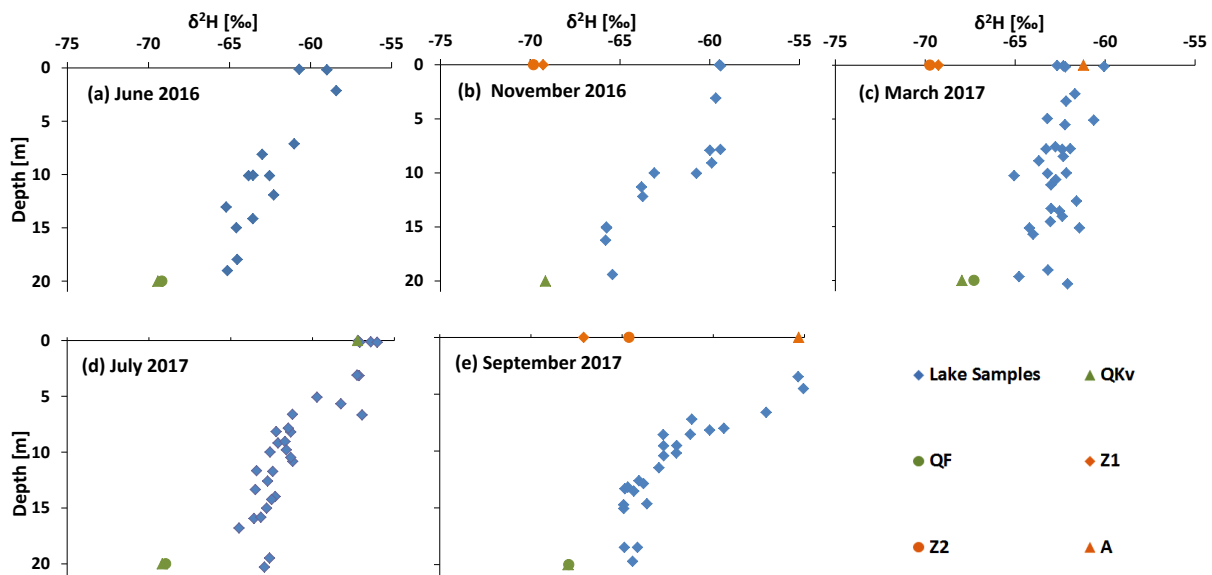


Figure 29 The plots indicate $\delta^2\text{H}$ in [‰] on the x-axis vs. depth in [m] on the y-axis in (a) June 2016 (b) November 2016 (c) March 2017 (d) July 2017 (e) September 2017.

In June 2016 $\delta^2\text{H}$ values lay within -58.4‰ and -60.7‰ at the upper part of the water column and subsequently decrease slightly down to -65.2‰ at a depth of 13.0 m. From 13.0 m down to the deepest point of the lake a recurring increase was measured up to -64.5‰ . QKv and QF indicate $\delta^2\text{H}$ signatures of -69.2‰ and -69.4‰ .

From 0.0 m to 7.8 m the lake show constant $\delta^2\text{H}$ values between -59.4‰ and -59.7‰ in November 2016. From 10.0 m until 15.0 m a lowering of $\delta^2\text{H}$ ratios was measured down to -65.8‰ which subsequently stays almost constant to the deepest point of the lake and an isotopic signature of -65.4‰ . QKv, Z1 and Z2 indicate $\delta^2\text{H}$ values of -69.2‰ , -69.3‰ and -69.8‰ .

Measurements of March 2017 exhibit some slight alterations in $\delta^2\text{H}$ signature between -65.1‰ and -60.1‰ along the entire water column. QKv, QF, Z1, Z2 and A show an isotopic ratio of -68.0‰, -67.3‰, -69.3‰, -69.7‰ and -61.2‰, respectively.

In July 2017 $\delta^2\text{H}$ ratios do not indicate strong fluctuations at the upper 3.0 m of the water column where values between -65.1‰ and -60.1‰ were measured. From 3.0 m to 16.8 m $\delta^2\text{H}$ values decrease continuously down to -64.5‰. Close to the deepest point of the lake slightly increased $\delta^2\text{H}$ ratios of -62.9‰ and -62.6‰ were measured. QKv, QF and A indicate isotopic signatures of -69.2‰, -69.0‰ and -57.3‰.

In the month of September 2017 $\delta^2\text{H}$ ratios between -55.4‰ and -54.4‰ were recorded in the uppermost 4.5m of the water column. Between 4.5m and 11.5m the lake water gets continuously enriched in light isotopes with depth. A $\delta^2\text{H}$ signature from -64.9‰ to -63.0‰ was measured between 11.5m down to the deepest zone of the lake. QKv and QF show similar values of -68.0‰ and -67.2‰. The $\delta^2\text{H}$ ratio for Z1, Z2 and A is -67.1‰, -64.6‰ and -55.3‰, respectively.

Groundwater Mixing Ratio

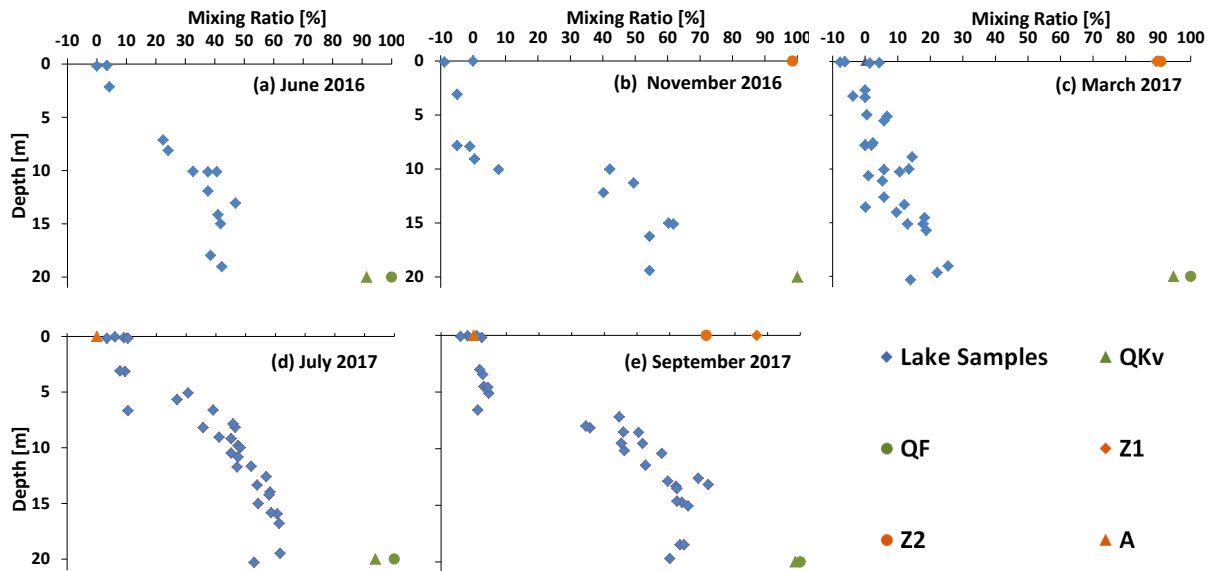


Figure 30 Groundwater mixing ratio in [%] vs. depth in [m] in the months of (a) June 2016 (b) November 2016 (c) March 2017 (d) July 2017 (e) September 2017.

In June 2016 groundwater ratio increases between the water surface and 10.0 m from 0.0%-3.4% to 32.6%-37.7%. From 10.0 m to the deepest point of the lake groundwater ratios change slightly between 37.7% and 47.0%. QF represents the groundwater and has therefore a groundwater ratio of 100.0% while QKv reveals a groundwater ratio of 100.0%.

According to November 2016 calculations show that there is no groundwater in the upper 10.0 m of the water column. From 10.0 m to 15.0 m groundwater ratio increases to 61.8%. The percentage of groundwater subsequently decreases slightly between 15.0 m and 21.4 m with a ratio of 54.4%. QKv, Z1 and Z2 are 100.0%, 100.0% and 98.5%, respectively.

A slight continuous increase with depth was calculated for groundwater ratio within the entire water column of the lake in March 2017. The surface values lay within -7.7% and 4.3% and ratios close to the deepest area of the lake fluctuate between 13.9% and 25.5%. For the sampling points QKv, QF, Z1, Z2 and A following percentages were calculated: 94.7%, 100.0%, 89.4% and 90.9%, respectively.

When regarding the measurements of July 2017, it can be distinguished that slight alterations in groundwater ratio were calculated between 0.0 m and 3.0 m with values from 3.4% to 10.4%. From 3.0 m to 15.0 m an increase of groundwater ratio was recorded, wherefrom slightly changing values between 52.7% and 61.6% were calculated. QF, QKv and A show percentages of 93.6%, 100.0% and 0%, respectively.

For the upper 6.6 m of the water column low groundwater ratios between -4.0% and 4.6% were calculated in September 2017. At a depth from 6.6 m to 12.6 m the percentage of groundwater ratio increases continuously wherefrom it reveals only slight alterations between 59.4% and 71.8% down to the deepest zone of the lake. QF and QKv indicate groundwater ratios around 100.0%. Sampling points Z1, Z2 and A show a groundwater ratio of 86.7%, 71.2% and 71.2%, respectively.

3.2 Quantification of groundwater inlets of Lake Steißlingen

Saturation Index of Calcite

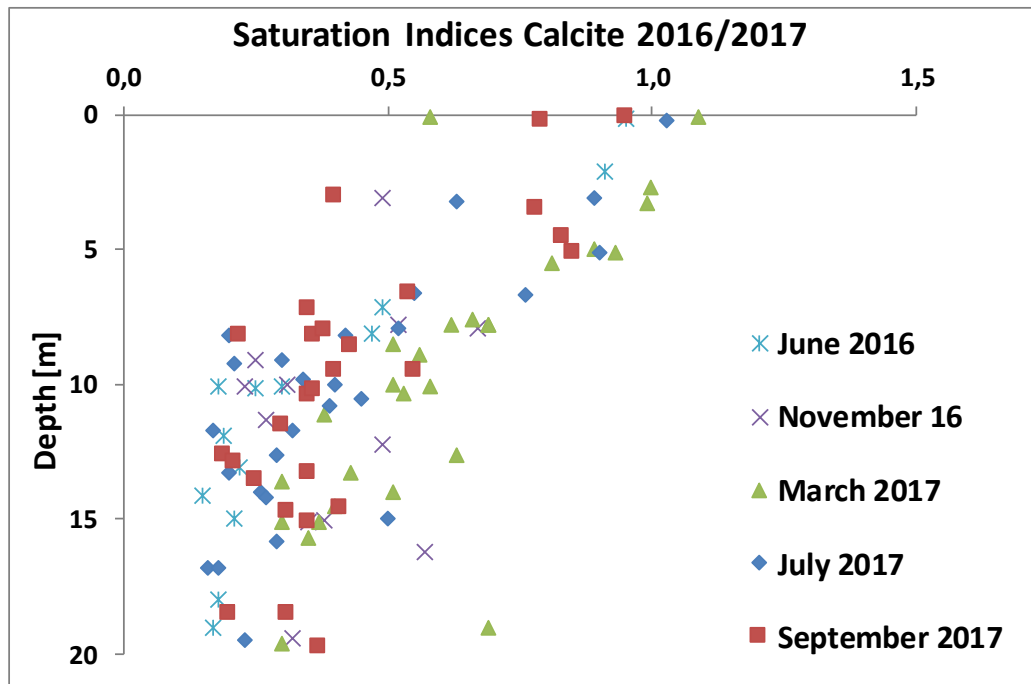


Figure 31 Calcite Saturation indices of Lake Steißlingen from different seasons of 2016/2017 (calculated with Phreeqc) against depth.

The saturation index of calcite gets defined as: $SI_{\text{Calcite}} = \log(IAP_{\text{Calcite}}/K_{\text{Calcite}})$. If $SI_{\text{Calcite}} = 0$, there is equilibrium between the solution and the mineral. An $SI < 0$ indicates subsaturation and an $SI > 0$ supersaturation.

Saturation indices of Calcite decreases with depth throughout the entire year in Lake Steißlingen. In the upper 5.5m SI_{Calcite} -values from 0.40 up to 1.09 were calculated. A smaller range of SI_{Calcite} -values were recorded from 5.5m down to the bottom of the lake from 0.15 to 0.76. All values show supersaturation, but the upper 5.5m get dominated by higher SI_{Calcite} values when comparing it to the water layers below 5.5m.

Inverse Modeling by Phreeqc

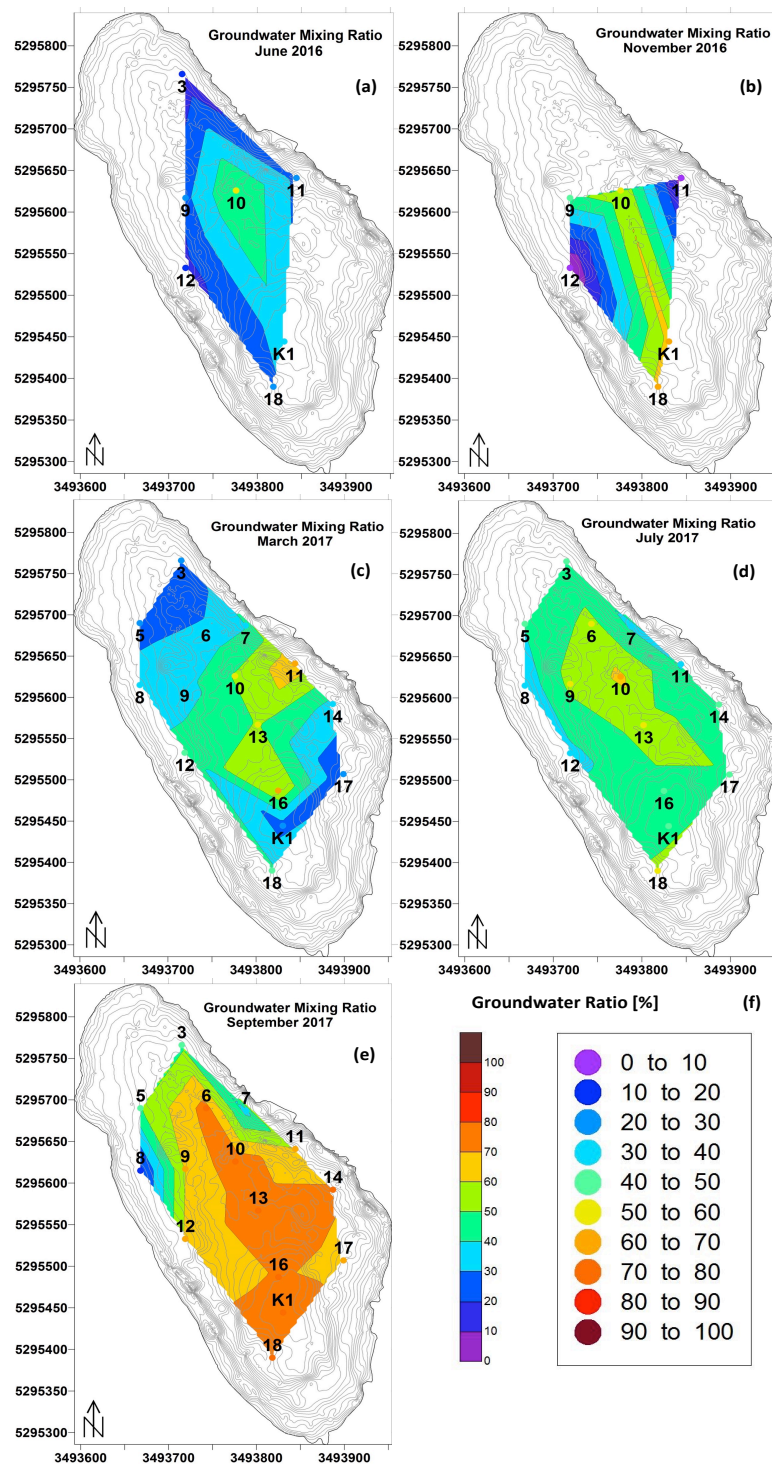


Figure 32 Calculated groundwater mixing ratio (based on Phreeqc) in [%] with interpolation between the sampling points 2016/2017 (a)-(e) June16, Nov 16, March17, July 17, Sept17; (f) legend.

For the delineation of Phreeqc data, which was calculated by inverse modeling only bottom values of the lake were used where most ratio of ground water gets assumed.

In the circumference nearby sampling point 10 in the middle of the lake a groundwater ratio of 40%-60% can be found in June 2016 around 14.1 m. This decreases with approaching to the lakes southern part, whereat 30%-40% groundwater at a depth of 19.0 m is found. Close to the shore line a low groundwater ratio of 10%-30% was calculated between 7.1 m and 11.0 m depth and again in 18.0 m in the middle of the lake (sampling points 3, 9, 12, 18 and 11).

In November 2016 groundwater ratios decrease from the middle of the lake to the direction of the shore line. The middle of the lake (sampling point 9, 10, K1, 18) in a depth between 12.2 m to 19.4 m indicates a groundwater ratio between 40%-70%. At the margin of the lake where samples were taken at a depth of 7.9 m and 9.1 m (sampling point 11, 12) groundwater ratios show values between 0%-40%.

The bottom water values in the month of March 2017 indicate a groundwater ratio between 40%-70% in the middle area of Lake Steißlingen between 7.8 m and 10.3 m and from 15.1 m to 19.6 m (sampling point 7, 11, 12 and 16). Moving towards the north-western and south-eastern part of the lake a descent of groundwater with values between 10%-40% is observed between 7.6 m to 13.6 m and from 19.0 m to 20.3 m.

In a depth between 8.2 m and 15.8 m (sampling point 3, 5, 18, 17, 14) in the middle of Lake Steißlingen, a groundwater ratio from 40%-70% was calculated by Phreeqc in July 2017. Towards the north-eastern and western shore side groundwater ratios are smaller between 30%-40% around 6.6 m to 9.8 m (sampling point 8, 11 and 12).

In September 2017 groundwater ratios from 70%-80% were found between 12.6 m and 19.7 m (sampling point 6, 10, 13, 14, 16, K1, 18) in the center of the lake. Around the middle of the lake but closer to its margin a slightly lower groundwater ratio of 60%-70% was calculated between 8.6 m and 12.9 m (sampling point 9, 12, 17, 11). Groundwater ratios decrease down to 30%-60% in the northern, north eastern and eastern part of the lake at a depth of 7.2 m to 8.5m. A low groundwater ratio of 20%-30% was calculated in 6.6 m depth (sampling point 8).

3.3 Stratification and mixing dynamics within Lake Steißlingen (EnviWatch)

During the cold months of November 2017, December 2016/2017 and January 2017 an air temperature range that lies within -14.3°C to 8.3°C was recorded. In spring and fall months (February 2017, March 2017, April 2017, October 2017) temperature values show a slight shift towards warmer temperatures compared to November, December and January, and values from -5.2°C to 23.2°C were measured. Another shift towards warmer air temperature was measured in summer of 2017 (May 2017 to September 2017) with values between 3.3°C and 32.2°C .

Most wind velocities measured fluctuate between 0.0 km/h and 5.0 km/h during the measurement phase of EnviWatch between December 2016 and 2017. Two stronger wind velocities, compared to the rest of the results, were recorded at the 18th of August 2017 with 9.5 km/h and at the 21st of November 2011 with 8.1 km/h .

During the entire measuring phase between December 2016 and December 2017 pressure values fluctuate between 931.0 hPa and 990.0 hPa .

In December 2016 and January 2017 solar radiation fluctuates between 0.0 W/m^2 and 514.8 W/m^2 . From February 2017 to April 2017 solar radiation show alterations within a bigger range between 0.0 W/m^2 and 1178.6 W/m^2 . Solar radiation indicates the highest fluctuations within the whole year from 0.0 W/m^2 to 1208.1 W/m^2 between May 2017 and September 2017. Between October 2017 and December 2017 solar radiation values constantly alter from 0.0 W/m^2 to 994.4 W/m^2 . From 30th of October 2017 until the 31st of December 2018 the values for solar radiation fluctuate between 0.0 W/m^2 and 861.1 W/m^2 . Due to a 24/7 measurement the values 0.0 W/m^2 for the night time were also included.

Low monthly precipitation rates were measured in a range of 0.7 mm to 31.1 mm from December 2016 to March 2017. In the months from April 2017 to August 2017 precipitation rates increased with monthly precipitation values between 97.1 mm and 135.1 . Whereat hereby the month of May 2017 indicates an exception with a lower monthly precipitation rate of 51.9 mm . In September 2017 and November 2017 monthly precipitation rates are similar with values of 74.0 mm and 65.1 mm , respectively. During October 2017 and December 2017 measurements show smaller precipitation values of 31.8 mm and 27.1 mm , respectively.

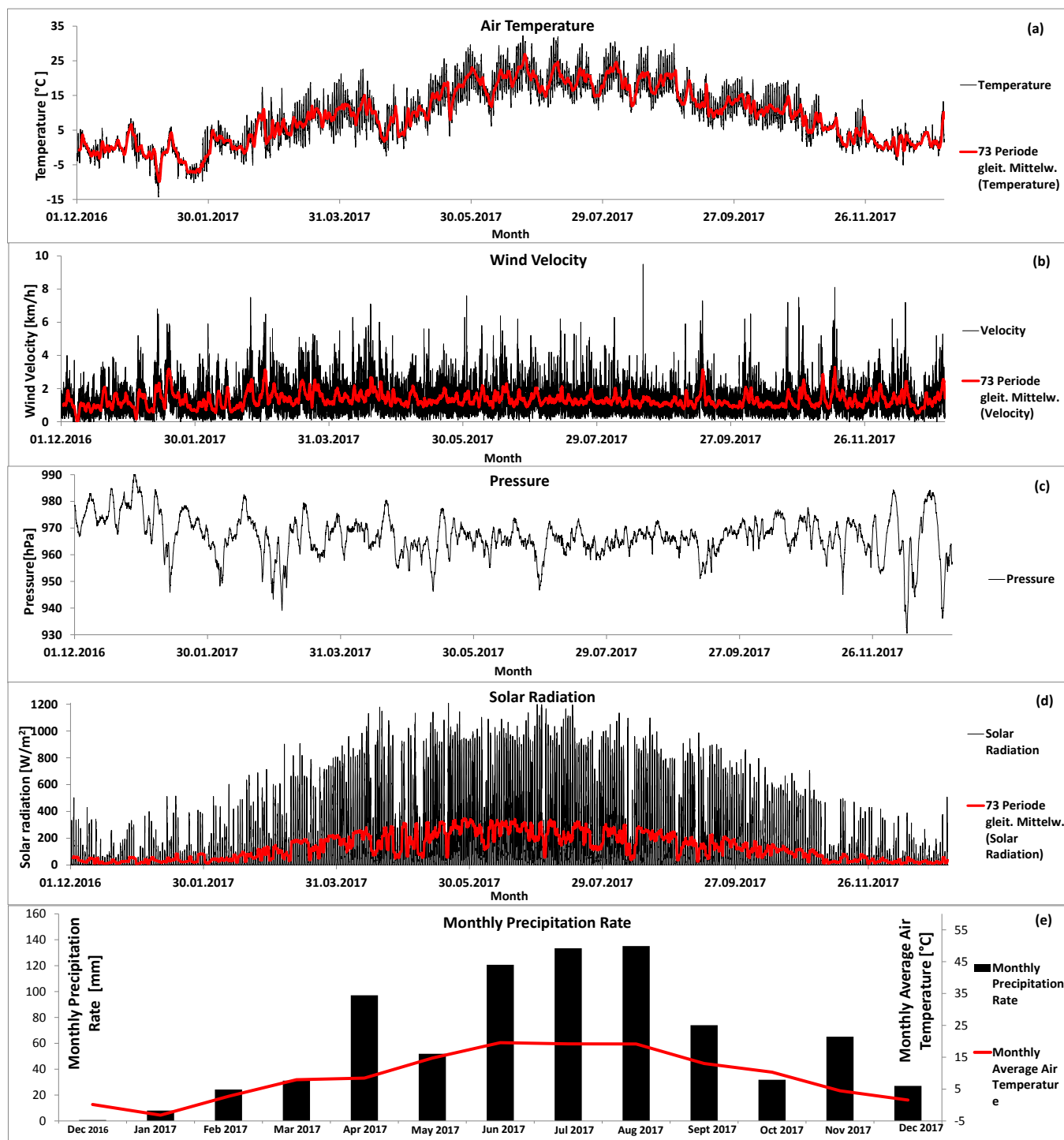


Figure 33 Following meteorological parameters were measured in 2016/2017 at EnviWatch station: (a) Air temperature, (b) wind velocity, (c) pressure, (d) solar radiation and (e) monthly precipitation rate.

4 Discussion

4.1 Error Discussion

Various faults can occur during sampling, measurement, handling, evaluation and transport which will be discussed and explained in this chapter.

Due to a low concentration close to the detection limit of ammonium and nitrate, low accuracies were calculated for the measurements of NH_4^+ ($\pm 13.0\%$) and NO_2^- ($\pm 15.3\%$) compared to Na^+ ($\pm 1.1\%$), K^+ ($\pm 3.4\%$), Ca^{2+} ($\pm 1.7\%$), Mg^{2+} ($\pm 0.8\%$), Cl^- ($\pm 0.8\%$), NO_3^- ($\pm 0.5\%$) and SO_4^{2-} (2.1%) that show concentrations within an appropriate value range for a precise analysis. Therefore, the results of Ammonium and Nitrite are mainly useful for proving its abundance. For further data evaluation this deficit has to be considered.

The measurements on the ground of the lake were not done directly at its bottom due to technical restrictions, but at about 0.0 m-1.0 m away from the sediment. Due to this fact measurements could not have been done directly at the bottom of the lake, which can impede punctual groundwater detection. On the other hand side this technique was implemented because the water sampler, equipped with measuring sensors, should not tangent the sediment which prevents a disturbance of the measurement process and protects the sensitive equipment that was used.

During the measuring campaign in November 2016 a defect of the CTD occurred wherefore the oxygen concentration was only calculated from measured oxygen saturations. Inaccuracies can occur because a different calculation method was applied compared to the one used by the intern oxygen sensor.

In June 2016 sampling point SS5 shows noticeable deviating values for several parameters (Chloride, Sulfate, EC, pH, alkalinity, water hardness, NH_4 , Na^+ , K^+ , Ca^{2+} , Mg^{2+}) at a depth of 14.0 m. A measurement error can be excluded, which can be explained by the fact that the sample was measured several times and the parameters were measured by using different sampling bottles and different instruments. Thus, it is statistically improbable that all bottles get contaminated simultaneously and several instrumentations show measuring mistakes for the same sample.

The water sample which was taken at QF already experienced a pumping process which might have changed temperature due to contact of a warmer environment such as near soil surface

areas or the atmosphere, which furthermore can lead to a slight change of dissolved oxygen values.

Furthermore, the measurement of pH and TA of QF and QKv could deviate from its real value. This can be explained by a degassing effect when groundwater gets in contact with the atmosphere (Hofmann, 2011). To avoid a strong exchange with the atmosphere and a degassing effect, the sampling bottles were directly filled up under continuous flowing water without headspace in the bottle and subsequently transported smoothly, followed by an immediate measurement in the laboratory. Moreover QF, which gets assumed as the main groundwater source of Lake Steißlingen, could not have been sampled in November 2016 because the pump was closed due to protection against pipeline freezing. This lack could make comparison difficult between groundwater and lake samples, as well as the groundwater reference values of QF and other months.

After sampling, the bottles were stored on the rubber boat and in the car until the end of the sampling day. We tried to keep the exposure time in the sun for the bottles as short as possible, but this can have influence on pH and alkalinity results because CO₂ degassed due to heating and shaking of the water samples.

The number of sampling points of the measuring campaign is smaller for the first sampling date in June 2016 and November 2016 compared to the other months. But the quantity of the sampling points does not influence data evaluation, which can be explained by the fact that measurements mainly show same results within the respective depths of the water layers in the entire lake.

As depth was measured with the CTD by a winch, some inaccuracies occur for the pressure measurements and thus the depth, but they can be assumed to be minimal and therefore negligible.

At some sampling points, depth intervals have a long way away from each other, which makes it more inaccurate to interpret the part in-between. The parameters measured with the CTD however recorded values along the entire water column and do not show considerable differences compared to the punctual measurements at the respective sampling point depths.

The localization of the sampling points during sampling and measuring was slightly imprecise, depending on the weather conditions that caused strong to light movements of the boat and the GPS accuracy of ± 1.0 m-5.0 m.

EnviWatch was only controlled every three months, so extern disturbance such as bathing people or stormy weather conditions might have changed some of the measurements. Due to the fact that the parameters were measured in short intervals for a long period thus a big amount of data is available and does not affect the general trend of the results throughout the year.

4.2 Hydrochemistry and Stratification of Lake Steißlingen

This chapter describes the general hydrochemistry and stratification of Lake Steißlingen over the year, whereat the aspect of incoming groundwater was hereby excluded and gets discussed in chapter 4.3 and 4.4.

Lake Steißlingen shows a typical thermohaline stratification within the temperate zone due to seasonal temperature and density anomalies throughout the year (Spirkaneder, 2016). During summer months (June 2016, July 2017 and September 2017) a strong temperature gradient with depth is perceived, caused by high temperature in the surface layer in contrast to constant colder bottom values, which can be explained by higher global insolation and warmer air temperatures. This effectuates a strong stratification within this period of the year (See Figure 34 (a)) and influences the processes in the upper layer of the lake which is closest and in exchange to the atmosphere. In the months of June 2016, March 2017, July 2017 and September 2017 a typically thermocline can be distinguished within the water column which leads to the assumption that the epilimnion occurs in a depth from 0.0 m to between 3.0 m and 5.0 m (See Figure 34 (a)). The hypolimnion within these months is between 8.0 m and 10.0 m down to the deepest point in the water column. This can be seen from CTD results of K1 (See Figure 34 (a)), which is representative for the entire lake, because same trends were measured with depth and show a horizontal homogeneity. The development of the epi- and hypolimnion, and thus the expansion of the metalimnion, depends on the season.

The temperature stratification correlates well with the CTD results of electrical conductivity for the measuring campaign in 2016/2017 (See Figure 34(b)), whereat EC starts to increase in a specific depth between epi- and metalimnion depending on the measuring month. The low EC values in the epilimnion can be explained by biological consumption during the months of biological activity and the fact that surface inlets do not fungate as ion source for the epilimnion of the lake due to a low recharge value of 2.0 l/s (Spirkaneder, 2016).

A temperature anomaly occurs between the month of November and December in both years (2016/2017) for about ten days, depending on the year. This phenomenon is caused by a denser water layer between 10.0 m and 18.0 m, which indicates a slightly higher water temperature of around 0.7°C-1.0°C depth compared to the layers below and above (See Figure 35).

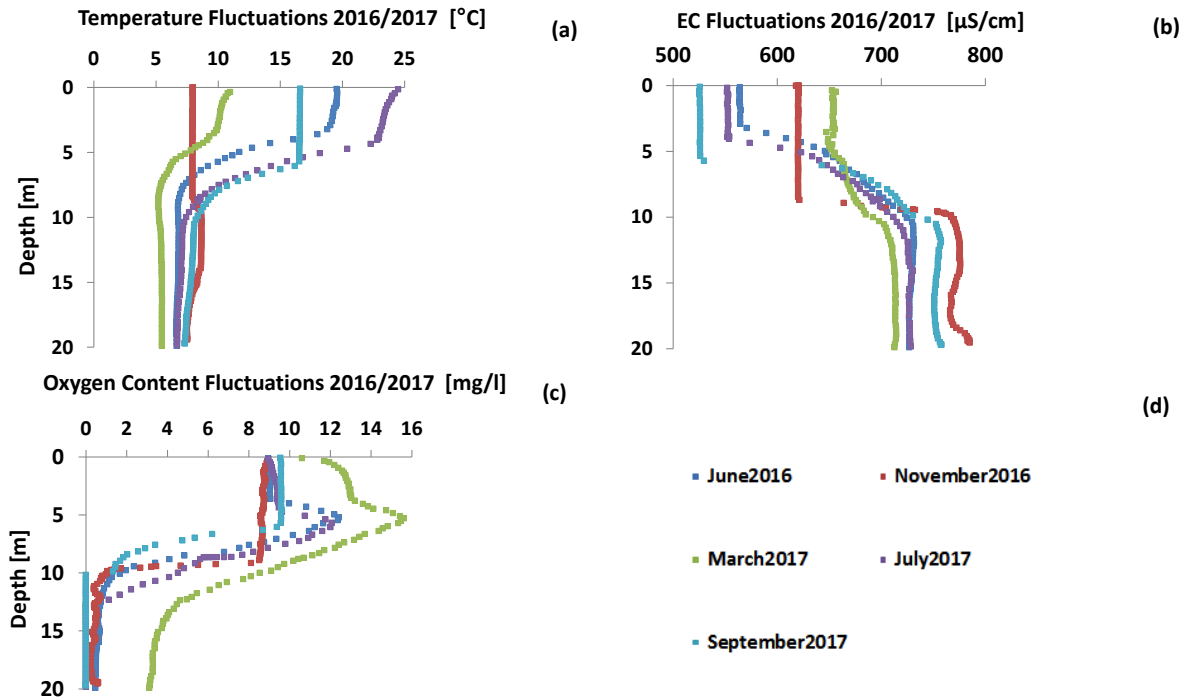


Figure 34 (a) represents temperature, (b) electrical conductivity and (c) represents dissolved oxygen fluctuation in 2016/2017 of the measurement of CTD depth profile which is representative for the entire lake on station K1.

Lake Steißlingen only approaches an entire mixing process, which facilitates an exchange of ions, dissolved oxygen and temperature between the stratification layers and is quite unusual compared to other lakes such as Lake Constance which usually experiences a complete annual circulation. According to Sundaram et al. (1971) a homothermal temperature stratification of 4.0°C, where water indicates the highest density, can be supposed for temperate lakes in early spring months. Lake Steißlingen indicates a comparatively warm hypolimnion and only approaches 4.0°C for a short time in winter with a measured temperature of 4.6°C. A comparatively warm hypolimnion can be caused by climate change and can therefore cause an incomplete mixture of the lake according to Wahl et al. (2014), which gets excluded for Lake Steißlingen due to a high groundwater ratio. The reason for the unusual temperature anomaly within the water column gets discussed in chapter 4.4. Despite the phenomenon of an incomplete mixing process, Lake Steißlingen gets classified as monomictic by LUBW (2014). The mixing approach happens between November 2016 and March 2017, assumable in December, where depth profiles show almost consistent temperature values within the entire water column (See Figure 35). The exchange effect between hypo- and epilimnion of this process can be perceived chemically, isotopically and physically in March 2017 and its approach to concentration homogeneity within the entire water column for several parameters (K, $\delta^{18}\text{O}$, $\delta^2\text{H}$, SO_4^{2-} , Cl^- , Mg^{2+} , Ca^{2+} , $\text{NH}_4^+\text{-N}$, water hardness, EC).

The lakes stratification can also be distinguished chemically (O_2 , TA, pH, water hardness, Na^+ , Ca^{2+} , Mg^{2+} , Cl^- , $SI_{Calcite}$) and isotopically (2H , ^{18}O) due to different concentrations and signatures depending on the layers. The parameters of oxygen, δ^2H , $\delta^{18}O$, CO_3^{2-} , $SI_{Calcite}$ and pH show decreased values in the hypolimnion compared to the epilimnion.

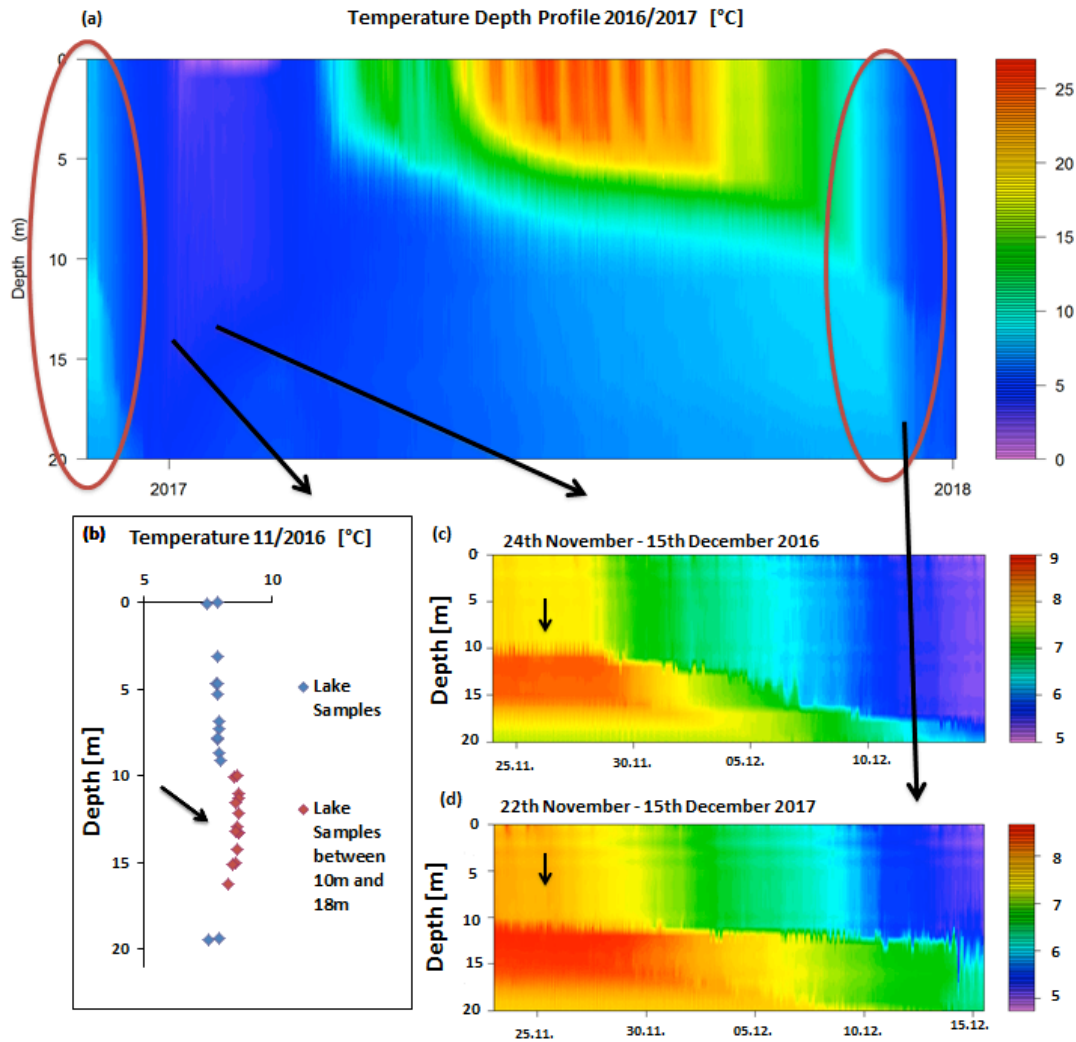


Figure 35 Temperature depth profile for November 2016 to December 2017 (a), November-December 2016 (c), November-December 2017 (d) measured with the thermistor chain and a large-scale delineation of temperature in November 2016 (b) measured with the CTD.

Whereas TA, water hardness, K^+ , Na^+ , Ca^{2+} , Mg^{2+} , Cl^- and HCO_3^- indicate increased concentrations in the hypolimnion when comparing it to the upper layer of Lake Steißlingen.

The parameter of water hardness gets influenced by Ca^{2+} , Mg^{2+} , pH and HCO_3^- concentrations and shows differences between hypolimnion and epilimnion. An average water hardness of 16.2°dH/5.8 ½ mmol/l in the epilimnion and 19.8°dH/7.1 ½ mmol/l in the hypolimnion is observed

and gets defined as “etwas hart” to “hart” according to “Härtegrade von Wasser nach Klut-Olzewski” (Langguth, 2004).

Table 1 Arithmetic water composition of the epilimnion and metalimnion, hypolimnion, QF and QKv and the assumed groundwater composition:

Sampling area	Mg2+ [mg/l]	Ca2+ [mg/l]	K+ [mg/l]	Na+ [mg/l]	Cl- [mg/l]	SO42- [mg/l]	HCO3- [mg/l]	CO32- [mg/l]	NH4+-N [µg/l]	NO3-N [µg/l]
Epi- and metalimnion (Arithmetic mean)	25,0	75,3	2,2	15,7	30,8	41,9	287,5	1,2	310	1082
Hypolimnion (Arithmetic mean)	26,9	98,2	2,4	16,6	32,4	42,3	367,7	0,4	895	1012
QF (Arithmetic mean)	27,6	96,4	1,1	4,5	8,7	37,5	359,3	0,4	75	3020
QKv (Arithmetic mean)	25,6	121,0	11,7	17,1	31,5	31,4	421,9	0,4	21	7456
Groundwater (33,5% QKv + 66,5% QF)	26,9	104,6	4,7	8,7	16,3	35,5	380,3	0,4	57	4508

The average $\delta^2\text{H}$ composition of the epilimnion in 2016/2017 is slightly enriched in heavy isotopes with -58.4‰ compared to -63.74‰ in the hypolimnion with a slight shift towards light isotopes. In the epilimnion a $\delta^{18}\text{O}$ signature of -7.36‰ was measured, which is enriched in heavy isotopes when comparing it to -8.45‰ in the hypolimnion. The shift towards a heavy isotope signature is caused by an evaporation effect at the surface of the lake.

In the epilimnion the average chloride and potassium concentrations during the measurement period in 2016 and 2017 are 30.8 mg/l and 2.2 mg/l, respectively (See Table 1). For Cl⁻ increased concentrations between 31.7 mg/l and 32.0 mg/l were measured in March 2017 at the water surface of Lake Steißlingen, which is attributable to street salting against street freezing at two streets nearby during winter (LUBW, 2014).

The average NO₃-N composition of Lake Steißlingen has a concentration of 1.1 mg/l in the epilimnion and 1.0 mg/l in the hypolimnion in 2016/2017, which considerably increased compared to the measuring campaigns in 2014 with 0.7 mg/l and 1987 with 0.6 mg/l (LUBW, 2014; See Table 1). An explanation for the increase of nitrate with time could be linked to the raise of agricultural land use in the vicinity of Lake Steißlingen.

For the measuring campaign in 2016/2017 average calcium and magnesium values of 75.3 mg/l and 25.1 mg/l in the epilimnion of the lake were recorded (See Table 1). In the hypolimnion of Lake Steißlingen higher average calcium and magnesium concentrations of 98.2 mg/l and 26.9 mg/l were measured in 2016/2017 and are supposed to be conservative elements (See Figure 39 (a) and Table 1). So, magnesium, calcium and alkalinity concentrations are higher in the hypolimnion compared to the epilimnion. The increased calcium concentration in the hypolimnion can be explained by a lower pH of around 7.5 combined with a higher dissolution rate.

Another reason for the concentration difference of calcium in the water column, is a higher biological consumption of nutrients close to the sunlight reaching area of the water column. The

high productivity in the epilimnion of the lake can cause a drop down of CO_2 and thus a pH change to basic conditions around 8.2, which furthermore causes a shift of the carbonic acid equilibrium (Hofmann, 2011). A rise of biological activity gets assumed in the months of March 2017, July 2017 and September 2017 due to increased chlorophyll A contents caused by algae bloom and occurring high concentrations of cyanobacteria within this period of the year measured by LUBW (2014). This process gets supported by a decrease of CO_2 solubility with increasing water temperatures during warmer months and a shift to higher pH conditions (Hofmann, 2011). Therefore, the shift of the carbonic acid equilibrium in combination with increased biological activity and CO_2 solubility can lead to the precipitation of calcite particles (Hofmann, 2011) and explains the occurrence of lake whitening in the months of March 2017, July 2017 and September 2017. The calculations of Phreeqc mainly show $\text{SI}_{\text{Calcite}}$ -values around 0.8 in the upper 5.5m in these months, which indicate a strong calcite supersaturation according to Müllegger (2013). The calcite supersaturation can cause precipitation of calcite and thus strengthens the presumption of lake whitening.

Phreeqc calculations showed that values of $\text{SI}_{\text{Calcite}}$ also demonstrate a variation with lake depth. The $\text{SI}_{\text{Calcite}}$ values calculated for the upper 5.5m mainly lay around 0.8 and are mostly higher compared to the hypolimnion, where calcite saturation indices from 0.15 to 0.76 occur. The Ca^{2+} and HCO_3^- concentrations of the hypolimnion can rise due to a fall of calcite particles in the water column originating from the epilimnion and a subsequent dissolution below the compensation depth of the lake, where more CO_2 gets produced than consumed and lowers pH (See Figure 42). Therefore, all values of $\text{SI}_{\text{Calcite}}$ indicate moderate to strong supersaturation, which is typical for calcium and carbonate rich lake systems like Lake Steißlingen (Koschel, 1997). $\text{SI}_{\text{Calcite}}$ values >0 can be clarified by the fact that the lake indicates a higher CO_2 partial pressure compared to the atmosphere, which leads to a degassing effect resulting in a higher saturation index for calcite. The higher $\text{SI}_{\text{Calcite}}$ values at the upper 5.5m, compared to the water body below, can be explained by stronger photosynthetic activity and the connected assimilation of CO_2 and HCO_3^- , which can lead to calcite precipitation (Müllegger, 2013). Despite positive $\text{SI}_{\text{Calcite}}$ values, calcite dissolution can occur in Lake Steißlingen because according to Eusterhues (2000) calcite is verifiable in the sediment of the lake system. The dissolution of calcite might appear through increased CO_2 concentration caused by bacterial respiration of organic material close to or at the surface of the sediment.

The saturation index for calcite was calculated by Phreeqc Interactive 3.4.0-12927. Therefore, the conservative and major parameters of each sample (pH, T [°C], alkalinity as HCO_3^- [mg/l], dissolved oxygen [mg/l], Ca^{2+} [mg/l], Mg^{2+} [mg/l], K^+ [mg/l], Na^+ [mg/l], N(5) as NH_4^+ [mg/l], Cl^- [mg/l], N(-3) as NO_3^- [mg/l], S(6) as SO_4^{2-} [mg/l], ^2H [‰], ^{18}O [‰]), measured during the five measuring campaigns, were included in the input file and the calculation of $\text{SI}_{\text{Calcite}}$ by Phreeqc. For the precision of the calculation, the species of $\text{NH}_4\text{-N}$, $\text{NO}_3\text{-N}$, SO_4^{2-} and alkalinity were written as N(5) as NH_4^+ , N(-3) as NO_3^- , S(6) as SO_4^{2-} and alkalinity as HCO_3^- . Another reason why alkalinity was written as “alkalinity as HCO_3^- ” is because in natural waters at a pH between 7.3-8.3

alkalinity equates approximately the HCO_3^- content. When TA is written as alkalinity only, Phreeqc uses the equivalent molar mass of $M=1/z \cdot M_{\text{CaCO}_3}$ for the calculation instead of $M=1/z \cdot M_{\text{HCO}_3^-}$, which would falsify the results.

The average oxygen concentrations of 7.6 mg/l in the epilimnion and 1.3 mg/l in the hypolimnion in 2016/2017 for Lake Steißlingen are low compared to other lakes in Baden-Württemberg like Bergsee and Rohrsee with an average O_2 concentration of 9.8 mg/l and 9.0 mg/l, respectively in 2014. It is noticeable that during the months of June 2016, March 2017 and July 2017 O_2 , with concentrations of 10.8 mg/l to 15.7 mg/l, are higher around 5.0 m depth within the water column. Additionally, a supersaturation of oxygen between 101.9% and 133.1% occurs within these months around 5m. A driving factor for this occurrence is the oxygen producing photosynthesis in connection with high solar insolation during these months. This assumption is supported by a CO_2 deficit in the upper layer during June 2016, March 2017 and July 2017 and same findings in former studies (LUBW, 2014).

In contrast to that suboxic to dysoxic conditions were recorded in June 2016, November 2016, June 2016 and July 2017 from a depth of around 10.0 m down to the bottom of the lake with a value range of 0.2 mg/l to 1.3 mg/l (Tyson et al., 1991). Slightly higher oxygen contents between 2.9 mg/l and 3.9 mg/l were measured in March 2017 from 14.0 m down to the lake floor and thus suboxic conditions are assumed for this part of Lake Steißlingen during this period of the year. These seasonal fluctuations get represented clearly at the CTD profile of K1 (See Figure 34 (c)).

As it can be seen from the measurement of chemical parameters enhanced nutrient values and almost anoxic conditions occur in the hypolimnion, which is typical for thermally stratified lakes (Rimmer et al., 2005). According to Rimmer et al. (2005) vertical mixture between epi- and hypolimnion influences geochemical and biological processes, which gets further discussed in the following.

The natural concentrations of SO_4^{2-} , O_2 , Fe^{2+} , H_2S , NO_3^- etc. get driven by oxidation and reduction processes in ground waters and marine sediments, which determines stability and solubility of components (Appelo et. al, 2005). These processes also occur in lacustrine systems and happen due to the essential energy extract of available elements in the aqueous system by microbiological activity and electron transfer reactions (Bertleff, 2001). Due to Berner (1981) microorganisms firstly use up the element with the most efficient energy state, for example oxygen, and subsequently migrate to the next substance that delivers energy when the first is limited or completely consumed, for example NO_3^{2-} . These redox processes (See Figure 36 equation (1)-(9)) happen in a certain succession caused by energetic differences: $\text{O}_2 > \text{NO}_3^- > \text{Mn}^{2+} > \text{Fe}^{2+} > \text{H}_2\text{S} > \text{CH}_4 > \text{Fe}^{2+}$ (See Figure 38).

As mentioned before suboxic conditions prevail from 14.0 m down to the bottom of Lake Steißlingen in March 2017, whereat dysoxic to suboxic conditions prevail away from 10.0 m down to the bottom of Lake Steißlingen during the other months (June 2016, November 2016,

July 2017 and September 2017). The low oxygen concentration in the hypolimnion in March 2017 gets explained by an incomplete mixture of the lake (Gilfedder, 2018). This causes that between March 2017 and July 2017 O₂ was already consumed by aerobic respiration (See Figure 36 equation (1)) in the hypolimnion followed by a dysoxic to suboxic period.

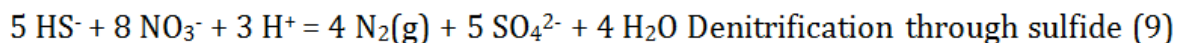
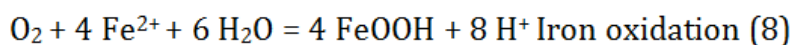
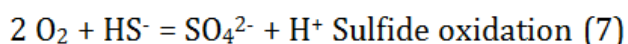
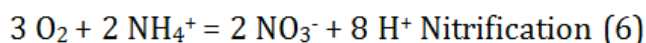
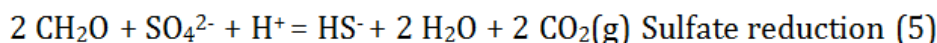
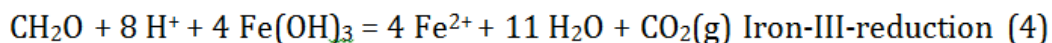
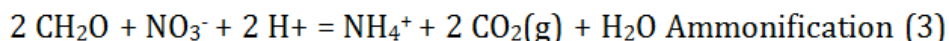
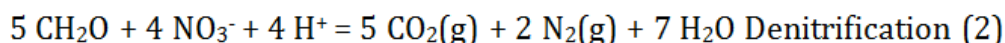
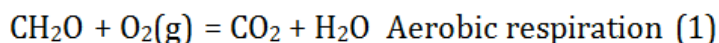


Figure 36 Redox processes that can happen under specific energetic conditions in the water column or the pore water of the sediment.

During the dysoxic to suboxic phase a parallel decrease of nitrate and increased values of NH₄-N were recorded from around 10.0 m to the deepest measured point of the lake and leads to the assumption of occurring nitrate reduction (See Figure 36 equation (2)) caused by oxygen depletion (Rimmer et al., 2005).

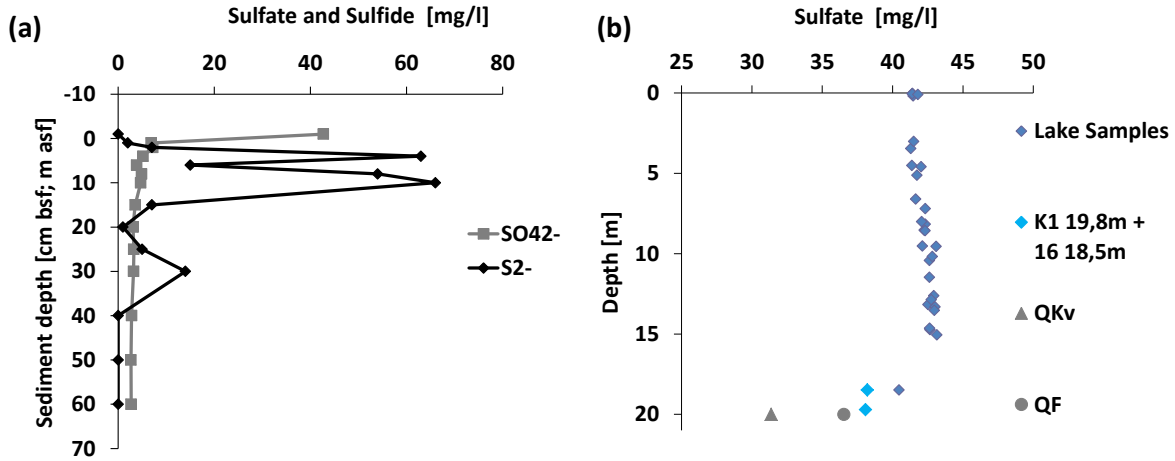


Figure 37 (a) Sulfate and sulfide concentrations within the pore water at station 13 and. (b) sulfate concentration within the water column in Lake Steißlingen September 2017 against water/sediment depth.

This concentration change gets explained by the fact that nitrate reduction favors the accumulation of ammonium (Bertleff, 2001). When comparing these months to March 2017, where suboxic conditions are assumed, NO₃-N concentrations increase, whereas NH₄-N contents are lower from around 10.0 m down to the deepest point of the lake which can be explained by the process of nitrification (Figure 36 equation (6)).

It is noticeable that a strong descent of sulfate is observed within the water column at a depth of around 18.0 m to 19.0 m for sampling point K1 in November 2016 and for sampling points K1 and 18 in September 2017. Furthermore, a smell of sulfur and a white precipitation on the sediment was perceived for these samples during the measurement campaign in November 2016 and September 2017. Since it is known that a descent of sulfate can cause formation of HS⁻ (See Figure 36 equation (5)) it gets assumed that this process of microbiological sulfate reduction as an alternative energy source for oxygen takes place in the hypolimnion of Lake Steißlingen close to and in the sediment. Simultaneously formed S²⁻ in the sediment can diffuse into the water column where it gets reoxidised to sulfate. The pore water observations indicate that SO₄²⁻ suddenly starts to decrease on top of the sediment, whereas contemporaneously S²⁻ increases.

The redox reactions and concentrations of nitrate reduction, ammonification and sulfate-reduction indicate lake stratification indirectly caused by the low dissolved oxygen content in the hypolimnion of the lake. Furthermore, those processes lead to a formation of CO₂ (See Figure 36 equations (1), (2), (3) and (5)), which consequently is partly responsible for a pH descent in the meta- and hypolimnion of Lake Steißlingen.

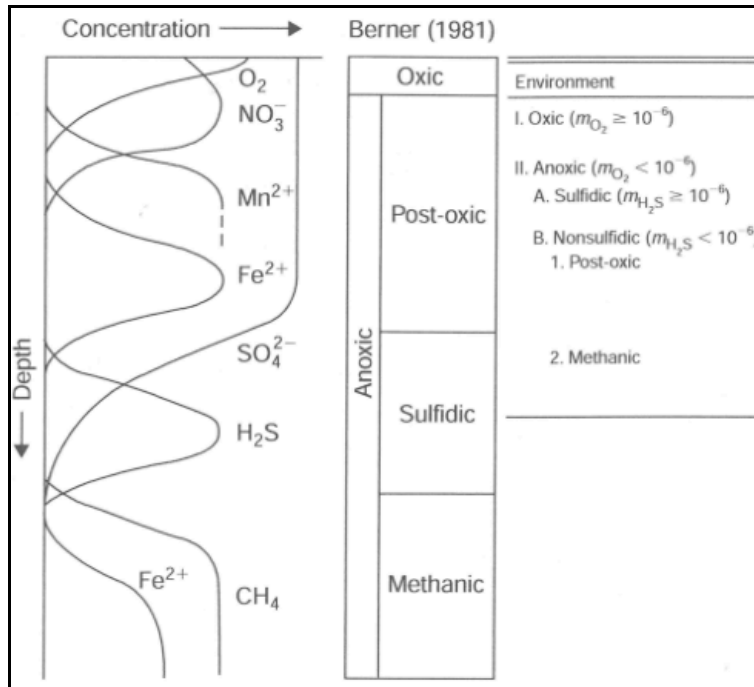


Figure 38 Succession of redox processes in a natural aqueous system (Appelo, 2005).

Due to measurements of LUBW (2014) cyanobacteria concentrations indicate higher values from the date of March 2014 until November 2014 compared to the months of December 2014 and February 2014 and a present bloom below 5m depth. Also, the results of 2016/2017 show that increased values of Chlorophyll A were recorded within a depth below 5m, which is probably caused by the productivity of cyanobacteria. Lake Steißlingen gets defined as mesotroph by LUBW (2014) due to an annual average Chlorophyll A concentration of 8.9 $\mu\text{g/l}$ in 2014. The delineation of the piper diagram shows (See Figure 39) that all water samples can be defined as alkaline-earth and carbonate type (Kralik et al., 2004). This water type is typical for Pleistocene sands which can be found in the aquifer layer of Lake Steißlingen where groundwater is assumed to originate from (Bertleff, 2001). The water samples show a mixture of groundwater type 2 and 3 which is a changeover between relatively young confined groundwater and normal confined groundwater with recently formed groundwater and good flow rate conditions that is already lasted sometime in the aquifer (Hotzan, 2011).

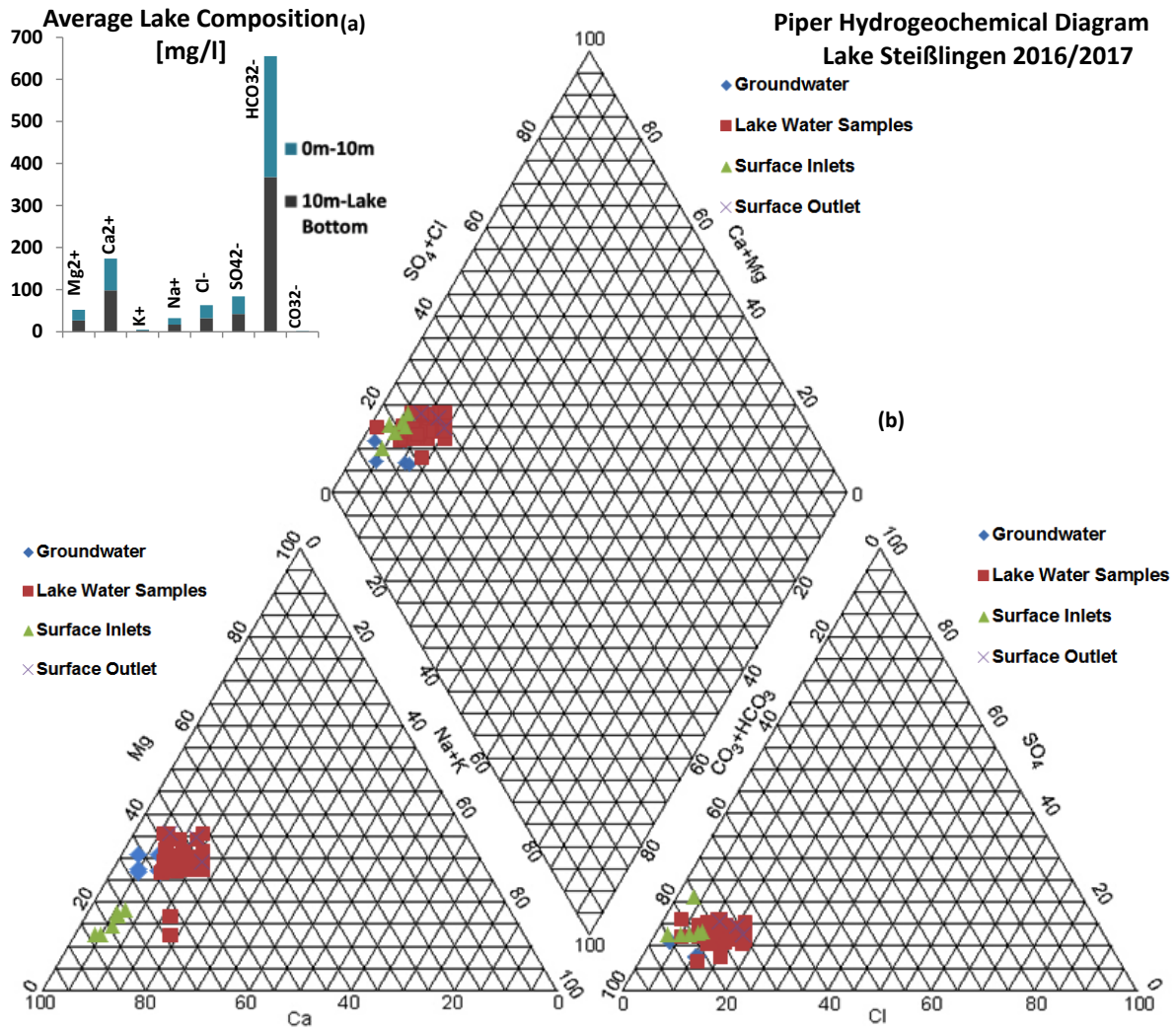


Figure 39 (a) Delineation of average lake composition for measuring campaigns during 2016/2017 (Domenico and Schwartz, 1997) (b) Piper hydro-geochemical diagram (Carlos, Molano) for Lake Steißlingen measuring campaigns during 2016/2017.

4.3 Groundwater Inflow to Lake Steißlingen

Since several years submerge groundwater inlets have been presumed in Lake Steißlingen by researchers as well as the inhabitants of Steißlingen (Eusterhues, 2000; LUBW, 2014; Schneider, 2000). This assumption gets confirmed by the study of Gilfedder et al. (2018), where clear groundwater signals from 750 to 944 Bq/m³ via ²²²Rn tracer method were measured in the middle and at the north-eastern side of Lake Steißlingen between 11.0 m and 14.0 m. Remarkable high radon activities were found at sampling profile SS5 and SS2 in a depth below 8 m by Gilfedder et al. (2018) (See Figure 10). SS5 and SS2 lie close to our sampling point 10 as well as 13, which gets discussed in more detail in a different part of 4.3. The activity and concentration of ²²²Rn is much higher in groundwater (1000-100000 Bq/m³) compared to lakes (only a few Bq/m³) (Arnoux et al., 2017). ²²²Rn can be formed through decay of ²³⁸Uranium ($T_{1/2}=3.82$ d) and transport in an aquifer consisting of a rock or sediment (Spirkaneder, 2016). The high volatility and short half-life of ²²²Rn effectuate a low activity in surface waters such as lakes (Spirkaneder, 2016). It gets assumed that groundwater enters the lake in the middle at a depth of 10.0 m to 15.0 m around sampling point 10 and 13, where the highest groundwater ratios were calculated between June and September.

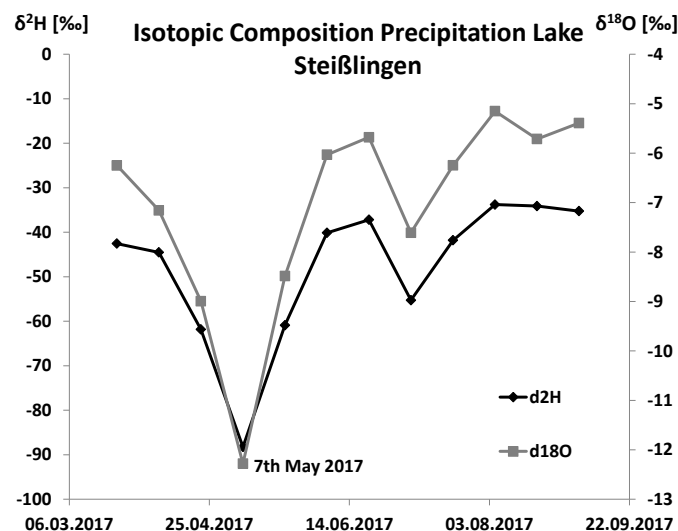


Figure 40 Isotopic composition of collected precipitation between March 2017 and September 2017 (Personal disclosure of data by Dirk Sachse (GFZ Potsdam)).

Previous studies reveal that water stable isotopes were found as natural tracer to detect and quantify groundwater inflow to lakes (Arnoux et al, 2016; Bertleff, 2001; Hofmann et al., 2011). Therefore, the method of groundwater tracing with stable isotopes of hydrogen and oxygen was also applied in this study.

Precipitation was collected and isotopically evaluated by GFZ Potsdam (Personal disclosure of data by Dirk Sachse) between March 2017 and September 2017. In figure 31 it can be seen that the isotopic precipitation composition of $\delta^{18}\text{O}$ lays within -5.15‰ and -8.99‰ between March 2017 and September 2017. Unusual low $\delta^{18}\text{O}$ values for this period of the year of -12.28‰ towards a shift to a lighter isotope signature was measured on the 7th of May, 2017. Due to an unusual cold period of two weeks and snow event at the end of April 2017, its subsequent evaporation and precipitation of the snowmelt, the descent in isotopic composition of $\delta^{18}\text{O}$ can be explained. This negative shift in isotopic signature is caused by the effect of lowered evaporation rates in colder periods and thus the lack of getting isotopically heavier. The same trend was observed with $\delta^2\text{H}$ that indicates a low isotopic ratio of -88.26‰ on the 7th of May, 2017 and a ratio between -33.7‰ and -55.26‰ in the warm period.

The local meteoric water line (LMWL) shows the relationship between isotopic ratios of oxygen and hydrogen of precipitation within the area of Lake Steißlingen (See Figure 41). Additional data of LUBW and GFZ Potsdam were delineated on the LMWL plot to show its connection and possible occurring physical changes (evaporation, precipitation, lake mixing) that the water was exposed to.

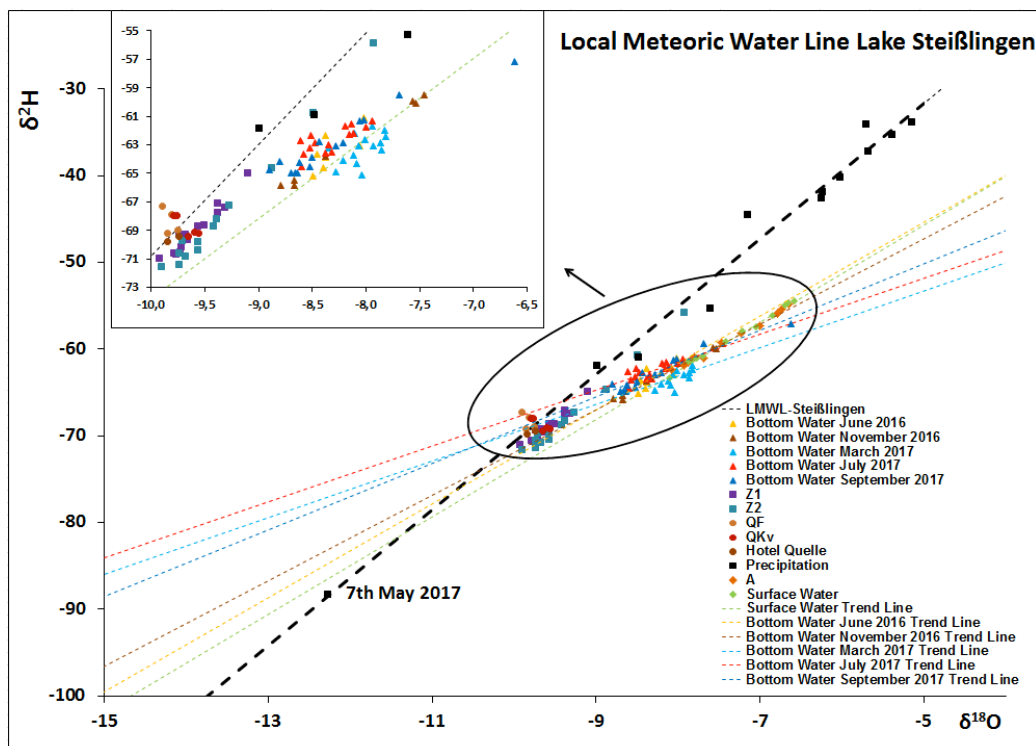


Figure 41 Local Meteoric Water Line Lake Steißlingen constructed with data by GFZ and LUBW 2016/2017.

The distribution of precipitation data on LMWL is caused by different seasonal temperatures and thus a change in evaporation rates, which causes a change of isotopic composition. The isotope composition of precipitation measurements between March 2017 and September 2017 form a clear trend line and are scattered mainly on the upper part of it, showing an enrichment of heavy hydrogen and oxygen isotopes (See Figure 40). Hereby, a remarkable depletion in heavy isotopes was observed on the 7th of May 2017 with a $\delta^{18}\text{O}$ and $\delta^2\text{H}$ value of -12.28‰ and -88.26‰, respectively. Hereby the effect of snowmelt precipitation can be seen. Additionally, similar low values can be assumed for the cold winter months.

The isotopic compositions of surface inlets (Z1, Z2) scatter on the LMWL of Steißlingen and the adjacent groundwater sampling points showing the average annual precipitation signal, and thus support the assumption that surface inlets get fed by rainwater. The isotopic signature between surface inlet and “surface lake water” (surface runoff) differentiates strongly because surface lake water does not get influenced intensely by surface inlets. Moreover, processes that occur during the residence time of water in the lake change the isotopic composition. Such effects could be evaporation, dilution through precipitation events, formation of ice or a different isotopic composition of groundwater that mainly feeds the lake. This can be clearly distinguished by the isotopic ratio of surface inlets, which differentiates from that of the surface runoff that gets assumed as surface lake water. So, the surface water shows that $\delta^2\text{H}$ and $\delta^{18}\text{O}$ is heavier in contrast to the LMWL signals, which indicates that the main influenced process is evaporation. Additionally, the deeper water shows lighter isotopic signals than the surface water which indicates another water source like groundwater. The deviation of water constitution between surface inlet and “surface lake water” (surface runoff) can also be seen when regarding the Piper Diagram, where outlet points do not scatter at the same area compared to inlet points (See Figure 39).

The possible groundwater sources for Lake Steißlingen are QF, QKv and Hotel Quelle (GFZ data) and show isotopic signatures that lay on and close to the LMWL and represent the annual average of the precipitation signals (See Figure 41). Therefore, the assumption that the aquifers of QF, QKv and Hotel Quelle get recharged by local precipitation gets confirmed.

The isotopic signature of surface runoff and the surface water of Lake Steißlingen, which show similar values, differentiate from that of the groundwater (See Figure 41). Thus, the points of surface runoff and surface lake water form another isotopic trend line, due to an isotopic ratio shift, showing the intensity of evaporation on the lake surface, denominated as the lake specific evaporation line. The isotopic ratio shift towards $\delta^2\text{H}$ is caused by an evaporation effect at the surface of the lake because it is in contact to the atmosphere and directly affected by sunlight that causes a stronger fractionation of $\delta^2\text{H}$. The stronger fractionation rate of $\delta^2\text{H}$, compared to $\delta^{18}\text{O}$ in the water body is caused by an evaporation effect at the surface and can be explained by the mass difference effect between the lighter H isotopes and heavier O isotopes.

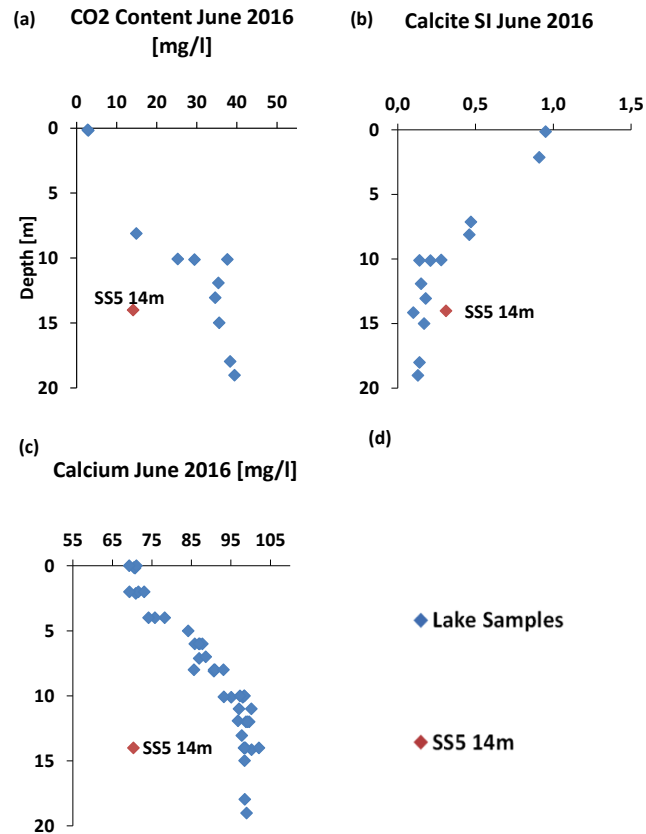


Figure 42 Depth profiles of June 2016 (a) CO₂ content in [mg/l] (b) SI Calcite (c) Ca²⁺ concentration

The approximate residence time of water in a lake can be determined on the basis of its isotopic composition and thus its position on the evaporation line of a lake (Hofmann et al., 2011; personal communication Leis Albrecht, March 6, 2018). The greater the deviation of the isotopic ratio from the LMWL, the greater the sum of evaporation rate of the water and hence the greater the residence time of water in a lake (Clark et al., 1997; personal communication Leis Albrecht, March 6, 2018). The position of lake water at Lake Steißlingen indicates a moderate fractionation shift along the lake-specific evaporation line which leads to the presumption of a moderate residence time of lake water. This assumption gets confirmed by calculations of Gilfedder et al. (2018) and a calculated residence time between 1.7 and 2.8 years. Lakes that get mainly fed by strong surface inflows show a water residence time of a few days (Hessisches Landesamt für Umwelt und Geologie, 2014). Lake Steißlingen however, shows a residence time of 1.7 and 2.8 years and gets therefore classified as “mäßig lang” (Mauersberger und Kopp, 2006). The size of Lake Steißlingen in combination with its residence time of water gets categorized as “stark durchflossen” (Schönborn et al., 2013).

The most striking result for several parameters (EC, TA, pH, water hardness, NH_4^+ , Na^+ , K^+ , Ca^{2+} , Mg^{2+} , Cl^- , SO_4^{2-} , CO_2 , $\text{SI}_{\text{Calcite}}$) shows sampling point SS5 with a groundwater ratio of 46,0% in 14.0 m with deviating values compared to other sampling points at the same depth (Figure 42). As an example, Lake Steißlingen shows an average chloride concentration of 32.4 mg/l at a depth of around 14.0 m. This anomaly was also observed for the parameters of Na^+ , NH_4^+ and SO_4^{2-} in groundwater and lake water.

The CO_2 content of SS5 is 14.2 mg/l, whereat other points in the same depth show values around 35.5 mg/l (Figure 42). Hereby a punctual groundwater inlet gets excluded. This can be explained by the fact that the CO_2 content too low and the SI of calcite >0 (See Figure 32). Due to respiration and microbiological processes, CO_2 gets produced in the soil air, thus the partial pressure of groundwater is increased when comparing it to the atmosphere and causes a decrease in pH (Hofmann et al., 2011). A direct groundwater inlet would therefore show enhanced CO_2 values and a negative $\text{SI}_{\text{Calcite}}$, which refers to calcite undersaturation. Also, when comparing SS5 with SS2, which both indicate high ^{222}Rn activities in this depth, it can be seen that SS2 shows unremarkable values for the same parameters like other sampling points in the same depth. The comparison of SS5 and SS2 also leads to the assumption that a punctual groundwater inlet can be excluded due to similar high ^{222}Rn activities but different values for above mentioned parameters. A measurement error can be excluded, which can be explained by the fact that the sample was measured several times and the parameters were measured by using different sampling bottles and different instruments. Thus, it is statistically improbable that all bottles get contaminated simultaneously and several instrumentations show measuring mistakes for the same sample. Practically seen an interchange of samples can be excluded due to a structured sampling. However, it is most plausible to explain the strong deviating values when comparing it to the rest of the sampling points. Moreover, a contamination of the water samples could also be the reason for the value shift at SS5 but seems unlikely due to a clean and exact sampling process. The anomalous values are therefore not comprehensible. To gain a plausible explanation, a more accurate investigation for this sampling point would be necessary and the sampling would have to be implemented again in the same depth. However, other indications for the occurrence of groundwater and possible groundwater inlets were found, which will be discussed subsequently.

In March 2017 a slightly increased $\text{NO}_3\text{-N}$ value of 1876 $\mu\text{g/l}$ was measured in the middle of the lake compared to the other sampling points at around 15m depth. The remarkable result is located adjacently to the area where high ^{222}Rn activities occur at around the same depth (Figure 43). An increased value of $\text{NO}_3\text{-N}$ might be an indicator for incoming groundwater nearby due to the fact that the groundwater around Lake Steißlingen comprises high $\text{NO}_3\text{-N}$ contents with an annual average concentration of 4508 $\mu\text{g/l}$. The high concentration difference between the sampling point at 15m depth and the groundwater can be explained by an immediate dilution effect of incoming groundwater in its surrounding lake water. The occurrence of accumulated $\text{NO}_3\text{-N}$ concentrations will be discussed in chapter 4.4 in more detail.

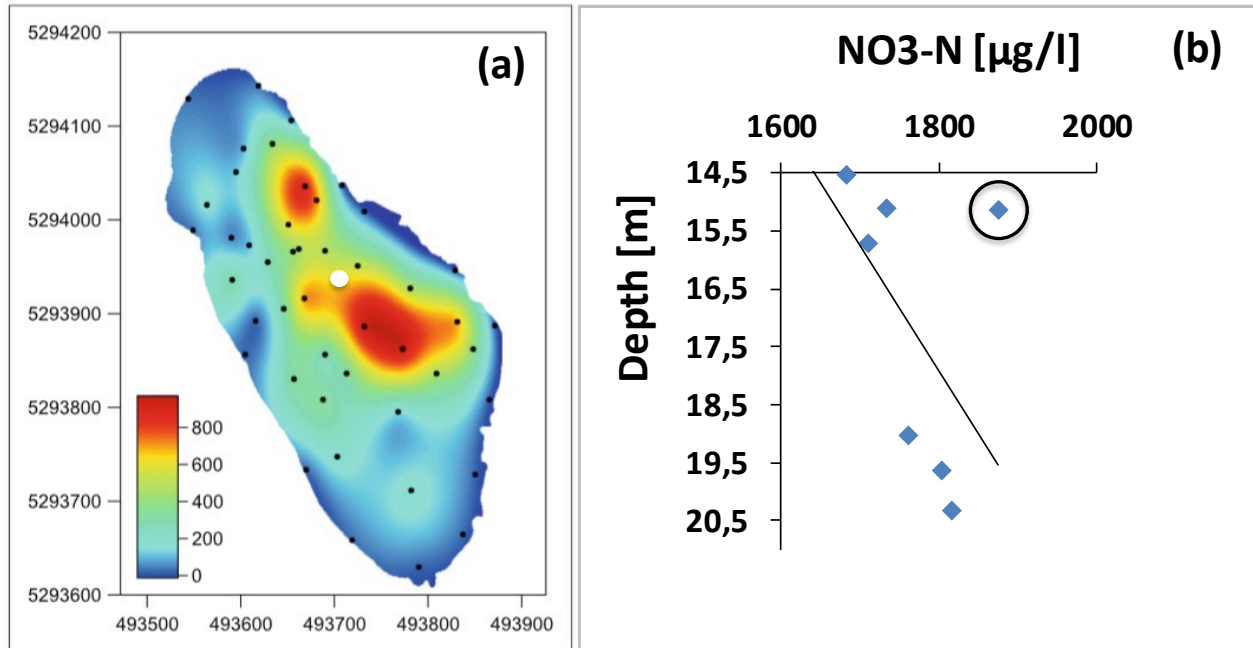


Figure 43 (a) Distribution of ^{222}Rn activities by Gilfedder et al. (2018) (b) $\text{NO}_3\text{-N}$ values of the hypolimnion in March 2017

When regarding $\delta^{18}\text{O}$ signatures in September 2017 below the metalimnion, two minimally deviating values occur at a depth of around 13 m in the middle and north-easterly of Lake Steißlingen. The $\delta^{18}\text{O}$ composition of these two points are slightly decreased with -8.8‰ and -8.9‰ compared to the other values in the same depth and an isotopic signature around -8.5‰ . Therefore, the deviating values reveal a shift towards the groundwater average isotopic signature of -9.7‰ in September 2017, which could indicate groundwater hot spots around this region of the lake. This assumption gets supported by the fact that also high radon activities were measured close and at these areas in the middle and north-east of the lake (See Figure 44). Our results therefore might show that groundwater not only occurs in spring and summer months at the middle and north-eastern side of the lake (Gilfedder et al., 2018), but also during other periods of the year, such as autumn.

The results of $\delta^{18}\text{O}$ reveal slight changes at a depth of 13.0 m, but only in September and not definite. Therefore, other methods were applied to gain high resolution data for groundwater ratios in Lake Steißlingen. At the beginning the groundwater ratio was calculated by the following binary isotopic equation of mixture between lake water and groundwater and the assumption of QF and QKv being the groundwater source:

$$X_L = \left(\frac{\delta^{18}\text{O}_{\text{Lake sample}} - \delta^{18}\text{O}_{\text{Lake water}}}{\delta^{18}\text{O}_{\text{Groundwater}} - \delta^{18}\text{O}_{\text{Lake water}}} \right) * 100$$

The results of this equation show an approach of how much groundwater can be found in the different layers of Lake Steißlingen. The calculation of groundwater ratio with stable oxygen isotopes showed a maximum of 71.8% in September 2017.

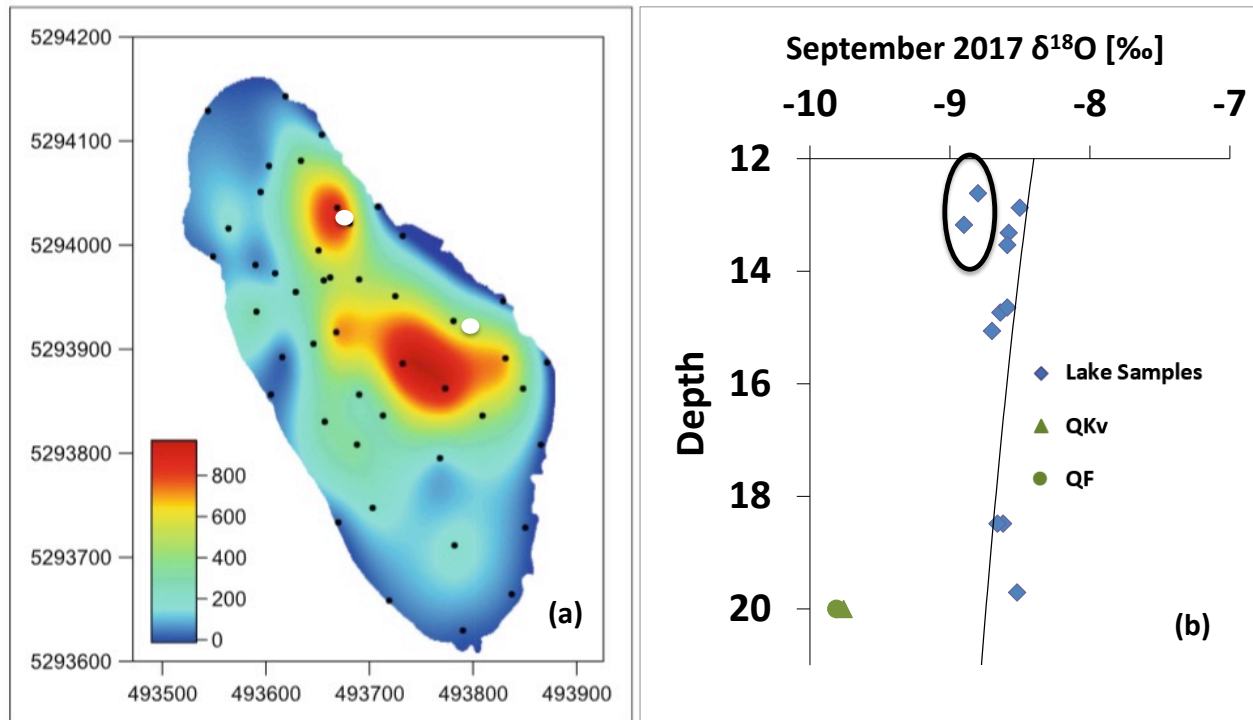


Figure 44 (a) Distribution of ^{222}Rn activities by Gilfedder et al. (2018) (b) $\delta^{18}\text{O}$ values of the hypolimnion in September 2017

To get more accurate results for the groundwater ratio in Lake Steißlingen, inverse modelling tool by Phreeqc Interactive 3.4.0-12927 was applied. The inverse model calculates how much of the average lake water solution and groundwater solution can be found in the bottom lake water solution. The solutions of surface inlets were excluded as a potential end member, because Phreeqc did not calculate feasible groundwater ratios with it. This can be explained by the fact that surface inlets indicate a relatively small catchment area and do not have a strong impact to the hydrochemistry of Lake Steißlingen due to a dry up in summer months and a low precipitation rate in winter months. All models found by Phreeqc showed similar or same groundwater ratios and only differentiated slightly in the amount of degassed CO_2 and precipitated calcite. Therefore, one appropriate model was chosen for each point for the delineation the results that will be discussed in the following sections (See Figure 32).

The most remarkable result to emerge from Phreeqc is that the main occurrence of groundwater can be proven in the hypolimnion. Even in the water layers of the epilimnion groundwater could be verified strongly diluted.

Another noticeable result to emerge from Phreeqc data is that seasonal alterations of groundwater ratio occur. Concerning the seasons only, without regarding the year, a clear increase of groundwater ratio can be distinguished between summer and fall months. At the beginning of summer, the highest groundwater ratios indicate sampling point 10 and SS5 at a depth of around 15m with 50.9% and 46.0%. The highest groundwater ratio found in July indicates 61.9% at sampling point 10. The maximum of groundwater found within the period of the measuring campaign is 77.2% in September 2017 in 14.7 m and 15.1 m at sampling point 10 and 13. In November maximum groundwater values around 60% are found in 15.0 m, 16.2 m and 19.4 m at sampling point 10, 18 and K1. In March the effect of the mixing approach in winter, where an exchange between hypo- and epilimnion occurs, can be clearly seen, because varying groundwater ratios within the entire water column are found (See Figure 45 (a)).

Because of this the maxima of groundwater ratio and its accumulation occur between June and September, which reveals that a distinct water layer gets formed around 15m. The distinct groundwater layer is in exchange with the water layer below, which finally causes a mixing of the entire hypolimnion and thus explains high groundwater ratios down to a depth of 19.4 m in November. Therefore, in the time between June and September an advancing accretion of groundwater can be observed in the entire hypolimnion due to a complete mixing process and a constant groundwater inflow (See Figure 45(a)). In the months between June and September bottom water values of the epilimnion and metalimnion around and above 9.0 m, indicate low groundwater ratios, because no groundwater is assumed there. But also, the epilimnion and metalimnion indicate a slight increase in groundwater ratio, which is caused by a heat exchange between the two surface layers and the incoming groundwater layer.

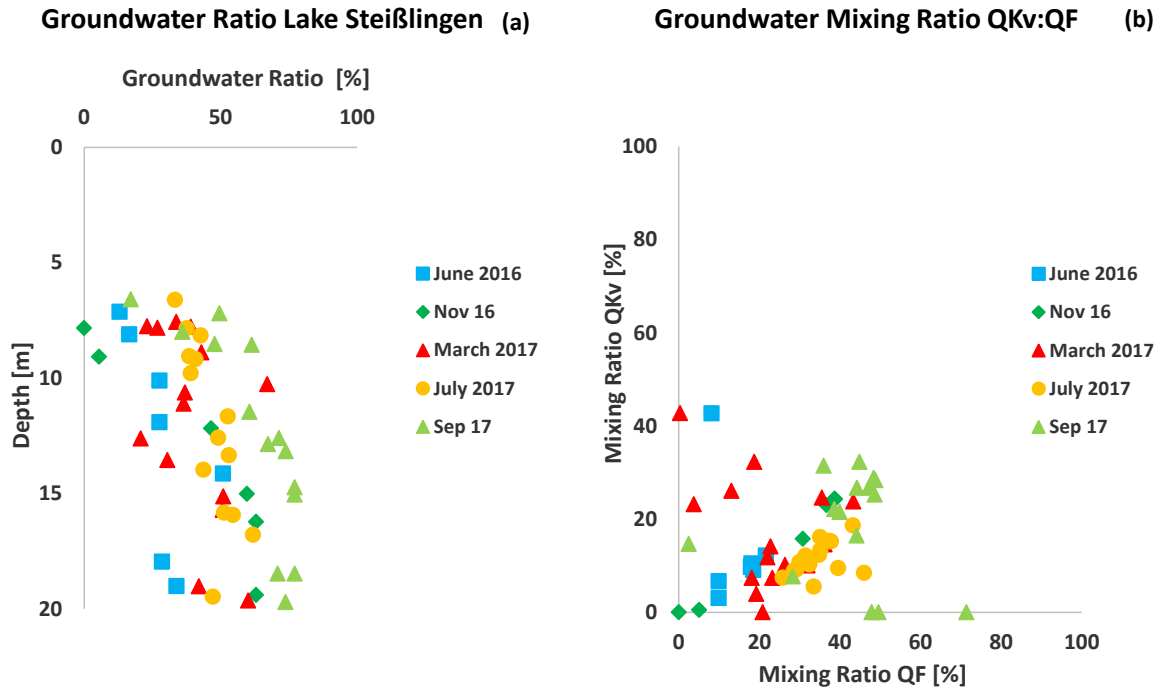


Figure 45 (a) Groundwater Ratio of Lake Steißlingen against depth calculated by Phreeqc Inverse Modeling (b) Groundwater Mixing Ratio of QKv versus QF calculated with Phreeqc Inverse Modeling.

Moreover, the results of isotopic parameters measured within this study also confirm the assumption that a seasonal enhancement of groundwater can be found mainly around 10.0 m to 15m and its subsequent exchange with the hypolimnion between summer and fall months. Hardly any groundwater is present from the surface of the water column down to around 10.0 m. The bottom water values of June 2016, November 2017, July 2017 and September 2017 are remarkable at a depth of around 13.0 m to 18.5 m and show a shift towards groundwater signature (QF, QKv) (See Figure 45 (b)). This confirms on the one hand the occurrence of a groundwater layer and its exchange with the water layer below. Besides that, groundwater samples scatter on and around the trend lines of bottom water values and thus clearly shows the influence of incoming groundwater (See Figure 41). Some bottom water values of June, November, July and September lay directly on the trend line of the surface water, which can be explained by their sampling depths around and above 9.0 m closer to the surface where barely any groundwater can be found. In Figure 41 Local Meteoric Water Line Lake Steißlingen constructed with data by GFZ and LUBW 2016/2017. it can be seen that the isotope values of March 2017 scatter mainly on the trend line of the surface water which is an effect of the entire mixing approach phenomenon of Lake Steißlingen during winter months.

The delineation of the groundwater mixing ratio between QKv and QF indicates a remarkable shift towards QF and a clear trend during the measuring period. No trend can be distinguished in March 2017, which was presumably caused by the approach of entire mixing the months before

(See Figure 45 (b)). Due to an unchanging mixing ratio of QKv and QF during June 2016, November 2016, July 2017 and September 2017 it can be presumed that incoming groundwater originates from one aquifer layer within these months. This leads to the assumption that precipitation and the constitution of the aquifer that it is flowing through forms the groundwater with ratios of about two thirds QF and one third QKv mixes up in the aquifer.

The assumption of the formation of a distinct layer through incoming groundwater also gets confirmed by water temperature and the phenomenon of inverse stratification in November 2016 (See Figure 46). An increased water temperature value of 9°C can be distinguished at a depth of around 15m. The influence of water temperature through groundwater income will get discussed in chapter 4.4 more explicit.

Through observations of this study, it can be predicated that groundwater recharges Lake Steißlingen, which gets confirmed by previous research and measurements of this area (Eusterhues, 2000; LUBW, 2014; Spirkaneder, 2016). The amount of groundwater that recharges the lake was assumed to be 8-17 l/s by Gilfedder et al. (2018), which effectuates a maximum groundwater ratio of 70%-80% in Lake Steißlingen. The percentage of groundwater in Lake Steißlingen is relatively high when comparing it to other lakes with a groundwater ratio of for example 14% (Schmidt et al., 2010).

A direct punctual localization of groundwater with the basis of chemical parameters was not accomplishable due to the fact that small groundwater outlets are assumed. Moreover, a dilution effect through precipitation occurs. This study however shows that Lake Steißlingen gets mainly fed by groundwater which gets mostly proven in the hypolimnion of the lake through the depth profiles of chemical parameters. The conservative and less reactive elements Ca^{2+} , Cl^- , Na^+ and K^+ indicate similar, but slightly decreased concentrations in the hypolimnion, compared to the groundwater samples of QKv and QF. The slight concentration difference between groundwater and lake water can be explained by the above mention dilution effect. Hence, groundwater mainly feeds Lake Steißlingen while surface inlets can be excluded as main water source for Lake Steißlingen. This can be explained by the fact that contents of Ca^{2+} , Cl^- and Na^+ remarkably differentiate compared to the hypolimnion and the groundwater.

The groundwater and lake water in the hypolimnion of other parameters, such as sulfate and $\text{NO}_3\text{-N}$, indicate a concentration difference. The shift in concentration can hereby be explained by a reactive behavior due to biological activities of these substances.

For the specification of this groundwater detection method a higher concentrated horizontal and vertical measuring grid with bottom water samples closer to the sediment would be mandatory.

Moreover, a new finding of this study is that groundwater firstly forms a distinct layer, followed by a mixture due exchange processes with the water layer below and thus piles up in the hypolimnion between March and September. This amount of data and information shows the

regions of groundwater income but is still not sufficient for the exact and punctual localization of a groundwater outlet. Nevertheless, it can be reasonably expected that groundwater generally influences the chemistry, stratification and thus mixing dynamic of Lake Steißlingen. The highest influence gets assumed in around 10.0 m – 15.0 m depth where groundwater enters the lake and forms a layer in the middle and north-easterly of the lake, which can be clearly seen by the results of isotopic parameters, Phreeqc modelling and the temperature isopleth diagram.

4.4 Impacts on Lake Steißlingen through Groundwater Inflow

Groundwater was often ignored in the history of lake research (Rosenberry et al., 2015). The study of Hofmann et al. (2011) reveals how groundwater can change lake systems according to several factors, such as its hydrochemistry, its seasonal groundwater inlet and its isotopic composition. Also, groundwater inflow can change the lakes water circulation and thus its stratification, which can influence the alteration of water densities (Boehrer et al., 2008).

According to Sundaram et al. (1971) a homo-thermal temperature stratification of 4°C, where water indicates the highest density, can be supposed for temperate lakes in early spring months. The occurrence of a temperature shift down to 4°C was not observed for Lake Steißlingen due to its strong influence of incoming groundwater, which exhibits a higher water temperature compared to the lake water. Therefore, the water temperature in the hypolimnion of the lake does not reach the state of highest density at 4°C. This might impede the mixing process of the lake during winter months among other things.

Lake Constance is monomictic and gets mainly fed by surface recharge, which causes that water temperatures in the hypolimnion do not get influenced by external factors. Therefore, the lake forms an epilimnion with a maximal thickness of 20.0 m wherefrom the thermocline begins (IGKB, 2004). This study reveals that the thermocline of Lake Steißlingen is comparatively shallow throughout the year, starting at a depth of 3.0 m to 10.0 m depending on the season. The unusual shift of the thermocline can be explained by a permanent “lift up” through incoming groundwater and the resulting density difference between the metalimnion and the groundwater layer.

Most monomictic lakes indicate a regular temperature stratification throughout the year in the hypolimnion (Hupfer et al., 2009), whereat Lake Steißlingen shows an uneven temperature stratification by forming two separate layers within the hypolimnion. This occurrence can be seen in the hypolimnion due to a time shift concerning the lakes water temperature between the upper layer of incoming groundwater and lower layer of the lake. The lag in temperature increase can be explained by the process of heat exchange between groundwater layer and bottom water layer (See Figure 46).

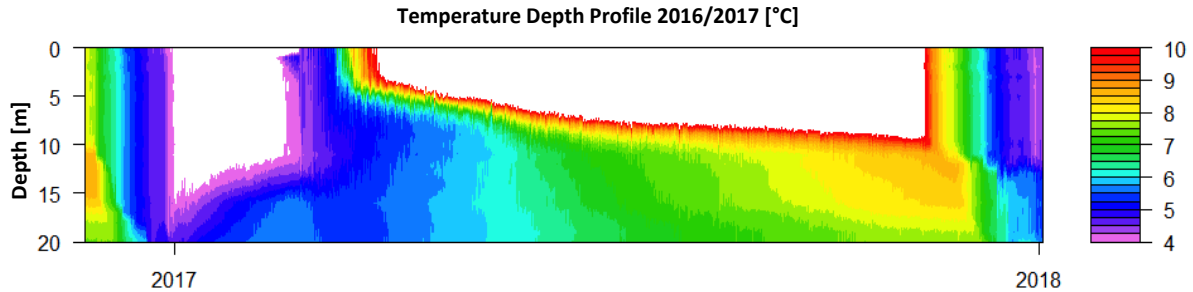


Figure 46 Isopleth diagram 2016/2017 including temperatures between 4°C and 10°C at station K1 measured with the thermistor chain at the permanent measuring station.

Due to Gilfedder et al. (2018) the groundwater, that enters Lake Steißlingen at a depth of 11.0 m to 14.0 m, is anoxic. The accumulation of anoxic groundwater and dissolved ions in the hypolimnion is probably a reason for a stable stratification and possibly explains the phenomenon of only approaching a mixing event during winter months. Furthermore, the hydrochemistry in the hypolimnion changes through intensified mineralization and remineralization processes such as consumption of nitrate and sulfate and formation of H_2S and NH_4^+ caused by the fact that anoxic groundwater enters the lake. The ratio of groundwater increases throughout the year between March 2017 and September 2017. So, after the formation of the stratification, firstly the small amount of dissolved O_2 gets used up in the hypolimnion through respiration. Subsequently the lake stays suboxic to dysoxic caused by the income of anoxic groundwater and non-mixing of the lake. Those processes cause an increase of CO_2 and a decrease of pH in the hypolimnion among other things. This shows a new finding and underlines that not only extern factors such as ice layers, warm summers and non-turbulent weather conditions determine the stabilization of the lakes stratification (Eusterhues, 2000), but also the incoming groundwater, which is probably the driving factor.

When regarding the results of isotope measurements, the physically unchanged $\delta^{18}\text{O}$ values in the hypolimnion show a shift towards the $\delta^{18}\text{O}$ groundwater signal. Controversial to that, the epilimnion is enriched in heavy ^{18}O isotopes and $\delta^{18}\text{O}$ signature is therefore more positive (Figure 28). This is due to the interaction between surface lake water and the atmosphere where evaporation and precipitation occur. An exception was observed in March 2017, where all values lay closer to the $\delta^{18}\text{O}$ groundwater signal, which can be explained by the mixing approach between epi- and hypolimnion and low precipitation and evaporation rates during winter months. The same trends were observed for $\delta^2\text{H}$ (Figure 29). Thus, groundwater, being the main water source of Lake Steißlingen, has an influence on its isotopic composition.

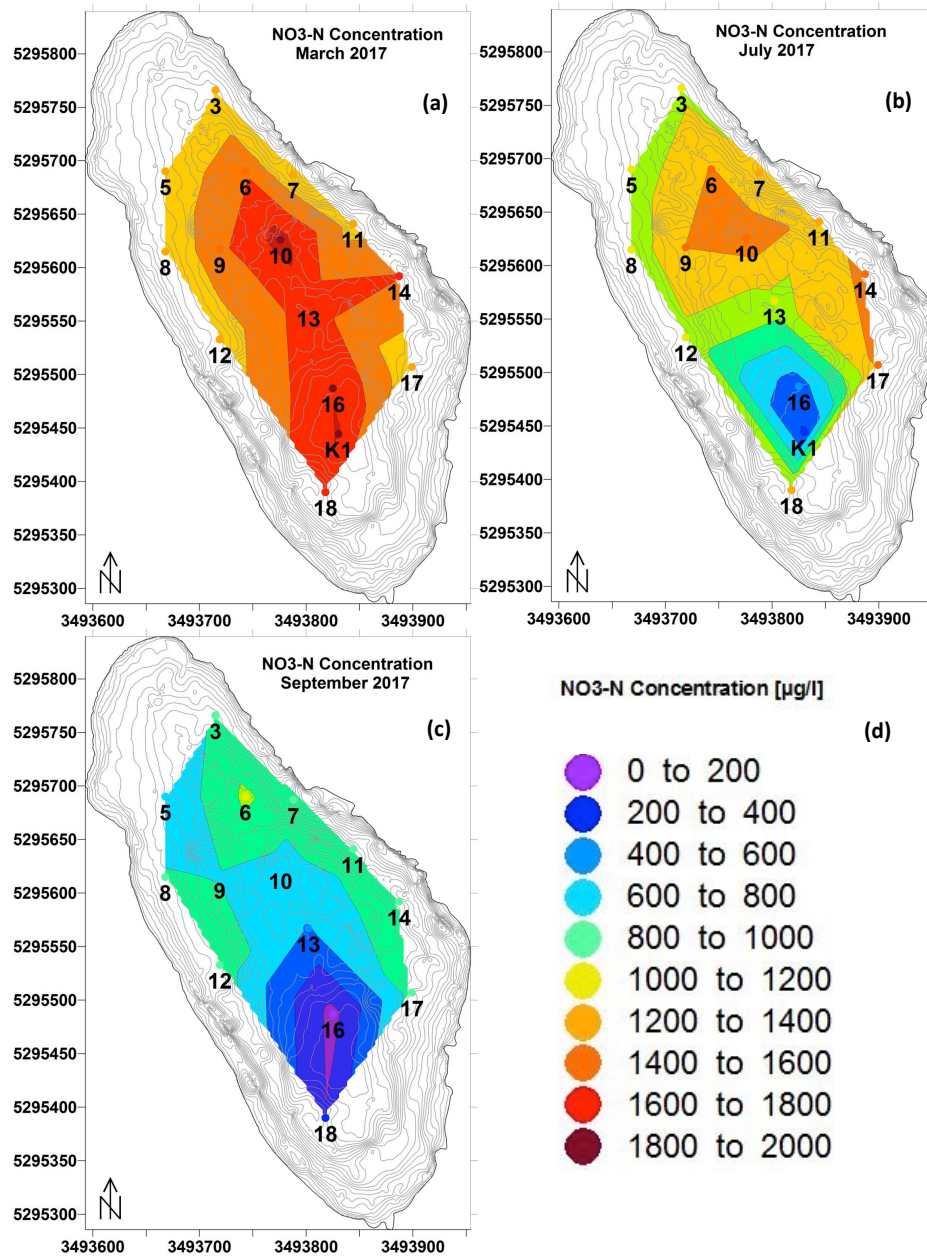


Figure 47 NO₃-N concentration in [µg/l] (d) in March 2017 (a), July 2017 (b) and September 2017 (c). Sampling points plotted in Gauß Krüger coordinates (d) legend.

Lake Constance (Obersee), defined as a meromictic system and mainly fed by surface inlets, indicate lower annual average NO₃-N concentrations compared to Lake Steißlingen that gets fed by groundwater (Güde et al., 2016). The NO₃-N concentration of groundwater is increased, compared to lake water, due to agricultural land use. Thus, groundwater functions as a NO₃-N source for the lake and provides it as an energy source for nitrate reducing bacteria in the suboxic to dysoxic hypolimnion. The income of nitrate through groundwater can be clearly seen in Figure 47 in the NO₃-N depth progression in March 2017. Hereby NO₃-N gets accumulated up

to 1200 µg/l - 2000 µg/l around sampling point 10 at a depth of 15.1 m, because it does not get consumed due to availability of dissolved oxygen as an energy source for organisms in the hypolimnion during March 2017. Between July 2017 and September 2017 suboxic to dysoxic conditions dominate the hypolimnion, which causes ammonification and thus the consumption of nitrate Figure 47. Therefore, the results of March 2017 explicitly show that incoming groundwater functions as nitrate provider.

The range of chloride concentration for Lake Constance, mainly fed by surface inlets, lays within 5.1 mg/l and 7.3 mg/l (Güde et al., 2016) and is low compared to Lake Steißlingen. The concentration of chloride with 32.4 mg/l is enhanced in the hypolimnion of Lake Steißlingen compared to the epilimnion with 30.8 mg/l (See table 1). It gets assumed that the chloride content of groundwater increases during its pathway. This is mainly caused by street salting at the streets above the aquifer. Moreover, chloride gets easily dissolved in the soil and does not get consumed biologically by organisms and does therefore not affect chloride concentration. The same occurrence and explanation also gets observed for sodium (See table 1). Due to Dr. Mohr R. (personal communication, March 14, 2018) it can be excluded that sodium chloride bearing parts occur in the quaternary layer in this area, therefore the lithology of the aquifer itself does not function as sodium or chloride source.

According to Eusterhues (2000) sulfate concentrations are remarkably high for fresh waters in Lake Steißlingen. It furthermore indicates a slight increase in sulfate between 1987 and 2014 (LUBW, 2014). The average sulfate concentration is unremarkably lower in with 35.5 mg/l groundwater compared to the hypolimnion with 42.3 mg/l (See table 1). Our results prove the assumption of previous studies that incoming groundwater functions as sulfate source (Kürfgen, 1999; LUBW, 2014). This is due to a carbonatic aquifer that can comprise sulfate (Van der Veen, 2003), agricultural land use (Van der Veen, 2003) and street salting (LUBW, 2014), where sulfates can be present as accessory minerals (Niedersächsisches Ministerium für Umwelt, Energie, Bauen und Klimaschutz, 2018). Moreover, it gets assumed that possible pyrite oxidation occurs in the sediment during the months of the mixing approach due to suboxic conditions, which can lead to production of sulfate.

The groundwater (QF, QKv) indicates an increased calcium concentration of 104.6 mg/l compared to the hypolimnion with 98.2 mg/l. It gets assumed that the actual groundwater comprises an even higher concentration of calcium than measured here, because the water of sampling points QF and QKv already experienced a degassing effect at the time of sampling. Different conditions get supposed in the aquifer with a higher CO₂ partial pressure that causes a pH shift and changes the carbonate balance system (Hofmann, 2011). Therefore, even higher calcium concentrations can be expected in the groundwater as measured in the samples. So, when the groundwater enters the lake a punctual degassing effect occurs that shortly raises pH and decreases Ca²⁺ concentration. The pH of the lake is smaller compared to the punctual outcome of groundwater, which promotes dissolution of Ca²⁺. Thus, the incoming groundwater of

Lake Steißlingen can be seen as a source of calcium among other things. Another process that delivers Ca^{2+} is the epilimnion where calcareous particles get precipitated by algae that can descends in the water column down to the hypolimnion where a recurring dissolution occurs caused by a lower pH.

The positive $\text{SI}_{\text{Calcite}}$ values calculated for Lake Steißlingen indicate a supersaturation and lead to calcite precipitation, which is typical for calcareous rich catchment areas (Koschel et al., 1997). However, calcite can presumably dissolve due to an effect by incoming groundwater denominated as mixture corrosion. This phenomenon can appear when two slightly oversaturated solutions with different water temperatures and calcium concentrations (groundwater and lake water) mix. This mixing process can lead to an excess of CO_2 and momentary change of $\text{SI}_{\text{Calcite}}$ that results in calcite dissolution.

Figure 27 shows that lake water samples and groundwater samples lay within the same area of the Piper Plot and get therefore characterized as carbonate type that clearly indicates groundwater influence in the hydrochemistry of Lake Steißlingen. This argument gets strengthened by the fact of high HCO_3^- and Ca^{2+} concentrations of 367.7 mg/l and 98.2 mg/l in the hypolimnion and underlines the assumption of accumulation of carbonatic groundwater there.

An average electrical conductivity of 655.3 $\mu\text{S}/\text{cm}$ and 844.7 $\mu\text{S}/\text{cm}$ was measured for both groundwater samples in 2016/2017, which is typical for surface near groundwaters (Bertleff, 2001). The incoming groundwater makes up 66.5% of QF and 33.5% of QKv which is about 718.7 $\mu\text{S}/\text{cm}$ of its average values that lay close to the average EC of the hypolimnion with 728.1 $\mu\text{S}/\text{cm}$. This result highlights again that Lake Steißlingen gets fed mainly by groundwater due the similarity of EC in the hypolimnion and the groundwater. This can also be seen in the month of June 2016 (See Figure 48).

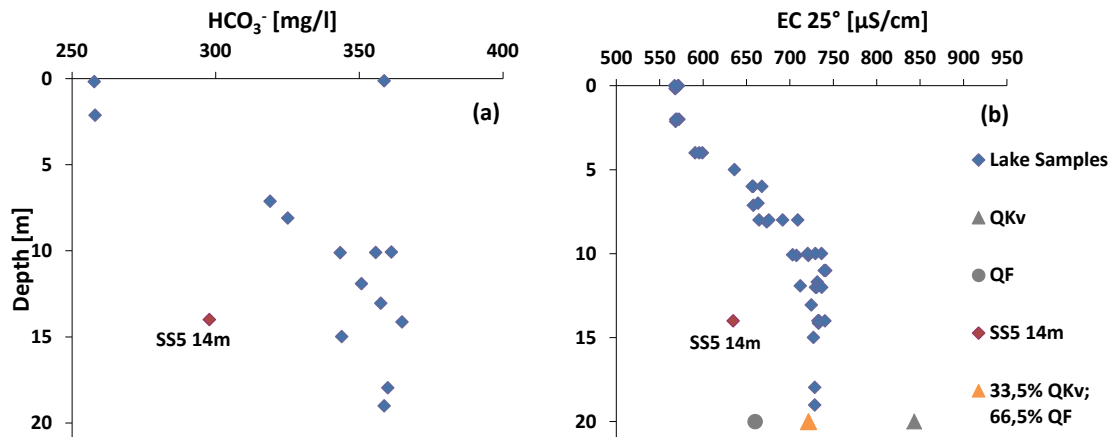


Figure 48 (a) HCO_3^- concentration in mg/l and (b) EC in $\mu\text{S}/\text{cm}$ against depth in June 2016.

5 Conclusion

The results of this study emphasize again the importance of groundwater – and surface water interactions in a lake system. The aims of this study were: The applicability of a groundwater tracing method from Lake Constance to Lake Steißlingen, the localization and origin of groundwater, the quantification of groundwater ratio, the mixing and distribution of groundwater and its influence to the lake circulation and seasonal alterations of groundwater recharge. This study reveals new findings, proofs and ideas for improvement, which will be shown in this chapter.

Within this study it could be proven that methods, which were developed for examinations at Lake Constance, are conferrable to a lake that indicates a difference in size and water volume. With the application of physical, chemical and isotopically measurements at Lake Steißlingen in 2016/2017, an insight to the lake stratification, seasonal variability and its groundwater ratio could be comprehended. To gain more accurate values for groundwater ratio and saturation indices of Lake Steißlingen, Phreeqc modelling and inverse modelling comprising all measured parameters (physical, chemical and isotopically), were utilized.

With the help of former geological surveys, a southwest-northeast running geological section could be interpolated. The geological interpretation of the subsurface leads to the assumption of a high permeable, quaternary lens at a sea level of 425-430 NN that cuts the lake at a depth of around 15m. Examinations of this study reveal that a distinct groundwater layer gets formed at a depth of around 14.0 m-15.0 m, where the quaternary aquifer tangents Lake Steißlingen. The natural tracer method with hydrogen – and oxygen isotopes showed that the water in the hypolimnion originate from local precipitation that infiltrates into the quaternary aquifer layer and finally flow into Lake Steißlingen. The incoming groundwater functions as NO_3^- , Cl^- , Na^+ , Ca^{2+} and HCO_3^- source, which was observed by the depth profiles of chemical parameters. This study is the first step towards enhancing the understanding of the geological conditions in the subsurface around Lake Steißlingen.

The formation of the hypolimnion, the accumulation of groundwater and non-mixing of the lake, cause an oxygen depletion between spring and fall months. This causes on the one hand the formation of NH_4^+ and HS^- through biological activity. On the other hand, suboxic conditions cause an increase of NO_3^- consumption by organisms. An exception was observed in March 2017 where the lake does not show a strong stratification after its mixing approach, causing suboxic conditions, under which NO_3^- does not get consumed immediately. Therefore, this month NO_3^- functions as groundwater indicator as NO_3^- shows punctual enhanced values in the middle of the lake at a depth of ~15m. NO_3^- gets accumulated at the location where groundwater enters the lake.

The calculation of groundwater ratio with stable oxygen isotopes showed a maximum of 71.8% in September 2017. The maximum value in September 2017 and other sampling points that also indicate high groundwater ratios, are located in the middle and north-easterly of the lake. A new finding within this thesis is the application of inverse modelling by Phreeqc that is more suitable and accurate for the calculation of groundwater ratios in a lake compared to a simple calculation of isotope ratios, due to the inclusion of several chemical, physical and isotopical parameters. Phreeqc calculations reveal a maximum groundwater ratio of 77.2%, which could be identified for September 2017. The sampling points with the highest groundwater ratios calculated are located in the middle and north-eastern side of the lake. For a better spatial resolution of groundwater localization, future research is needed.

The incoming groundwater to Lake Steißlingen causes the phenomenon of a “lake in a lake”. Between summer and fall months groundwater accumulates at a depth of around 15m forming a distinct water layer above the hypolimnion due to difference in density and water temperature. Then the groundwater layer and the layer below starts to interact with each other by exchanging heat, which finally causes a mixing process of the entire hypolimnion in fall months. This causes a homogeneity of the hypolimnion. During November 2016, an inverse stratification of the entire lake was being observed between epilimnion and the homogeneous hypolimnion, caused by warmer incoming groundwater.

While the hypolimnion of Lake Steißlingen gets fed by incoming groundwater providing ions and nutrients, the epilimnion is full of ion consuming organisms due to photogenic activity. This occurrence affects the stratification of Lake Steißlingen that gets rated as distinctly stable between spring and fall. The stable thermal and chemical stratification causes that Lake Steißlingen does not circulate entirely, but approaching a mixing event through exchange processes between epi- and hypolimnion.

This thesis gives mankind an idea of the lake system itself and the localization and ratio of groundwater in connection with its seasonal influence to the mixing dynamics, occurring redox reactions and stratification of Lake Steißlingen. To gain a more accurate spatial resolution for groundwater tracing within Lake Steißlingen, future studies should include a more precise hydrogeological analysis concerning real groundwater samples from groundwater wells, drilling cores with a grain size analysis for the determination of hydrogeological parameters and a higher amount of measurements closer to the sediment.

6 References

- Anibas C, Fleckenstein JH, Volze N, Buis K, Verhoeven R, Meire P, Batelaan O. Transient or steady-state? Using vertical temperature profiles to quantify groundwater-surface water exchange. *Hydrological Processes* Vol 23, 2165-2177 (2009)
- Arnoux M, Gibert-Brunet E, Barbecot F, Guillon S, Gibson J, Noret A. Interactions between groundwater and seasonally ice-covered lakes: Using water stable isotopes and radon-222 multilayer mass balance models. *Hydrological Processes* Vol 31, 2566-2581 (2017)
- Apello CAJ, Postma D. *Geochemistry, groundwater and pollution*. 2nd edition A.A. Balkema, Amsterdam (2005)
- Berner RA. A new geochemical classification of sedimentary environments. *Journal of Sedimentary Petrology* Vol 51, 0359-0365 (1981)
- Bertleff B, Plum H, Selg M, Szenkler C. *Hydrogeologische Erkundung Baden-Württemberg (Singen) Beiheft hydrogeologischer Bau Mappe 1. Bericht des Landesamt für Geologie, Rohstoffe und Bergbau (LGRB), Freiburg, pp. 23. (2005)*
- Bertleff B, Plum H, Schuff J, Stichler W, Storch DH, Trapp C. Wechselwirkungen zwischen Baggerseen und Grundwasser. *Bericht des Landesamt für Geologie, Rohstoffe und Bergbau – Baden – Württemberg, Freiburg, pp. 64 (2001)*
- Bohrer B, Schultze M. Stratification of Lakes. *Reviews of Geophysics* Vol 46, 10-15 (2008)
- Bundesanstalt für Geowissenschaften und Rohstoffe (BGR). *Geologische Übersichtskarte der Bundesrepublik Deutschland 1:200.000 (GÜK200) - CC 8718 Konstanz (2007)* (<https://produktcenter.bgr.de/terraCatalog/DetailResult.do?fileIdentifier=D83A4470-C0AC-4222-B4A7-BF82B62F205F>); last call up: 28.08.2017
- Bundesministerium für Umwelt, Naturschutz und Reaktorsicherheit (BMU). *Wasser im 21. Jahrhundert – Material für Bildung und Information. Druck Center Meckenheim, Berlin (2008)*
- Deutscher Wetterdienst. *Niederschlag: langjährige Mittelwerte 1981-2010 (generiert: 01.06.2017).* (http://www.dwd.de/DE/leistungen/klimadatendeutschland/mittelwerte/nieder_8110_akt.html.html?view=nasPublication&nn=16102); last call up: 04.09.2017
- Dimova N, Burnett WC, Chanton JP, Corbett J. Application of radon-222 to investigate groundwater discharge into small shallow lakes. *Journal of Hydrology* Vol 486, 112-122 (2013)

- Eusterhues K. Die Sedimente des Steißlinger Sees (Hegau, Süddeutschland) - Ein Archiv für zeitlich hoch aufgelöste geochemische Untersuchungen zu Umweltveränderungen im Holozän. Dissertation, Georg-August-Universität zu Göttingen (2000)
- Eusterhues K, Heinrich H, Schneider J. Geochemical response on redox fluctuations in Holocene lake sediments, Lake Steißlingen, Southern Germany. *Chemical Geology* Vol 222, 1-22 (2005)
- Eusterhues K, Lechterbeck J, Schneider J, Wolf-Brozio U. Late – and Post-Glacial evolution of lake Steißlingen (I). Sedimentary history, palynological record and inorganic geochemical indicators. *Palaeogeography, Palaeoclimatology, Palaeoecology* Vol 187, 341-371 (2002)
- Fleckenstein J, Krause S, Hannah D, Boano F. Groundwater-surface water interactions: New methods and models to improve understanding of processes and dynamics. *Advances in Water Resources* Vol 33, 1291-1295 (2010)
- Galler J, Eutrophierung (Ursachen und Maßnahmen). Landwirtschaftskammer Salzburg, Beratungsbroschüre, pp. 23 (2013)
- Garfunkel Z, Greiling RO. The implications of foreland basins for the causative tectonic loads. EGU Stephan Mueller Special Publication Series, 1, 3-16 (2002)
- Genereux D, Bandopadhyay I. Numerical investigation of lake bed seepage patterns: effects of porous medium and lake properties. *Journal of Hydrology* Vol 241, 286-303 (2001)
- Geoportal der Geodateninfrastruktur Baden-Württemberg (GDI-BW). (<http://www.geoportal-bw.de/geoportal/opencms/de/geoviewer.html>); last call up: 11.9.2017)
- Gilfedder B, Pfeiffer S, Pöschke F, Spirkander A. Grundwasserzufluss zum Steißlinger See und Folgen für die Wasserchemie. *Grundwasser* Vol 23, 155 - 165. (2018)
- Gleeson T, Befus K, Jasechko S, Luijendijk E, Cardenas B. The global volume and distribution of modern groundwater. *Nature Geoscience* Vol 9, 161-167 (2015)
- Güde H, Straile D. Bodensee – Ökologie und anthropogene Belastungen eines tiefen Voralpensees. *Limnologie aktuell*, Band 15. Schweizerbart, Stuttgart (2016)
- Hessisches Landesamt für Umwelt und Geologie: Gütebewertung Seen 2014 - Bereich Regierungspräsidium Gießen (2014) .
(https://www.hlnug.de/fileadmin/dokumente/wasser/seen/Seenbericht_2014_RP-Giessen.pdf); last call up: 05.04.2018
- Hotzan G. Die Formierung und Entwicklung des Chemismus natürlicher Grundwässer, ihre Widerspiegelung in hydrogeochemischen Genesemodellen sowie ihre Klassifizierung auf hydrogeochemisch-genetischer Grundlage. *Brandenburgische Geowissenschaftliche Beiträge* 1/2-2011, 77-91 (2011)

- Hötzl H. Origin of the Danube-Aach system. Environmental Geology Vol 27, 87-96 (1996)
- Hofmann T, Müllegger C. Abschlussbericht: Einfluss von Nassbaggerungen auf die Oberflächen- und Grundwasserqualität. Forschungsprojekt Nassbaggerungen (2011)
- IGKB. Der Bodensee, Zustand – Fakten – Perspektiven. Druckerei Uhl, pp. 177 (2004)
- Kalbus E, Reinstorf F, Schirmer M. Measuring methods for groundwater – surface water interactions: a review. Hydrology and Earth System Sciences Vol 10, 873-887 (2006)
- Koschel R, Kasprzak P, Schreiber A. Kalzitfällung und Nahrungskettenmanipulation. Laufener Seminarbeiträge 3, 61-76 (1997)
- Kralik M, Wyhlidal S, Philippitsch R. Erläuterungen zur Wasserisotopenkarte Österreichs: Der Niederschlags-, Oberflächenwasser-, Grundwasser- und Tiefengrundwasserstationen. Bericht des Bundesministerium für Land-, Forstwirtschaft, Umwelt und Wasserwirtschaft, Wien, pp. 30 (2015)
- Kralik M, Zieritz I, Grath J, Vincze G, Philippitsch R, Pavlik H. Hydrochemische Karte Österreichs oberflächennaher Grundwasserkörper und Fließgewässer – Mittelwerte von Wassergüteehebungsdaten Bericht des. Umweltbundesamt GmbH, Wien, pp. 16 (2004)
- Krause S, Hannah D, Fleckenstein J, Heppell C, Kaeser D, Pickup R, Pinay G, Robertson A, Wood P. Inter-disciplinary perspectives on processes in the hyporheic zone. Ecohydrology Vol 4, 481-499 (2010)
- Kürfgen G. Petrographische und geochemische Untersuchungen an den jüngsten, laminierten Sedimenten des Steißlinger Sees (Hegau). Diplomarbeit, Institut für Geologie und Dynamik der Lithosphäre der Georg-August-Universität zu Göttingen (1999)
- LaBaugh J, Winter T, Rosenberry D, Schuster P, Reddy M, Aiken G. Hydrological and chemical estimates of the water balance of a closed-basin lake in north central Minnesota. Water Resources Research Vol 33, 2799-2812 (1997)
- Landesamt für Geologie, Rohstoffe und Bergbau (LGRB). LGRB-Kartenviewer (2017) (<http://maps.lgrb-bw.de>); last call up: 11.09.2017
- Landesanstalt für Umwelt, Messungen und Naturschutz Baden-Württemberg (LUBW). ISF Jahresbericht, Karlsruhe, pp. 115 (2014)
- Landesanstalt für Umwelt, Messungen und Naturschutz Baden-Württemberg (LUBW). Document „Stammdaten_Grundwassermessstellen_SteisslingerSee“ was made available by groundwater department of LUBW (state July 2016)
- Landesanstalt für Umwelt, Messungen und Naturschutz Baden-Württemberg (LUBW). Zukünftige Klimaentwicklung in Baden-Württemberg, Karlsruhe, pp. 31 (2013)

- Langguth HR, Voigt R. Hydrogeologische Methoden. 2. Auflage Springer-Verlag Berlin Heidelberg GmbH, pp. 1006 (2004)
- Lechterbeck J. „Human Impact“ oder „Climatic Change“? Zur Vegetationsgeschichte des Spätglazials und Holozäns in hochauflösenden Pollenanalysen laminierter Sedimente des Steißlinger Sees. Dissertation, geowissenschaftliche Fakultät der Eberhard-Karls-Universität Tübingen (2000)
- Lewis E., Wallace D., Allison LJ. Program developed for CO₂ system calculations. Brookhaven National Lab., Dept. of Applied Science, Upton, NY (United States) Oak Ridge National Lab., Carbon Dioxide Information Analysis Center, TN (United States), Report ORNL/CDIAC-105 (1998)
- Mauersberger R, Kopp D. Klassifikation der Seen für die Naturraumerkundung des norddeutschen Tieflandes – Archiv für Naturschutz und Landschaftsforschung 45, 51-89 (2006)
- Millero FJ, Graham TB, Huang F, Bustos-Serrano H, Pierrot D. Dissociation constants of carbonic acid in seawater as a function of salinity and temperature. Marine Chemistry Vol 100, 80-94 (2006)
- Müllegger C. Der Einfluss von Nassbaggerungen auf die Grundwasserqualität, Hydrochemische, mikrobiologische und isotopenhydrologische Untersuchungen an fünf österreichischen Baggerseen, Dissertation, Universität Wien (2013)
- Niedersächsisches Ministerium für Umwelt, Energie, Bauen und Klimaschutz. Grundwasserbericht Niedersachsen, Hannover (2014) (<https://www.umwelt.niedersachsen.de/themen/wasser/grundwasser/grundwasserbericht/grundwasserbeschaffenheit/queteparameter/grundprogramm/sulfat/sulfat-137612.html>); last call up: 16.03.2018
- Parkhurst, DL, Apello CAJ. User's guide to PHREEQC (Version 2) - A computer program for speciation, Batch-reaction, one-dimensional transport, and inverse geochemical calculations. Water-Resources Investigations Report, 99-4259 (1999)
- Peschtrich K. Die Entwicklung der Umweltbelastung vom Mittelalter bis zur Neuzeit im Gebiet des Steißlinger Sees. Dissertation, Geowissenschaftliches Zentrum der Universität Göttingen (2005)
- Rosenberry D, Lewandowski J, Meinikmann K, Nützmann G. Groundwater- the disregarded component in lake water and nutrient budgets. Part 1: effects of groundwater on hydrology. Hydrological Processes Vol 29, 2895-2921 (2015)
- Schlunegger F, Kissling E. Slab rollback orogeny in the Alps and evolution of the Swiss Molasse basin. Nature Communications Vol 6, 1-10 (2015).

- Schmidt A, Gibson JJ, Santos IR, Schubert M, Tattrie K, Weiss H. The contribution of groundwater discharge to the overall water budget of two typical Boreal lakes in Alberta/Canada estimated from a radon mass balance. *Hydrology and Earth System Sciences* Vol 14, 79-89 (2010)
- Schneider J. Abschlussbericht: Die Entwicklungsgeschichte des Steißlinger Sees (Hegau) als Spiegel sich verändernder Klima- und Umweltbedingungen während der letzten 15.000 Jahre. Ein Standardprofil für den westlichen Bodenseeraum. Abschlussbericht DFG-Projekt 16/19-4 (2000)
- Schönborn W, Risse-Buhl U. Lehrbuch der Limnologie, 2. Auflage Schweizerbart Stuttgart, pp. 669 (2013)
- Sea & Sun Technology GmbH. CTD90 m Memory probe –Manual and operating instructions. Version 1 (2002)
- Sebok E, Duque C, Kazmierczak J, Engesgaard P, Nilsson B, Karan S, Frandsen M. High-resolution distributed temperature sensing to detect seasonal groundwater discharge into Lake Væng, Denmark. *Water Resources Research* Vol 49, 5355-5368 (2013)
- Spirkaneder A. Interaktion von Grund- und Seewasser und daraus resultierende Folgen für die Wasserqualität am Steißlinger See, Bachelorarbeit Universität Bayreuth (2016)
- Sundaram TR, Rehm RG. Formation and Maintenance of Thermoclines in Temperate Lakes. *AIAA Journal* Vol 9, 1322-1329 (1971)
- Tepe Y, Türkmen A, Mutlu E, Ates A. Some Physicochemical Characteristics of Yarseli Lake, Hatay, Turkey. *Turkish Journal of Fisheries and Aquatic Sciences* Vol 5, 35-42 (2005)
- Tyson RV, Pearson TH. Modern and ancient continental shelf anoxia: an overview. *Geological Society Special Publication* Vol 58, 1-24 (1991)
- Van der Veen A. Schwefelspeziation und assoziierte Metalle in rezenten Sedimenten. Dissertation, Gemeinsame Naturwissenschaftliche Fakultät der Technischen Universität Carolo-Wilhemina zu Braunschweig (2003)
- Vogt T, Hoehn E, Schneider P, Freund A, Schirmer M, Cirpka OA. Fluctuations of electrical conductivity as a natural tracer for bank filtration in a losing stream. *Advances in Water Resources* Vol 33, 1296-1308 (2010)
- Wahl B, Peeters F. Effect of climatic changes on stratification and deep-water renewal in Lake Constance assessed by sensitivity studies with a 3D hydrodynamic model. *Limnol. Oceanogr.* Vol 59, 1035-1052 (2014)

Wolf U. Nähr- und Schadstoffbelastung kleiner Seen in Baden Württemberg unter Berücksichtigung der Sedimentationsgeschichte. Die Rolle der kleinen Stehgewässer im regionalen Verbund. Dissertation Georg-August-Universität Göttingen (1994)

Appendix

A) Table of Figures

Figure 1 Geographical location of the research area (constructed with QGIS OpenLayers plugin, print composer)	6
Figure 2 Geology of Southwestern-Germany, France and Switzerland (Hötzl, 1996)	7
Figure 3 Geological map of the research area Steißlingen (LGRB, 2017). The denomination and interpretation of the faults is based on the study of Barnikol-Schlamm (1994).	8
Figure 4 Geological section of the survey area Lake Steißlingen; drawn manually and digitalized by Microsoft PowerPoint integrating data of LRGB (2017), LUBW and GDI-BW (2017).	12
Figure 5 Surface catchment area of Lake Steißlingen (Compiled by LUBW (Obad) copyright by LUBW Baden-Württemberg based on "räumlichen Informations- und Planungssystem" (RIPS) and Siedlung „ATKIS-DLM25 BW" copyright Landesamt für Geoinformation und Landentwicklung Baden-Württemberg, Stuttgart (www.lgl-bw.de) Az 2851 (2011))	14
Figure 6 Interpolation of measured ²²² Radon activities and assumed groundwater inlets (black mark) at the bottom of Lake Steißlingen (Spirkaneder, 2016)	15
Figure 7 Isoleth map of (a) water temperature (b) ammonium (c) O ₂ and (d) Ca ²⁺ in 2014.	16
Figure 8 Physical-chemical parameters of Lake Steißlingen in 2014 and 1987 (LUBW, 2014)	17
Figure 9 Defined measuring Grid in Gauß-Krüger coordinate system with black sampling points (data LUBW), orange sampling points (University of Bayreuth) and purple sampling points (data GFZ Potsdam that gets involved in chapter 4) (constructed with Surfer ®)	19
Figure 10 Measuring grid map of Lake Steißlingen in Gauß-Krüger coordinates.	30
Figure 11 Data of water temperature measurements of Lake Steißlingen from different seasons with the references Z, Q and A against water depth. (a) June 2016, (b) November 2016, (c) March 2017, (d) July 2017 and (e) September 2017. The x-axis demonstrates water temperature in [°C] and the y-axis shows water depth in [m].	31
Figure 12 Depth profiles of EC measured by titration (T=25°C) in [µS/cm] (x-axis) vs. depth (y-axis) for the months of (a) June 2016, (b) November 2016, (c) March 2017, (d) June 2017 and (e) September 2017.	32
Figure 13 The plots of (a) June 2016, (b) November 2016, (c) March 2017, (d) July 2017 and (e) September 2017 show dissolved oxygen in [mg/l] plotted on the x-axis and depth in [m].	34
Figure 14 Oxygen saturation in [%] vs. depth in [m] in (a) June 2016 (b) November 2016 (c) March 2017 (d) July 2017 and (e) September 2017.	35

Figure 15 The delineation shows turbidity in FTU (x-axis) versus depth in [m] (y-axis) of the sampling campaigns in (a) June 2016, (b) November 2016, (c) March 2017, (d) July 2017 and (e) September 2017 of Lake Steißlingen. A different scale for the graph of September 2017 was chosen, because sampling point 1 is deviating strongly due to plant growth. 36

Figure 16 pH-value vs. water depth in [m] in (a) June 2016, (b) November 2016, (c) March 2017, (d) July 2017 and (e) September 2017. 37

Figure 17 Chlorophyll A contents in [$\mu\text{g/l}$] on the x-axis vs. depth in [m] on the y-axis in (a) June 2016, (b) November 2016, (c) March 2017, (d) July 2017 and (e) September 2017. Because of strong Chlorophyll A fluctuations between the seasons, different scales were chosen depending on the concentration range. 39

Figure 18 The results of TA in (a) June 2016, (b) November 2016, (c) March 2017, (d) July 2017 and (e) September 2017 plotted in [mmol/l] on the x-axis vs. depth in [m] on the y-axis. 40

Figure 19 The results of Lake Steißlingen for water hardness were plotted on the x-axis in [$\frac{1}{2}$ mmol/l] with corresponding depths on the y-axis in [m] in (a) June 2016, (b) November 2016, (c) March 2017, (d) July 2017 and (e) September 2017. 41

Figure 20 Chloride concentration in [mg/l] on the x-axis vs. depth in [m] in the months of (a) June 2016, (b) November 2016, (c) March 2017, (d) July 2017 and (e) September 2017. 43

Figure 21 Sulfate concentration in [mg/l] on the x-axis vs. depth in [m] on the y-axis in (a) June 2016, (b) November 2016, (c) March 2017, (d) July 2017 and (e) September 2017. 44

Figure 22 $\text{NO}_3\text{-N}$ values on the x-axis in [$\mu\text{g/l}$] vs. depth in [m] on the y-axis in (a) June 2016, (b) November 2016, (c) March 2017, (d) July 2017 and (e) September 2017. 45

Figure 23 Ammonium concentration on the x-axis in [$\mu\text{g/l}$] vs. depth in [m] on the y-axis in (a) June 2016, (b) November 2016, (c) March 2017, (d) July 2017 and (e) September 2017. 47

Figure 24 Sodium concentration in [mg/l] on the x-axis and depth in [m] on the y-axis in (a) June 2016, (b) November 2016, (c) March 2017, (d) July 2017 and (e) September 2017. 48

Figure 25 The illustration of potassium concentrations on the x-axis in [$\mu\text{g/l}$] with depth in [m] on the y-axis in (a) June 2016, (b) November 2016, (c) March 2017, (d) July 2017 and (e) September 2017. 49

Figure 26 Calcium concentration at Lake Steißlingen in (a) June 2016, (b) November 2016, (c) March 2017, (d) July 2017 and (e) September 2017. The x-axis demonstrates calcium in [$\frac{1}{2}$ mmol/l] and the y-axis shows water depth in [m]. 50

Figure 27 Magnesium concentration in and around Lake Steißlingen in (a) June 2016, (b) November 2016, (c) March 2017, (d) July 2017 and (e) September 2017. The x-axis demonstrates magnesium in [$\frac{1}{2}$ mmol/l] and the y-axis shows depth in [m]. 52

Figure 28 $\delta^{18}\text{O}$ values in [‰] on x-axis vs. depth in [m] on y-axis in (a) June 2016, (b) November 2016, (c) March 2017, (d) July 2017 and (e) September 2017.	54
Figure 29 The plots indicate $\delta^2\text{H}$ in [‰] on the x-axis vs. depth in [m] on the y-axis in (a) June 2016 (b) November 2016 (c) March 2017 (d) July 2017 (e) September 2017.	55
Figure 30 Groundwater mixing ratio in [%] vs. depth in [m] in the months of (a) June 2016 (b) November 2016 (c) March 2017 (d) July 2017 (e) September 2017.	56
Figure 31 Calcite Saturation indices of Lake Steißlingen from different seasons of 2016/2017 (calculated with Phreeqc) against depth.	58
Figure 32 Calculated groundwater mixing ratio (based on Phreeqc) in [%] with interpolation between the sampling points 2016/2017 (a)-(e) June16, Nov 16, March17, July 17, Sept17; (f) legend.	59
Figure 33 Following meteorological parameters were measured in 2016/2017 at EnviWatch station: (a) Air temperature, (b) wind velocity, (c) pressure, (d) solar radiation and (e) monthly precipitation rate.	62
Figure 34 (a) represents temperature, (b) electrical conductivity and (c) represents dissolved oxygen fluctuation in 2016/2017 of the measurement of CTD depth profile which is representative for the entire lake on station K1.	66
Figure 35 Temperature depth profile for November 2016 to December 2017 (a), November-December 2016 (c), November-December 2017 (d) measured with the thermistor chain and a large-scale delineation of temperature in November 2016 (b) measured with the CTD.	67
Figure 36 Redox processes that can happen under specific energetic conditions in the water column or the pore water of the sediment.	71
Figure 37 (a) Sulfate and sulfide concentrations within the pore water at station 13 and. (b) sulfate concentration within the water column in Lake Steißlingen September 2017 against water/sediment depth.	72
Figure 38 Succession of redox processes in a natural aqueous system (Appelo, 2005).	73
Figure 39 (a) Delineation of average lake composition for measuring campaigns during 2016/2017 (Domenico and Schwartz, 1997) (b) Piper hydro-geochemical diagram (Carlos, Molano) for Lake Steißlingen measuring campaigns during 2016/2017.	74
Figure 40 Isotopic composition of collected precipitation between March 2017 and September 2017 (Personal disclosure of data by Dirk Sachse (GFZ Potsdam)).	75
Figure 41 Local Meteoric Water Line Lake Steißlingen constructed with data by GFZ and LUBW 2016/2017.	76

Figure 42 Depth profiles of June 2016 (a) CO ₂ content in [mg/l] (b) SiCalcite (c) Ca ²⁺ concentration	78
Figure 43 (a) Distribution of ²²² Rn activities by Gilfedder et al. (2018) (b) NO ₃ -N values of the hypolimnion in March 2017	80
Figure 44 (a) Distribution of ²²² Rn activities by Gilfedder et al. (2018) (b) δ ¹⁸ O values of the hypolimnion in September 2017	81
Figure 45 (a) Groundwater Ratio of Lake Steißlingen against depth calculated by Phreeqc Inverse Modeling (b) Groundwater Mixing Ratio of QKv versus QF calculated with Phreeqc Inverse Modeling.	83
Figure 46 Isopleth diagram 2016/2017 including temperatures between 4°C and 10°C at station K1 measured with the thermistor chain at the permanent measuring station.	87
Figure 47 NO ₃ -N concentration in [µg/l] (d) in March 2017 (a), July 2017 (b) and September 2017 (c). Sampling points plotted in Gauß Krüger coordinates (d) legend.	88
Figure 48 (a) HCO ₃ ⁻ concentration in [mg/l] and (b) EC in [µS/cm] against depth in June 2016.	90

B) List of Tables

Table 1 Arithmetic water composition of the epilimnion and metalimnion, hypolimnion, QF and QKv and the assumed groundwater composition:

68

Sampling area	Mg2+ [mg/l]	Ca2+ [mg/l]	K+ [mg/l]	Na+ [mg/l]	Cl- [mg/l]	SO42- [mg/l]	HCO3- [mg/l]	CO32- [mg/l]	NH4+-N [µg/l]	NO3-N [µg/l]
Epi- and metalimnion (Arithmetic mean)	25,0	75,3	2,2	15,7	30,8	41,9	287,5	1,2	310	1082
Hypolimnion (Arithmetic mean)	26,9	98,2	2,4	16,6	32,4	42,3	367,7	0,4	895	1012
QF (Arithmetic mean)	27,6	96,4	1,1	4,5	8,7	37,5	359,3	0,4	75	3020
QKv (Arithmetic mean)	25,6	121,0	11,7	17,1	31,5	31,4	421,9	0,4	21	7456
Groundwater (33,5% QKv + 66,5% QF)	26,9	104,6	4,7	8,7	16,3	35,5	380,3	0,4	57	4508

C) Physical, Chemical and Isotopic Parameters

Sampling Point	Date	Time	Depth	Water T	EC	O2	O2	ChlA	Turbidity	pH	TA	Water hardness
		h	m	°C	µS/cm	%	mg/l	mg/l	FTU		mmol/l	°dH
SZ_GW_SteißlingerSee_01	21.06.2016	13:00	4,5	12,55	n.a.n.	112,1	11,7	1,4	10,5	n.a.n.	n.a.n.	n.a.n.
SZ_GW_SteißlingerSee_02	21.06.2016	13:04	5,0	10,21	n.a.n.	101,9	11,2	1,3	8,7	n.a.n.	n.a.n.	n.a.n.
SZ_GW_SteißlingerSee_03	21.06.2016	11:00	7,1	8,42	658,0	76,5	8,9	1,0	5,9	7,79	5,25	17,88
SZ_GW_SteißlingerSee_03	21.06.2016	11:00	2,1	19,78	568,5	98,2	8,9	1,2	6,5	8,22	4,29	15,11
SZ_GW_SteißlingerSee_04	21.06.2016	13:10	2,8	19,09	n.a.n.	107,2	9,8	2,0	13,9	n.a.n.	n.a.n.	n.a.n.
SZ_GW_SteißlingerSee_05	21.06.2016	13:13	7,0	7,67	n.a.n.	54,9	6,5	0,9	5,9	n.a.n.	n.a.n.	n.a.n.
SZ_GW_SteißlingerSee_06	21.06.2016	13:16	12,9	7,06	n.a.n.	4,2	0,5	1,3	11,1	n.a.n.	n.a.n.	n.a.n.
SZ_GW_SteißlingerSee_07	21.06.2016	13:20	7,4	7,47	n.a.n.	47,1	5,6	1,1	6,5	n.a.n.	n.a.n.	n.a.n.
SZ_GW_SteißlingerSee_08	21.06.2016	13:25	5,8	9,51	n.a.n.	103,3	11,6	2,2	10,5	n.a.n.	n.a.n.	n.a.n.
SZ_GW_SteißlingerSee_09	21.06.2016	10:50	11,9	7,07	711,9	6,2	0,7	2,7	8,8	7,43	5,76	18,73
SZ_GW_SteißlingerSee_10	21.06.2016	10:35	14,1	6,89	733,0	4,3	0,5	1,3	7,9	7,35	5,99	19,48
SZ_GW_SteißlingerSee_10	21.06.2016	10:35	10,1	7,02	721,3	15,1	1,8	2,2	9,0	7,41	5,84	19,14
SZ_GW_SteißlingerSee_10	21.06.2016	10:35	0,2	19,82	568,0	97,6	8,9	0,4	4,0	8,25	4,29	14,73
SZ_GW_SteißlingerSee_11	21.06.2016	10:27	10,1	7,12	707,6	16,5	2,0	1,3	15,5	7,50	5,64	18,56
SZ_GW_SteißlingerSee_12	21.06.2016	10:14	8,1	7,24	673,4	56,2	6,7	0,9	5,2	7,77	5,35	18,05
SZ_GW_SteißlingerSee_13	21.06.2016	10:20	15,0	6,80	n.a.n.	6,7	0,8	1,7	11,6	n.a.n.	n.a.n.	n.a.n.
SZ_GW_SteißlingerSee_14	21.06.2016	10:25	11,9	6,99	n.a.n.	7,4	0,9	1,2	8,7	n.a.n.	n.a.n.	n.a.n.
SZ_GW_SteißlingerSee_15	21.06.2016	10:11	6,9	7,84	n.a.n.	90,3	10,5	1,0	5,6	n.a.n.	n.a.n.	n.a.n.
SZ_GW_SteißlingerSee_16	21.06.2016	10:06	18,8	6,69	n.a.n.	3,8	0,5	1,0	9,7	n.a.n.	n.a.n.	n.a.n.
SZ_GW_SteißlingerSee_17	21.06.2016	10:03	12,5	6,91	n.a.n.	5,3	0,6	1,4	9,6	n.a.n.	n.a.n.	n.a.n.
SZ_GW_SteißlingerSee_18	21.06.2016	09:09	18,0	6,74	728,6	4,9	0,6	1,1	13,1	7,41	5,91	19,60
SZ_GW_SteißlingerSee_18	21.06.2016	09:09	13,1	6,90	724,7	4,4	0,5	1,9	8,5	7,45	5,87	19,55
SZ_GW_SteißlingerSee_19	21.06.2016	09:29	12,0	6,89	n.a.n.	5,8	0,7	1,9	11,3	n.a.n.	n.a.n.	n.a.n.
SZ_GW_SteißlingerSee_20	21.06.2016	09:03	11,7	6,84	n.a.n.	5,4	0,6	3,1	10,1	n.a.n.	n.a.n.	n.a.n.
SZ_GW_SteißlingerSee_K1	21.06.2016	09:35	19,0	6,65	728,6	3,9	0,5	1,0	16,2	7,40	5,93	19,59
SZ_GW_SteißlingerSee_K1	21.06.2016	09:35	15,0	6,78	727,2	5,6	0,7	1,3	7,3	7,44	5,89	19,61
SZ_GW_SteißlingerSee_K1	21.06.2016	09:35	10,1	6,79	703,2	13,8	1,7	2,6	8,4	7,57	5,65	18,90
SZ_GW_SteißlingerSee_K1 OW	21.06.2016	09:35	0,1	19,54	568,6	98,1	9,0	0,7	6,7	8,27	4,28	15,04
SZ_St_SS2 0m	20.06.2016	n.a.n.	0,0	n.a.n.	571,3	n.a.n.	n.a.n.	n.a.n.	n.a.n.	8,22	4,29	15,07
SZ_St_SS2 2m	20.06.2016	n.a.n.	2,0	n.a.n.	572,3	n.a.n.	n.a.n.	n.a.n.	n.a.n.	8,20	4,29	15,10
SZ_St_SS2 4m	20.06.2016	n.a.n.	4,0	n.a.n.	599,2	n.a.n.	n.a.n.	n.a.n.	n.a.n.	8,08	4,59	15,96
SZ_St_SS2 6m	20.06.2016	n.a.n.	6,0	n.a.n.	657,6	n.a.n.	n.a.n.	n.a.n.	n.a.n.	7,91	5,21	17,72
SZ_St_SS2 8m	20.06.2016	n.a.n.	8,0	n.a.n.	664,7	n.a.n.	n.a.n.	n.a.n.	n.a.n.	7,80	5,27	17,89
SZ_St_SS2 10m	20.06.2016	n.a.n.	10,0	n.a.n.	720,6	n.a.n.	n.a.n.	n.a.n.	n.a.n.	7,48	5,86	19,53
SZ_St_SS2 12m	20.06.2016	n.a.n.	12,0	n.a.n.	729,7	n.a.n.	n.a.n.	n.a.n.	n.a.n.	7,45	5,87	19,56
SZ_St_SS2 14m	20.06.2016	n.a.n.	14,0	n.a.n.	732,4	n.a.n.	n.a.n.	n.a.n.	n.a.n.	7,66	5,95	19,83
SZ_St_SS4 0m	20.06.2016	n.a.n.	0,0	n.a.n.	571,6	n.a.n.	n.a.n.	n.a.n.	n.a.n.	8,27	4,30	15,08
SZ_St_SS4 2m	20.06.2016	n.a.n.	2,0	n.a.n.	570,2	n.a.n.	n.a.n.	n.a.n.	n.a.n.	8,26	4,27	14,97
SZ_St_SS4 4m	20.06.2016	n.a.n.	4,0	n.a.n.	591,0	n.a.n.	n.a.n.	n.a.n.	n.a.n.	8,16	4,50	15,70
SZ_St_SS4 5m	20.06.2016	n.a.n.	5,0	n.a.n.	636,3	n.a.n.	n.a.n.	n.a.n.	n.a.n.	8,06	4,97	17,01
SZ_St_SS4 6m	20.06.2016	n.a.n.	6,0	n.a.n.	657,1	n.a.n.	n.a.n.	n.a.n.	n.a.n.	8	5,15	17,46
SZ_St_SS4 7m	20.06.2016	n.a.n.	7,0	n.a.n.	663,4	n.a.n.	n.a.n.	n.a.n.	n.a.n.	7,94	5,24	17,72
SZ_St_SS4 8m	20.06.2016	n.a.n.	8,0	n.a.n.	675,8	n.a.n.	n.a.n.	n.a.n.	n.a.n.	7,89	5,4	17,69
SZ_St_SS5 0m	21.06.2016	n.a.n.	0,0	n.a.n.	567,3	n.a.n.	n.a.n.	n.a.n.	n.a.n.	8,22	4,29	14,77
SZ_St_SS5 2m	21.06.2016	n.a.n.	2,0	n.a.n.	568,7	n.a.n.	n.a.n.	n.a.n.	n.a.n.	8,22	4,27	14,71
SZ_St_SS5 4m	21.06.2016	n.a.n.	4,0	n.a.n.	595,5	n.a.n.	n.a.n.	n.a.n.	n.a.n.	8,11	4,53	15,41
SZ_St_SS5 6m	21.06.2016	n.a.n.	6,0	n.a.n.	656,8	n.a.n.	n.a.n.	n.a.n.	n.a.n.	7,9	5,2	17,26
SZ_St_SS5 8m	21.06.2016	n.a.n.	8,0	n.a.n.	691,9	n.a.n.	n.a.n.	n.a.n.	n.a.n.	7,63	5,51	18,05
SZ_St_SS5 10m	21.06.2016	n.a.n.	10,0	n.a.n.	736,5	n.a.n.	n.a.n.	n.a.n.	n.a.n.	7,42	5,88	n.a.n.
SZ_St_SS5 12m	21.06.2016	n.a.n.	12,0	n.a.n.	731,0	n.a.n.	n.a.n.	n.a.n.	n.a.n.	7,42	5,9	19,07
SZ_St_SS5 14m	21.06.2016	n.a.n.	14,0	n.a.n.	634,8	n.a.n.	n.a.n.	n.a.n.	n.a.n.	7,76	4,9	16,37
SZ_St_SK1	21.06.2016	n.a.n.	6,0	n.a.n.	667,8	n.a.n.	n.a.n.	n.a.n.	n.a.n.	7,95	5,32	17,42
SZ_St_SK2	21.06.2016	n.a.n.	8,0	n.a.n.	709,0	n.a.n.	n.a.n.	n.a.n.	n.a.n.	7,62	5,71	18,42
SZ_St_SK3	21.06.2016	n.a.n.	12,0	n.a.n.	736,9	n.a.n.	n.a.n.	n.a.n.	n.a.n.	7,49	5,93	19,17
SZ_St_SK4	21.06.2016	n.a.n.	11,0	n.a.n.	741,4	n.a.n.	n.a.n.	n.a.n.	n.a.n.	7,49	5,96	19,28
SZ_St_SK5	21.06.2016	n.a.n.	10,0	n.a.n.	729,4	n.a.n.	n.a.n.	n.a.n.	n.a.n.	7,53	5,91	19,03
SZ_St_SK6	21.06.2016	n.a.n.	14,0	n.a.n.	733,5	n.a.n.	n.a.n.	n.a.n.	n.a.n.	7,52	5,9	18,97
SZ_St_SK7	21.06.2016	n.a.n.	14,0	n.a.n.	733,5	n.a.n.	n.a.n.	n.a.n.	n.a.n.	7,56	5,93	19,02
SZ_St_SK8	21.06.2016	n.a.n.	14,0	n.a.n.	740,4	n.a.n.	n.a.n.	n.a.n.	n.a.n.	7,53	5,94	19,08
SZ_St_SK9	21.06.2016	n.a.n.	11,0	n.a.n.	739,8	n.a.n.	n.a.n.	n.a.n.	n.a.n.	7,54	6,02	19,34
SZ_GW_SteißlingerSee_QF	22.06.2016	n.a.n.	20,0	n.a.n.	660,0	n.a.n.	n.a.n.	n.a.n.	n.a.n.	7,45	5,94	19,08
SZ_GW_SteißlingerSee_QKv	22.06.2016	n.a.n.	20,0	n.a.n.	843,5	n.a.n.	n.a.n.	n.a.n.	n.a.n.	7,32	6,87	22

Sampling Point	Date	Time h	Depth m	Chloride mg/l	NO3-N µg/l	Sulfate mg/l	NH4-N µg/l	1/2 Calcium mmol/l	Magnesi mmol/l	Sodium mg/l	Potassium mg/l	² H ‰	¹⁸ O ‰
SZ_GW_SteiblingerSee_01	21.06.2016	13:00	4,5	n.a.n.	n.a.n.	n.a.n.	n.a.n.	n.a.n.	n.a.n.	n.a.n.	n.a.n.	n.a.n.	n.a.n.
SZ_GW_SteiblingerSee_02	21.06.2016	13:04	5,0	n.a.n.	n.a.n.	n.a.n.	n.a.n.	n.a.n.	n.a.n.	n.a.n.	n.a.n.	n.a.n.	n.a.n.
SZ_GW_SteiblingerSee_03	21.06.2016	11:00	7,1	30,61	1321,3	43,56	446,50	4,34	2,13	15,74	2,32	-61,01	-8,02
SZ_GW_SteiblingerSee_03	21.06.2016	11:00	2,1	28,85	1547,2	41,40	187,92	3,54	1,96	14,88	2,13	-58,42	-7,59
SZ_GW_SteiblingerSee_04	21.06.2016	13:10	2,8	n.a.n.	n.a.n.	n.a.n.	n.a.n.	n.a.n.	n.a.n.	n.a.n.	n.a.n.	n.a.n.	n.a.n.
SZ_GW_SteiblingerSee_05	21.06.2016	13:13	7,0	n.a.n.	n.a.n.	n.a.n.	n.a.n.	n.a.n.	n.a.n.	n.a.n.	n.a.n.	n.a.n.	n.a.n.
SZ_GW_SteiblingerSee_06	21.06.2016	13:16	12,9	n.a.n.	n.a.n.	n.a.n.	n.a.n.	n.a.n.	n.a.n.	n.a.n.	n.a.n.	n.a.n.	n.a.n.
SZ_GW_SteiblingerSee_07	21.06.2016	13:20	7,4	n.a.n.	n.a.n.	n.a.n.	n.a.n.	n.a.n.	n.a.n.	n.a.n.	n.a.n.	n.a.n.	n.a.n.
SZ_GW_SteiblingerSee_08	21.06.2016	13:25	5,8	n.a.n.	n.a.n.	n.a.n.	n.a.n.	n.a.n.	n.a.n.	n.a.n.	n.a.n.	n.a.n.	n.a.n.
SZ_GW_SteiblingerSee_09	21.06.2016	10:50	11,9	31,77	1529,6	44,12	874,36	4,83	2,20	16,25	2,34	-62,27	-8,38
SZ_GW_SteiblingerSee_10	21.06.2016	10:35	14,1	32,21	1474,0	44,16	1061,50	5,00	2,24	16,81	2,39	-63,56	-8,46
SZ_GW_SteiblingerSee_10	21.06.2016	10:35	10,1	31,83	1493,2	43,03	917,85	4,89	2,21	16,73	2,37	-62,53	-8,45
SZ_GW_SteiblingerSee_10	21.06.2016	10:35	0,2	28,89	1423,2	41,07	196,46	3,53	1,96	14,87	2,13	-58,99	-7,49
SZ_GW_SteiblingerSee_11	21.06.2016	10:27	10,1	31,81	1485,7	42,97	816,12	4,74	2,18	16,55	2,38	-63,82	-8,38
SZ_GW_SteiblingerSee_12	21.06.2016	10:14	8,1	31,11	1187,6	43,02	618,11	4,53	2,18	16,12	2,37	-62,98	-8,06
SZ_GW_SteiblingerSee_13	21.06.2016	10:20	15,0	n.a.n.	n.a.n.	n.a.n.	n.a.n.	n.a.n.	n.a.n.	n.a.n.	n.a.n.	n.a.n.	n.a.n.
SZ_GW_SteiblingerSee_14	21.06.2016	10:25	11,9	n.a.n.	n.a.n.	n.a.n.	n.a.n.	n.a.n.	n.a.n.	n.a.n.	n.a.n.	n.a.n.	n.a.n.
SZ_GW_SteiblingerSee_15	21.06.2016	10:11	6,9	n.a.n.	n.a.n.	n.a.n.	n.a.n.	n.a.n.	n.a.n.	n.a.n.	n.a.n.	n.a.n.	n.a.n.
SZ_GW_SteiblingerSee_16	21.06.2016	10:06	18,8	n.a.n.	n.a.n.	n.a.n.	n.a.n.	n.a.n.	n.a.n.	n.a.n.	n.a.n.	n.a.n.	n.a.n.
SZ_GW_SteiblingerSee_17	21.06.2016	10:03	12,5	n.a.n.	n.a.n.	n.a.n.	n.a.n.	n.a.n.	n.a.n.	n.a.n.	n.a.n.	n.a.n.	n.a.n.
SZ_GW_SteiblingerSee_18	21.06.2016	09:09	18,0	32,14	1071,9	43,13	1105,76	4,92	2,22	16,48	2,41	-64,53	-8,40
SZ_GW_SteiblingerSee_18	21.06.2016	09:09	13,1	32,05	1458,6	43,14	924,06	4,88	2,21	16,69	2,39	-65,21	-8,60
SZ_GW_SteiblingerSee_19	21.06.2016	09:29	12,0	n.a.n.	n.a.n.	n.a.n.	n.a.n.	n.a.n.	n.a.n.	n.a.n.	n.a.n.	n.a.n.	n.a.n.
SZ_GW_SteiblingerSee_20	21.06.2016	09:03	11,7	n.a.n.	n.a.n.	n.a.n.	n.a.n.	n.a.n.	n.a.n.	n.a.n.	n.a.n.	n.a.n.	n.a.n.
SZ_GW_SteiblingerSee_K1	21.06.2016	09:35	19,0	32,32	527,7	43,62	1306,88	4,94	2,23	16,65	2,43	-65,13	-8,49
SZ_GW_SteiblingerSee_K1	21.06.2016	09:35	15,0	32,08	1313,6	43,04	1014,91	4,91	2,22	16,46	2,40	-64,58	-8,48
SZ_GW_SteiblingerSee_K1	21.06.2016	09:35	10,1	31,59	1368,5	43,04	785,06	4,65	2,17	16,11	2,34	-63,55	-8,26
SZ_GW_SteiblingerSee_K1 C	21.06.2016	09:35	0,1	28,92	1432,0	41,11	193,35	3,52	1,96	14,93	2,14	-60,70	-7,57
SZ_St_SS2 0m	20.06.2016	n.a.n.	0,0	29,03	1431,8	41,23	186,36	3,55	1,97	14,95	2,19	n.a.n.	n.a.n.
SZ_St_SS2 2m	20.06.2016	n.a.n.	2,0	29,00	1428,4	41,30	195,68	3,57	1,98	15,02	2,15	n.a.n.	n.a.n.
SZ_St_SS2 4m	20.06.2016	n.a.n.	4,0	29,44	1392,2	42,08	211,21	3,90	2,05	15,53	2,22	n.a.n.	n.a.n.
SZ_St_SS2 6m	20.06.2016	n.a.n.	6,0	31,10	1153,9	43,41	442,62	4,35	2,14	15,79	2,30	n.a.n.	n.a.n.
SZ_St_SS2 8m	20.06.2016	n.a.n.	8,0	30,83	1253,3	42,89	456,59	4,28	2,12	15,83	2,32	n.a.n.	n.a.n.
SZ_St_SS2 10m	20.06.2016	n.a.n.	10,0	31,86	1353,8	43,23	904,65	4,91	2,24	16,55	2,42	n.a.n.	n.a.n.
SZ_St_SS2 12m	20.06.2016	n.a.n.	12,0	32,25	1467,7	43,39	948,13	4,97	2,23	16,56	2,39	n.a.n.	n.a.n.
SZ_St_SS2 14m	20.06.2016	n.a.n.	14,0	32,43	1500,2	44,15	958,23	5,09	2,29	16,87	2,46	n.a.n.	n.a.n.
SZ_St_SS4 0m	20.06.2016	n.a.n.	0,0	n.a.n.	n.a.n.	n.a.n.	n.a.n.	n.a.n.	n.a.n.	n.a.n.	n.a.n.	n.a.n.	n.a.n.
SZ_St_SS4 2m	20.06.2016	n.a.n.	2,0	29,13	1440,3	41,40	215,87	3,64	2,02	15,39	2,23	n.a.n.	n.a.n.
SZ_St_SS4 4m	20.06.2016	n.a.n.	4,0	29,07	1465,6	41,68	222,86	3,78	2,01	15,21	2,20	n.a.n.	n.a.n.
SZ_St_SS4 5m	20.06.2016	n.a.n.	5,0	30,81	1207,4	43,30	354,09	4,20	2,13	15,79	2,30	n.a.n.	n.a.n.
SZ_St_SS4 6m	20.06.2016	n.a.n.	6,0	31,15	1159,3	43,50	427,86	4,38	2,16	15,94	2,34	n.a.n.	n.a.n.
SZ_St_SS4 7m	20.06.2016	n.a.n.	7,0	31,31	1176,3	43,57	490,76	4,42	2,16	15,98	2,31	n.a.n.	n.a.n.
SZ_St_SS4 8m	20.06.2016	n.a.n.	8,0	31,64	1134,5	43,73	576,95	4,53	2,17	16,07	2,34	n.a.n.	n.a.n.
SZ_St_SS5 0m	21.06.2016	n.a.n.	0,0	29,16	1431,3	41,42	142,10	3,46	1,92	14,58	2,15	n.a.n.	n.a.n.
SZ_St_SS5 2m	21.06.2016	n.a.n.	2,0	29,16	1427,7	41,45	150,64	3,46	1,93	14,68	2,14	n.a.n.	n.a.n.
SZ_St_SS5 4m	21.06.2016	n.a.n.	4,0	29,83	1341,2	42,23	232,96	3,70	1,99	14,89	2,09	n.a.n.	n.a.n.
SZ_St_SS5 6m	21.06.2016	n.a.n.	6,0	31,26	1141,7	43,61	424,76	4,29	2,11	15,53	2,24	n.a.n.	n.a.n.
SZ_St_SS5 8m	21.06.2016	n.a.n.	8,0	31,61	1173,3	43,37	722,16	4,54	2,14	15,83	2,30	n.a.n.	n.a.n.
SZ_St_SS5 10m	21.06.2016	n.a.n.	10,0	32,60	1597,6	43,81	900,76	4,91	2,19	16,28	2,35	n.a.n.	n.a.n.
SZ_St_SS5 12m	21.06.2016	n.a.n.	12,0	32,40	1476,3	43,51	927,94	4,93	2,22	16,41	2,37	n.a.n.	n.a.n.
SZ_St_SS5 14m	21.06.2016	n.a.n.	14,0	29,52	1454,8	41,81	192,58	3,51	1,95	14,71	2,07	n.a.n.	n.a.n.
SZ_St_SK1	21.06.2016	n.a.n.	6,0	31,85	1134,2	43,84	445,72	4,34	2,13	16,25	2,26	n.a.n.	n.a.n.
SZ_St_SK2	21.06.2016	n.a.n.	8,0	31,80	1168,8	43,47	800,59	4,65	2,17	16,02	2,31	n.a.n.	n.a.n.
SZ_St_SK3	21.06.2016	n.a.n.	12,0	32,47	1594,2	43,80	917,85	4,95	2,21	16,35	2,36	n.a.n.	n.a.n.
SZ_St_SK4	21.06.2016	n.a.n.	11,0	32,63	1694,5	43,82	940,37	5,00	2,22	16,56	2,35	n.a.n.	n.a.n.
SZ_St_SK5	21.06.2016	n.a.n.	10,0	32,01	1401,7	43,39	903,09	4,86	2,21	16,21	2,34	n.a.n.	n.a.n.
SZ_St_SK6	21.06.2016	n.a.n.	14,0	32,69	1427,5	43,77	934,93	4,92	2,22	16,49	2,34	n.a.n.	n.a.n.
SZ_St_SK7	21.06.2016	n.a.n.	14,0	32,66	1392,4	43,71	955,90	4,91	2,21	16,43	2,37	n.a.n.	n.a.n.
SZ_St_SK8	21.06.2016	n.a.n.	14,0	32,54	1428,6	43,50	946,58	4,91	2,21	16,74	2,37	n.a.n.	n.a.n.
SZ_St_SK9	21.06.2016	n.a.n.	11,0	32,56	1608,0	43,53	945,02	4,84	2,17	16,21	2,33	n.a.n.	n.a.n.
SZ_GW_SteiblingerSee_QF	22.06.2016	n.a.n.	20,0	8,89	3277,4	39,10	47,37	4,88	2,32	4,57	1,08	-69,17	-9,9
SZ_GW_SteiblingerSee_Qkv	22.06.2016	n.a.n.	20,0	32,75	7731,4	31,83	19,41	6,01	2,09	17,32	12,46	-69,42	-9,7

Sampling Point	Date	Time	Depth	Water T	EC	O2	O2	ChlA	Turbidity	pH	TA	Water hardness
		h	m	°C	µS/cm	%	mg/l	mg/l	FTU		mmol/l	°dH
SZ_GW_SteißlingerSee_01	23.11.2016	10:28	4,7	7,85	n.a.n.	68,3	7,9	35,1	27,3	n.a.n.	n.a.n.	n.a.n.
SZ_GW_SteißlingerSee_02	23.11.2016	10:32	5,3	7,85	n.a.n.	70,1	8,1	92,7	19,8	n.a.n.	n.a.n.	n.a.n.
SZ_GW_SteißlingerSee_03	23.11.2016	10:35	7,9	7,86	622,9	70,7	8,2	2,5	0,5	7,88	4,78	16,58
SZ_GW_SteißlingerSee_03	23.11.2016	10:35	3,1	7,86	623,1	70,4	8,1	2,4	0,4	7,88	4,78	16,56
SZ_GW_SteißlingerSee_04	23.11.2016	10:55	4,7	7,87	n.a.n.	70,0	8,1	3,2	2,4	n.a.n.	n.a.n.	n.a.n.
SZ_GW_SteißlingerSee_05	23.11.2016	10:52	8,7	7,93	n.a.n.	35,6	4,1	30,0	0,0	n.a.n.	n.a.n.	n.a.n.
SZ_GW_SteißlingerSee_06	23.11.2016	10:47	13,3	8,68	n.a.n.	3,8	0,4	29,5	0,0	n.a.n.	n.a.n.	n.a.n.
SZ_GW_SteißlingerSee_07	23.11.2016	11:19	11,0	8,68	n.a.n.	3,9	0,4	7,1	0,0	n.a.n.	n.a.n.	n.a.n.
SZ_GW_SteißlingerSee_08	23.11.2016	10:59	7,3	7,92	n.a.n.	56,4	6,5	23,4	0,0	n.a.n.	n.a.n.	n.a.n.
SZ_GW_SteißlingerSee_09	23.11.2016	11:02	12,2	8,72	746,5	5,0	0,6	2,7	6,7	7,40	6,15	20,28
SZ_GW_SteißlingerSee_10	23.11.2016	11:07	15,0	8,61	778,1	4,5	0,5	30,2	0,0	7,37	6,55	21,37
SZ_GW_SteißlingerSee_10	23.11.2016	11:07	10,0	8,55	663,3	32,3	3,7	5,2	2,2	7,69	5,20	17,64
SZ_GW_SteißlingerSee_10	23.11.2016	11:07	0,0	7,90	622,5	75,4	8,7	2,2	0,4	7,96	4,81	16,57
SZ_GW_SteißlingerSee_11	23.11.2016	11:44	9,1	7,97	638,6	66,4	7,6	6,1	3,4	7,88	4,98	17,00
SZ_GW_SteißlingerSee_12	23.11.2016	11:33	7,8	7,91	623,3	69,8	8,0	3,5	0,6	7,97	4,78	16,45
SZ_GW_SteißlingerSee_13	23.11.2016	11:28	14,2	8,67	n.a.n.	4,1	0,5	2,7	5,3	n.a.n.	n.a.n.	n.a.n.
SZ_GW_SteißlingerSee_14	23.11.2016	11:24	13,2	8,68	n.a.n.	4,3	0,5	8,8	5,6	n.a.n.	n.a.n.	n.a.n.
SZ_GW_SteißlingerSee_15	23.11.2016	11:39	6,8	7,92	n.a.n.	69,2	8,0	2,6	0,8	n.a.n.	n.a.n.	n.a.n.
SZ_GW_SteißlingerSee_16	23.11.2016	12:50	19,4	7,49	n.a.n.	3,4	0,4	23,1	3,6	n.a.n.	n.a.n.	n.a.n.
SZ_GW_SteißlingerSee_17	23.11.2016	12:52	12,9	8,66	n.a.n.	5,8	0,7	0,2	0,0	n.a.n.	n.a.n.	n.a.n.
SZ_GW_SteißlingerSee_18	23.11.2016	11:54	16,2	8,27	772,8	2,0	0,2	2,2	9,7	7,41	6,49	21,10
SZ_GW_SteißlingerSee_18	23.11.2016	11:54	11,3	8,69	741,3	8,9	1,0	2,5	3,3	7,48	6,13	20,14
SZ_GW_SteißlingerSee_19	23.11.2016	12:55	13,2	8,62	n.a.n.	2,6	0,3	0,2	0,0	n.a.n.	n.a.n.	n.a.n.
SZ_GW_SteißlingerSee_20	23.11.2016	12:59	11,5	8,61	n.a.n.	3,0	0,3	37,4	9,3	n.a.n.	n.a.n.	n.a.n.
SZ_GW_SteißlingerSee_K1	23.11.2016	10:05	19,4	7,52	785,1	4,0	0,5	2,7	4,3	7,35	6,90	20,79
SZ_GW_SteißlingerSee_K1	23.11.2016	10:05	15,1	8,48	775,8	2,7	0,3	2,1	2,4	7,45	6,54	21,10
SZ_GW_SteißlingerSee_K1	23.11.2016	10:05	10,0	8,64	733,4	8,8	1,0	3,3	1,2	7,54	6,01	19,76
SZ_GW_SteißlingerSee_K1	23.11.2016	10:05	0,1	7,95	626,4	76,1	8,8	1,9	0,1	8,06	4,82	16,48
SZ_GW_SteißlingerSee_Qkv	23.11.2016	09:25	20,0	11,90	843,2	n.a.n.	n.a.n.	n.a.n.	n.a.n.	7,40	6,97	22,54
SZ_GW_SteißlingerSee_Z1	23.11.2016	10:26	0,0	9,40	901,0	n.a.n.	n.a.n.	n.a.n.	n.a.n.	7,70	7,30	26,54
SZ_GW_SteißlingerSee_Z2	23.11.2016	10:46	0,0	8,70	806,2	n.a.n.	n.a.n.	n.a.n.	n.a.n.	7,81	7,09	19,52

Sampling Point	Date	Time	Depth	Chloride	NO3-N	Sulfate	NH4-N	1/2 Calcium	1/2 Magnesium	Sodium	Potassium	² H	¹⁸ O
		h	m	mg/l	µg/l	mg/l	µg/l	mmol/l	mmol/l	mg/l	mg/l	‰	‰
SZ_GW_SteißlingerSee_01	23.11.2016	10:28	4,7	n.a.n.	n.a.n.	n.a.n.	n.a.n.	n.a.n.	n.a.n.	n.a.n.	n.a.n.	n.a.n.	n.a.n.
SZ_GW_SteißlingerSee_02	23.11.2016	10:32	5,3	n.a.n.	n.a.n.	n.a.n.	n.a.n.	n.a.n.	n.a.n.	n.a.n.	n.a.n.	n.a.n.	n.a.n.
SZ_GW_SteißlingerSee_03	23.11.2016	10:35	7,9	30,42	1175,8	41,95	311,4	3,88	2,05	15,65	2,38	-59,99	-7,54
SZ_GW_SteißlingerSee_03	23.11.2016	10:35	3,1	30,60	1134,9	42,23	307,5	3,86	2,05	15,56	2,27	-59,66	-7,46
SZ_GW_SteißlingerSee_04	23.11.2016	10:55	4,7	n.a.n.	n.a.n.	n.a.n.	n.a.n.	n.a.n.	n.a.n.	n.a.n.	n.a.n.	n.a.n.	n.a.n.
SZ_GW_SteißlingerSee_05	23.11.2016	10:52	8,7	n.a.n.	n.a.n.	n.a.n.	n.a.n.	n.a.n.	n.a.n.	n.a.n.	n.a.n.	n.a.n.	n.a.n.
SZ_GW_SteißlingerSee_06	23.11.2016	10:47	13,3	n.a.n.	n.a.n.	n.a.n.	n.a.n.	n.a.n.	n.a.n.	n.a.n.	n.a.n.	n.a.n.	n.a.n.
SZ_GW_SteißlingerSee_07	23.11.2016	11:19	11,0	n.a.n.	n.a.n.	n.a.n.	n.a.n.	n.a.n.	n.a.n.	n.a.n.	n.a.n.	n.a.n.	n.a.n.
SZ_GW_SteißlingerSee_08	23.11.2016	10:59	7,3	n.a.n.	n.a.n.	n.a.n.	n.a.n.	n.a.n.	n.a.n.	n.a.n.	n.a.n.	n.a.n.	n.a.n.
SZ_GW_SteißlingerSee_09	23.11.2016	11:02	12,2	32,24	1124,5	42,40	917,8	5,03	2,21	16,52	2,39	-63,73	-8,38
SZ_GW_SteißlingerSee_10	23.11.2016	11:07	15,0	32,86	1053,8	42,46	1125,2	5,36	2,27	16,81	2,43	-65,76	-8,79
SZ_GW_SteißlingerSee_10	23.11.2016	11:07	10,0	31,15	1015,9	42,09	497,7	4,24	2,11	15,89	2,33	-60,74	-7,72
SZ_GW_SteißlingerSee_10	23.11.2016	11:07	0,0	30,57	1128,8	41,89	316,8	3,87	2,06	15,61	2,32	-59,46	-7,56
SZ_GW_SteißlingerSee_11	23.11.2016	11:44	9,1	30,88	1078,7	42,09	374,3	4,01	2,08	15,69	2,28	-59,89	-7,57
SZ_GW_SteißlingerSee_12	23.11.2016	11:33	7,8	30,62	1133,3	42,12	322,3	3,86	2,06	15,57	2,30	-59,40	-7,46
SZ_GW_SteißlingerSee_13	23.11.2016	11:28	14,2	n.a.n.	n.a.n.	n.a.n.	n.a.n.	n.a.n.	n.a.n.	n.a.n.	n.a.n.	n.a.n.	n.a.n.
SZ_GW_SteißlingerSee_14	23.11.2016	11:24	13,2	n.a.n.	n.a.n.	n.a.n.	n.a.n.	n.a.n.	n.a.n.	n.a.n.	n.a.n.	n.a.n.	n.a.n.
SZ_GW_SteißlingerSee_15	23.11.2016	11:39	6,8	n.a.n.	n.a.n.	n.a.n.	n.a.n.	n.a.n.	n.a.n.	n.a.n.	n.a.n.	n.a.n.	n.a.n.
SZ_GW_SteißlingerSee_16	23.11.2016	12:50	19,4	n.a.n.	n.a.n.	n.a.n.	n.a.n.	n.a.n.	n.a.n.	n.a.n.	n.a.n.	n.a.n.	n.a.n.
SZ_GW_SteißlingerSee_17	23.11.2016	12:52	12,9	n.a.n.	n.a.n.	n.a.n.	n.a.n.	n.a.n.	n.a.n.	n.a.n.	n.a.n.	n.a.n.	n.a.n.
SZ_GW_SteißlingerSee_18	23.11.2016	11:54	16,2	32,84	902,2	42,43	1112,8	5,27	2,25	16,76	2,54	-65,80	-8,67
SZ_GW_SteißlingerSee_18	23.11.2016	11:54	11,3	32,52	954,4	42,54	894,6	5,03	2,22	16,56	2,42	-63,80	-8,57
SZ_GW_SteißlingerSee_19	23.11.2016	12:55	13,2	n.a.n.	n.a.n.	n.a.n.	n.a.n.	n.a.n.	n.a.n.	n.a.n.	n.a.n.	n.a.n.	n.a.n.
SZ_GW_SteißlingerSee_20	23.11.2016	12:59	11,5	n.a.n.	n.a.n.	n.a.n.	n.a.n.	n.a.n.	n.a.n.	n.a.n.	n.a.n.	n.a.n.	n.a.n.
SZ_GW_SteißlingerSee_K1	23.11.2016	10:05	19,4	32,57	213,0	26,72	2838,2	5,36	2,28	16,82	2,52	-65,42	-8,67
SZ_GW_SteißlingerSee_K1	23.11.2016	10:05	15,1	33,02	877,8	42,54	1143,8	5,37	2,28	16,90	2,44	-65,74	-8,82
SZ_GW_SteißlingerSee_K1	23.11.2016	10:05	10,0	32,17	975,2	42,21	838,6	4,94	2,21	16,55	2,38	-63,09	-8,42
SZ_GW_SteißlingerSee_K1	23.11.2016	10:05	0,1	30,70	1147,8	42,02	322,3	3,91	2,08	15,72	2,30	-59,39	-7,38
SZ_GW_SteißlingerSee_Qkv	23.11.2016	09:25	20,0	30,90	7279,4	31,45	10,1	6,12	2,12	17,03	11,76	-69,15	-9,60
SZ_GW_SteißlingerSee_Z1	23.11.2016	10:26	0,0	23,31	7877,4	66,45	18,6	7,84	1,76	12,77	1,73	-69,28	-9,74
SZ_GW_SteißlingerSee_Z2	23.11.2016	10:46	0,0	8,82	3000,0	69,10	23,3	7,80	1,19	5,68	3,97	-69,81	-9,57

Sampling Point	Date	Time h	Depth m	Water T °C	EC µS/cm	O2 %	O2 mg/l	ChlA mg/l	Turbidity FTU	pH	TA mmol/l	Water hardness °dH
SZ_GW_SteißlingerSee_01	28.03.2017	09:55	4,8	8,14	n.a.n.	133,1	15,7	45,3	2,4	n.a.n.	n.a.n.	n.a.n.
SZ_GW_SteißlingerSee_02	28.03.2017	10:03	6,1	6,79	n.a.n.	119,7	14,5	87,1	1,3	n.a.n.	n.a.n.	n.a.n.
SZ_GW_SteißlingerSee_03	28.03.2017	10:08	7,8	5,40	662,9	71,6	9,0	7,9	0,6	8,03	5,38	18,20
SZ_GW_SteißlingerSee_03	28.03.2017	10:08	2,7	9,88	656,7	111,4	12,6	7,1	0,5	8,29	5,33	18,02
SZ_GW_SteißlingerSee_04	28.03.2017	10:22	3,2	9,39	n.a.n.	114,1	13,0	10,3	0,5	n.a.n.	n.a.n.	n.a.n.
SZ_GW_SteißlingerSee_05	28.03.2017	10:27	7,8	5,48	661,9	83,2	10,5	47,0	2,2	8,03	5,34	18,06
SZ_GW_SteißlingerSee_06	28.03.2017	10:34	13,6	5,58	690,4	12,7	1,6	33,8	8,8	7,60	5,57	18,77
SZ_GW_SteißlingerSee_06	28.03.2017	10:34	8,5	5,27	669,8	70,6	8,9	7,8	0,5	7,84	5,38	18,15
SZ_GW_SteißlingerSee_06	28.03.2017	10:34	3,3	9,60	656,3	113,5	12,9	9,1	0,5	8,28	5,31	17,95
SZ_GW_SteißlingerSee_06	28.03.2017	10:34	0,0	10,71	657,1	103,5	11,5	1,5	0,7	8,29	5,32	17,98
SZ_GW_SteißlingerSee_07	28.03.2017	10:46	7,8	5,42	665,3	79,5	10,0	12,7	0,7	7,96	5,33	17,99
SZ_GW_SteißlingerSee_08	28.03.2017	10:51	7,6	5,33	664,0	84,9	10,7	37,9	1,3	8,01	5,29	17,88
SZ_GW_SteißlingerSee_09	28.03.2017	10:54	11,1	5,47	690,8	43,2	5,4	30,8	5,3	7,67	5,68	19,05
SZ_GW_SteißlingerSee_10	28.03.2017	11:15	15,1	5,57	710,0	28,8	3,6	78,7	5,6	7,57	5,74	19,30
SZ_GW_SteißlingerSee_10	28.03.2017	11:15	10,1	5,30	680,0	61,6	7,8	5,6	0,4	7,77	5,42	18,27
SZ_GW_SteißlingerSee_10	28.03.2017	11:15	5,0	7,07	659,1	130,3	15,6	48,9	1,4	8,21	5,32	17,96
SZ_GW_SteißlingerSee_10	28.03.2017	11:15	0,1	11,43	658,5	108,2	11,8	2,6	0,3	8,30	5,33	18,04
SZ_GW_SteißlingerSee_11	28.03.2017	11:28	10,3	5,28	675,6	62,0	7,8	6,4	0,8	7,85	5,39	18,16
SZ_GW_SteißlingerSee_12	28.03.2017	11:37	8,9	5,30	672,9	70,5	8,9	11,6	0,4	7,89	5,38	18,14
SZ_GW_SteißlingerSee_13	28.03.2017	11:44	15,7	5,51	705,8	24,5	3,1	8,6	2,3	7,63	5,66	19,03
SZ_GW_SteißlingerSee_13	28.03.2017	11:44	10,6	5,25	675,5	58,6	7,4	5,0	0,5	7,91	5,40	18,22
SZ_GW_SteißlingerSee_13	28.03.2017	11:44	5,5	6,39	662,9	123,7	15,2	60,1	1,0	8,14	5,32	17,96
SZ_GW_SteißlingerSee_13	28.03.2017	11:44	0,2	11,02	658,0	104,7	11,5	2,3	0,3	8,31	5,36	18,15
SZ_GW_SteißlingerSee_14	28.03.2017	12:02	13,3	5,48	699,1	35,8	4,5	60,3	1,9	7,72	5,64	18,95
SZ_GW_SteißlingerSee_15	28.03.2017	12:12	7,9	5,37	n.a.n.	82,9	10,4	52,3	3,6	n.a.n.	n.a.n.	n.a.n.
SZ_GW_SteißlingerSee_16	28.03.2017	12:54	19,6	5,51	712,6	29,8	3,7	60,5	0,0	7,57	5,73	19,23
SZ_GW_SteißlingerSee_16	28.03.2017	12:54	14,5	5,44	702,7	31,3	3,9	3,0	0,5	7,68	5,63	18,96
SZ_GW_SteißlingerSee_17	28.03.2017	13:06	12,6	5,37	668,9	39,0	4,9	5,9	1,5	7,97	5,32	17,96
SZ_GW_SteißlingerSee_18	28.03.2017	13:15	19,0	5,49	709,6	25,3	3,2	20,5	2,7	7,62	5,73	19,28
SZ_GW_SteißlingerSee_18	28.03.2017	13:15	14,0	5,48	676,2	27,1	3,4	2,5	1,1	7,82	5,42	18,36
SZ_GW_SteißlingerSee_19	28.03.2017	13:24	13,0	5,48	n.a.n.	30,0	3,8	5,9	2,2	n.a.n.	n.a.n.	n.a.n.
SZ_GW_SteißlingerSee_20	28.03.2017	13:32	11,3	5,36	n.a.n.	17,6	2,2	5,8	0,0	n.a.n.	n.a.n.	n.a.n.
SZ_GW_SteißlingerSee_K1	28.03.2017	13:43	20,3	5,48	712,9	23,0	2,9	52,2	0,0	7,61	5,71	19,21
SZ_GW_SteißlingerSee_K1	28.03.2017	13:43	15,1	5,48	705,5	28,2	3,5	2,9	0,7	7,67	5,64	19,01
SZ_GW_SteißlingerSee_K1	28.03.2017	13:43	10,0	5,25	685,8	67,5	8,5	5,6	0,5	7,82	5,45	18,41
SZ_GW_SteißlingerSee_K1	28.03.2017	13:43	5,1	7,37	660,1	129,5	15,4	45,9	1,2	8,25	5,33	18,05
SZ_GW_SteißlingerSee_K1	28.03.2017	13:43	0,1	12,65	659,2	98,0	10,6	0,5	0,3	8,33	5,32	18,01
SZ_GW_SteißlingerSee_QF	28.03.2017	09:27	20,0	11,20	843,6	n.a.n.	n.a.n.	n.a.n.	n.a.n.	7,49	6,97	22,53
SZ_GW_SteißlingerSee_QF	28.03.2017	09:56	20,0	8,90	648,9	n.a.n.	n.a.n.	n.a.n.	n.a.n.	7,62	5,87	19,28
SZ_GW_SteißlingerSee_Z1	28.03.2017	11:25	0,0	8,10	901,0	n.a.n.	n.a.n.	n.a.n.	n.a.n.	7,90	7,30	28,72
SZ_GW_SteißlingerSee_Z2	28.03.2017	11:01	0,0	9,90	941,6	n.a.n.	n.a.n.	n.a.n.	n.a.n.	8,15	8,01	26,16
SZ_GW_SteißlingerSee_A	28.03.2017	13:38	0,0	12,00	660,9	n.a.n.	n.a.n.	n.a.n.	n.a.n.	8,32	5,30	17,98

Sampling Point	Date	Time	Depth	Chloride	NO3-N	Sulfate	NH4-N	1/2 Calcium	1/2 Magnesium	Sodium	Potassium	² H	¹⁸ O
		h	m	mg/l	µg/l	mg/l	µg/l	mmol/l	mmol/l	mg/l	mg/l	‰	‰
SZ_GW_SteißlingerSee_01	28.03.2017	09:55	4,8	n.a.n.	n.a.n.	n.a.n.	n.a.n.	n.a.n.	n.a.n.	n.a.n.	n.a.n.	n.a.n.	n.a.n.
SZ_GW_SteißlingerSee_02	28.03.2017	10:03	6,1	n.a.n.	n.a.n.	n.a.n.	n.a.n.	n.a.n.	n.a.n.	n.a.n.	n.a.n.	n.a.n.	n.a.n.
SZ_GW_SteißlingerSee_03	28.03.2017	10:08	7,8	31,11	1207,9	42,31	403,8	4,36	2,09	15,64	2,25	-61,94	-7,83
SZ_GW_SteißlingerSee_03	28.03.2017	10:08	2,7	31,18	1223,2	42,25	427,1	4,36	2,10	15,64	2,24	-61,68	-7,78
SZ_GW_SteißlingerSee_04	28.03.2017	10:22	3,2	n.a.n.	n.a.n.	n.a.n.	n.a.n.	n.a.n.	n.a.n.	n.a.n.	n.a.n.	n.a.n.	n.a.n.
SZ_GW_SteißlingerSee_05	28.03.2017	10:27	7,8	31,64	1230,3	43,05	493,1	4,38	2,11	15,57	2,23	-62,38	-7,82
SZ_GW_SteißlingerSee_06	28.03.2017	10:34	13,6	31,64	1571,8	42,74	660,8	4,58	2,14	15,90	2,27	-62,53	-8,01
SZ_GW_SteißlingerSee_06	28.03.2017	10:34	8,5	31,47	1272,9	42,76	528,0	4,41	2,11	15,70	2,24	-62,33	-7,91
SZ_GW_SteißlingerSee_06	28.03.2017	10:34	3,3	31,23	1220,5	42,38	472,1	4,38	2,11	15,62	2,23	-62,17	-7,78
SZ_GW_SteißlingerSee_06	28.03.2017	10:34	0,0	31,73	1238,6	42,75	427,9	4,37	2,10	15,70	2,30	-62,67	-7,69
SZ_GW_SteißlingerSee_07	28.03.2017	10:46	7,8	31,51	1232,1	42,80	491,5	4,38	2,11	15,63	2,27	-63,28	-7,86
SZ_GW_SteißlingerSee_08	28.03.2017	10:51	7,6	31,37	1216,2	42,67	487,7	4,38	2,11	15,64	2,25	-62,76	-7,87
SZ_GW_SteißlingerSee_09	28.03.2017	10:54	11,1	31,84	1550,6	43,11	636,0	4,59	2,15	15,91	2,29	-63,01	-7,93
SZ_GW_SteißlingerSee_10	28.03.2017	11:15	15,1	32,12	1875,9	43,19	636,7	4,77	2,18	16,20	2,32	-64,21	-8,09
SZ_GW_SteißlingerSee_10	28.03.2017	11:15	10,1	31,60	1380,9	42,87	554,4	4,53	2,15	15,96	2,27	-63,20	-7,94
SZ_GW_SteißlingerSee_10	28.03.2017	11:15	5,0	31,57	1220,5	42,89	458,9	4,42	2,12	15,75	2,27	-63,21	-7,83
SZ_GW_SteißlingerSee_10	28.03.2017	11:15	0,1	31,74	1243,8	43,03	440,3	4,40	2,12	15,76	2,26	-62,32	-7,66
SZ_GW_SteißlingerSee_11	28.03.2017	11:28	10,3	31,76	1311,1	42,99	573,8	4,49	2,14	15,91	2,31	-65,06	-8,04
SZ_GW_SteißlingerSee_12	28.03.2017	11:37	8,9	31,53	1277,0	42,76	558,3	4,46	2,14	15,80	2,27	-63,68	-8,12
SZ_GW_SteißlingerSee_13	28.03.2017	11:44	15,7	32,35	1710,3	43,64	726,0	4,73	2,18	16,13	2,28	-64,00	-8,21
SZ_GW_SteißlingerSee_13	28.03.2017	11:44	10,6	31,86	1349,1	43,17	569,2	4,50	2,15	15,90	2,26	-62,74	-7,84
SZ_GW_SteißlingerSee_13	28.03.2017	11:44	5,5	31,53	1215,1	42,79	494,6	4,43	2,13	15,82	2,28	-62,23	-7,94
SZ_GW_SteißlingerSee_13	28.03.2017	11:44	0,2	31,74	1243,1	43,02	483,0	4,45	2,14	15,89	2,29	-62,21	-7,85
SZ_GW_SteißlingerSee_14	28.03.2017	12:02	13,3	31,91	1610,2	43,30	608,8	4,68	2,17	16,09	2,30	-63,00	-8,07
SZ_GW_SteißlingerSee_15	28.03.2017	12:12	7,9	n.a.n.	n.a.n.	n.a.n.	n.a.n.	n.a.n.	n.a.n.	n.a.n.	n.a.n.	n.a.n.	n.a.n.
SZ_GW_SteißlingerSee_16	28.03.2017	12:54	19,6	32,41	1802,9	43,65	528,0	4,81	2,23	16,87	2,33	-64,79	-8,28
SZ_GW_SteißlingerSee_16	28.03.2017	12:54	14,5	32,29	1683,2	43,56	618,1	4,76	2,20	16,42	2,32	-63,04	-8,20
SZ_GW_SteißlingerSee_17	28.03.2017	13:06	12,6	31,55	1249,0	42,92	508,6	4,50	2,16	16,05	2,33	-61,59	-7,94
SZ_GW_SteißlingerSee_18	28.03.2017	13:15	19,0	32,50	1761,6	43,78	775,7	4,82	2,21	16,42	2,33	-63,18	-8,35
SZ_GW_SteißlingerSee_18	28.03.2017	13:15	14,0	31,96	1394,7	43,34	623,5	4,58	2,17	16,08	2,30	-62,38	-8,02
SZ_GW_SteißlingerSee_19	28.03.2017	13:24	13,0	n.a.n.	n.a.n.	n.a.n.	n.a.n.	n.a.n.	n.a.n.	n.a.n.	n.a.n.	n.a.n.	n.a.n.
SZ_GW_SteißlingerSee_20	28.03.2017	13:32	11,3	n.a.n.	n.a.n.	n.a.n.	n.a.n.	n.a.n.	n.a.n.	n.a.n.	n.a.n.	n.a.n.	n.a.n.
SZ_GW_SteißlingerSee_K1	28.03.2017	13:43	20,3	32,68	1816,2	44,00	777,3	4,84	2,21	16,47	2,34	-62,09	-8,11
SZ_GW_SteißlingerSee_K1	28.03.2017	13:43	15,1	32,33	1733,8	43,57	729,9	4,70	2,19	16,28	2,32	-61,43	-8,19
SZ_GW_SteißlingerSee_K1	28.03.2017	13:43	10,0	32,09	1473,1	43,46	639,1	4,61	2,17	16,12	2,27	-62,16	-8,10
SZ_GW_SteißlingerSee_K1	28.03.2017	13:43	5,1	31,52	1231,6	42,80	469,8	4,41	2,12	15,74	2,27	-60,63	-7,96
SZ_GW_SteißlingerSee_K1	28.03.2017	13:43	0,1	31,96	1253,1	43,32	443,4	4,48	2,16	16,02	2,29	-60,06	-7,91
SZ_GW_SteißlingerSee_QKv	28.03.2017	09:27	20,0	31,04	7285,3	31,06	60,6	6,15	2,15	16,68	11,43	-67,96	-9,79
SZ_GW_SteißlingerSee_QF	28.03.2017	09:56	20,0	8,49	2919,8	36,80	142,9	4,88	2,28	4,50	1,11	-67,29	-9,90
SZ_GW_SteißlingerSee_Z1	28.03.2017	11:25	0,0	28,59	7334,7	60,57	187,9	7,73	1,90	15,59	1,79	-69,27	-9,68
SZ_GW_SteißlingerSee_Z2	28.03.2017	11:01	0,0	11,26	3171,6	106,99	121,9	9,00	1,70	9,06	11,77	-69,74	-9,71
SZ_GW_SteißlingerSee_A	28.03.2017	0,57	0,0	4,50	2,16	16,04	2,35	-61,20	-7,82	16,044	2,35	-61,2	-7,82

Sampling Point	Date	Time h	Depth m	Water T °C	EC µS/cm	O2 %	O2 mg/l	ChlA mg/l	Turbidity FTU	pH	TA mmol/l	Water hardness °dH
SZ_GW_SteißlingerSee_01	05.07.2017	12:29	4,7	21,36	n.a.n.	72,2	6,4	49,1	19,8	n.a.n.	n.a.n.	n.a.n.
SZ_GW_SteißlingerSee_02	05.07.2017	12:36	5,3	17,69	n.a.n.	113,7	10,9	7,9	7,8	n.a.n.	n.a.n.	n.a.n.
SZ_GW_SteißlingerSee_03	05.07.2017	12:16	8,2	9,65	690,0	48,0	5,5	10,8	12,6	7,44	5,59	18,84
SZ_GW_SteißlingerSee_03	05.07.2017	12:16	3,2	22,84	565,1	107,8	9,2	1,5	6,8	7,95	4,11	14,67
SZ_GW_SteißlingerSee_04	05.07.2017	12:43	4,3	21,83	n.a.n.	94,6	8,3	5,5	23,9	n.a.n.	n.a.n.	n.a.n.
SZ_GW_SteißlingerSee_05	05.07.2017	12:10	9,2	8,36	681,4	18,4	2,2	10,2	2,7	7,49	5,42	18,28
SZ_GW_SteißlingerSee_06	05.07.2017	11:51	13,3	7,31	716,1	2,1	0,2	6,9	7,3	7,45	5,76	19,31
SZ_GW_SteißlingerSee_06	05.07.2017	11:51	8,2	9,32	646,6	59,3	6,8	8,6	4,5	7,75	5,06	17,34
SZ_GW_SteißlingerSee_06	05.07.2017	11:51	3,1	22,93	565,7	108,5	9,3	1,5	6,7	8,22	4,16	14,69
SZ_GW_SteißlingerSee_06	05.07.2017	11:51	0,0	24,01	566,3	103,5	8,8	0,9	6,4	8,05	4,11	14,70
SZ_GW_SteißlingerSee_07	05.07.2017	11:47	9,1	8,31	671,9	42,8	5,0	13,3	6,9	7,61	5,26	17,86
SZ_GW_SteißlingerSee_08	05.07.2017	12:52	6,6	12,49	664,0	82,8	8,8	5,5	12,7	7,79	5,39	18,19
SZ_GW_SteißlingerSee_09	05.07.2017	12:59	11,7	7,33	725,2	3,8	0,5	26,2	6,0	7,41	5,82	19,45
SZ_GW_SteißlingerSee_10	05.07.2017	13:07	16,8	7,23	750,4	4,1	0,5	0,1	0,0	7,34	6,39	20,91
SZ_GW_SteißlingerSee_10	05.07.2017	13:07	11,7	7,13	682,7	11,0	1,3	13,5	3,9	7,62	5,40	18,21
SZ_GW_SteißlingerSee_10	05.07.2017	13:07	6,7	12,37	568,7	101,6	10,8	2,8	4,9	8,23	4,16	14,65
SZ_GW_SteißlingerSee_10	05.07.2017	13:07	0,1	24,39	567,5	103,5	8,7	2,1	6,6	8,14	4,14	14,61
SZ_GW_SteißlingerSee_11	05.07.2017	11:40	9,8	7,90	698,4	38,0	4,5	15,6	4,6	7,61	5,53	18,52
SZ_GW_SteißlingerSee_12	05.07.2017	13:23	7,9	9,99	686,3	66,2	7,5	7,2	6,2	7,77	5,46	18,37
SZ_GW_SteißlingerSee_13	05.07.2017	13:30	15,9	6,95	742,9	5,6	0,7	49,1	0,0	7,39	6,13	20,18
SZ_GW_SteißlingerSee_13	05.07.2017	13:30	10,8	7,25	693,8	24,5	3,0	20,2	5,1	7,67	5,57	18,61
SZ_GW_SteißlingerSee_13	05.07.2017	13:30	5,7	15,94	587,5	123,3	12,1	3,1	4,5	8,19	4,40	15,30
SZ_GW_SteißlingerSee_13	05.07.2017	13:30	0,2	24,36	566,8	103,3	8,7	0,6	6,5	8,28	4,18	14,71
SZ_GW_SteißlingerSee_14	05.07.2017	11:30	14,0	7,19	731,6	3,1	0,4	27,5	0,0	7,49	5,87	19,97
SZ_GW_SteißlingerSee_15	05.07.2017	13:46	7,5	10,54	n.a.n.	71,8	8,0	5,8	11,4	n.a.n.	n.a.n.	n.a.n.
SZ_GW_SteißlingerSee_16	05.07.2017	13:51	19,5	6,76	738,9	3,1	0,4	0,6	0,0	7,44	6,22	20,25
SZ_GW_SteißlingerSee_16	05.07.2017	13:51	14,2	6,97	734,6	3,3	0,4	8,5	4,9	7,49	5,96	19,75
SZ_GW_SteißlingerSee_17	05.07.2017	14:08	12,6	7,10	735,6	3,1	0,4	10,8	8,8	7,51	6,01	19,83
SZ_GW_SteißlingerSee_18	05.07.2017	14:25	15,8	6,89	741,5	2,4	0,3	10,2	6,9	7,49	6,36	20,68
SZ_GW_SteißlingerSee_18	05.07.2017	14:25	10,5	7,30	702,8	26,8	3,2	39,5	4,2	7,72	5,62	18,73
SZ_GW_SteißlingerSee_19	05.07.2017	14:21	11,0	7,28	n.a.n.	14,7	1,8	32,4	8,3	n.a.n.	n.a.n.	n.a.n.
SZ_GW_SteißlingerSee_20	05.07.2017	14:49	11,2	7,28	n.a.n.	11,0	1,3	3,1	12,5	n.a.n.	n.a.n.	n.a.n.
SZ_GW_SteißlingerSee_K1	05.07.2017	14:35	20,3	6,74	741,5	2,6	0,3	0,6	0,0	7,50	6,06	19,77
SZ_GW_SteißlingerSee_K1	05.07.2017	14:35	15,0	7,03	737,1	2,9	0,4	5,1	5,8	7,54	5,99	19,79
SZ_GW_SteißlingerSee_K1	05.07.2017	14:35	10,0	7,44	716,9	37,6	4,5	39,6	4,7	7,65	5,74	19,11
SZ_GW_SteißlingerSee_K1	05.07.2017	14:35	5,1	18,19	620,3	115,0	10,8	3,7	5,6	8,16	4,78	16,34
SZ_GW_SteißlingerSee_K1	05.07.2017	14:35	0,2	24,48	568,5	106,8	9,0	1,5	6,5	8,34	4,19	14,68
SZ_GW_SteißlingerSee_QKv	05.07.2017	17:00	20,0	13,50	851,3	n.a.n.	n.a.n.	n.a.n.	n.a.n.	7,52	7,04	22,50
SZ_GW_SteißlingerSee_QF	05.07.2017	10:00	20,0	16,80	660,3	n.a.n.	n.a.n.	n.a.n.	n.a.n.	7,46	5,94	19,32
SZ_GW_SteißlingerSee_Z1	05.07.2017	n.a.n.	0,0	n.a.n.	n.a.n.	n.a.n.	n.a.n.	n.a.n.	n.a.n.	n.a.n.	n.a.n.	n.a.n.
SZ_GW_SteißlingerSee_Z2	05.07.2017	n.a.n.	0,0	n.a.n.	n.a.n.	n.a.n.	n.a.n.	n.a.n.	n.a.n.	n.a.n.	n.a.n.	n.a.n.
SZ_GW_SteißlingerSee_A	05.07.2017	n.a.n.	0,0	26,30	565,9	n.a.n.	n.a.n.	n.a.n.	n.a.n.	8,39	4,19	14,65

Sampling Point	Date	Time h	Depth m	Chloride mg/l	NO3-N µg/l	Sulfate mg/l	NH4-N µg/l	1/2 Calcium mmol/l	1/2 Magnesium mmol/l	Sodium mg/l	Potassium mg/l	² H ‰	¹⁸ O ‰
SZ_GW_SteißlingerSee_01	05.07.2017	12:29	4,7	n.a.n.	n.a.n.	n.a.n.	n.a.n.	n.a.n.	n.a.n.	n.a.n.	n.a.n.	n.a.n.	n.a.n.
SZ_GW_SteißlingerSee_02	05.07.2017	12:36	5,3	n.a.n.	n.a.n.	n.a.n.	n.a.n.	n.a.n.	n.a.n.	n.a.n.	n.a.n.	n.a.n.	n.a.n.
SZ_GW_SteißlingerSee_03	05.07.2017	12:16	8,2	31,33	1144,0	42,09	458,9	4,44	2,11	15,98	2,21	-62,22	-8,16
SZ_GW_SteißlingerSee_03	05.07.2017	12:16	3,2	30,82	1200,7	41,76	89,3	3,14	2,04	15,79	2,24	-57,16	-7,06
SZ_GW_SteißlingerSee_04	05.07.2017	12:43	4,3	n.a.n.	n.a.n.	n.a.n.	n.a.n.	n.a.n.	n.a.n.	n.a.n.	n.a.n.	n.a.n.	n.a.n.
SZ_GW_SteißlingerSee_05	05.07.2017	12:10	9,2	31,17	1072,3	41,84	421,7	4,38	2,12	16,06	2,24	-62,11	-8,12
SZ_GW_SteißlingerSee_06	05.07.2017	11:51	13,3	31,98	1413,5	42,48	518,7	4,61	2,15	16,31	2,23	-63,50	-8,38
SZ_GW_SteißlingerSee_06	05.07.2017	11:51	8,2	30,98	1122,9	42,01	285,8	4,03	2,10	15,93	2,23	-61,33	-7,84
SZ_GW_SteißlingerSee_06	05.07.2017	11:51	3,1	30,97	1211,3	41,96	87,0	3,14	2,05	15,81	2,23	-57,28	-7,01
SZ_GW_SteißlingerSee_06	05.07.2017	11:51	0,0	30,82	1249,5	41,66	87,0	3,15	2,04	15,88	2,31	-57,20	-6,96
SZ_GW_SteißlingerSee_07	05.07.2017	11:47	9,1	31,44	1225,1	42,39	361,9	4,25	2,11	16,07	2,27	-61,68	-8,00
SZ_GW_SteißlingerSee_08	05.07.2017	12:52	6,6	30,99	1068,1	42,41	287,3	4,19	2,09	15,83	2,21	-61,23	-7,94
SZ_GW_SteißlingerSee_09	05.07.2017	12:59	11,7	31,87	1404,0	42,83	545,1	4,75	2,18	16,31	2,27	-63,42	-8,32
SZ_GW_SteißlingerSee_10	05.07.2017	13:07	16,8	32,60	1521,0	42,66	674,0	4,97	2,20	16,48	2,33	-64,49	-8,60
SZ_GW_SteißlingerSee_10	05.07.2017	13:07	11,7	31,40	1246,7	42,40	424,0	4,37	2,13	16,31	2,25	-62,43	-8,18
SZ_GW_SteißlingerSee_10	05.07.2017	13:07	6,7	30,89	1201,1	41,84	94,0	3,16	2,04	15,84	2,23	-56,97	-7,09
SZ_GW_SteißlingerSee_10	05.07.2017	13:07	0,1	30,86	1205,4	41,82	91,6	3,16	2,05	15,91	2,24	-56,44	-7,05
SZ_GW_SteißlingerSee_11	05.07.2017	11:40	9,8	31,79	1330,3	42,67	436,4	4,56	2,17	16,46	2,27	-61,60	-8,19
SZ_GW_SteißlingerSee_12	05.07.2017	13:23	7,9	31,56	1142,6	42,86	364,2	4,41	2,13	16,01	2,25	-61,48	-8,14
SZ_GW_SteißlingerSee_13	05.07.2017	13:30	15,9	32,29	1134,9	42,48	701,2	4,92	2,21	16,60	2,30	-63,58	-8,58
SZ_GW_SteißlingerSee_13	05.07.2017	13:30	10,8	31,67	1295,5	42,70	409,2	4,49	2,15	16,21	2,24	-61,21	-8,19
SZ_GW_SteißlingerSee_13	05.07.2017	13:30	5,7	30,94	1193,0	42,03	121,9	3,40	2,07	15,87	2,22	-58,27	-7,58
SZ_GW_SteißlingerSee_13	05.07.2017	13:30	0,2	30,98	1212,2	41,95	98,6	3,19	2,06	16,00	2,24	-56,05	-7,09
SZ_GW_SteißlingerSee_14	05.07.2017	11:30	14,0	32,14	1444,4	42,60	583,2	4,83	2,20	16,57	2,31	-62,28	-8,51
SZ_GW_SteißlingerSee_15	05.07.2017	13:46	7,5	n.a.n.	n.a.n.	n.a.n.	n.a.n.	n.a.n.	n.a.n.	n.a.n.	n.a.n.	n.a.n.	n.a.n.
SZ_GW_SteißlingerSee_16	05.07.2017	13:51	19,5	32,41	482,3	42,65	889,9	4,87	2,20	16,55	2,31	-62,63	-8,61
SZ_GW_SteißlingerSee_16	05.07.2017	13:51	14,2	32,26	1402,8	42,66	608,0	4,90	2,22	16,73	2,32	-62,50	-8,50
SZ_GW_SteißlingerSee_17	05.07.2017	14:08	12,6	32,21	1425,9	42,73	606,5	4,86	2,20	16,63	2,30	-62,75	-8,47
SZ_GW_SteißlingerSee_18	05.07.2017	14:25	15,8	32,32	1202,2	42,57	673,2	4,90	2,21	16,63	2,30	-63,16	-8,52
SZ_GW_SteißlingerSee_18	05.07.2017	14:25	10,5	31,93	1352,7	42,89	461,3	4,58	2,16	16,32	2,25	-61,33	-8,12
SZ_GW_SteißlingerSee_19	05.07.2017	14:21	11,0	n.a.n.	n.a.n.	n.a.n.	n.a.n.	n.a.n.	n.a.n.	n.a.n.	n.a.n.	n.a.n.	n.a.n.
SZ_GW_SteißlingerSee_20	05.07.2017	14:49	11,2	n.a.n.	n.a.n.	n.a.n.	n.a.n.	n.a.n.	n.a.n.	n.a.n.	n.a.n.	n.a.n.	n.a.n.
SZ_GW_SteißlingerSee_K1	05.07.2017	14:35	20,3	32,26	372,5	42,77	911,6	4,89	2,21	16,56	2,32	-62,94	-8,35
SZ_GW_SteißlingerSee_K1	05.07.2017	14:35	15,0	32,27	1296,0	42,62	629,8	4,90	2,21	16,67	2,30	-62,81	-8,39
SZ_GW_SteißlingerSee_K1	05.07.2017	14:35	10,0	31,96	1456,8	42,74	498,5	4,71	2,18	16,44	2,30	-62,60	-8,21
SZ_GW_SteißlingerSee_K1	05.07.2017	14:35	5,1	30,85	1163,8	42,04	173,2	3,77	2,09	15,92	2,24	-59,73	-7,69
SZ_GW_SteißlingerSee_K1	05.07.2017	14:35	0,2	31,06	1209,9	42,01	94,7	3,18	2,06	16,06	2,28	-57,11	-6,88
SZ_GW_SteißlingerSee_Qkv	05.07.2017	17:00	20,0	30,83	7426,2	31,21	10,1	6,06	2,14	16,88	11,36	-69,18	-9,56
SZ_GW_SteißlingerSee_QF	05.07.2017	10:00	20,0	8,85	2969,5	37,59	5,4	4,79	2,27	4,52	1,07	-68,97	-9,75
SZ_GW_SteißlingerSee_Z1	05.07.2017	n.a.n.	0,0	n.a.n.	n.a.n.	n.a.n.	n.a.n.	n.a.n.	n.a.n.	n.a.n.	n.a.n.	n.a.n.	n.a.n.
SZ_GW_SteißlingerSee_Z2	05.07.2017	n.a.n.	0,0	n.a.n.	n.a.n.	n.a.n.	n.a.n.	n.a.n.	n.a.n.	n.a.n.	n.a.n.	n.a.n.	n.a.n.
SZ_GW_SteißlingerSee_A	05.07.2017	n.a.n.	0,0	31,12	1203,4	42,14	102,5	3,21	2,11	16,35	2,30	-57,25	-6,78

Sampling Point	Date	Time h	Depth m	Water T °C	EC µS/cm	O2 %	O2 mg/l	ChlA mg/l	Turbidity FTU	pH	TA mmol/l	Water hardness °dH
SZ_GW_SteißlingerSee_01	22.09.2017	11:16	4,6	16,54	n.a.n.	93,7	9,1	25,5	52,8	n.a.n.	n.a.n.	n.a.n.
SZ_GW_SteißlingerSee_02	22.09.2017	11:13	5,0	16,53	n.a.n.	96,2	9,4	3,4	0,8	n.a.n.	n.a.n.	n.a.n.
SZ_GW_SteißlingerSee_03	22.09.2017	11:20	8,5	9,26	675,5	12,5	1,4	9,7	2,1	7,64	5,37	18,19
SZ_GW_SteißlingerSee_03	22.09.2017	11:20	3,5	16,60	533,7	99,7	9,7	2,9	0,6	8,27	3,8	13,80
SZ_GW_SteißlingerSee_04	22.09.2017	11:11	3,8	16,50	n.a.n.	92,0	9,0	3,5	1,9	n.a.n.	n.a.n.	n.a.n.
SZ_GW_SteißlingerSee_05	22.09.2017	11:02	7,2	11,34	675,6	23,9	2,6	3,5	2,7	7,58	5,45	18,33
SZ_GW_SteißlingerSee_06	22.09.2017	11:38	13,2	8,05	762,9	3,9	0,5	2,6	0,0	7,38	6,34	20,91
SZ_GW_SteißlingerSee_06	22.09.2017	11:38	8,2	9,66	647,6	15,4	1,7	8,0	0,6	7,72	5,04	17,25
SZ_GW_SteißlingerSee_06	22.09.2017	11:38	3,0	16,61	533,9	100,3	9,7	2,5	0,5	8,28	3,79	13,72
SZ_GW_SteißlingerSee_06	22.09.2017	11:38	0,2	16,87	534,2	99,4	9,6	1,1	0,4	8,27	3,77	13,64
SZ_GW_SteißlingerSee_07	22.09.2017	11:32	8,0	9,73	641,4	17,0	1,9	8,2	0,8	7,72	4,95	16,91
SZ_GW_SteißlingerSee_08	22.09.2017	10:57	6,6	13,38	628,7	69,7	7,2	9,1	1,6	7,75	4,88	16,66
SZ_GW_SteißlingerSee_09	22.09.2017	10:46	11,5	8,58	718,9	5,4	0,6	0,0	0,0	7,52	5,83	19,30
SZ_GW_SteißlingerSee_10	22.09.2017	10:32	14,7	7,94	761,0	3,0	0,4	4,4	5,1	7,47	6,4	20,78
SZ_GW_SteißlingerSee_10	22.09.2017	10:32	9,5	8,69	675,0	8,2	0,9	8,4	1,1	7,7	5,37	17,98
SZ_GW_SteißlingerSee_10	22.09.2017	10:32	4,5	16,56	534,0	99,4	9,7	4,8	0,6	8,32	3,84	13,75
SZ_GW_SteißlingerSee_10	22.09.2017	10:32	0,0	16,75	533,8	98,5	9,5	1,2	0,5	8,31	3,83	13,70
SZ_GW_SteißlingerSee_11	22.09.2017	10:20	10,4	8,15	721,9	4,6	0,5	6,4	1,7	7,56	6,06	19,90
SZ_GW_SteißlingerSee_12	22.09.2017	09:43	8,6	9,35	699,9	15,3	1,7	8,0	1,1	7,67	5,66	18,77
SZ_GW_SteißlingerSee_13	22.09.2017	09:48	15,1	7,80	757,9	2,8	0,3	8,2	2,8	7,51	6,42	20,76
SZ_GW_SteißlingerSee_13	22.09.2017	09:48	10,2	8,17	694,2	6,8	0,8	19,0	1,0	7,62	5,62	18,68
SZ_GW_SteißlingerSee_13	22.09.2017	09:48	5,1	16,56	533,9	99,3	9,6	5,5	0,6	8,34	3,87	13,77
SZ_GW_SteißlingerSee_13	22.09.2017	09:48	0,1	16,69	534,2	98,8	9,6	1,4	0,6	8,36	3,86	13,74
SZ_GW_SteißlingerSee_14	22.09.2017	10:14	12,6	8,04	757,9	3,9	0,5	3,1	2,2	7,36	6,29	20,65
SZ_GW_SteißlingerSee_15	22.09.2017	09:40	7,5	11,14	n.a.n.	22,2	2,4	10,2	1,4	n.a.n.	n.a.n.	n.a.n.
SZ_GW_SteißlingerSee_16	22.09.2017	09:28	18,5	7,36	758,2	2,7	0,3	4,4	3,5	7,48	6,47	20,37
SZ_GW_SteißlingerSee_16	22.09.2017	09:28	13,3	7,99	752,7	2,9	0,3	2,6	1,6	7,53	6,24	20,22
SZ_GW_SteißlingerSee_17	22.09.2017	09:01	12,9	8,15	743,7	2,9	0,3	6,2	13,6	7,41	6,13	20,13
SZ_GW_SteißlingerSee_18	22.09.2017	08:36	18,5	7,34	755,3	3,3	0,4	2,8	2,9	7,38	6,38	20,40
SZ_GW_SteißlingerSee_18	22.09.2017	08:36	13,5	7,94	749,8	3,1	0,4	2,4	1,0	7,43	6,23	20,27
SZ_GW_SteißlingerSee_19	22.09.2017	08:56	10,6	8,07	n.a.n.	4,6	0,5	6,2	3,1	n.a.n.	n.a.n.	n.a.n.
SZ_GW_SteißlingerSee_20	22.09.2017	08:26	9,8	8,48	n.a.n.	6,5	0,8	7,2	1,3	n.a.n.	n.a.n.	n.a.n.
SZ_GW_SteißlingerSee_K1	22.09.2017	09:09	19,7	7,32	762,2	3,1	0,4	4,3	3,4	7,54	6,52	20,45
SZ_GW_SteißlingerSee_K1	22.09.2017	09:09	14,6	7,84	759,0	3,0	0,4	2,8	1,0	7,58	6,33	20,38
SZ_GW_SteißlingerSee_K1	22.09.2017	09:09	9,5	8,61	717,3	12,5	1,4	7,2	0,8	7,78	5,84	18,78
SZ_GW_SteißlingerSee_K1	22.09.2017	09:09	4,6	16,56	533,9	98,8	9,6	4,8	0,6	8,3	3,82	13,57
SZ_GW_SteißlingerSee_K1	22.09.2017	09:09	0,1	16,60	533,2	98,3	9,6	1,8	0,5	8,31	3,85	13,64
SZ_GW_SteißlingerSee_QKv	22.09.2017	13:50	20,0	12,90	841,6	82,0	8,6	n.a.n.	n.a.n.	7,3	6,73	21,98
SZ_GW_SteißlingerSee_QF	22.09.2017	07:34	20,0	17,20	651,9	94,2	9,2	n.a.n.	n.a.n.	7,49	5,9	19,62
SZ_GW_SteißlingerSee_Z1	22.09.2017	13:30	0,0	12,80	912,4	79,1	8,3	n.a.n.	n.a.n.	7,83	8,01	26,74
SZ_GW_SteißlingerSee_Z2	22.09.2017	12:25	0,0	13,40	951,9	67,5	7,0	n.a.n.	n.a.n.	7,83	9,35	28,32
SZ_GW_SteißlingerSee_A	22.09.2017	12:20	0,0	17,00	533,8	109,5	10,5	n.a.n.	n.a.n.	8,27	3,79	13,73

Sampling Point	Date	Time	Depth	Chloride	NO3-N	Sulfate	NH4-N	1/2 Calcium	1/2 Magnesium	Sodium	Potassium	² H	¹⁸ O
		h	m	mg/l	µg/l	mg/l	µg/l	mmol/l	mmol/l	mg/l	mg/l	‰	‰
SZ_GW_SteißlingerSee_01	22.09.2017	11:16	4,6	n.a.n.	n.a.n.	n.a.n.	n.a.n.	n.a.n.	n.a.n.	n.a.n.	n.a.n.	n.a.n.	n.a.n.
SZ_GW_SteißlingerSee_02	22.09.2017	11:13	5,0	n.a.n.	n.a.n.	n.a.n.	n.a.n.	n.a.n.	n.a.n.	n.a.n.	n.a.n.	n.a.n.	n.a.n.
SZ_GW_SteißlingerSee_03	22.09.2017	11:20	8,5	31,63	837,9	42,24	476,0	4,29	2,12	16,07	2,29	-61,26	-8,06
SZ_GW_SteißlingerSee_03	22.09.2017	11:20	3,5	30,41	993,7	41,30	58,2	2,89	2,01	15,66	2,20	-55,35	-6,67
SZ_GW_SteißlingerSee_04	22.09.2017	11:11	3,8	n.a.n.	n.a.n.	n.a.n.	n.a.n.	n.a.n.	n.a.n.	n.a.n.	n.a.n.	n.a.n.	n.a.n.
SZ_GW_SteißlingerSee_05	22.09.2017	11:02	7,2	31,67	616,3	42,32	570,0	4,29	2,11	16,01	2,27	-61,18	-8,02
SZ_GW_SteißlingerSee_06	22.09.2017	11:38	13,2	32,66	1036,7	42,51	929,5	5,11	2,21	16,63	2,37	-64,69	-8,9
SZ_GW_SteißlingerSee_06	22.09.2017	11:38	8,2	31,62	874,0	42,32	412,3	4,06	2,10	15,94	2,25	-60,2	-7,73
SZ_GW_SteißlingerSee_06	22.09.2017	11:38	3,0	30,58	998,0	41,50	61,3	2,85	1,99	15,50	2,19	-54,4	-6,64
SZ_GW_SteißlingerSee_06	22.09.2017	11:38	0,2	30,54	992,6	41,46	59,8	2,87	2,01	15,61	2,21	-54,65	-6,66
SZ_GW_SteißlingerSee_07	22.09.2017	11:32	8,0	31,43	877,4	42,07	373,5	3,93	2,08	15,92	2,25	-59,42	-7,69
SZ_GW_SteißlingerSee_08	22.09.2017	10:57	6,6	31,06	822,7	41,64	310,6	3,64	2,07	15,92	2,25	-57,1	-6,62
SZ_GW_SteißlingerSee_09	22.09.2017	10:46	11,5	32,31	786,6	42,62	671,7	4,74	2,18	16,41	2,37	-62,98	-8,28
SZ_GW_SteißlingerSee_10	22.09.2017	10:32	14,7	32,75	744,6	42,66	987,7	5,11	2,23	16,79	2,40	-64,92	-8,64
SZ_GW_SteißlingerSee_10	22.09.2017	10:32	9,5	31,48	905,6	42,11	424,0	4,17	2,13	16,18	2,30	-62,01	-8,04
SZ_GW_SteißlingerSee_10	22.09.2017	10:32	4,5	30,48	994,4	41,37	58,2	2,88	2,01	15,63	2,20	-55,06	-6,68
SZ_GW_SteißlingerSee_10	22.09.2017	10:32	0,0	30,52	993,3	41,41	58,2	2,88	2,01	15,63	2,21	-54,62	-6,61
SZ_GW_SteißlingerSee_11	22.09.2017	10:20	10,4	32,42	912,9	42,61	678,7	4,80	2,19	16,56	2,35	-62,72	-8,44
SZ_GW_SteißlingerSee_12	22.09.2017	09:43	8,6	32,19	920,3	42,31	496,2	4,56	2,17	16,38	2,31	-62,75	-8,21
SZ_GW_SteißlingerSee_13	22.09.2017	09:48	15,1	33,08	586,0	43,14	990,8	5,09	2,24	16,83	2,39	-64,91	-8,7
SZ_GW_SteißlingerSee_13	22.09.2017	09:48	10,2	32,18	923,3	42,82	507,1	4,54	2,20	16,63	2,36	-62,03	-8,07
SZ_GW_SteißlingerSee_13	22.09.2017	09:48	5,1	30,76	1002,3	41,73	68,3	2,89	2,01	15,67	2,21	-54,94	-6,73
SZ_GW_SteißlingerSee_13	22.09.2017	09:48	0,1	30,50	991,9	41,40	69,9	2,90	2,02	15,75	2,22	-54,62	-6,52
SZ_GW_SteißlingerSee_14	22.09.2017	10:14	12,6	33,06	968,0	42,93	922,5	5,13	2,24	16,85	2,40	-64,08	-8,8
SZ_GW_SteißlingerSee_15	22.09.2017	09:40	7,5	n.a.n.	n.a.n.	n.a.n.	n.a.n.	n.a.n.	n.a.n.	n.a.n.	n.a.n.	n.a.n.	n.a.n.
SZ_GW_SteißlingerSee_16	22.09.2017	09:28	18,5	32,64	132,4	38,20	1559,3	5,06	2,24	16,78	2,46	-64,16	-8,62
SZ_GW_SteißlingerSee_16	22.09.2017	09:28	13,3	32,99	817,3	43,02	864,3	5,05	2,24	16,82	2,41	-64,85	-8,58
SZ_GW_SteißlingerSee_17	22.09.2017	09:01	12,9	32,65	876,7	42,74	769,5	4,99	2,23	16,79	2,38	-63,83	-8,5
SZ_GW_SteißlingerSee_18	22.09.2017	08:36	18,5	32,77	207,8	40,45	1370,6	5,05	2,23	16,74	2,41	-64,88	-8,66
SZ_GW_SteißlingerSee_18	22.09.2017	08:36	13,5	32,93	855,5	42,96	834,8	5,05	2,23	16,80	2,42	-64,36	-8,59
SZ_GW_SteißlingerSee_19	22.09.2017	08:56	10,6	n.a.n.	n.a.n.	n.a.n.	n.a.n.	n.a.n.	n.a.n.	n.a.n.	n.a.n.	n.a.n.	n.a.n.
SZ_GW_SteißlingerSee_20	22.09.2017	08:26	9,8	n.a.n.	n.a.n.	n.a.n.	n.a.n.	n.a.n.	n.a.n.	n.a.n.	n.a.n.	n.a.n.	n.a.n.
SZ_GW_SteißlingerSee_K1	22.09.2017	09:09	19,7	33,17	169,7	38,07	1573,2	5,07	2,24	16,82	2,44	-64,43	-8,52
SZ_GW_SteißlingerSee_K1	22.09.2017	09:09	14,6	32,72	835,2	42,63	869,7	5,06	2,24	16,81	2,41	-63,64	-8,59
SZ_GW_SteißlingerSee_K1	22.09.2017	09:09	9,5	32,32	946,5	43,09	552,1	4,68	2,19	16,54	2,37	-62,73	-8,25
SZ_GW_SteißlingerSee_K1	22.09.2017	09:09	4,6	30,97	1008,0	42,02	61,3	2,88	2,02	15,70	2,22	-54,71	-6,72
SZ_GW_SteißlingerSee_K1	22.09.2017	09:09	0,1	30,79	1003,7	41,79	65,2	2,93	2,05	15,99	2,28	-54,58	-6,45
SZ_GW_SteißlingerSee_Qkv	22.09.2017	13:50	20,0	32,00	7382,9	31,38	4,7	5,85	2,03	17,76	11,72	-67,96	-9,76
SZ_GW_SteißlingerSee_QF	22.09.2017	07:34	20,0	8,47	2913,2	36,53	103,3	4,69	2,23	4,38	1,10	-67,92	-9,81
SZ_GW_SteißlingerSee_Z1	22.09.2017	13:30	0,0	22,71	5832,3	61,30	25,6	7,84	1,84	12,49	1,52	-67,11	-9,38
SZ_GW_SteißlingerSee_Z2	22.09.2017	12:25	0,0	8,55	6995,9	67,76	40,4	8,53	1,35	7,09	7,85	-64,62	-8,88
SZ_GW_SteißlingerSee_A	22.09.2017	12:20	0,0	30,36	991,7	41,22	74,5	2,86	2,00	15,57	2,21	-55,32	-6,58

D) Results of Phreeqc SI_{Calcite} and Inverse Modeling

Name	Date	SI_Anhydrite	SI_Aragonite	SI_Calcite	SI_CO2	SI_Dolomite	SI_Gypsum	Density [g/cm3]
Solution 1_Abfluss	22.09.2017	-2,44	0,64	0,79	-2,98	1,44	-2,05	0,99911
Solution 2_K1 0m Oberflächenwert	22.09.2017	-2,44	0,69	0,84	-3,02	1,54	-2,04	0,99919
Solution 3_Zufluss 1	22.09.2017	-2	0,82	0,98	-2,26	1,28	-1,56	1,00004
Solution 4_Zufluss 2	22.09.2017	-1,93	0,93	1,08	-2,19	1,33	-1,49	1,00002
Solution 5_Quelle Kreisverkehr	22.09.2017	-2,37	0,09	0,25	-1,83	-0,01	-1,92	0,99991
Solution 6_Quelle Friedhof	22.09.2017	-2,33	0,23	0,38	-2,03	0,46	-1,94	0,99917
Solution 7_Mischwasser- K1 BW	22.09.2017	-2,38	0,19	0,35	-2,09	0,19	-1,87	1,00039
Solution 7_Mischwasser-3 BW-5	22.09.2017	-2,44	0,64	0,79	-2,98	1,43	-2,04	0,99918
Solution 7_Mischwasser-3	22.09.2017	-2,36	0,18	0,34	-2,26	0,26	-1,88	1,00020
Solution 7_Mischwasser-5	22.09.2017	-2,9	0,17	0,33	-2,18	0,27	-2,44	0,99997
Solution 7_Mischwasser-6 BW-5	22.09.2017	-2,38	0,22	0,38	-2,36	0,37	-1,90	1,00015
Solution 7_Mischwasser-6 BW-10	22.09.2017	-2,44	0,64	0,79	-2,99	1,44	-2,05	0,99918
Solution 7_Mischwasser-6	22.09.2017	-2,32	0,02	0,18	-1,96	-0,15	-1,82	1,00034
Solution 7_Mischwasser-7	22.09.2017	-2,39	0,21	0,36	-2,37	0,35	-1,91	1,00014
Solution 7_Mischwasser-8	22.09.2017	-2,4	0,37	0,53	-2,26	0,77	-1,97	0,99979
Solution 7_Mischwasser-9	22.09.2017	-2,34	0,12	0,27	-2,12	0,08	-1,84	1,00028
Solution 7_Mischwasser-10 BW-5	22.09.2017	-2,38	0,22	0,38	-2,32	0,34	-1,89	1,00024
Solution 7_Mischwasser-10 BW-10	22.09.2017	-2,45	0,69	0,84	-3,03	-1,53	-2,05	1,00123
Solution 7_Mischwasser-10	22.09.2017	-2,32	0,12	0,27	-2,03	0,05	-1,82	1,00036
Solution 7_Mischwasser-11	22.09.2017	-2,34	0,17	0,33	-2,14	0,18	-1,84	1,00032
Solution 7_Mischwasser-12	22.09.2017	-2,35	0,26	0,41	-2,27	0,40	-1,86	1,00022
Solution 7_Mischwasser-13 BW - 5	22.09.2017	-2,35	0,18	0,34	-2,23	0,23	-1,85	1,00030
Solution 7_Mischwasser-13 BW-10	22.09.2017	-2,44	0,71	0,86	-3,05	1,58	-2,04	0,99919
Solution 7_Mischwasser-13 BW	22.09.2017	-2,32	0,16	0,31	-2,07	0,13	-1,82	1,00037
Solution 7_Mischwasser-14 BW	22.09.2017	-2,31	0	0,15	-1,94	-0,19	-1,81	1,00034
Solution 7_Mischwasser-16 BW-5	22.09.2017	-2,32	0,17	0,32	-2,1	0,16	-1,82	1,00035
Solution 7_Mischwasser-16 BW	22.09.2017	-2,37	0,12	0,28	-2,04	0,05	-1,87	1,00039
Solution 7_Mischwasser-17 BW	22.09.2017	-2,33	0,02	0,17	-2	-0,15	-1,82	1,00038
Solution 7_Mischwasser-18 BW-5	22.09.2017	-2,32	0,06	0,22	-2,01	-0,06	-1,82	1,00035
Solution 7_Mischwasser-18	22.09.2017	-2,35	0,01	0,16	-1,96	-0,18	-1,84	1,00038
Solution 7_Mischwasser-K1 BW-5	22.09.2017	-2,33	0,22	0,38	-2,14	0,27	-1,82	1,00036
Solution 7_Mischwasser-K1 BW-10	22.09.2017	-2,34	0,38	0,54	-2,36	0,62	-1,85	1,00028

Name	Date	SI_Anhydrite	SI_Aragonite	SI_Calcite	SI_CO2	SI_Dolomite	SI_Gypsum	Density [g/cm3]
Solution 1_Abfluss	05.07.2017	-2,32	0,97	1,11	-3,01	2,19	-2,03	0,99707
Solution 2_K1 0m Oberflächenwert	05.07.2017	-2,34	0,89	1,03	-2,97	2,01	-2,03	0,99754
Solution 5_Quelle Kreisverkehr	05.07.2017	-2,36	0,37	0,52	-2,01	0,56	-1,92	0,99986
Solution 6_Quelle Friedhof	05.07.2017	-2,31	0,2	0,35	-2	0,40	-1,92	0,99925
Solution 7_Mischwasser-K1 BW	05.07.2017	-2,34	0,09	0,25	-2,09	-0,01	-1,82	1,00040
Solution 7_Mischwasser-3 BW-5	05.07.2017	-2,35	0,48	0,62	-2,59	1,16	-2,02	0,99793
Solution 7_Mischwasser-3 BW	05.07.2017	-2,35	0,01	0,16	-2,05	-0,10	-1,87	1,00018
Solution 7_Mischwasser-5 BW	05.07.2017	-2,37	0,02	0,18	-2,12	-0,09	-1,87	1,00027
Solution 7_Mischwasser-6 BW	05.07.2017	-2,35	0	0,16	-2,06	-0,16	-1,85	1,00035
Solution 7_Mischwasser-6 BW-5	05.07.2017	-2,39	0,25	0,4	-2,39	0,42	-1,90	1,00018
Solution 7_Mischwasser-6 BW-10	05.07.2017	-2,36	0,75	0,89	-2,86	1,71	-2,03	0,99791
Solution 7_Mischwasser-7 BW	05.07.2017	-2,37	0,12	0,28	-2,24	0,13	-1,88	1,00027
Solution 7_Mischwasser-8 BW	05.07.2017	-2,35	0,38	0,53	-2,38	0,72	-1,90	0,99988
Solution 7_Mischwasser-9 BW	05.07.2017	-2,34	-0,02	0,13	-2,02	-0,22	-1,83	1,00035
Solution 7_Mischwasser-10 BW-5	05.07.2017	-2,37	0,13	0,29	-2,25	0,12	-1,86	1,00034
Solution 7_Mischwasser-10 BW-10	05.07.2017	-2,44	0,6	0,76	-2,93	1,28	-2,00	0,99982
Solution 7_Mischwasser-10 BW	05.07.2017	-2,33	-0,05	0,11	-1,92	-0,28	-1,82	1,00038
Solution 7_Mischwasser-11 BW	05.07.2017	-2,35	0,16	0,32	-2,23	0,18	-1,85	1,00031
Solution 7_Mischwasser-12 BW	05.07.2017	-2,34	0,35	0,5	-2,37	0,59	-1,87	1,00015
Solution 7_Mischwasser-13 BW-5	05.07.2017	-2,36	0,21	0,37	-2,28	0,27	-1,85	1,00035
Solution 7_Mischwasser-13 BW	05.07.2017	-2,34	-0,02	0,14	-1,99	-0,22	-1,83	1,00039
Solution 7_Mischwasser-14 BW	05.07.2017	-2,34	0,07	0,23	-2,09	-0,04	-1,83	1,00037
Solution 7_Mischwasser-16 BW-5	05.07.2017	-2,34	0,08	0,24	-2,09	-0,03	-1,82	1,00039
Solution 7_Mischwasser-16 BW	05.07.2017	-2,34	0,04	0,19	-2,03	-0,12	-1,83	1,00040
Solution 7_Mischwasser-17 BW	05.07.2017	-2,34	0,1	0,26	-2,1	0,02	-1,83	1,00038
Solution 7_Mischwasser-18 BW-5	05.07.2017	-2,35	0,28	0,43	-2,33	0,39	-1,85	1,00035
Solution 7_Mischwasser-18 BW	05.07.2017	-2,34	0,1	0,26	-2,06	0,01	-1,83	1,00040
Solution 7_Mischwasser-K1 BW-5	05.07.2017	-2,34	0,33	0,48	-2,3	0,48	-1,83	1,00038
Solution 7_Mischwasser-K1 BW-10	05.07.2017	-2,35	0,22	0,38	-2,25	0,28	-1,84	1,00035
Solution 7_Mischwasser-K1 BW-15	05.07.2017	-2,34	0,75	0,9	-2,77	1,58	-1,96	0,99896

Name	Date	SI_Anhydrite	SI_Aragonite	SI_Calcite	SI_CO2	SI_Dolomite	SI_Gypsum	Density [g/cm3]
Solution 1_Abfluss	28.03.2017	-2,33	0,92	1,07	-2,92	1,77	-1,88	0,99995
Solution 2_K1 0m Oberflächenwert	28.03.2017	-2,32	0,94	1,09	-2,93	1,82	-1,88	0,99987
Solution 3_Zufluss 1	28.03.2017	-2,04	0,78	0,93	-2,39	1,13	-1,55	1,00047
Solution 4_Zufluss 2	28.03.2017	-1,75	1,14	1,29	-2,59	1,77	-1,28	1,00043
Solution 5_Quelle Kreisverkehr	28.03.2017	-2,37	0,3	0,46	-2	0,38	-1,91	1,00013
Solution 6_Quelle Friedhof	28.03.2017	-2,38	0,25	0,4	-2,2	0,36	-1,89	1,00024
Solution 7_Mischwasser - K1 BW	28.03.2017	-2,34	0,16	0,32	-2,23	0,11	-1,81	1,00043
Solution 7_Mischwasser-3 BW-5	28.03.2017	-2,36	0,85	1	-2,9	1,60	-1,88	1,00016
Solution 7_Mischwasser-3 BW	28.03.2017	-2,39	0,52	0,68	-2,66	0,86	-1,86	1,00041
Solution 7_Mischwasser-5 BW	28.03.2017	-2,38	0,52	0,68	-2,66	0,86	-1,85	1,00041
Solution 7_Mischwasser-6 BW-5	28.03.2017	-2,38	0,33	0,49	-2,47	0,47	-1,85	1,00041
Solution 7_Mischwasser-6 BW-10	28.03.2017	-2,36	0,83	0,99	-2,89	1,56	-1,88	1,00018
Solution 7_Mischwasser-6 BW	28.03.2017	-2,37	0,12	0,28	-2,23	0,04	-1,84	1,00041
Solution 7_Mischwasser-7 BW	28.03.2017	-2,38	0,45	0,61	-2,59	0,71	-1,85	1,00041
Solution 7_Mischwasser-8 BW	28.03.2017	-2,38	0,5	0,66	-2,64	0,81	-1,85	1,00041
Solution 7_Mischwasser-9 BW	28.03.2017	-2,36	0,2	0,36	-2,28	0,20	-1,83	1,00042
Solution 7_Mischwasser-10 BW-5	28.03.2017	-2,37	0,41	0,57	-2,54	0,63	-1,84	1,00042
Solution 7_Mischwasser-10 BW-10	28.03.2017	-2,37	0,73	0,89	-2,83	1,31	-1,86	1,00035
Solution 7_Mischwasser-10 BW-15	28.03.2017	-2,37	0,41	0,57	-2,54	0,63	-1,84	1,00042
Solution 7_Mischwasser-10 BW	28.03.2017	-2,35	0,11	0,27	-2,19	0,02	-1,82	1,00043
Solution 7_Mischwasser-11 BW	28.03.2017	-2,37	0,35	0,51	-2,48	0,52	-1,84	1,00041
Solution 7_Mischwasser-12 BW	28.03.2017	-2,38	0,39	0,55	-2,52	0,59	-1,85	1,00041
Solution 7_Mischwasser-13 BW-10	28.03.2017	-2,37	0,65	0,81	-2,76	1,13	-1,86	1,00038
Solution 7_Mischwasser-13 BW	28.03.2017	-2,35	0,17	0,32	-2,25	0,13	-1,82	1,00043
Solution 7_Mischwasser-14 BW	28.03.2017	-2,36	0,25	0,41	-2,34	0,31	-1,83	1,00043
Solution 7_Mischwasser-16 BW-5	28.03.2017	-2,35	0,22	0,38	-2,3	0,23	-1,82	1,00043
Solution 7_Mischwasser-16 BW	28.03.2017	-2,34	0,11	0,27	-2,19	0,03	-1,81	1,00043
Solution 7_Mischwasser-17 BW	28.03.2017	-2,38	0,46	0,62	-2,6	0,74	-1,85	1,00044
Solution 7_Mischwasser-18 BW-5	28.03.2017	-2,36	0,33	0,49	-2,45	0,47	-1,83	1,00042
Solution 7_Mischwasser-18 BW	28.03.2017	-2,35	0,53	0,69	-2,57	0,85	-1,82	1,00044
Solution 7_Mischwasser-K1 BW-5	28.03.2017	-2,35	0,19	0,35	-2,3	0,18	-1,82	1,00042
Solution 7_Mischwasser-K1 BW-10	28.03.2017	-2,36	0,33	0,49	-2,45	0,47	-1,83	1,00042
Solution 7_Mischwasser-K1 BW-15	28.03.2017	-2,37	0,77	0,93	-2,87	1,40	-1,86	1,00034

Name	Date	SI_Anhydrite	SI_Aragonite	SI_Calcite	SI_CO2	SI_Dolomite	SI_Gypsum	Density [g/cm3]
Solution 2_K1 0m Oberflächenwert	23.11.2016	-2,41	0,51	0,67	-2,72	0,92	-1,91	1,00027
Solution 3_Zufluss 1	23.11.2016	-1,99	0,6	0,76	-2,19	0,75	-1,5	1,00037
Solution 4_Zufluss 2	23.11.2016	-1,96	0,69	0,85	-2,31	0,76	-1,47	1,00039
Solution 5_Quelle Kreisverkehr	23.11.2016	-2,36	0,22	0,37	-1,91	0,22	-1,91	1,00005
Solution 7_Mischwasser-K1 BW	23.11.2016	-2,51	0,03	0,19	-1,9	-0,13	-2	1,00039
Solution 7_Mischwasser-K1 OW+15	23.11.2016	-2,3	0,13	0,29	-2	0,08	-1,81	1,00033
Solution 7_Mischwasser-K1OW+10	23.11.2016	-2,33	0,17	0,32	-2,12	0,17	-1,84	1,00029
Solution 7_Mischwasser-18 BW -5	23.11.2016	-2,32	0,12	0,27	-2,06	0,07	-1,83	1,00029
Solution 7_Mischwasser-18 BW	23.11.2016	-2,31	0,07	0,23	-1,97	-0,05	-1,81	1,00036
Solution 7_Mischwasser-12 BW	23.11.2016	-2,41	0,41	0,57	-2,63	0,72	-1,91	1,00026
Solution 7_Mischwasser-11 BW	23.11.2016	-2,4	0,35	0,51	-2,53	0,6	-1,9	1,00027
Solution 7_Mischwasser-10 BW	23.11.2016	-2,3	0,05	0,21	-1,93	-0,09	-1,81	1,00032
Solution 7_Mischwasser-10 OW+10	23.11.2016	-2,37	0,2	0,36	-2,32	0,3	-1,88	1,00025
Solution 7_Mischwasser-9 BW	23.11.2016	-2,32	0,03	0,19	-1,98	-0,1	-1,83	1,00029
Solution 7_Mischwasser-3 BW-5	23.11.2016	-2,41	0,32	0,47	-2,55	0,54	-1,91	1,00027
Solution 7_Mischwasser-3 BW	23.11.2016	-2,41	0,32	0,48	-2,55	0,54	-1,91	1,00027

Name	Date	SI_Anhydrite	SI_Aragonite	SI_Calcite	SI_CO2	SI_Dolomite	SI_Gypsum	Density [g/cm3]
Solution 2_K1 0m Oberflächenwert	20.06.2016	-2,35	0,81	0,95	-2,92	1,72	-1,99	0,99867
Solution 5_Quelle Kreisverkehr	20.06.2016	-2,35	0,14	0,3	-1,84	0,1	-1,91	0,99984
Solution 6_Quelle Friedhof	20.06.2016	-2,29	0,2	0,35	-1,99	0,39	-1,9	0,99925
Solution 7_Mischwasser-K1BW	20.06.2016	-2,33	-0,02	0,13	-2,01	-0,24	-1,81	1,00040
Solution 7_Mischwasser-3 BW	20.06.2016	-2,35	0,32	0,47	-2,42	0,51	-1,86	1,00026
Solution 7_Mischwasser- 3BW - 5	20.06.2016	-2,35	0,76	0,91	-2,86	1,63	-1,98	0,99862
Solution 7_Mischwasser-9 BW	20.06.2016	-2,33	0	0,15	-2,05	-0,19	-1,81	1,00037
Solution 7_Mischwasser- 10 OW +10	20.06.2016	-2,33	-0,02	0,14	-2,02	-0,22	-1,82	1,00038
Solution 7_Mischwasser- 10 BW	20.06.2016	-3,11	0,05	0,1	-1,96	-0,3	-2,6	1,00036
Solution 7_Mischwasser- 11 BW	20.06.2016	-2,34	0,06	0,21	-2,12	-0,06	-1,83	1,00036
Solution 7_Mischwasser- 12 BW	20.06.2016	-2,36	0,3	0,46	-2,4	0,45	-2,4	1,00034
Solution 7_Mischwasser_18 BW	20.06.2016	-2,33	-0,01	0,14	-2,02	-0,22	-1,82	1,00039
Solution 7_Mischwasser- 18 BW-5	20.06.2016	-2,33	0,03	0,18	-2,06	-0,13	-1,82	1,00038
Solution 7_Mischwasser-K1 OW+10	20.06.2016	-2,35	0,12	0,28	-2,19	0,06	-1,84	1,00038
Solution 7_Mischwasser-K1OW+15	20.06.2016	-2,33	0,02	0,17	-2,05	-0,16	-1,82	1,00039

Inverse Modelling										
Name	Depth	Date	Solution 1	Solution 2	Solution 3	Solution 4	Solution 5	Solution 6	Solution 7	Control
			A	Lake OW	Z1	Z2	QKV	QF	Mixture	
3 BW (QKv QF OW)	7,13	21.06.2016	n.a.n.	87,01	n.a.n.	n.a.n.	3,08	9,91	100	100,0
K1 BW (QKv QF OW)	19,01	21.06.2016	n.a.n.	66,17	n.a.n.	n.a.n.	12,19	21,64	100	100,0
9 BW (QKv QF OW)	11,92	21.06.2016	n.a.n.	72,45	n.a.n.	n.a.n.	9,08	18,47	100	100,0
10 BW (QKv QF OW)	14,14	21.06.2016	n.a.n.	49,15	n.a.n.	n.a.n.	42,71	8,14	100	100,0
11 BW (QKv QF OW)	10,11	21.06.2016	n.a.n.	72,39	n.a.n.	n.a.n.	9,70	17,90	100	100,0
12 BW (QKv QF OW)	8,11	21.06.2016	n.a.n.	83,45	n.a.n.	n.a.n.	6,66	9,90	100	100,0
18 BW (QKv QF OW)	17,96	21.06.2016	n.a.n.	71,45	n.a.n.	n.a.n.	10,47	18,08	100	100,0
9 BW(QKv OW "QF")	12,18	23.11.2016	n.a.n.	53,42	n.a.n.	n.a.n.	15,77	30,81	100	100,0
10 BW (QKv OW "QF")	15,02	23.11.2016	n.a.n.	40,28	n.a.n.	n.a.n.	23,05	36,67	100	100,0
11 BW (QKv OW "QF")	9,07	23.11.2016	n.a.n.	94,45	n.a.n.	n.a.n.	0,48	5,06	100	100,0
12 BW (QKv OW "QF")	7,83	23.11.2016	n.a.n.	100,00	n.a.n.	n.a.n.	0,00	0,00	100	100,0
18 BW (QKv OW "QF")	16,23	23.11.2016	n.a.n.	36,89	n.a.n.	n.a.n.	24,40	38,70	100	100,0
K1 BW (QKv OW "QF")	19,40	23.11.2016	n.a.n.	36,90	n.a.n.	n.a.n.	24,27	38,82	100	100,0
3 BW (QKv QF OW)	7,76	28.03.2017	n.a.n.	76,85	n.a.n.	n.a.n.	3,92	19,23	100	100,0
5 BW (QKv QF OW)	7,82	28.03.2017	n.a.n.	73,09	n.a.n.	n.a.n.	23,20	3,71	100	100,0
6 BW (QKv QF OW)	13,56	28.03.2017	n.a.n.	69,44	n.a.n.	n.a.n.	7,36	23,20	100	100,0
7 BW (QKv QF OW)	7,78	28.03.2017	n.a.n.	60,87	n.a.n.	n.a.n.	26,09	13,04	100	100,0
8 BW (QKv QF OW)	7,58	28.03.2017	n.a.n.	66,18	n.a.n.	n.a.n.	11,77	22,05	100	100,0
9 BW (QKv QF OW)	11,11	28.03.2017	n.a.n.	63,49	n.a.n.	n.a.n.	10,16	26,35	100	100,0
10 BW (QKv QF OW)	15,13	28.03.2017	n.a.n.	48,97	n.a.n.	n.a.n.	32,27	18,76	n.a.n.	100,0
11 BW (QKv QF OW)	10,27	28.03.2017	n.a.n.	32,87	n.a.n.	n.a.n.	23,79	43,34	100	100,0
12 BW (QKv QF OW)	8,89	28.03.2017	n.a.n.	56,93	n.a.n.	n.a.n.	42,75	0,32	100	100,0
13 BW (QKv QF OW)	15,71	28.03.2017	n.a.n.	49,17	n.a.n.	n.a.n.	14,59	36,23	100	100,0
14 BW (QKv QF OW)	10,63	28.03.2017	n.a.n.	63,04	n.a.n.	n.a.n.	14,16	22,80	100	100,0
16 BW (QKv QF OW)	19,65	28.03.2017	n.a.n.	39,84	n.a.n.	n.a.n.	24,63	35,53	100	100,0
17 BW (QKv QF OW Z1 Z2)	12,62	28.03.2017	n.a.n.	79,17	n.a.n.	n.a.n.	0,00	20,83	100	100,0
18 BW (QKv QF OW)	19,03	28.03.2017	n.a.n.	57,92	n.a.n.	n.a.n.	10,06	32,02	100	100,0
K1 BW (QKv QF OW)	20,32	28.03.2017	n.a.n.	74,51	n.a.n.	n.a.n.	7,37	18,12	100	100,0
3 BW (QKv OF OW)	8,16	05.07.2017	n.a.n.	57,32	n.a.n.	n.a.n.	10,28	32,41	100	100,0
5 BW (QKv OF OW)	9,18	05.07.2017	n.a.n.	59,24	n.a.n.	n.a.n.	10,81	29,95	100	100,0
6 BW (QKv OF OW)	13,35	05.07.2017	n.a.n.	47,00	n.a.n.	n.a.n.	15,23	37,78	100	100,0
7 BW (QKv OF OW)	9,05	05.07.2017	n.a.n.	61,50	n.a.n.	n.a.n.	9,23	29,27	100	100,0
8 BW (QKv OF OW)	6,62	05.07.2017	n.a.n.	66,78	n.a.n.	n.a.n.	7,43	25,79	100	100,0
9 BW (QKv QF OW)	11,66	05.07.2017	n.a.n.	47,42	n.a.n.	n.a.n.	15,35	37,24	100	100,0
10 BW (QKv QF OW)	16,79	05.07.2017	n.a.n.	38,13	n.a.n.	n.a.n.	18,67	43,20	100	100,0
11 BW (QKv QF OW)	9,80	05.07.2017	n.a.n.	60,96	n.a.n.	n.a.n.	5,53	33,51	100	100,0
12 BW (QKv QF OW)	7,85	05.07.2017	n.a.n.	62,47	n.a.n.	n.a.n.	8,96	28,56	100	100,0
13 BW (QKv QF OW)	15,94	05.07.2017	n.a.n.	45,52	n.a.n.	n.a.n.	8,47	46,01	100	100,0
14 BW (QKv QF OW)	13,98	05.07.2017	n.a.n.	56,34	n.a.n.	n.a.n.	12,20	31,47	100	100,0
16 BW (QKv QF OW)	19,48	05.07.2017	n.a.n.	52,84	n.a.n.	n.a.n.	12,33	34,83	100	100,0
17 BW (QKv QF OW)	12,59	05.07.2017	n.a.n.	50,94	n.a.n.	n.a.n.	9,53	39,54	100	100,0
18 BW (QKv QF OW)	15,83	05.07.2017	n.a.n.	48,76	n.a.n.	n.a.n.	16,14	35,10	100	100,0
K1 BW (QKv QF OW)	20,30	05.07.2017	n.a.n.	51,49	n.a.n.	n.a.n.	13,37	35,14	100	100,0
K1 BW (QKv QF OW)	19,71	22.09.2017	n.a.n.	26,11	n.a.n.	n.a.n.	25,25	48,64	100	100,0
3 BW (QKv QF OW)	8,53	22.09.2017	n.a.n.	52,09	n.a.n.	n.a.n.	0,00	47,91	100	100,0
5 BW (QKv QF OW)	7,20	22.09.2017	n.a.n.	50,38	n.a.n.	n.a.n.	0,00	49,62	0	100,0
6 BW (QKv QF OW)	13,17	22.09.2017	n.a.n.	26,05	n.a.n.	n.a.n.	26,73	47,22	100	100,0
7 BW (QKv QF OW)	8,00	22.09.2017	n.a.n.	63,97	n.a.n.	n.a.n.	7,70	28,33	100	100,0
8 BW (QKv QF OW)	6,60	22.09.2017	n.a.n.	82,82	n.a.n.	n.a.n.	14,69	2,50	100	100,0
9 BW (QKv QF OW)	11,47	22.09.2017	n.a.n.	39,34	n.a.n.	n.a.n.	16,49	44,17	100	100,0
10 BW (QKv QF OW)	14,73	22.09.2017	n.a.n.	22,77	n.a.n.	n.a.n.	28,86	48,37	100	100,0
11 BW (QKv QF OW)	n.a.n.	22.09.2017	n.a.n.	39,26	n.a.n.	n.a.n.	22,13	38,61	0	100,0
12 BW (QKv QF OW)	8,56	22.09.2017	n.a.n.	38,51	n.a.n.	n.a.n.	21,58	39,91	100	100,0
13 BW (QKv QF OW)	15,06	22.09.2017	n.a.n.	22,80	n.a.n.	n.a.n.	32,32	44,88	100	100,0
14 BW (QKv QF OW)	12,60	22.09.2017	n.a.n.	28,57	n.a.n.	n.a.n.	0,00	71,43	100	100,0
16 BW (QKv QF OW)	18,48	22.09.2017	n.a.n.	29,07	n.a.n.	n.a.n.	26,73	44,21	n.a.n.	100,0
17 BW (QKv QF OW)	12,87	22.09.2017	n.a.n.	32,57	n.a.n.	n.a.n.	31,47	35,96	100	100,0
18 BW (QKv QF OW)	18,48	22.09.2017	n.a.n.	22,77	n.a.n.	n.a.n.	28,38	48,85	100	100,0